ISAS - INTERNATIONAL SCHOOL
FOR ADVANCED STUDIES

Characterisation of the Rotavirus NSP5 phosphorylation and study of its function with selected intracellular antibodies

Thesis Submitted for the Degree of
Doctor Philosophiae

Candidate:
Fulvia Vascotto

Supervisor:
Dr. Oscar Burrone

Academic Year 2002/2003

SISSA - SCUOLA
NTERNAZIONALE
SUPERIORE
I STUDI AVANZATI
TRIESTE
Via Beirut 2-4

TRIESTE

Characterisation of the Rotavirus NSP5 phosphorylation and study of its function with selected intracellular antibodies

Thesis Submitted for the Degree of
Doctor Philosophiae

Candidate:
Fulvia Vascotto

Supervisor:
Dr. Oscar Burrone

Academic Year 2002/2003

INDEX:

List of abbreviations

3D = three-dimentional
= Angstrom
Amp = ampicellin
ATP = adenosine triphosphate
BAB = basic acidic basic
BSA = bovine serum albumin
Ci = Curie
C-terminal = carboxy-terminal
C60 = rotavirus strain
CMV = cytomegalovirus
cpe = cytopathic effect
CryoEM = cryoelectron microscopy
kDa = kilo Dalton
dil = dilution
DLP = double layered particles
DMEM = Dulbecco modified Eagle Medium
DMSO = dimethilsulfoxide
DMP = di-methylpimelidate
DOC = deoxycolate
ds = double shell (= double layer particles)
DSP = dithiobis (succinimidylpropionate
dsRNA = double stranded RNA
DTT = di-thio-eritol
E.coli = Escherichia coli
EGFP = eukariotic green fluorescence protein
EM = electron microscopy
ENS = enteric nervous system
ER = endoplasmic reticulum
FACS = fast analytical cell system
FCS= fetal calf serum
FITC = fluorescein
G418 = gentamycin
GlcNAc = N-Acetyl glucosamine
GST = Glutathion-S-transferase
h = hours
HRP = horse raddish peroxidase
Kan = kanamycin
Ib = intrabody
Ig = immunoglobulin
IP3 = inositol 1,4,5-trisphosphat
IPTG = isopropyl β-D-thiogalactopyraniside
λ-Ppase = lambda protein phosphatase
LB = Luria Bertani Broth
MA104 = fetal rhesus monkey kidney cells
mAmp = milli Ampere
Met = methionine
min = minute
MMP = metalloproteases
moi = molteplicity of infection
N-terminal = amino-terminal
NSP1-NSP6 = non structural protein
nt = nucleotides
o/n = over-night
^{o}C = celsius degrees
OD = optical density
ORF = open reading frame
OSU = rotavirus strain
PAGE = polyacrylamide gel electrophoresis
PBS = phosphate buffer saline
P-BSA = PBS+BSA
PEST = protease domain
PFA = paraformaldehyde
pfu = plque forming unit
pi = post infection
^{32}Pi = inorganic phosphate
PMSF = protease inhibitor
RI = relication intermediate
RNAse = Ribonuclease
RITC = rhodamine
rpm = rotation per minute
RT = room temperature
^{35}S = solfour
SA11 = rotavirus strain
ScFv = single chain fragment V
SDS = sodium dodecil sulfate
SF = serum free
sec = seconds
ss = single shell immature viral particles
ssRNA = single stranded RNA
SV40 = simian virus 40
SVP = subviral particles
TBB = tetrabromo-2-azabenzimidazole
TNT = coupled transcription and translation
Ts = temperature sensitive
U = unit
UTR = untranslated region
UV = ultraviolet
V = Volt
VLP = virus like particles (from baculovirus)
VLS = viroplam-like structure
VP1-VP7 = viral structural proteins
vTF7.3 = vaccinia virus strain

Introduction (1)

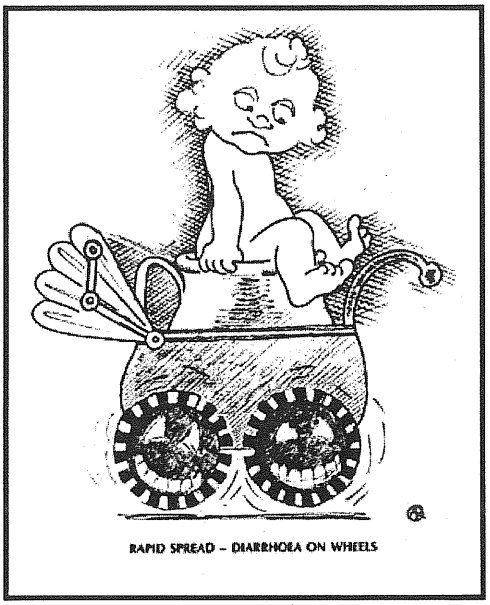

Rotaviruses, the most common diarrheal pathogen in children worldwide, are classified as a genus within the family *Reoviridae*. Mature rotavirus particles were observed in 1973 by electron microscopy in the duodenal epithelium of children with diarrhea as structures of 65-75 nm diameter and subsequently designed as rotavirus (Latin *rota* = wheel) because of their appearance (Figure 1). They possess a triple-layered icosahedral capsid which surrounds 11 dsRNA fragments each coding for a protein, for a total number of 6 structural proteins (VP) and 5 non-structural proteins (NSP) found only in infected cells (Figure 2). Although the structural proteins have been largely characterised, the non-structural ones have been detected in various stages of the rotavirus replication cycle, but for some of them specific functions have not yet been completely established. They play a role as helper proteins supporting virus replication, packaging, assembly and ssRNA stabilisation [55].

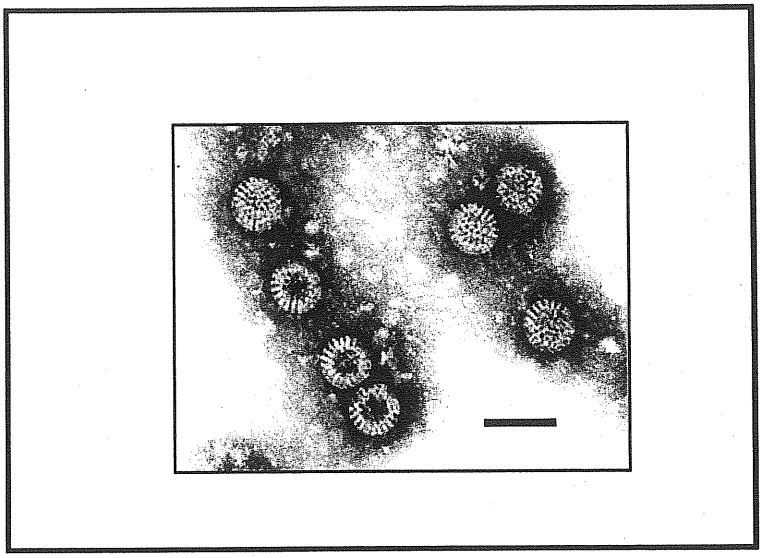

Figure 1: Note the wheel-like appearance of some of the rotavirus particles. The observance of such particles gave the virus its name ("rota" being the Latin word meaning wheel). Bar = 100 nanometers. Source: Cell culture. Method: Negative-stain Transmission Electron Microscopy
By F.P. Williams, U.S. Environmental Protection Agency.

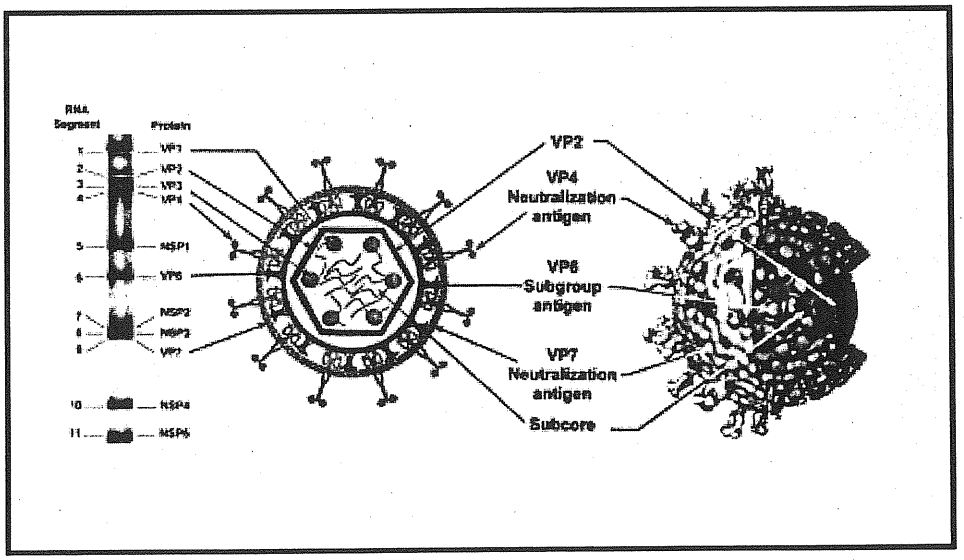

Figure 2: Gene coding assignments and three-dimensional structure of rotavirus particles. Double-stranded RNA segments separated on polyacrylamide gel (**left**) code for individual proteins, which are localized in the schematic of virus particle (**centre**) or in different protein shells of virus (**right**). Outer capsid proteins VP4 and VP7 are neutralization antigens, which induce neutralizing antibody; protein that makes up intermediate protein shell, VP6, is the subgroup antigen [55].

Rotavirus epidemiology and vaccination

Rotavirus infection accounts for ~45% of severe diarrheal diseases in infants and young children in both developed and developing countries. In the USA, rotavirus causes ~ 20 to 40 death, 55.000 hospitalisations and 500.000 physician visits that cost in excess of US$ 1 billion annually. The outcome of infection is more devastating in developing countries, where an estimate 600.000 deaths occur annually, and surviving children may fail to thrive (Figure 3).

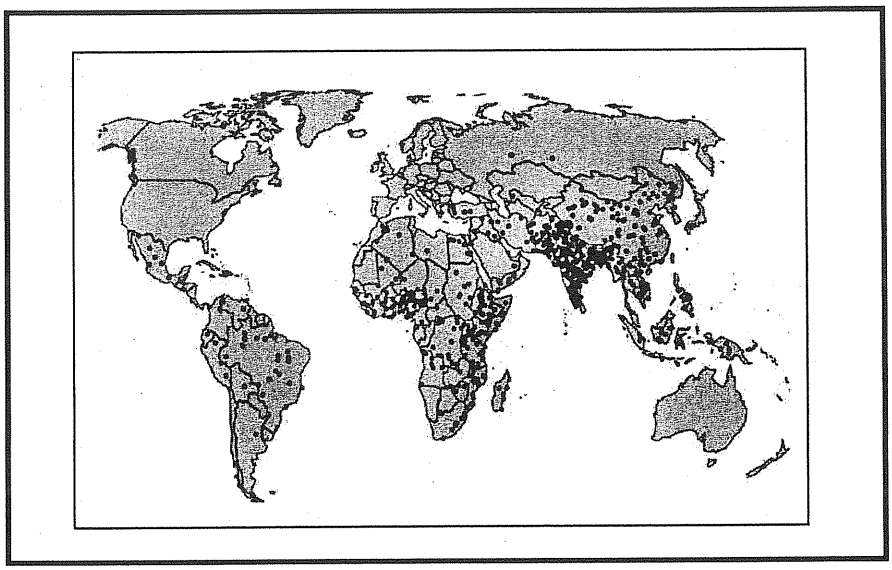

Figure 3: Estimated global distribution of the 800,000 annual deaths caused by rotavirus diarrhea [135, 67].

These statistics support the global need for an effective vaccine. Unfortunately, the live-attenuated rhesus rotavirus (RRV)-tetravalent vaccine (TV), the first rotavirus vaccine licensed, was withdrawn from the market [195] because of a temporal association with intussusception. Intussussception, an invagination of one portion of intestine into an immediately adjacent section, was the most common cause of intestinal obstruction in small children but the cause(s) of RRV-TV remain unclear. However, a model for rotavirus-induced intussusception in mice has recently been developed, useful to test whether rotavirus vaccine candidates pose a risk of intussusception in children [39]. This unexpected setback emphasized the need to better understand the mechanisms underlying rotavirus pathogenesis, including details of the molecular interactions between rotavirus and cells of the gastrointestinal tract [36, 135].

Rotavirus ethiology

Despite the prevalence of rotavirus infection and extensive studies in animal models, rotavirus pathogenesis and the mechanism underlying the intestinal fluid loss in rotavirus diarrhea are not completely known. There is evidence that transcription- and replication-defective rotaviruses cause diarrhea in animal models, suggesting that rotavirus attachment or entry into cells is sufficient for the induction of diarrhea [170].

Rotaviruses have a limited tissue tropism, with infection restricted to cells of the small intestine, and infect fully differentiated enterocytes via their apical surface. During infection the mucosal architecture undergoes remodelling, which results in the stunting of the villi, flattening and loss of enterocytes. The generation of diarrhea is a multifactorial process involving Ca^{2+}-dependent secretory processes of mediators, water and electrolytes, as well as the induction of cell death in the different cell types that compose the intestinal epithelium. In particular recently it has been reported the induction of apoptosis, involving mitochondria, but caspase-3 independent process, in human intestinal epithelial Caco-2 cells by rotavirus infection [25].

It was also been demonstrated that purified NSP4 causes diarrhea in young mice in an age-dependent, dose-dependent and specific manner. So, it is proposed that NSP4 acts as an enterotoxin, because it has toxin-like effect when transiently expressed in cells and is capable of inducing secretory diarrhea in neonatal mice; these effects are selectively blocked by anti-NSP4 antibodies [12, 56, 83]. Moreover, NSP4 directly causes the inhibition of the Na+-D-glucose symporter (SGLT1) [78]. This effect, implying a concomitant inhibition of water absorption, is postulated to play a mechanicistic role in the pathogenesis of rotavirus diarrhea.

Another interesting discovery is that rotavirus evokes intestinal fluid and electrolyte secretion by systemic activation of the enteric nervous system (ENS) in the intestinal wall. Four different drugs that inhibit ENS were tested; these significantly attenuated the intestinal secretory response to rotavirus, strongly suggesting that ENS participates in the virus induced electrolyte and fluid secretion [109]. A possible interpretation of the ENS action, is that the increasing of Ca^{2+} concentration induced by NSP4, may trigger the release of amines or peptides from the endocrine cells of the gut to stimulate dendrites or free nerve endings located underneath the epithelial layer, thereby activating secretory nervous reflexes. Moreover, as a possible therapeutic approach, the intestinal secretion

that activate ENS via the intestinal endocrine cells can be significantly inhibited by the calcium channels blockers, which markedly attenuate the release of amines and peptides from these cells [184]. Besides, specific neurotransmitters were identified in the pathophysiology of a viral intestinal pathogen. In fact, serotonin and vasoactive intestinal peptide (VIP) are involved in rotavirus (RRV) induced fluid secretion [97].

In trying to explain how rotavirus loses its infectivity in adults, a model has recently been proposed in which the simultaneous presence of two categories of cellular receptors is necessary for symptomatic diarrhea [12]. One of the two is essential for virus entry and gene expression, but not needed in disease, whereas the second may regulate NSP4-specific functions. According to this model, the concentration of NSP4 receptor may be substantially reduced in adult animals, thus resulting in no disease.

Virion structure

Three-dimensional structural analyses have been carried out using cryoelectron microscopy and computer image reconstruction procedures on different members of *Reoviridae* family, as bluetongue virus (BTV) of the Orbivirus genus and several strains of Reovirus genus [55, 158]. The overall organisation is similar among these viruses, and an interesting question has risen about why these viruses are so complex. The complex nature of the structural organisation may have evolved as a direct consequence of the requirement for transcribing multiple dsRNA genome segments within a particular enzymatic complex. However, the distinctive feature of rotavirus genus is the presence of 120 protruding spikes (VP4) and of 132 channels per virion linking the outer surface with the inner core (about 140Å deep) (Figure 4) [158].

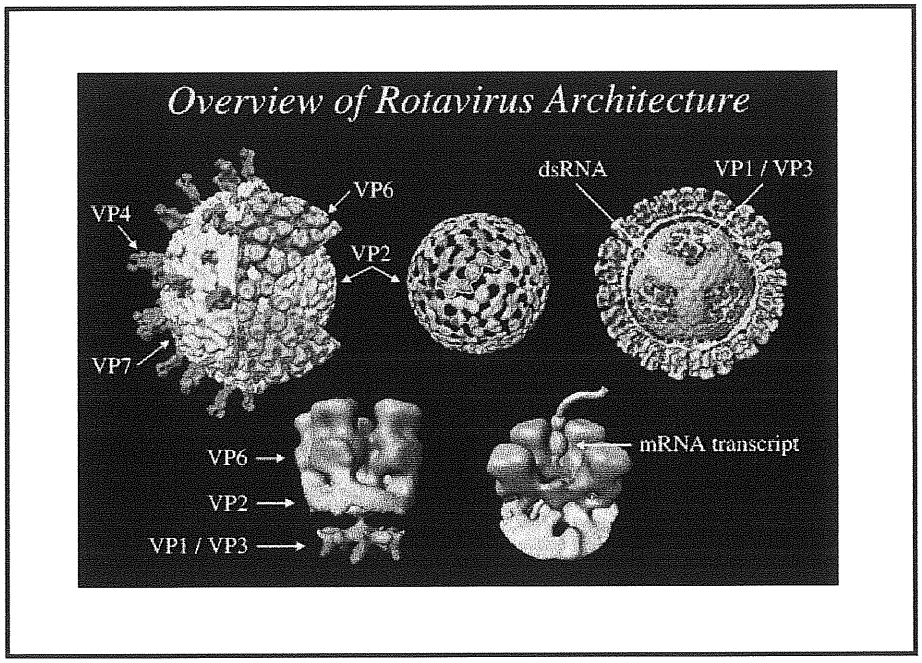

Figure 4: Organisation of proteins and dsRNA genome in rotavirus particles carried out by using electron cryomicroscopy and computer image-processing techniques. **(Upper left)** Three-dimensional structure of the mature triple-layer rotavirion, in which portions of the outer (VP4 and VP7) and intermediate shells have been removed. **(Upper centre)** Representation of the T=2 core formed by 120 copies of VP2. The white boundary indicates the interaction between the two molecules of VP2 along the twofold axis. Note the 10 molecules of VP2 making up the pentamer, 5 are positioned close to the fivefold axis (red) while the other 5 originate further away from the axis. **(Upper right)** Cutaway of the intermediate and core layers of protein, displaying protrusions of the RNA polymerase, VP1, and the capping enzyme VP3, at the fivefold axes into the interior of the core, where they are surrounded by the dsRNA genome arranged as dodecahedron. **(Lower left)** Side view illustrating the three-dimensional organisation of the proteins through the fivefold axis of a double-layered particle (DLP). The VP1-VP3 complex extends as "flower-petal" from the VP2 pentamers. VP2 has a RNA binding activity and may form a platform on which the VP1 carries out RNA synthesis. **(Lower right)** Proposed path of mRNA transit through the inner capsid. For clarity, one of the five trimers of VP6 (blue) has been removed, exposing a portion of the underlying VP2 layer (green) along with the plug of mRNA (pink) seen in the centre of the channel. Shown in grey is a cartoon representation of the potential path of an mRNA transcript (tube diameter ~10A) exiting through the VP2 and VP6 layers. Figure published by B. V. V. Prasad [160, 159].

Rotaviruses have icosaheral symmetry with T=131 for the two outer layers. Three types of channels can be distinguished according to their position and size (12 type I, 60 type II and 60 type III) (Figure 5) [55]. Type II and III channels are about 55Å wide while type I have a narrower and more circular opening around 40Å in diameter and they are defined only by VP6. The base of the type I channels is closed in the centre by the VP2 pavement [99, 159]. Type I channels are involved in importing metabolites required for RNA transcription and exporting the nascent mRNA [99].

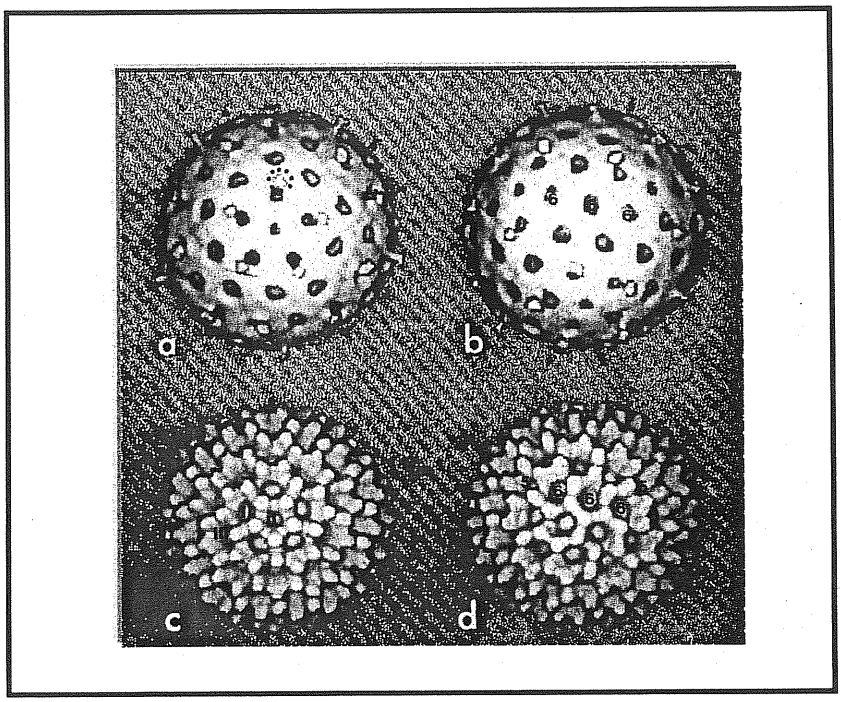

Figure 5: Surface representation of the 3-dimensional structures of double and single-shelled rotavirions along the icosahedral fivefold axis (a and c) and along the icosahedral three-fold axis (b and d). The channels I, II, III are indicated. In b and d a pair of neighbouring fivefold axes (50 and the 6-co-cordinatoed positions (6) relating them are shown to illustrate T=13*l* (*levo*). [160].

The outer layer of the virus gets 120Å long surface spikes composed by 120 copies of VP4 (dimers) which have a bilobed structure (Figure 2, 4) [157]. The VP4 spike interacts with 2 molecules of VP7, both involved in the cell recognition and entry, but inside its larger globular domain of VP4 interacts with 6 molecules of VP6 surrounding the type II channels [169]. The second protein of the outer layer is the glycoprotein VP7 represented in 780 molecules as trimers. VP4-VP7 and VP4-VP6 interactions imply that VP4 may structurally participate in maintaining the precise geometric register between the inner and the outer layers [158].

The surface of the intermediate layer (or double-layered particles DLP) is composed by 780 molecules of VP6, forming 260 capsomeric units arranged in trimers [160, 198]. The inner layer possesses a T=1 symmetry, formed by 120 molecules of VP2 arranged as 60 dimers. The inner layer surrounds the 11 genome dsRNA fragments, which are highly ordered [55]. Further inside the inner shell localises 12 molecules of VP1, (RNA-dependent RNA polymerase) and VP3 (guanyl-transferase, as capping enzyme) per virion [157] in direct contact with the genome, but further structural studies are required to understand their internal organization in the rotavirus particles. The outer surface of VP2 provides a structural platform for assembly of VP6 trimers, preventing aggregation of the core

particles (VP1, VP2, VP3 and genome), which are known to be high hydrophobic proteins [154] (Figure 6).

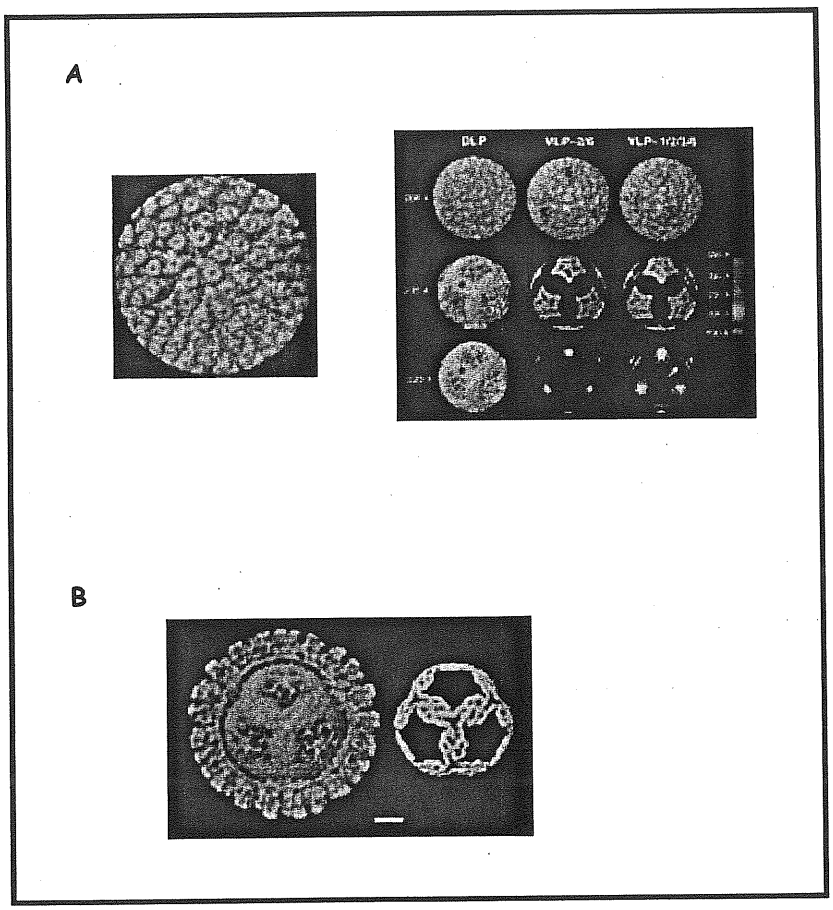

Figure 6: A. Surface representation of the 3-dimensional structure of the DLP at a resolution of 19Å viewed along the icosahedral 3-fold axis. VP6 is stained in blue. The 5-fold positions on one of the icosahedral facets are shown. An original feature is the hole at the centre of each VP6 trimer. **B.** Structural organisation of RNA inside rotavirus. Left, cutaway from the 19Å structure of the rotavirus DLP, showing internal organisation. VP2 is represented in green and VP6 in blue. VP1-VP3 complex at the 5-fold axes is shown in red. Portions of VP2 at the 5-fold axis are shown in green. Right, the icosahedral shell of the ordered RNA (yellow), showed separately for clarity. Each strand is about 20 Å in diameter. The strands are separated from each other by 25-30 Å. Scale bar, 100Å. These figures are modified from [159].

Baculovirus-expressed viral like particles (VLP) were very important in obtaining the first three-dimensional organisation of the *Reoviridae* genome [154]. Different types of recombinant VLP were compared by cryoelectron microscopy and native transcriptionally active DLP were purified from viral infected cells. Interestingly, VLP-DLP comparative structural analysis also helped in the localisation of the virus transcription complex. Viral dsRNA forms a dodecahedral structure in which the RNA double helices appear as a tube of 20Å diameter, interacting closely with the inner capsid layer (VP2) and packed around the enzyme complex (Figure 6). The extensive ordering genome may be critical for the endogenous transcriptase activity, perhaps facilitating a

RNA movement through the enzyme complex, driving the continuous exit of newly synthesized mRNA. Although it is not possible to determine the position of the different dsRNA segments, it is possible to hypothesise that a substantial portion of each genome fragment could interact with the VP1-VP3 complex.

Rotavirus genome

Rotavirus genome consists of 11 segments of base paired double stranded RNA with a size range of 0.6 to 3.3 Kbp. Rotavirus dsRNA genes could be purified and resolved according to their length on 10% polyacrilamide gels, resolving rotavirus genome fragments into 11 bands (Figure 2). Deproteinased rotavirus dsRNA genome is not infectious, reflecting the need viral RNA polymerase in genome transcription and replication. The newly replicated dsRNA genome is formed within nascent subviral particles in viroplasms, and free dsRNA or free ssRNA with negative polarity were never found in infected cells [55].

The genome sequences of the different rotavirus strains show general features about the structure of each genome segment, and are A+U rich (58-67%) (Figure 7 and 8). Peculiarities in rotavirus genome are also common to other members of Reoviridae family (reovirus, cytoplasmic polyhedrosis virus, orbivirus) and to other virus families with segmented genome (*Ortomyxoviradae*, *Arenaviridae*, *Bunyaviridae*) as the capped structures and 3' conserved sequences [55].

Segment	Base pairs	G + C (%)	Noncoding sequences 5'	Noncoding sequences 3'	First AUG is a favored sequence for initiation	Additional long ORF	Amino acids
1	3,302	34.6	18	17	Yes	No	1,088
2	2,690	32.9	16	28	Yes	No	881
3	2,591	28.9	49	35	Yes	No	835
4	2,362	34.7	9	22	Yes	No	776
5	1,581	33.9	32	73	Yes	No	491
6	1,356	38.6	23	139	Yes	No	397
7	1,104	33.5	25	131	No	Yes (2-i)	315 (312,306)
8	1,059	35.5	46	59	Yes	No	317
9	1,062	35.9	48	33	No	Yes (1-i)	326 (297)
10	751	40.2	41	182	Yes	Yes (2-i)	175
11	667	38.6	21	49	Yes	Yes (1-o)	198 (92)

Figure 7: Nucleotide sequences of rotavirus genome segments.

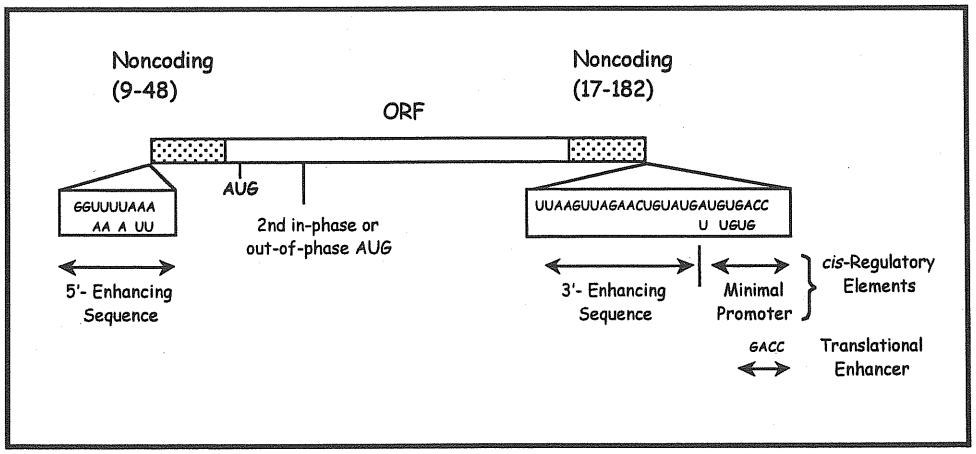

Figure 8: Major feature of rotavirus gene structure. The prototype SA11 genome segments range size from 667 bp (segment 11) to 3302 bp (segment 1). The bottom arrows shows *cis*-regulatory elements of rotavirus mRNA required for replication of transcripts assayed in a cell-free replication system [146, 192]. The 5'- and 3'-noncoding regions at the termini of the mRNA are predicted to interact to form a panhandle structure [143, 146]. The penultimate 5'-GACC is a translation enhancer [55].

Rotavirus dsRNA segments contain cap structures at the 5' end of the positive strand RNA [55], while lacking in the 3'-end polyadenilation signals [120]. Each (+) RNA segment starts with a 5'-guanidine followed by a set of conserved sequences that are part of the 5' non-coding sequences (called untranslated region, UTR). Usually, the 5' UTR is followed by a unique open reading frame (ORF), coding for a single protein product ending with the stop codon and then another conserved untranslated region at 3' termini (3' UTR) with two terminal cytidine. Each fragment of the rotavirus genome features different lengths of the 5'- and 3'-UTR. Although some of the genes possess additional in-phase (genes 7, 9 and 10) or out-of-phase ORFs (gene 11), current evidence indicates that they are monocystronic, except possibly for genes 9 [27] and 11 [119]. Gene transcription starts under strong initiation codon based on Kozak's rules. The strong conservation of 5' and 3' terminal UTRs in rotavirus genome segments suggests that they contain signals important for transcription, RNA transportation and replication. Indeed cis-acting signals that promote minus-strand synthesis and translation were found in rotavirus UTRs. Moreover, each mRNA must carry a unique signal in order to be distinguished from the other fragments during the packaging of the viral genome, but so far assembly or encapsidation signals remain unknown [144].

Reassortants and rearrangements

An interesting aspect of segmented viruses in general, and of rotavirus in particular, is the ability of the virions to assemble a precise set of genome segments into newly made virions. Understanding how this occurs remains a major challenge, as this knowledge might lead to the development of reverse genetic systems to study the gene functions of these viruses. In the absence of a reverse genetic system, genetic analysis has exploited the fact that the genome segments can undergo reassortment during mixed infections [55]. The number of packed RNA segments is invariably 11, there seems to be much less constraint on the length of individual RNA fragment assembled into mature virus particles. Genome rearrangements are mechanisms, which generate heterogeneity in RNA segment mobility in cognate RNA fragments, which consist of concatamerisation and duplication with evident changes in gel mobility. Viruses containing rearranged genome fragments are generally not defective either structurally or functionally. Biophysical characterization of viruses with rearranged segments have shown that up to 1800 additional nucleotides can be packaged into particles, without causing detectable changes in particle diameter or in sedimentation values. However, the density of particles containing rearranged genomes may be increased proportionally to the additional base pairs added [121]. These studies indicate that rotavirus have a considerable capacity of packaging additional RNA, although the upper limit is obscure [55].

Virus rearrangements of segments 5, 6, 8, 10 and 11 have been characterised [69]. Modifications in fragment 11 are very frequent, although the reason for this is appearing unknown, there seems that these viruses have some selective advantage [75, 35] (better growth or stability), which made them more easily detectable [117, 118].

Moreover, a series of temperature-sensitive mutants of rotavirus have been characterised [111, 33] and their different infective phenotypes (Figure 9) were important to rotavirus gene assignment and proteins function.

Mutant group	Prototype mutant	ssRNA	dsRNA	Protein	Host shut-off	Mapped to genome segment (protein)
A	tsA (778)	100	75	100	+	4 (VP4)
B	tsB (339)	5	5	25	+	3 (VP3)
C	tsC (606)	5	5	25	+	1 (VP1)
D	tsD (975)	100	100	150	+	NA
E	tsE (400)	<5	<5	20	+	8 (NSP2)
F	tsF (2124)	100	<5	20	-	2 (VP2)
G	tsG (2130)	100	<5	20	-	6 (VP6)
H	tsG (2384)	100	100	10	-	NA
I	tsH(2403)	100	100	100	-	NA
J	tsJ (2131)	100	75	100	+	NA

Data from Gombold et al. [44] and Ramig et al. [40]

Figure 9: Summary of the characteristic of rotavirus temperature sensitive mutants.

Genome segment	Protein product	Nascent polv-peptide (M_r)	Mature protein modified	Location in virus particles	Number of molecules per virion[c]	Function
1	VP1	125,005 (125K)	—	Inner core	ND	RNA polymerase
2	VP2	102,431 (94K)	Cleaved	Inner core	120	RNA binding
3	VP3	98,120 (88K)	—	Inner core	ND	Guanylyltrans-ferase
4	VP4 (VP5* + VP8*)	86,782 (88K)	Cleaved VP5* (529) VP8 (247)[e]	Outer capsid	120	Hemagglutinin, neutralization antigen, pro-tease-enhanced infectivity, viru-lence, putative fusion region, cell attachment
5	NSP1 (NS53)	58,654 (53K)	—	Nonstructural		Slightly basic, zinc finger, RNA binding
6	VP6	44,816 (41K)	—	Inner capsid	780	Hydrophobic, trimer, subgroup antigen
7	NSP3 (NS34)	34,600 (34K)	—	Nonstructural		Slightly acidic, RNA binding
8	NSP2 (NS35)	36,700 (35K)	—	Nonstructural		Basic, RNA binding
9	VP7	37,368 (38K)	Cleaved signal sequence, high mannose clycosylation and trimming	Outer capsid	780	RER integral membrane glyco-protein neutraliza-tion antigen, bicistronic gene , two hydrophobic NH_2-terminal regions
10	NSP4 (NS28)	20,290 (28K)	29K–28K, uncleaved signal sequence, high mannose glycosylation and trimming	Nonstructural		RER transmem-brane glyco-protein, role in morphogenesis, three hydro-phobic NH_2-terminal regions
11	NSP5 (NS26)	21,725 (26K)	28K, phosphorylated *O*-glycosylated	Nonstructural		Slightly basic, rich in serine and threonine, RNA binding

Figure 10: Summary of the characteristics of rotavirus structural (VP) and non-structural (NSP) proteins [1].

Rotavirus structural proteins

VP1, the RNA-dependent RNA polymerase, the core shell protein VP2 and the guanylyltransferase VP3 form the rotavirus open cores involved in the process of RNA transcription and replication.

VP1 (gene 1 in SA11 strain, 125 kDa) functions as both the viral transcriptase and replicase when associated with VP2 [142]. Several findings prove that VP1 is the viral polymerase:

1. VP1 binds nucleotides and specifically the 3' end of viral mRNA [146].
2. UV cross-linking of the photoreactable nucleotide azido-adenosine triphosphate (ATP) to VP1 inhibits transcription mediated by VP1 [186].
3. Temperature-sensitive (tsC) mutants of gene 1 do not synthesise ssRNA at non-permissive temperature [70, 30].
4. VP1 expressed in baculovirus has replication activity only with the co-expression of VP2 [142].

VP1 interacts with VP2 and VP3 forming the viral core particles [200], but in the infected cells VP1 interacts with the NSP2 in a specific structural and functional manner [7, 3].

VP2 (gene 2, 102 kDa) the most abundant protein of the inner core, is the second viral RNA binding protein, but contrary to VP1, its N-terminus binds non specifically ss and dsRNA [19]. The temperature-sensitive mutant of gene 2 (tsF) do not synthesise ss and dsRNA at not permissive temperature and have improper viral capsid assembly [111, 177].

VP3 (gene 3, 98 kDa) is the minor protein component of the core of rotavirions that binds unspecifically only ssRNA. VP3 has a non-specific guanylyltransferase activity [152] that caps viral and non-viral ssRNAs *in vitro*, while not on dsRNA [101]. It has recently been demonstrated that open cores contain methyltransferase activity [31] confirming that VP3 is a multifunctional capping enzyme.

The three major structural proteins VP4, VP6 and VP7 are the most extensively studied proteins because of their important biochemical, antigenic and biological roles in rotavirus replication and assembly.

VP4 (gene 4, ~88 kDa) is an unglycosylated protein of the rotavirus outer layer, present on the surface of the outer layer of mature virions as 60 dimer spikes with lobed heads [197, 157]. The involvement of VP4 in cell binding was suggested by analysis of VP4 containing virus like particles expressed in baculovirus [42]. Both sialic acid-dependent and

independent virus-cell attachments are mediated by VP4 [107, 106] through the recognition of cellular integrin receptor (39). Efficient infectivity of rotavirus in cell culture requires trypsin cleavage of VP4 into 2 fragments, VP8* (28 kDa) and VP5* (60 kDa), respectively the N- and the C-terminal portion of VP4, both of which remain associated with the virion [106, 37]. Specific cleavage site is mapped on the highly conserved Arginine 247 [9, 65] generating the two products (VP5*and VP8*), which remain linked through an intrachain disulphide bond [141]. Other two cleavage sites exist: R241 and R231. The first (R241) does not correlate with the enhancement of rotavirus infectivity and the second (R231) is not conserved in the different virus strains. VP4 cleavage results in the enhancement of viral infectivity, heightening virus penetration into cells, but not cell attachment [62, 37]. Although, the mechanism of activation of rotavirus infectivity is unknown, it has recently been proposed that the trypsin treatment of triple-layer particles (TLP) induces some conformational change on the outer layer proteins mainly ordering the VP4 spikes, otherwise icosahedral disordered in untreated TLP [43]. Virus penetration is probably due to the permeabilization of cell membranes by VP5* [49]. In fact, site-directed mutagenesis of the VP5* hydrophobic domain (VP5*-HD, residues 385 to 404) has demonstrated the importance of this region of VP5* in inducing membrane permeability [52]. VP8* is the viral hemagglutinin [59], whose structure has recently been analysed by X-ray crystallography and NMR spectrometry. It has been found that discovering that VP8* has a β-sandwich fold characteristic of the galectines [51].

The VP4 localisation was monitored at different levels in infected cells:

1. in the space between the periphery of the viroplasms, outside of the ER [131]
2. in the plasma membrane [131]
3. in the cytoplasm with β-tubulin of the microtubule network [131]
4. associated with the glycoprotein VP7 [131]
5. in the peroxisomes driven by a type 1 peroxisomal targeting signals (PTS1) present in the C-terminal of VP4 [128]

A very intriguing fact about VP8* concerns its role as activator of intracellular signalling pathways, which is discussed below, in the specific paragraph "Rotavirus infection and cellular response".

VP4 induces neutralising antibodies and protective immunity in animals and in children. Using a murine rotavirus model, it has been demonstrated that intragastric

administration of VP4-peptide protects subjects from challenge with virulent rotavirus [87], suggesting their potential use in rotavirus vaccine and therapy.

VP6 (gene 6, 45 kDa) is the major structural component of the virions, highly conserved along the different rotavirus strains, and highly hydrophobic and immunogenic. VP6 forms a tight trimer with a central Zn^{2+} ion it composed to has two distinct domains: a distal β-barrel domain and a proximal α-helical domain, which interact with the outer and inner layer of the virion respectively [115] VP6 protein expressed in baculovirus spontaneously forms trimers and was mapped the domains responsible for the trimerisation (residues 246-314) and for the interaction with the other viral structural proteins forming DLP (residues 251-397) [2, 28]. VP6 N-terminus has an amphiphatic α-helix critical for virus assembly. Temperature sensitive mutant virus of VP6 gene (tsG) showed an assembly negative phenotype, indicating that VP6 N-terminus is important in VP6 transporting to viroplasmic inclusions for double layer particles assembly [111]. Removal of VP6 from double layered particles results in a loss of polymerase activity associated to viral transcription [15, 28]. This evidence is supported by the results of further experiment in which mAb direct against VP6 induced a conformational change in VP6 trimer, thus rendering the particle transcriptionally incompetent and preventing the elongation of initiated transcripts [58, 66, 100].

VP7 (gene 9, 37 kDa), the outermost capsid protein, contains up to three N-glycosylation sites, only two of which are apparently used. VP7 protein is synthesised/associated to the rough ER [194] and has a highly conserved signal peptide with a cleavage site at glutamine 51 [172]. VP7 lacks the characteristic sequence KDEL important in confering ER retention, but contains a conserved region with hydrophobic aminoacids (consensus peptide LPXTG), which acts as the signal sequence in directing VP7 to ER [54]. The manner by which VP7 remains in the ER is unresolved. After the insertion into ER membranes, VP7 remains constantly associated with the membrane but with a luminal orientation [91].

As VP4, VP7 is the virus protein responsible for integrin-mediated virus-cell binding, its aminoacidic sequence containig tripeptides sequences (GPR and LDV), which are ligands respectively for integrins αxβ2 and α4β1 [41]. In VP7, these sequences are embedded in a disintegrin-like domain, which also shows sequence similarity to fibronectin and the Tie receptor tyrosine kinase [41].

Protein folding of VP7 requires ATP and cellular factors for correct disulfide bond formation [126]. Structural reconstruction has shown that VP7 is a trimeric complex, which forms oligomers with VP4 and NSP4 in infected cell [110]. Recently, it was also found that the endogenous ER-associated chaperone calnexin interacts with the ER-associated rotavirus proteins, (VP7 and NSP4) [125] thus promoting their folding and assembly during viral infection.

Rotavirus non-structural proteins

Properties of most non-structural proteins are only beginning to be understood. So far, it has been observed that non-structural proteins possess a basic charge; that most of them are able to bind RNA and are present in subviral particles with replicase activity and that ts mutants that map to their segments have RNA replication negative phenotype [30, 78]. These data suggest that the rotavirus non-structural proteins function as part of the replication complex, as chaperones to transport RNAs or proteins to the sites of RNA replication, assembly and packaging.

Rotavirus **NSP1** (gene 5, 55kDa) shows extreme sequence diversity among different serotypes, even among viruses isolated from the same species. The first 150 aa exhibit a greater degree of conservation, including three basic regions and a cystein-rich domain. Studies of this region demonstrate RNA-binding activity of NSP1 (1- 81 aa), specific for elements located at the 5' end of viral mRNAs [143, 84]. The highly conserved cysteine-rich region forms a zinc finger motif (nucleotides 156 to 248) and seems to be essential for NSP1 RNA-binding activity [133, 174]. The carboxyl-terminal 233 aa of NSP1 are not required for rotavirus replication *in vitro* and deletion of the cystein rich region (up to 500 nucleotides) originated non-defective reassortant rotavirus mutant that normally replicates in cultured cells [84, 86] although the plaques were small [174]. In infected cells, NSP1 is present in association with the cytoskeletal matrix, [84] however, a large amount of NSP1 is diffused in the cytosol [85].

NSP2 (gene 8) (35 KDa) is highly conserved in the different rotavirus strains [143] and the region between residues 54 and 87 (see figure 9) shows high similarity with bacterial metallo-proteinases (30% identity, 70% similarity) [16]. NSP2, as NSP5, accumulates in viroplasms [148], characteristic electrodense structures in the cytoplasm of infected cells were also viral structural proteins (VP1, VP2 and VP6) localise cooperationing in the viral replication and packaging. Moreover, NSP2 was found associated to purified immature particles ("sub-viral particles") with replicase activity [139, 81].

Cells infected with NSP2 temperature sensitive mutants (tsE) contain few viroplasms, lack replication intermediates with replicase activity and produce empty virus particles lacking RNA, thus suggesting an essential role in RNA replication process or packaging and may coordinate virion assembly [30]. UV crosslinking of virus infected cells has demonstrated that NSP2 possesses a non specific RNA-binding capacity with a strong preference for ss over dsRNA, for which it display a little affinity [8, 93, 175]. *In vivo* chemical (DSP)-crosslinking of infected cells and specific immunoprecipitation revealed that NSP2 interacts with the viral RNA polymerase VP1 [92 3] suggesting that NSP2 is directly linked to the replicase complex. However, it has been demonstrated in our laboratory that a direct interaction of NSP2 with NSP5 regulates NSP5 phosphorylation state (Figure 14) [3].

Sedimentation analysis of NSP2 expressed in infected cells or in the reticulocyte-dependent translation system, showed that it assembles into multimers of approximately 10S [92]. However, it was shown that the C-terminally His-tagged NSP2 expressed in bacteria (rNSP2) did not exist as an octameric complex. Interestingly, the authors revealed that rNSP2 possessed an associated nucleoside triphosphatase (NTPase) activity *in vitro*. rNSP2 in the presence of Mg^{2+} catalysed the hydrolysis of each of the four NTPs to NDPs with equal efficiency [175]. It has also been demonstrated that NSP2 posses a helix destabilizing activity similar to that of other known viral helicases. rNSP2 disrupts DNA-RNA and RNA-RNA duplexes, while Mg^{2+} or other divalent cations inhibit the activity of NSP2. However under conditions where NSP2 works as an NTPase, its helix-destabilizing activity is less sensitive to the presence of Mg^{2+}, suggesting that in the cellular environment the two activities may function together. The similar helicase activity of σNS of reovirus suggests a common mechanism of unwinding viral m-RNA prior to packaging and concomitant dsRNA synthesis [176].

A recent X-ray structure of rNSP2 showed an octameric organisation, which is functional and with more compact conformation in the binding of RNA and ADP. The NSP2 monomer has two distinct domains: the N-terminal domain has a new (unique) fold and the C-terminal domain resembles the ubiquitous cellular histidine triad (HIT) group of nucleotide hydrolases. This structural similarity suggests that the NTP-binding site is located inside the cleft between the 2 domains. Prominent grooves running diagonally across the doughnut-shaped octamer are probable locations for RNA binding [89].

Moreover, the NSP2 temperature-sensitive (tsE), which is able to form octamers in bacteria caused disruption of the tsE octamers and yielded polydisperse NSP2 aggregates

at non-permissive temperature and exposure to Mg^{2+}. Their biochemical analysis showed the loss of RNA-binding, helix-destabilising and NTPase activity. These results support the idea that NSP2 octamers are the fully functional form of NSP2 to support packaging and/or replication [177].

It was proposed that NSP2 functions as a molecular motor, catalysing the packaging of viral mRNA into core-like replication intermediates through the energy derived from its NTPase activity [168].

NSP3 (gene 7, 36 kDa) is a viral protein with a diffuse cytoplasmic distribution as revealed with immunofluorescence technique of virus infected cell showing no localisation of NSP3 in viroplasms [7]. NSP3 is a rotavirus sequence-specific RNA binding protein that binds specifically the non polyadenylated 3'-end of rotavirus mRNAs [153], on the GACC minimal sequence located from nucleotides 8 to 15 [154, 155]. NSP3 consists of two readily separated domains. The N-terminal domain (1-170 residues) binds the rotavirus mRNA 3' consensus and simultaneously the C-terminal domain (206-315 residues) binds a portion of the host initiator factor eIF4G (the eukaryotic translation initiation factor 4G) a multipurpose adaptor protein responsible for delivering capped and polyadenylated mRNAs to the ribosome [151, 188, 187]. The interaction of NSP3 with eIF4G subunit has been demonstrated using the last C-terminal 107 aminoacids of NSP3 in the two-hybrid system [151]. Moreover, recombinant NSP3 is responsible for translation enhancement of viral mRNA in transfected cells [188]. Interestingly, the amount of cellular poly(A)-binding protein (PABP) present in eIF4G complexes decreases during rotavirus infection [151] suggesting that NSP3 is working as a functional analogue of PABP. Since the binding sites of eIF4G for PABP and NSP3 overlap, and its affinity for NSP3 is stronger than for PABP, it occurs an increased translational activity of the viral mRNA, while translation of host mRNAs is rendered less efficient [124, 188]. Another important aspect of the eIF4G-PABP interaction during the translation process is the mRNA circularisation [191]. The functional consequences of mRNA circularisation for the full complement of cellular mRNAs have not yet been addressed. Circularisation of mRNAs is mediated by eIF4G, which brings together the cap-binding protein eIF4E, the RNA helicase eIF4A (at 5'- m-RNA) and the poly (A)-binding protein (PABP) (at 3'-mRNA). These interactions promote translation initiation via the interaction of the eIF4G with eIF3 on the 43S ribosomal pre-initiation complex. A critical link of such circular mRNAs is evicted *in vitro* from eIF4G by NSP3 via its C-terminus [150], which is thereby able to interfere with 5'-3' circularisation of cellular capped and poly(A) m-RNAs [76, 134], and

suggesting that mRNA circularisation can also occur for viral mRNAs [76]. These results indicate that rotavirus hijacks the cell synthesis machinery and so NSP3 is responsible for the shut-off of cellular protein synthesis [187].

The X-ray structure of the RNA binding domain of NSP3 shows that N-terminal domain forms an unusual, highly asymmetric heart-shaped homodimer with a medial RNA binding cleft. High affinity recognition of the 3' terminal tetrenucleotide of viral RNA is achieved by an extensive network of non-covalent interactions [50].

NSP4 (gene 10, 20 kDa), a non-structural glycosylated protein, is found in the ER membrane. The amino-terminus of NSP4 has a non-cleavable signal sequence to ER retention, connected through a protease-resistant α-helical coiled-coil stem with the C-terminus protruding in the cytoplasm [179]. The cytoplasmic C-terminal domain of NSP4 acts as viral receptor in binding immature double layered viral particles (immature capsid particles, ICP) and to mediate the budding of immature virions into the lumen of the ER [10 11], where the final steps of viral morphogenesis takes place. The structural model of NSP4 cytoplasmic region suggests that four NSP4 molecules tetramerise through their four flexible C-terminal 28 aminoacids projecting from the ER [179], which seems to form a core-metal-binding site (Sr^{2+} and Ca^{2+}) [18, 132].

Purified NSP4 or a peptide of the C-terminal of NSP4 (residues 114 to 135) is sufficient to induce diarrhea in young mice in a age-dependent and dose-dependent manner, thus acting as a viral enterotoxin [12, 201]. Moreover, NSP4 peptide 114-135 is a specific inhibitor of the Na^+-D-glucose symporter (SGLT1), while peptide 464-483 inhibits Na^+-L-leucine symport during rotavirus infection *in vivo* [78]. The enterotoxin effect demonstrated by a cleavage product of NSP4 (112-175) secreted from infected cells in a non-classical way, i.e. through a Golgi apparatus-independent mechanism that involves the microtubule and actin microfilaments network [201]. The NSP4 enterotoxin effect depends on trans-epithelial chloride secretion by calcium-dependent signalling pathway. NSP4 is in fact the only viral protein noted to be responsible for the increase in cytosolic calcium concentration observed in rotavirus-infected cells [182].

Interestingly, glycosylation of NSP4 is required for removal of the transient envelope from ER-budding mature viral particles; in fact treatment of infected cells with tunicamycin maintains enveloped viral particles [130, 147]. Consistently, NSP4 possesses a direct membrane-destabilization activity (MDA, residues 114-135) that may cause ER membrane damage and possibly play a role in the removing of the transient viral envelope

[20, 181]. Recent studies suggest that the membrane-destabilizing and the enterotoxic properties of NSP4 may be mediated by different regions of the polypeptide [20].

NSP5 is the ORF product of gene 11, with 198 aa and a molecular weight around 26 kDa. A second internal ORF (from 52° nt) has been described, encoding for a shorter protein of 92 aa (22kDa) called NSP6 [119, 185]. Up to now very few reports have found a particular role of NSP6 in infected cells, probably due to its low level of expression. Besides, NSP6 is not an ubiquitous protein among different rotavirus strains; in fact it is absent in Rotavirus group C and in some strains of group A, such as porcine OSU strain [75]

The NSP5 aminoacid sequence is highly conserved among the different rotavirus species [103] and no mutants in NSP5 gene were ever found, suggesting that NSP5 may play a fundamental role in rotavirus cycle [28, 64, 73-75]. Some rotavirus strains carry a head-to-tail duplicated gene 11, resulting in an identical NSP5 protein and no effects on virus replication [35, 64, 96]. There is no sequence structure prediction for NSP5 and the sequence characteristics still have unknown significance. As shown in figure 11, NSP5 primary sequence is characterised by an overall high content of serine (21%) and threonine (4.5%), which is higher in the last N-terminal 131 aminoacids (30.5%). Moreover, a "basic-acid-basic domain" (BAB) of highly charged 49 aminoacid residues (60% charged residues), is located between residues 131 and 179, similar to that found in other RNA binding proteins.

```
1/                                          31/4
GGC TTT TAA AGC GCT ACA GTG atg tct ctc agc att gac gta acg agt ctt ccc tca att
                           M   S   L   S   I   D   V   T   S   L   P   S   I

61/14                                       91/24
tct tct agt atc ttt aaa aat gaa tcg tct tct aca acg tca act ctt tct gga aaa tct
S   S   S   I   F   K   N   E   S   S   S   T   T   S   T   L   S   G   K   S

121/34                                     151/44
att ggt agg agt gaa cag tac att tca cca gat gca gaa gca ttc aat aaa tac atg ttg
I   G   R   S   E   Q   Y   I   S   P   D   A   E   A   F   N   K   Y   M   L

181/54                                      211/64
tcg aag tct cca gag gat att GGA CCa tct gat tct gct tca aac gat cca cta acc agc
S   K   S   P   E   D   I   G   P   S   D   S   A   S   N   D   P   L   T   S

241/74                                      271/84
ttt tcg att aga tcg aat gca gtt aag aca aat gca gac gct ggc gtg tct atg gat tca
F   S   I   R   S   N   A   V   K   T   N   A   D   A   G   V   S   M   D   S

301/94                                      331/104
tcg acg caa tca cga cct tca agt aac gtt ggg tgc gat caa gtg gat ttc tcc ctg act
S   T   Q   S   R   P   S   S   N   V   G   C   D   Q   V   D   F   S   L   T

361/114                                     391/124
aaa ggt att aat gtt agt gct aat ctt gat tca tgt gta tca atc tca act gat aat aaa
K   G   I   N   V   S   A   N   L   D   S   C   V   S   I   S   T   D   N   K

421/134                                     451/144
aag gag aaa tcc aag aaa gat aaa agt agg aaa cac tac ccg aga att gaa gca gat tct
K   E   K   S   K   K   D   K   S   R   K   H   Y   P   R   I   E   A   D   S

481/154                                     511/164
gac tct gaa gat tat gtt tta gat gat tca gat agt gat gac ggt aaa tgt aag aat tgt
D   S   E   D   Y   V   L   D   D   S   D   S   D   D   G   K   C   K   N   C

541/174                                     571/184
aaa tat aag aaa aag tac ttc gca cta aga atg agg atg aag caa gtc gca atg caa ttg
K   Y   K   K   K   Y   F   A   L   R   M   R   M   K   Q   V   A   M   Q   L

601/194                                     631
atc gaa gat ttg taa TGT CAA CCT GAG AGC ACA CTA GGG AGC TCC CCA CTC CCG TTT TGT
I   E   D   L   *

661
GAC C
```

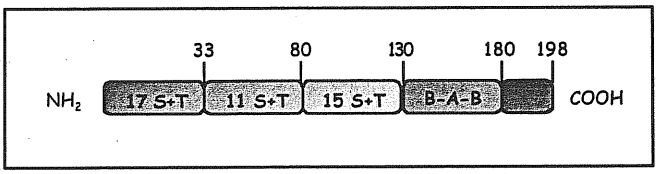

Figure 11: Nucleotide sequence of rotavirus SA11 gene 11, and aminoacid translation of NSP5. Underlined nucleotides represent the gene 11 5' and 3' untranslated region (UTRs). The bold letters indicate putative CK2 phosphorylation sites, while underlined letters PKC phosphorylation sites (results from PROSITE-EMBL). The 4 regions of NSP5 are indicated in different colourful boxes.

Up to now only three rotavirus non-structural proteins (NSP1, NSP2 and NSP3) have been prove to posses RNA binding ability: NSP3 and NSP1 are viral mRNA sequence specific binding proteins, while NSP2 possesses a non-specific RNA binding capacity for ds and ssRNA. Only recently has it been reported that NSP5 has no specific DNA and RNA-binding activity, recognizing ssRNA and dsRNA with similar affinities, thus

proposing a new function of NSP5, as an RNA-binding protein. In so doing NSP5 is involved in cooperating with NSP2 in the destabilization of RNA secondary structures, in the packaging of RNA and/or in the prevention of the interferon-induced dsRNA-dependent activation of the protein kinase PKR [189]. However, this possibility was accurately investigated in our laboratory, and no indications of RNA binding activity of NSP5 were ever found.

NSP5 protein sequence shows an interesting repeated motif (SDSD) in the C-terminal region, where there lie potential substrate sites for casein kinase II (S/TXXD/E) and for protein kinase C (S/TR/K) (figure11) [16, 54]. The last 18 C-terminal aminoacids of NSP5 are highly conserved [117, 119] and seem to be involved in the homomultimerization of NSP5 [185].

NSP5 was originally described with an apparent molecular mass of 26 kDa in SDS-PAGE [114] that further undergoes hyperphosphorylation and cytoplasmatic glycosylation changing its gel mobility [4, 74]. N-acetylglucosamine (NAcGlc) residues are added on serine residues (O-glycosylation) of NSP5 in the cytoplasm of infected cells [74]. NSP5 *in vivo* labelling with 1,6-[^{3}H]-glucosammine, shows that the NSP5 glycosylation occurs mainly on the 26 and 28 kDa species with no glycosylation in the hyperphosphorylated forms [4]. The main post-trascriptional modification of NSP5 is the hyperphosphorylation that produces forms from 28 to 32-34 kDa. NSP5 phosphorylation occurs only on serine and threonine residues and is sensitive to λ-phosphatase treatment (λ-Ppase), converting all the hyperphosphorylated species to an unique band of 26 kDa (figure 12) [4].

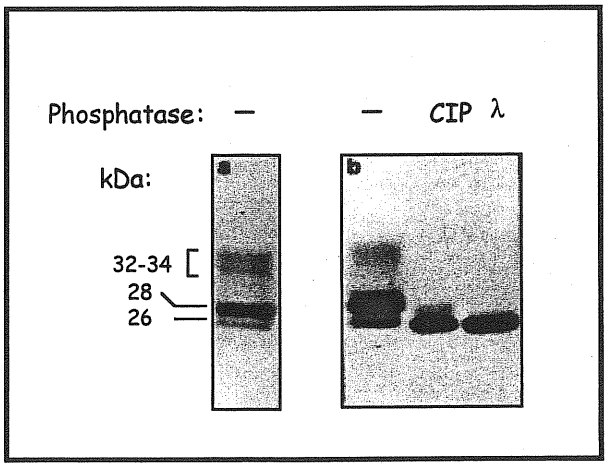

Figure 12: SDS-PAGE analysis of NSP5.
a. Immunoblot analysis of extracts of rotavirus infeceted cells and reacted with anti-NSP5 serum.
b. Immunoprecipitation of NSP5 from virus infected cells labelled with ^{35}S-Met. Calf intestinal phosphatase (CIP) and λ-Ppase treatments are indicated (5).

An important feature of NSP5 raises from different *in vitro* phosphorylation assays. In particular, incubation of NSP5 immunoprecipitated from viral infected cells, with [γ-^{32}P]-ATP showed a strong phosphorylation pattern (λ-Ppase sensitive), demonstrating that the already phosphorylated NSP5 can still be further phosphorylated *in vitro*. Several works based on results obtained with different phosphorylation assays proposed NSP5 as a kinase, capable of auotposphorylation [3, 17, 57, 156, 185]. NSP5 was shown to have a strong capacity of being phosphorylated in absence of any other viral proteins [3, 4] even if no relevant homology was ever found between NSP5 and all protein kinases so far described [3, 4, 17, 57, 156, 185]. NSP5 was also proposed as a new protein belonging to a "non conventional" kinase group [185].

Moreover, other works suggested a crucial role of NSP5 in viral replication and packaging, in cooperation with other viral proteins with which it was found to interact. In fact, NSP5 immunoprecipitated from rotavirus infected cells, [^{35}S]-Met labelled, treated *in vivo* with DSP (thiol-cleavable membrane permeable cross-linker of protein-protein interactions) was shown to specifically interact with VP1 and NSP2 (Figure 13) [3].

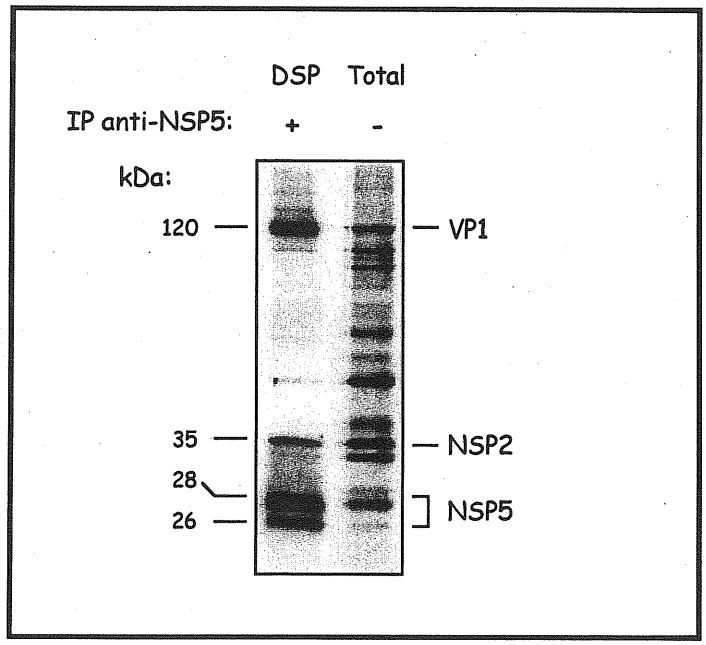

Figure 13: Analysis of DSP-crosslinked extracts from MA104 rotavirus infectred cells. ^{35}S[Met] labelled MA104 SA11 infected cells were DSP crosslinked (indicated) and immunoprecipitated with anti-NSP5 sera and loaded on SDS-PAGE gel.

Since NSP2 is a RNA binding protein, exposure of rotavirus infected cells to UV light was also used to detect if RNA molecules were present in the NSP5/NSP2/VP1 complex. The UV treatment is in fact a technique used mainly to covalently link nucleic acid to proteins (RNA/DNA-binding protein) and not protein to protein. In our laboratory

it was demonstrated that NSP5 immunoprecipitated from virus infected cells treated *in vivo* with UV light, was associated to NSP2 but not to VP1. To evaluate the possibility that RNA could form a "bridge" in the complex, RNase treatment was performed before immunoprecipitation. The result showed that the amount of NSP2 co-precipitated with anti-NSP5 antibodies was not affected. These results thus demonstrated that the interaction between NSP2 and NSP5 via RNA is highly unlike; rather a possible conformational modification/stabilisation of NSP2/viral RNAs by UV treatment could increase its affinity for NSP5 [3].

As mentioned above, an important consequence of the NSP2/NSP5 interaction arises from co-transfection experiments of the two proteins in MA104 cells. NSP2 is able to up-regulate the phosphorylation of NSP5 in the absence of all the other viral proteins (Figure 14). This interaction may cause conformational modifications enhancing the accessibility of NSP5 phosphorylation sites for kinase activities [3]. Based on the proof of this peculiar interaction between NSP5 and NSP2, NSP5 has been largely investigated in finding out possible functions and roles within the virus replicative cycle.

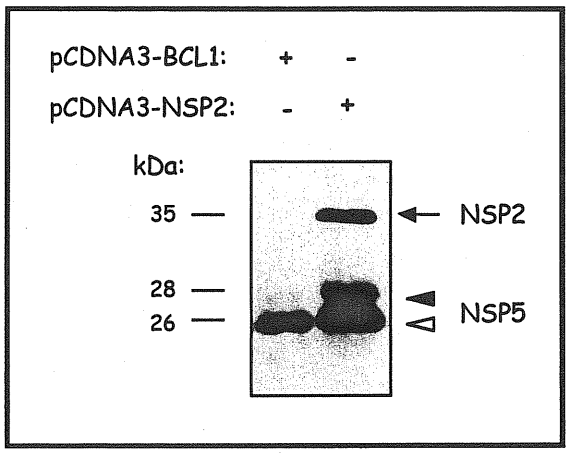

Figure 14: anti-NSP5 and NSP2 Western immunoblotting of MA104 cellular extracts of cotransfected with pCDNA3-NSP5 and an irrelevant protein BCL1 (lane 1) or pCDNA3-NSP5 with pCDNA3-NSP2 (lane 2). Open and closed arrowheads indicate the NSP5 26 kDa and the 28 kDa phosphorylated forms, respectively.

The most intriguing and discussed function of NSP5 is its autophosphorylation activity seen as a potential protein-kinase. The most recent results will be presented in this thesis about the phosphorylation state of NSP5, its potential kinase activity, and its interaction with NSP2.

Rotavirus replication cycle

GENERAL FEATURE OF ROTAVIRUS REPLICATION
1. Cultivation of most virus strains requires the addition of exogenous proteases (as trypsin) to the medium. This ensures activation of viral infectivity by cleaving the outer capsid protein VP4 in to VP5* and VP8* which remain associated to the virus.
2. Replication occurs totally in the cytoplasm of cells.
3. Since cells do not contain RNA-dependent-RNA-polymerases; the virus must supply the necessary enzymes for transcription and replication.
4. Transcripts serve both as mRNAs to produce proteins and as template for the synthesis of the viral negative strand RNAs to generate the dsRNA genome (replication).
5. The dsRNA segments are formed within the nascent subviral particles, and free dsRNA and free negative ssRNA is never found in infected cells.
6. Subviral particles form in association with viroplasms, and later on bud into ER to produce mature particles. During this process particles acquire their outer capsid.
7. Cell lysis releases particles from infected cells grown in monolayer

[55]

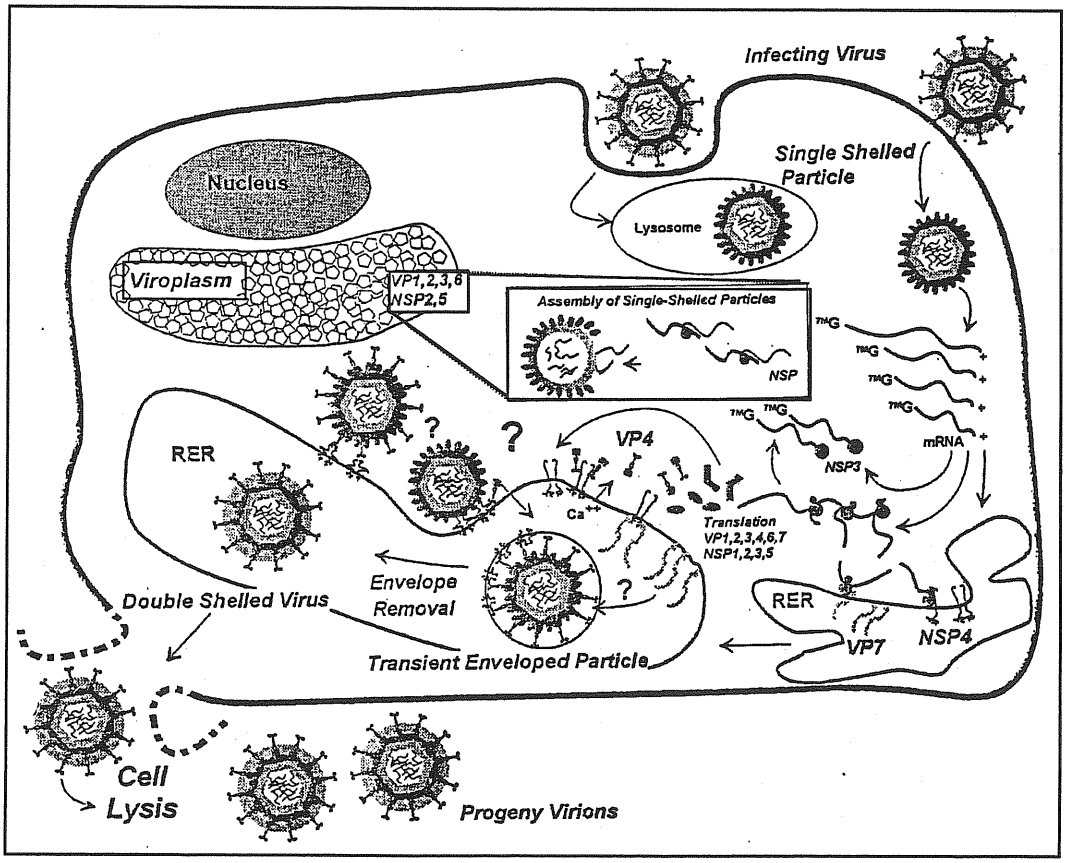

Figure 15: Schematic representation of the replicative cycle of rotavirus [55].

Virus adsorption:

The initial stages of rotavirus binding and entry into cells are complex. They involve a multistep process [123] (multiple receptors my be used sequentially or in a cell-type-specific manner) and are the central focus of much current investigation. Rotaviruses exhibit tissue- and cell-type-specific tropisms consistent with the existence of a specific host-cell-surface receptor(s) that mediates virus attachment or entry. However, the identity of the rotavirus cellular receptor remains controversial. Initially, animal rotaviruses were thought to require the presence of N-acetylneuraminic acid (sialic acid; SA) residues on the cell surface for efficient binding and infectivity. Analysis of a larger number of animal rotavirus strains for their dependence on SA for infectivity showed that most animal rotavirus strains are SA-independent, like human rotaviruses. Therefore, different results might have been obtained, depending on the SA-binding proprieties of the particular virus strain analysed. The binding of SA-dependent and SA-independent rotavirus to glyco-conjugates (glycoproteins, glycolipids and glycosphingolipids) has named several molecules as putative rotavirus receptors. The lack of correlation between ganglioside-binding pattern and host specificity indicates that additional interactions between rotavirus and cell surface are probably needed to confer host specificity.

The rotavirus outer capsid proteins VP4 and VP7 contain three peptidic sequences (DGE, GPR, LDV), which are also present in the sequences of very late antigen 2 VLA-2, (also known as $\alpha 2\beta 1$ integrin), very late antigen 4 (VLA-4; also known as $\alpha 4\beta 1$ integrin) [82-77]. Several studies demonstrate:

- $\alpha 2\beta 1$ and $\alpha 4\beta 1$ integrins expressed in poorly susceptible human erythroleukemic K562 cells, increase binding and infectivity for SA-dependent SA11 strain [82].
- susceptibility to rotavirus infection correlates with the amount of $\alpha 2\beta 1$ integrin expressed on the surface of 6 human cell lines tested [102].
- $\alpha 2\beta 1$ integrin alone is not responsible for entry into cells, but may serve as a post-attachment factor for both SA-dependent or SA-independent rotaviruses or rotavirus-integrin interactions may be required for signalling events necessary to initiate infection or viral entry.

Virus penetration and uncoating:

The VP4 spike protein of the outer layer is the virus attachment protein and trypsin treatment cleaves VP4 into VP5* and VP8*, enhancing the infectivity [106, 105].

Physiologically, proteolitic cleavage of VP4 occurs *in vivo* by the action of pancreatic protease inside the small intestine. The mechanism of rotavirus internalisation (penetration) into cells remains controversial, but two mechanisms have been proposed: direct penetration through the cell membrane and receptor-mediated endocytosis.

1. the direct membrane-penetration model is supported by the observation that the VP5* contains a putative fusion hyrofobic domain (aa 385-404), conserved in all rotavirus strains, which can permeabilse the lipid vesicle *in vitro* suggesting a role of VP5* in the cellular entry of rotavirus [49].

2. the mechanism of receptor-mediated endocytosis does not occur through a pH-dependent fusion mechanism. A recent receptor-mediated endocytosis model proposes that both rotavirus delivery into the cell and activation of transcription are Ca^{2+}-dependent processes [164].

Then, uptake of SA-dependent or SA-independent rotavirus is different on the polarized intestinal cells. SA-independent rotaviruses enter polarized cells by either the apical or basolateral surface of the cells, whereas SA-dependent only infect efficiently by the apical surface cells [36]. These studies show that SA-dependent or SA-independent rotaviruses enter cells through different mechanism and probably use different receptors [36].

Once the virus is internalised, a low cytoplasmic Ca^{2+} concentration induces the loss of the outer shell of the viral capsid in a process called "uncoating" [108]. During this event the VP4-VP7 layer is eliminated producing double layered particles (DLP), which become transcriptionally active only in this stage [38].

Rotavirus infection induces profound alterations in the morphology and biochemistry of the host cell. Rotavirus entry, activation of transcription, cell lyses and particle release are Ca^{2+}-dependent processes [164]. Viral protein synthesis is sufficient to increase the intracellular calcium concentration and there is evidence that the expression of the single rotavirus protein NSP4, directly influences the Ca^{2+} homeostasis [182, 183]. Ca^{2+} plays a role in the replication cycle and pathogenesis of other viruses such as poliovirus, Cocksackie virus, cytomegalovirus, vaccinia and measles virus and HIV [164]. It has been reported that differences in Ca2+ concentration after rotavirus infection provokes also severe structural alterations of the cytoskeleton network, even though not always dependent on Ca^{2+} concentration. Viral infection in cultured cells is associated with microtubule network disassembly (vimentin and tubulin disorganisation), F-actin disassembly and alteration in

intermediate filament (IF) keratins 8 and 18 and phosphoglycoproteins [21, 131, 190]. Rotavirus infection reduces sucrase-isomaltase expression in human intestinal epithelial cells by perturbing protein targeting and organization of microvillar cytoskeleton [107], and also lactase-phlorizin hydrolase, tested in human intestinal epithelial Caco-2 cells, impairing lactose digestion and thereby indirectly participating in the triggering of osmotic diarrhea [113].

Virus transcription:

Genome transcription is a critical stage in the viral life cycle, as the process by which the viral genetic information is presented to the host cell protein synthesis machinery for the production of viral proteins necessary for genome replication and virion assembly. Despite numerous architectural and organizational differences among the families of dsRNA viruses, numerous studies suggest that the basic mechanism of mRNA production may be similar in most, if not all, viruses having dsRNA genomes, and rotavirus was chosen as the transcription model system [100]. The viral transcriptase (VP1) is latent in triple layer particles, it is either activated by the uncoating process after virus cell entry or experimentally by chelating agents (EDTA, EGTA) that destabilise the outer layer. Viruses with dsRNA genomes contain all the necessary enzymatic machinery to synthesize complete mRNA transcripts within the core by the endogenous capsid-bound RNA-dependent RNA polymerase VP1, without virion disassembly. This enzyme directs also the copy of the parental (+) single strand template to regenerate the dsRNA genome (replication) [1, 120].

Interestingly, nucleotidic sequences in the viral mRNA UTR regions were shown to function as translation enhancers [34]. The infected eukaryotic host cells provide all the enzymatic activities needed to generate the 5'-cap required by the eukaryotic translation machinery. Rotavirus mRNA capping is directed by the multifunctional activity of the viral core protein VP3, which was found to possess guanylyltransferase and methyltransferase activities [101, 31].

One of the more striking observations about genome transcription in rotavirus is that it occurs efficiently only when the transcriptionally competent particles (DLP) have a full intact cores surrounded by VP6 [15]. This observation suggests that all of the components of the transcribing particles, including the viral genome, the transcription enzymes, and the viral inner capsid, function together to produce and release mRNA transcripts and that each component has a specific and critical role promoting the efficiency of this process.

Interesting observations confirm that the particles do indeed remain structurally intact during transcription. The structural integrity of the transcribing particles may be required to hold the components of the transcription machinery in their proper arrangements throughout repeated initiation-elongation cycles as well as to enable the efficient release of mRNA transcripts. A series of comparative structural and biochemical studies were carried out to demonstrate the importance of the integrity of the DLP particles during transcription [28].

The precise releasing pathway of mRNA through the VP2 layer is still not known. However, cryoelectron microscopy observations of transcribing viral particles have suggested the precise route that nascent viral mRNA molecules during the exit from viral particle. On the base of these observations, it is thus hypothesised that the viral nascent mRNA is exported through the VP2-VP6 made type I channels located at the ichosaedral fivefold axis of the DLPs [99]. Antibodies directed against specific sites VP6 thus can produce conformational and structural changes in the mRNA-release channels or perhaps can reduce the effective diameter of their opening [100, 58]. These results indicate that the integrity of the capsid is critical for the continuous translocation and efficient transcript elongation of nascent mRNA.

Virus replication and assembly:

Genome replication and formation of new virions occurs in the cytoplasm of infected cells at level of particular structures called viroplasms, highly electrondense aggregates with viral protein-RNA complex that are detected in the cytoplasm from the early stage of infection [29, 6, 148, 173]. During replication, positive single strand viral RNAs (mRNAs) serve as templates for the synthesis of progeny minus strands RNA to yield dsRNA [1, 137]. The dsRNA segments are never detected free in the cytoplasm but are transcribed and replicated within the viral capsid by RNA-dependent RNA polymerase (VP1), remaining immediately incorporated into virions and associated and protected into viral particles. Although not examined directly, it is assumed that rotavirus replication takes place in a conservative manner, thus both parental dsRNA strands remain within uncoated particles. Replication intermediates (RI) can be separated from infected cells through sedimentation on CsCl or sucrose gradients and consist in particles with inner most viral structural proteins (VP1, VP2, VP3, VP6) and of co-purified small amount of some of the NSPs (NSP3, NSP1, NSP2 and NSP5) [139].

Rotavirus RI, purified at the initial stage of virus replication, are associated to the nuclease-sensitive positive ssRNA template and were called sub-viral particles (SVP). Interestingly, these particles could support in vitro, in a cell free system, the synthesis of their own dsRNA genome, mRNAs [145, 137, 140, 81, 52]. *In vitro* genome synthesis by SVP occurs with elongation of nascent minus strands RNA from a positive strand RNA rotavirus used as template and co-purified with SVP. The process permits the formation of fully packaged particles with dsRNA and protected to nuclease digestion [139, 137]. From these experiments it was hypothesised that the replication of rotavirus genome consists in the moving of the RNA templates from outside to inside the replicative active particles.

In addition to RNA polymerase activity, open cores have been shown to contain a nonspecific guanylyltransferase activity that caps viral and nonviral RNAs *in vitro* [138]. Recently it was described that the initiation of the minus strand RNA by the rotavirus RNA polymerase in a cell-free system, involves a novel mechanism of initiation. It consists in the formation of a ternary complex consisting of the viral RNA-dependent RNA polymerase VP1, viral (+) strand RNA, and possibly a 5'-phosphorylated dinucleotide, that is, pGpG or ppGpG [32]. Several data indicate that VP1 in the absence of other viral proteins lacks replicase activity, even if alone is sufficient to bind viral ssRNA [146].

Analysis of different baculovirus expressed VLPs have demonstrated in fact that VP2 is required for the replicative activity and VP1/2 is the minimal replicase particle. Moreover, the role of VP2 in the replicase activity is most likely structural and VP3 is not required for replicase activity of VLPs [200].

In vitro replication reactions, using reporter template, were performed to map cis-acting elements that regulate replication. Templates with internal deletions indicated that no essential replication signals were present within the ORF of the different rotavirus RNA genes and that key elements were present in the 5' and 3' non coding UTRs. Terminal truncations of the reporter RNA showed that the minimum requirement for replication (minimal promoter) of (+) strand was contained in the 3'-terminal 7 nucleotides (nt 1056-1062) (5'-UGUGACC-3') and the conserved 3'-terminal -CC residues of all rotavirus genes are required for efficient replication [192, 193]. Analysis of additional chimeric templates demonstrated that sequences capable of enhancing replication from the minimal promoter were located immediately upstream of the 3' end minimal promoter and at the extreme 5' terminus of the template [192] and in same cases portion of the ORF [144]. The fact that the highly conserved termini differ between the genome segments probably reflects

the existence within them of unique packaging signals that allows the segments to be distinguished from one another during replication. Several authors used the *mfold* program to predict the secondary structures of the rotavirus mRNAs identifying different stem loop structures formed by 5' terminal sequence or by 3' terminal sequence, which can function as specific packaging signalling [63, 144]. However, the regulation of the packaging by which the correct set of 11 genome segments is encapsidated into each virion, remains a mystery and it is likely that some of the viral non-structural proteins may be involved in this process.

Virus release:

After the formation of the DLP particles containing exactly the 11 dsRNA fragments, the nascent viruses translocate into ER lumen likely through a specific interaction between VP6 of the DLP and the cytoplasmic domain of NSP4 [179, 178]. Here occurs the final assembly of the outer layer proteins VP4 and VP7. During this unique morphogenetic process, the viral particles under final maturation are transiently enveloped. In the case of inefficient virus maturation, membrane enveloped double layered virus particles are accumulated in the cytoplasm [173]. Exit of viruses from the ER and assembly with VP4 are less documented and involved a ternary complex containing NSP4, VP7 that were found as integral transmembrane proteins tightly associated with the ER membrane [26]. The localisation of VP4 has been identified in a fine reticular material associated with VP7 and NSP4 at the junction area of virus particles and the ER membrane on the cytoplasmic side of projecting ss (single shelled) particles, suggesting this is the site of assembly of ds (double shelled) particles [151]. Even if other observations demonstrate an extensive co-localization of NSP4, VP7 and VP4 in a ring-like or semicircular structure in close association with viroplasms [71].

Therefore it is difficult to reconciliate the hypothesis of a complete intra-reticular assembly of rotavirus with an exclusive extra-reticular localisation of VP4. Indeed, it has been recently demonstrated that, early after MA104 cell infection, VP4 was not localised within the ER but interacts with rafts on the membrane of the intestinal Caco-2 cells [165]. In this work they proposed for the first time that a non-enveloped virus is able to associate with rafts through a direct interaction with VP4. Based on this data they suggest that the infectious virions are formed at the level of rafts that act as a platform promoting virus assembly.

The release of mature rotaviruses from polarised intestinal cells occurs through a non-conventional vesicular transport mechanism from the ER to the apical plasma membrane that bypass the Golgi complex [90].

Rotavirus infection and cellular response

Several reports described many different interactions between viral and cellular proteins during virus infection, fundamental to drive all the cellular machineries for the interest of the virus to satisfy its aims.

Rotavirus infection determines the shut-off of the cellular protein synthesis [54] and four different cellular proteins were found specifically up regulated after virus infection. Two of them were identified as the ER-associated proteins BiP and endoplasmin, members of a family of glucose-regulated chaperone proteins [196]. Interestingly, the transcription of these genes is regulated directly by rotavirus ER-associated protein NSP4, in viral infected cells as well as in cells transiently expressing NSP4 alone [196]. The mechanism by which these genes are up regulated is not known; however, NSP4 does not seem to be associated with either BiP or endoplasmin. The important role of the correct viral protein glycosylation in the mechanism of viral envelope removing, was also confirmed by treatment of infected cells with tunicamycin, which acts in eukaryotic cells as inhibitor of N-glycosylation. This treatment did not abolish cell lysis but inhibited the liberation of particles [130]. In particular, the specific block of NSP4 glycosylation results in the maintaining of enveloped viral particles.

Recently, a large number of investigations involve the study of activation or inhibition of some cellular signalling pathway, where different cellular kinases are involved. In the context of rotavirus infection the response of enterocytes, its principal target is still largely unknown. However, an interesting research determined that rotavirus infected HT-29 cells express mRNA for several C-C and C-X-C chemokines as well as IFNs, GM-CSF [163] and IL-8 [171-24]. Moreover, rotavirus infection of HT-29 intestinal epithelial cells results in prompt activation of NF-kB (<2 h), STAT1, and ISG F3 (3 h). Genetically inactivated rotavirus and virus-like particles (VP2/4/6/7) assembled from baculovirus-expressed viral proteins also activated NF-kB. Since rotavirus particles, lacking genomic RNA, activate NF-kB suggested that rotavirus proteins direct cellular signalling responses [163]. In another work it has been identified a conserved TNFR-associated factor (TRAF) binding motifs exactly within the rotavirus VP8* (N-terminal of the cleavage product VP4). TRAFs (-1, -2, and -3) are bound by the rhesus rotavirus

VP8* protein through three discrete TRAF binding domains (conserved PXQXT motif). Expression of VP4 or VP8* from rhesus or human rotaviruses induced a 5-7-fold increase in NF-kB activity and synergistically enhanced TRAF2-mediated NF-kB activation. Mutagenesis of VP8* TRAF binding motifs abolished VP8* binding to TRAFs and the ability of the protein to activate NF-kB [98].

These findings demonstrate that rotavirus primarily activates NF-kB through a TRAF2-NF-kB-inducing kinase signalling pathway and that VP4 and VP8* proteins direct pathway activation through interactions with cellular TRAFs. On the contrary, transcriptional responses from AP-1 reporters were inhibited by VP8* and were not activated by rotavirus infection, suggesting the differential regulation of TRAF2 signalling responses by VP8*. Moreover VP8* blocked JNK activation directed by TRAF2 or TRAF5 but had no effect on JNK activation directed by TRAF6 or MEKK1. This establishes that fully cytoplasmic rotaviruses selectively engage signalling pathways, which regulate cellular transcriptional responses. These findings also demonstrate that TRAF2 interactions can disengage JNK signalling from NF-kB activation and thereby provide a new means for TRAF2 interactions to determine pathway-specific responses [98]. As a result, the ability of rotaviruses to selectively activate NF-kB provides a potential role for signalling pathway activation in both host immune response and viral pathogenesis.

Finally, a microarray approach was applied on RRV infected Caco-2 cells. This technique offers a large list of up- and down-regulated genes, which generally can be classified in genes encoding integral membrane proteins, IFN-regulated genes, transcriptional and translational regulators and Ca^{2+} metabolism-related genes. This general analysis provides a large view of the cellular response to rotavirus infection, although further studies are necessary for a better understanding of host-virus interactions [46].

Phosphorylation processes, protein kineses and virus cycles

A delicate balance between protein phosphorylation and dephosphorylation regulates the function of a variety of proteins in the cells; generally protein phosphorylation occurs at short linear sequence motifs that regulate protein activity, localisation and interaction. Moreover, several lines of evidence have suggested that the phosphorylation tightly regulate the function of viral proteins, interacting with host cellular kinases involved in the processes of virus replication and maturation. Some very

important events append commonly after virus infections as chemokines production (e.g. IL-8, IL-1, IL-6 IL-11, RANTES etc.) for activation and recruitment of neutrophils, lymphocytes and macrophages to the infected area, during an inflammatory process. Very interesting examples were already reported about rotavirus infection and the cellular response in the previous chapter "Rotavirus infection and cellular responses" of this thesis, but a larger list of examples are emerging for other viruses. Generally, it is very intriguing to see that different viruses can interfere with cellular processes (pathways) as a survive strategy, facilitating their replication and maturation and silencing possible responses of the host. Processes of phosphorylation/dephosphorylation again finely regulate most of these interactions involving different cellular kinase activated by viral proteins. Several viruses were studied and a very interesting example was reported for respiratory syncytial virus (RSV). The RSV infection inhibits apoptosis of the host cells and the inflammatory cytokine production activating NF-kB through the Phosphatidylinositol 3-Kinase–dependent pathways [180]. However, the effects of NF-kB on apoptosis are not necessarily anti-apoptotic, because NF-kB superfamily's factors are also involved in the activation of apoptotic events in other viral infections such as Reovirus [40]. Moreover, it was described the inhibition of NF-kB activity as a consequence of virus infection. Since NF-kB regulates a large number of genes involved in the inflammatory response, innate immune response, cell proliferation, and apoptosis, some authors proposed for the non-structural protein 5A (NS5A) of hepatitis C virus (HCV) the ability to escape immunosuppression to the virus, leading to persistent infection [136].

Several different examples are emerging about different cellular kinases as protein kinases C (PKC), protein kinase A (PKA), casein kinase 2 (CK2) and different viruses. During our work we focused our attention essentially on CK2, because it appears to be primarily involved in the phosphorylation of NSP5.

CK2 is a Ca2+/phospholipid-independent Serine/Threonine protein kinase able to use ATP (K_m ~10 μM) and GTP (K_m ~20 μM) as phosphor donor as few protein kinases can do. It is a ubiquitous (cytoplasmic and nuclear localisation) eukariotic protein kinase composed of two non-identical catalytic subunits α (42-44kDa) and α' (38 kDa) and two β regulatory subunits (26-41 kDa depending on the cell type), forming a heterotetramer complexes ($\alpha_2\beta_2$ or $\alpha\alpha'\beta_2$). The α subunits are catalytically active by themselves and have an MW of 42-44 kDa (α), while the β subunit (usually 26 kDa in animal cells) is inactive by itself but it stimulates the catalytic activity of 5- to 10- fold. It cause s the

stabilisation of the α and, more important, can change the specificity of its interaction with substrates and inhibitors [149, 5]. CK2 can autophosphorylate at the α subunits. This phosphorylation is very weak when the β subunit is absent. The fact that the β greatly enhances this autophosphorylation might be due to the fact that it causes the monomeric α to enter into the tetrameric form in which two α subunits may phosphorylated each other. CK2 has many nuclear and cytoplasmic substrates and may act to regulate the activity, stability and/or intracellular localisation of many cell growth control proteins. It very well known that CK2 plays important roles in the regulation of DNA replication, transcription and cell proliferation.

- *Enzymes involved in nucleic acid synthesis* (e.g. RNApol I, II DNA ligase, DNA topoisomerase I, II)
- *Transcription factors* (e.g. c-Myc, c-Myb, HPV E7, p53, c-Jun)
- *Signal transduction proteins* (e.g. $p34^{cdc-2}$, insulin receptor, calnexin, caldesmon)
- *Protein synthesis factors*
- *Cytoskeleton and structural proteins* (e.g. β-tubulin, Troponin-T, mysiosin)
- *Othre nuclear and nucleolar proteins* (e.g. nucleolin, HMG1, HMG14)

CK2 is one of oft the most intensively studied Ser/Thr kinases able to phosphorylate a diversity of proteins [5]. However, the regulation of CK2 activity toward its many substrates remains an enigma [45]. It has been reported that CK2 is involved in the phosphorylation of several viral proteins, as reported in the Table 1.

However, in several cases the role of CK2 during the viral cycles has not yet been fully understood, while in some cases phosphorylation involving CK2 have been well demonstrated for viral proteins resulting in modification in activity, localisation and interactions with other proteins or nucleic acid.

The case of the Protease (PR) and Reverse Transcriptase (RT) of HIV-1 are a clear example of protein activation following phosphorylation of both of them by CK2. PR plays an important role in the maturation of HIV-1, cleaving specifically and thus contributing to activate viral proteins such as the RT and other mature structural proteins like p17, p24, p7. In this particular case CK2 plays a role as a host mediator responsible for the stimulation of PR and RT activities in HIV-1-infected cells. In fact chemical inhibition kinase activity or mutation of the residues essential for PR activity lead to the production of immature and non-infectious viral particles, thus indicating that PR is required for viral infectivity [79].

Table 1:

PROTEIN	VIRUS	REFERENCE
Ribonucleotide Reductase (R1)	Herpes simplex virus 1	39
Immediate-Early IE63	Herpes simplex virus 1	22
Glycoprotein (gE-1)	Herpes simplex virus 1	127
Structural proteins of tegument VP1/2, VP13/14, VP22	Herpes simplex virus 1	129
Rev and Vpu	HIV-1	167
Protease (PR)	HIV-1	79
Reverse Transcriptase (RT)	HIV-1	80
Oncoprotein E7	HPV-16	162
Coat Protein (CP)	Potato virus A (PVA)	88
Movement Protein (MP)	Tomato mosaic virus (ToMV)	116
Non-Structural protein (NSs)	Rift Valley Fever Virus	95
Phosphoprotein (P)	Vesicular Syncytial Virus (VSV)	47
Phosphoprotein (P)	Respiratory Syncytial Virus (RSV)	104
Phosphoprotein (P)	Measles Virus	48
Non-structural NS35A	Hepatitis C Virus (HCV)	94
Phosphoprotein (P)	Chandipura Virus (CHP)	161

Another clear example of the role of CK2 for protein activation during viral cycle comes from the Respiratory Syncytial Virus (RSV). The Phosphoprotein (P) of human RSV is an essential component of the viral RNA polymerase, along with the large polymerase (L) and the nucleocapsid (N) protein. Five serines of P are substrate for CK2. Using recombinant viruses carrying P proteins point mutated in either 3 or all the 5 serines, Lu et al. demonstrated that the phosphorylation on P is required for efficient virus replication and budding [104].

Another example of Coat Protein (CP) of Potato Virus A (PVA), whose phosphorylation by CK2 on multiples sites strongly inhibited its RNA binding function, suggest a possible mechanism of cell-to-cell movement of the virus (as Movement Protein MP of Tabacco mosaic virus ToMV) by formation and/or stability of the viral ribonuclear (vRNP) complex. Based on this model, MP as CP are involved in assisting the spread of viral progeny from cell to cell. At middle and late stages of infection, a certain pool of viral RNA becomes excluded from replication through a strong cooperative interaction with CP and then is targeted to structurally modified plasmodesmata. During or after the translocation trough plasmadesmata, the cellular protein kinase CK2 phosphorylates CP,

decreasing its affinity towards viral RNA. Consequently, the translocation-incompetent vRNP complexes dissociate, allowing the viral RNA to start replication in the new infected cell [88].

CK2-dependent phosphorylation essential for protein-protein interaction, it was reported for the interaction of IE63 of HSV-1 with heterogeneous nuclear ribonuclear protein (hnRNP) and p32 using the two-hybrid system. p32 is a cellular protein involved in the splicing process as well as hnRNP. The formation of a complex p32-hnRNP-CK2 requires IE63 protein, which presents CK2 to p32. As a consequence p32 becomes phosphorylated and retained in the cytoplasm thus acting as a disruption element of the splicing complex. In summary IE63 contributes to the cell shutoff by interfering with the splincing mechanism [22].

An interesting research was conducted using two distinct classes of compounds, the flavonoids and the benzothiophenes, as potent inhibitors of HIV-1 transcription in chronically infected cells [23, 44] and suppressors of HIV-1 replication [23]. A report suggested the mechanism of action of these compounds interacting with CK2, demonstrating CK2 enzymatic inhibition as a common biochemical target of chrysin (flavonoid) and benzothiophenes. Further support for such a role come from a third chemically distinct compound, a common CK2 inhibitor 5,6-dichloro-1-β-D-ribofuranosylbensimidazole (DRB), which mimicked the antiviral proprieties of the other two inhibitors. DRB was originally recognised for its ability to inhibit RNA polymerase II-direct transcription, while leaving RNA polymerase-I and -III unaffected, however this effect was later ascribed to the ability of DRB to inhibit CK2 activity [199]. It was proposed that CK2 could be functionally linked, either directly or indirectly, to a component(s) critical for HIV-1 transcription. Although the protein substrates that link CK2 activity specifically to HIV-1 transcription have not been elucidated, the authors indicated that CK2 may regulate this process by phosphoylating of cellular proteins involved in HIV-1 transactivation, which contain multiple CK2 phosphorylation consensus sequences [45].

Aims (1):

1. Characterisation of the *in vivo* phosphorylation state of rotavirus NSP5 and its mutants in transfected cells
2. Analysis of the *in vivo* interaction of NSP2 and NSP5
3. Investigations of the putative autokinase activity of NSP5
4. Mapping of the phosphorylation sites of NSP5
5. Mapping of the regions of NSP5 involved in the activation of a cellular kinase(s) for its own phosphorylation
6. Characterisation of the cellular kinase(s) responsible for the NSP5 phosphorylation: role of casein kinase II (CK2)
7. Effects of specific protein kinase inhibitors in *in vitro* and *in vivo* phosphorylation assays

Materials and Methods (1)

Cells and viruses

MA104 cells are monkey epithelial kidney cells and are the permissive cell line for rotavirus infection.

MA104 cells were routinely cultured in Dulbecco modified Eagle Medium (DMEM) supplemented with 10% fetal calf serum (FCS), 2 mM L-glutamine and 50 µg/ml gentamycin (Gibco Laboratories) (complete medium).

For virus infection or DNA transfection, cell culture was maintained in absence of serum and antibiotics (serum free medium, SF).

Rotavirus simian 11 rotavirus (SA11 strain) was propagated and grown in MA104 cells. Briefly, the inoculum was activated in presence of 10 µg/ml of tripsin for 30 min at 37°C and let to absorb on the cell monolayer for 1 h at 37°C. Cells were thus washed and cultured in SF medium with 10 µg/ml tripsin until complete cytopathic effect (c.p.e.). For current virus propagation, cells were infected with virus at a multiplicity of infection (m.o.i.) of 5-10. Using this virus title the infection was completed usually after 15 h. The infective medium was frozen and thaw 3 times and than centrifuged at 3.000 rpm for 10 minutes to eliminate cellular debris. The inoculum was aliquoted and stored at -80°C.

Stable transfection of MA104 cells

The stable transfection of MA104 cells was performed with 6 µg of pcDNA3 constructs previously linearised by a single digestion (unique site SpeI) to permit the integration in the cellular genome. 3 to 4 h before the experiment fresh medium was added to MA104 cells to ensure are growing exponentially when they receive the DNA. The DNA was transfected using standard Calcium Phosphate technique. The cell were incubated o/n with the precipitates and then washed twice with PBS and maintained in selective medium (complete medium and 500 µg/ml Geneticin G-418 Invitrogen).

Transient transfections of MA104 cells

The cellular transfections were performed with 5 µg of pcDNA3-scFvs (Jetstar® purified) mixed with 7,5 µl of Transfectam® reagent (Promega) in 1 ml of SF. After 5 hours post transfection the cells were washed twice with PBS and incubated for 30 hours in complete medium at 37°C.

For co-transfection experiments, cells were transfected with 8 µg of total amount of DNA. CMV promoter of pEGFPN1 and pcDNA3 constructs drove the protein expression in mammalian cells.

Transient transfections of MA104 cells with Vaccinia virus

Cell transfections were performed in presence of Vaccinia virus infection. Vaccinia strain vTF7.3, recombinant for the T_7 RNA polymerase gene [60, 61], is used to obtain an efficient transient expression of genes under the control of the T_7 promoter. Since Vaccinia virus cycle is cytoplasmatic, exogenous gene transcription and translation are coupled in the cytoplasm of the transfected cells.

Before transfection, cells were infected with Vaccinia virus at multiplicity of 20 pfu/cell in SF. One hour later, the cells were washed and incubated with 1 ml of SF with a mixture of 5 µl of Transfectam® reagent (Promega) and 5 µg of plasmid DNA. The Transfectam-DNA mixture was maintained onto the cells for 16 h in the incubator at 37°C. Cells were then washed two times with PBS and analysed either by

immunoprecipitation or Western immunoblot. For co-transfection experiments, they were transfected 5 μg of total amount of pcDNA vectors.

Cellular lysis

Lysates (corresponding to $0.5x10^5$ cells) were prepared in 100 μl of TNN lysis buffer (100 mM Tris-HCl pH 8; 250 mM NaCl; 0.5% NP40; 1 mM PMSF, 20 Mm NEM and 5% glycerol) at 4°C. Extracts were spun at 10.000 g for 10 min and supernatants were stored at -80°C. Usually, 1/10 of extracts was loaded on SDS-PAGE for Western immunoblot and 1/2 was used for immunoprecipitation.

In vivo ^{32}P labelling

For ^{32}Pi labeling, 5 x 10^5 cells were transfected and 16 h later were washed three time with in phosphate-free minimal essential medium and than starved in 1 ml of the same medium for 30 min. Afterwards cells were incubated for 1 h at 37°C with 30 μl of carrier-free ^{32}Pi (10 mCi/ml; Amersham Pharmacia Biotech) and the cells were lysed as described before.

Chemical DSP-crosslinking

Living ^{35}S-Met labelled cell monolayers were washed twice with washing buffer (PBS-$Ca^{++}Mg^{++}$) and incubated with 600 μM of DSP (dithiobissuccinimidylpropionate) chemical crosslinker (Pierce) in 1.5 ml washing buffer at 4°C for 10 min. Than the crosslinker was eliminated with 3 washings steps for 5 min with washing buffer (50 mM Tris pH 7.5, 150 mM NaCl) and the excess of DSP was quenched. Cellular extracts were thus prepared in TNN lysis buffer with 20 mM iodoacetamide (Sigma) as antioxidant. After the immunoprecipitation, the crosslinked species were analysed in reducing conditions in SDS-PAGE.

Immunoprecipitations

Cellular extracts (unlabelled, ^{35}S, ^{32}P labelled) or GST fusion proteins (tested in the *in vitro* phosphorylation kinase assays) or TNT *in vitro* translated proteins, were diluted up to 100 μl with TNN buffer and incubated from 2 h to o/n at 4°C in presence of 1 μl of specific antisera (anti-NSP5, anti-NSP2 or anti-SV5 antibody) 1 mM PMSF and with 50 μl of 50% Protein-A Sepharose CL-4B beads (Pharmacia). Beads are than washed three times with TNN buffer. The samples were eluted by boiling in 4x Laemmli's sample loading buffer and the supernatants were loaded onto SDS-PAGE. Radioactive ^{35}S-Met gels are incubated with Fluorografy-Amplifyer (Amersham) for 30 min at RT to enhance the intensity of the radioactive signal. Radioactive ^{35}S-Met and ^{32}-P gels are fixed 30 min at RT in the fixing solution (10% acetic acid and 10% ethanol). Autoradiografy is performed at -80°C o/n using X-ray films (Kodak X-OMAT AR).

Western immunoblot analysis

The cellular extracts were resolved on a SDS-PAGE, transferred onto a PVDF membrane (Millipore), previously activated in methanol (2 min at RT), in a Tris-Glycine buffer (Tris 12.12 g/l, glycine 57.04 g/l and 20% methanol). The blockings, antibody incubations and washings of the membranes were performed in PBS 5% milk at RT.

The transferred proteins were reacted with primary sera (Table 1), and with the HRP-conjugated secondary antibodies at dilution suggested by the company.

The immunoreaction was analysed developing the membranes with the ECL-chemioluminescence system (Amersham).

Anti-NSP5 and anti-NSP2 antibodies

Balb/c mice, 6-7 weeks old, and guinea pigs were injected intraperitoneally with50 µg of protein or 100 µg for each boost respectively. Guinea pig and mouse anti-NSP5 and anti-NSP2 polyclonal antisera were obtained using GST fusion proteins. The boosts were repeated three times every 15 days and the animal were bleeded 1 week later. From each blood extraction was recovered 200 µl of serum for the mice and 0,5 ml for the guinea pigs.

Anti-NSP2 and anti-NSP5 sera were tested by Western immunoblot analysis on extracts of infected cells and uninfected cells. Hyperimmune sera were aliquoted and stored at -20°C in presence of 0.02% Sodium Azide (NaN_3).

The sera were used for Western immonoblotting analysis, immunofluorescences, and immunoprecipitations:

Technical application	antigen	animal	dilution
Western immunoblotting	NSP5	Guinea pig	1:3000
Western immunoblotting	NSP2	Guinea pig	1:3000
Western immunoblotting	NSP5	Mouse	1:1000
Western immunoblotting	NSP2	Mouse	1:1000
Immunofluorescence	NSP5	Guinea pig	1:100
Immunofluorescence	NSP2	Guinea pig	1:100
Immunofluorescence	NSP5	Mouse	1:100
Immunofluorescence	NSP2	Mouse	1:100
Immunoprecipitation	NSP5	Guinea pig	1µl in 150
Immunoprecipitation	NSP2	Guinea pig	1 µl in 150

Table 1: List of the sera produced in our laboratory with their sera dilutions for experimental applications.

Immunofluorescence microscopy and immunohistocheimistry

For indirect immunofluorescence microscopy, cells were washed twice with PBS supplemented with Ca^{++}/Mg^{++} (1mM each), fixed with 3,7% paraformaldeide (PFA) for 10 min at RT and washed three times with PBS. The cells were permeabilised with PBS-Triton 0,1% for 5 min at RT and washed again with PBS and prepared for the blocking with PBS-BSA 1% for 30 min at RT. Slides were incubated with the first antibody (1:100) in PBS-1% BSA for 1 h in a moist chamber at RT. After three washing in PBS, a secondary reaction was performed with RITC-conjugated secondary anibody (1:100) in PBS-1%BSA for 1 h. Samples were thus washed and mounted with ProLong mounting medium (Molecular Probes) and analysed either with the Argon-Helium double laser confocal microscopy (Zeiss) or with conventional UV-lamp microscopy (Nikon).

For double immunofluorescence experiments, two distinct rounds of primary antibodies incubation were performed, followed by a single secondary immunoreaction with a mixture of RITC-conjugated goat anti-guinea pig (Sigma) and FITC-conjugated goat anti-mouse (Dako) antibodies (both used at a dilution of 1:50 in PBS-1% BSA).

For immunohystocheimistry, the glasses were fixed with 2% PFA plus 0.2% gluteraldehyde in 0.1M Na-cocodilate buffer pH7.4 and incubated with specific mouse anti-NSP5 or mouse anti-NSP2 antisera. As secondary antibody was used an HRP-conjugated anti-mouse antibody (Dako). The immunodetection was obtained with diaminobenzidine (Sigma) and analysed with the conventional microscopy under transmitted light.

Electron microscopy

The electron microscopy experiments were obtained with the help and the supervision of Piero Giulianini of the University of Trieste.

Morphological electronical analysis of viroplasms or VLS

Cell monolayers were fixed for 30 min with 2% PFA and 2.5% glutaraldehyde in 0.1M cacodylate buffer (pH 7.5), at RT and post-fixed in 1% osmium tetroxide in the same buffer. They were dehydrated in a graded series of ethanol (70%, 96%, 100%) and embedded, via propylene oxide, in Araldite 502/Embed 812 (Electron Microscopy Sciences).

Immunogold labelling of viroplasms

Cells were fixed as before, washed four times with ice-cold PBS and permeabilized with 0.1% Triton X-100 in PBS for 5 minutes, at RT. Free aldehyde groups were then blocked with 0.02% glycine in PBS for 10 min. Cells were then incubated for 20 min with PBS-0.5% BSA (PBSA) containing 20% of normal goat serum. Incubation with the primary antibodies was then performed for 1 h at RT. Cells were washed six times (5 min each) with PBSA, at RT, and incubated for 1 hr at RT with the secondary antibodies (goat anti-mouse and rabbit anti-goat IgG 1nm gold conjugates (British Biocell International), diluted 1:100 in PBSA. After several rounds of PBSA/PBS washings, cells were treated with 1% glutaraldehyde in PBS for 15 minutes, washed again and treated with 0.5% osmium tetroxide in PBS for 15 minutes, at RT. After 3 washes with deionized water (milliQ water), gold-labelled cells were silver enhanced with HQ SilverTM Enhancement Kit (Nanoprobes) for 3 min, at RT and in the dark. Cells were rinsed 3 times with water and dehydrated with ethanol (70, 96 and 100%). Once dehydrated, cells were scraped off the plates, pelleted at 7,000 rpm for 10 min and embedded.

For pre-embedding EM of infected or transfected cells, monolayers were fixed directly on petri dish with EM grade 2% PFA and 0.2% gluteraldehyde in 0.1M Na-cocodilate buffer pH 7.4. After permeabilisation with Triton 0.1% and specific immunostaining, cells were post-fixed in 1% gluteraldehyde and in 05% osmium tetraoxide. Sections were cut using an ultramicrotome (Pabisch Top Ultra 150) and placed on 300 mesh uncoated nickel grids. The latter were stained with 2% aqueous uranyl acetate and 0.5% lead citrate (10 min each). Sections were observed under a Philips EM 208 transmission electron microscope, at 80 kV acceleration voltage. All measurements and statistical analyses were performed with an Image-Pro Plus ver 4.1 software (Media Cybernetics), on digitised images.

Purification of Histidine tagged proteins

Transfected cellular extracts were incubated for 1 h at 4°C with nickel beads, NTA-agarose (Amersham Pharmacia Biotech) equilibrated in 5 volume of loading buffer (20 mM imidazole, 5 mM DTT in PBS). The beads were washed with 10 volumes of washing buffer (35 mM imidazole, 5 mM DTT in PBS), and once with 35 mM imidazole, 5 mM DTT, 400 mM NaCl in PBS. The protein was eluted with 2 volumes of elution buffer (250 mM imidazole, 0.02% sodium azide, 5mM DTT in PBS) and dialysed in PBS containing 5mM DTT. The recovered protein was analysed by Western blotting using guinea pig anti-NSP5 sera.

Reticolocyte dependent transcription and translation

In vitro translated proteins were synthesised using the TNT-T_7 Coupled Reticolocyte Lysate System (Promega). 1 mg of circular template DNA plasmid was transcribed using 15 U T_7 RNA polymerase (Promega) and the transcripts was translates in rabbit reticulocyte lysates in the presence of 4 µl (1000 Ci/mmol) of ^{35}S-Methionine

and incubated at 30°C for 1,5 h. 1/10 of the *in vitro* transcribed polypeptides were immunoprecipitated with specific antibodies and analysed on SDS-PAGE gel.

Phosphatase treatment

Lambda protein phosphatase (λ-Ppase) (New England Biolabs) treatment was performed on the immunoprecipitationed Sepharose beads in a total volume of 40 µl of a reaction buffer (50mM Tris-HCl pH 7.8, 5mM DTT, 6mM $MnCl_2$, 100 µg/ml BSA) in presence of 80 U/µl λ-Ppase (New England Biolabs) and incubated at 30°C for 2h. The reaction was boiled in 4x Laemmly sample buffer and the supernatant loaded on SDS-PAGE.

In vitro *shift-phosphorylation assay*

The *in vitro* shift-phosphorylation assay was perform in a total volume of 50 µl of cellular extracts, containing 10 µl of *in vitro* translated protein, 15 µl of cellular extract, 5 µl of kinase buffer (50 mM Tris-HCl pH 8.0, 1.5 mM spermidine, 5 mM $MgCl_2$, 1 mM DTT and 50% glycerol). The reaction was incubated for 30 min at 37°C, stopped with 5 µl of 50 mM EDTA then immunoprecipitated with anti-NSP5 serum and loaded on 12% SDS-PAGE.

In vitro *phosphorylation assay*

The assay was performed with GST-NSP5 deletion mutants purified by G-Sepharose beads (Pharmacia). 1 µg of the eluted GST-NSP5 mutant was incubated for 25 minutes at 37°C in 50 µl of kinase buffer (Tris-HCl pH 8 5, 1.5 mM sperimidine, 5 mM $MgCl_2$, 1 mM DTT, 5% glycerol) containing 10 µCi of (3000Ci/mmol) [γ–^{32}P] ATP (Amersham). The reactions were stopped with 5 µl of EDTA 50mM, immunoprecipitated with anti- NSP5 serum and loaded a SDS-PAGE gel.

For the Casein kinase 2 (CK2) assay substrate were incubated in a total volume of 50µl of reaction buffer (50mM Hepes pH 7.8, 10mM $MgCl_2$, 150 mM NaCl and 0.5 mM DTT) containing with 5 units of recombinant GST-CKIIα /GST CKβ (26) supplemented with 4 µM ATP and 1 µCi [γ^{32}P]ATP(3000Ci/mol). The reaction was incubated for 25 min at 30°C then stopped with 5 µl of 50 mM EDTA and loaded on SDS-PAGE gel.

E. coli protein expression

GST fusion proteins were produced in *E. coli* DH5α. Cultures were induced with 3 mM IPTG for 3-4 h at 37°C. The bacteria was centrifuged and the pellet washed with ice cold PBS and resuspended in 1,5% laurilsarcosine-PBS and added 0,1µg/µl lysozime, 0,1µg/µl CLAP, 5mM DTT for sonication (6 times, 10s). The supernatant was supplemented with 1% Triton X-100 in PBS and equilibrated slurry beads Glutathione Sepharose 4 Fast Flow (Amersham Pharmacia Biotech). After rolling for 1 h at 4°C, the sample was centrifuged at 1000 x g for 5 min at 4°C and washed three times with 20 volumes of PBS-1%Triton X-100. Elution was performed with 2 volumes of elution buffer (50 mM Tris-HCl pH 8, 150 mM NaCl, 5 mM DTT, 0.1% Triton X-100, 50 mM reduced glutathione).

For a higher concentration of eluted GST fusion protein (approximately 1 µg/µl), the beads were treated with 2 volumes of elution buffer 1 (100 mM Triethylamine pH 12) centrifuged at 1000 x g for 5 min at 4°C and neutralised with 1 volume of elution buffer 2 (1 M Tris-HCl pH 8). The purified proteins were loaded and quantify on SDS-PAGE and analysed by Coomassie staining. The quantification was confirmed with Bradford assay.

Plasmid constructs

NSP5 containing plasmids

NSP5 original cDNA fragment, completed of its proper 5' and 3' ends untranslated regions (UTR), was cloned by Susana Gianbiagi from rotavirus total RNA in pBluescript

(pBlue-NSP5) and further subcloned in a pUC-derivated plasmid containing the T_7 promoter recognition region, to generate pT7+1/OSU11.
pCDNA3-ΔT, pCDNA3-Δ1, pCDNA3-ΔC29, pCDNA3-ΔC48, pCDNA3-Δ4T were obtained by PCR and were prepared by Ivka Afrikanova as described [3].
To obtain the pCDNA3-Δ2, pCDNA3-Δ3, pCDNA3-Δ4, pCDNA3-Δ1/Δ3, NSP5 internal deletion mutants, different PCR amplifications were performed by Elsa Fabbretti as described [54]. pCDNAHis$_6$-Δ1/Δ3 and pCDNA His$_6$-Δ1 were obtained by Catherine Eichwald inserting at the N-terminus the His$_6$ tag with oligonucleotides, 5'-AGCTTGTACCATGGGTCATCACCATCACCATCATGGTAC-3' and 5'-CATGATGGTGATGGTGATGACCCATGGTACA-3', and into HindIII/KpnI pCDNA3-Δ1/Δ3 and pCDNA3-Δ1.
pCDNA His$_6$-Δ1/Δ3(S→A) and the other serine mutants were obtained by double step PCR using internal oligonucleotides (5'-TCAGCATCTGCATCATCTAAAACATAATCTTC-3' and (5'-GATGCTGACGCTGAAGATTATGTTTTAGATGA-3') and cloned KpnI/BamHI in pCDNA(His)$_6$.

p-GEX-2T vectors for GST fusion proteins
To obtain GST-NSP5 fusion protein, BamHI-NSP5 restriction fragment was subcloned from pBlue-NSP5 to p-GEX-2T (pGEX-NSP5).
pGex2T vector was modified in pGex2T-KB changing BamHI site in KpnI and BamHI sites using a linker (5'-GATCGGGTACCAGGCGGATCCG-3').
GST-Δ1, Δ2, -Δ3, -Δ4, -ΔT, -Δ4T, -Δ1/Δ3, -Δ1ΔT, -4T were obtained by cloning the respective PCR fragments obtiained from pCDNA clones in pGex2T-KB (KpnI/BamHI) The oligonucleotides for the amplification were at 5' KpnATG-NSP5 (5'-CGGGGTACCATGTCTCTCAGC-3') and 3' SP6 for Δ2, Δ4. For ΔT, Δ4T were used 5' KpnATG-NSP5 with 3' ΔTBamStop (5'-CGCGGATCCTTAGTACTTTTTCTTA-3') or 3' Δ4TbamStop (5'-CGCGGATCCTTAAGTTGAGATTGAT-3'), respectively. GST-Δ1, -Δ1/Δ3, -4T, -Δ1/Δ3(S→A) were subcloned KpnI/BamHI from pCDNA vectors into pGex2T-KB.
GST-Δ1/ΔT were obtained KpnI/BamHI ffrgment form PCR on pCDNA-Δ1/ΔT with 5' D1 primer (5'-ATTGGTACCATGATTGGTAGGAG-3') and 3' ΔTbamStop.
pGex2T NSP2 was obtained cutting pBLSKS-NSP2 NcoI/XbaI, filled in and subcloned in pGEX2T(SmaI).
pEGFP-N1 vectors for EGFP fusion proteins
To obtain NSP5-EGFP fusion protein, Elsa Fabbretti amplified the coding region of NSP5 from pCDNA3-NSP5 with the oligonucleotides EcoRI-ATG-NSP5 (5'-AAgaattcATGTCTCTCAGCATTGAC-3') and NSP5-PstI-up (5'-GATCCTTActgcagCAAATCTTCGATCAATTGCA-3') to obtain an NSP5 PCR fragment, that was restricted with EcoRI-PstI to lack of the 3'-end stop codon. To frame at the amino terminus NSP5 sequence with EGFP (eukariotic mutagenised version) obtaining pEGFP-NSP5 plasmid, the fragment was thus cloned in the respective polylinker sites of the original pEGFP-N1 vector (Clontech). The pEGFP-Δ2 was obtained by PCR by Catherine Eichwald as described [54].
NSP2 containing plasmids
The complete NSP2 coding region was amplified by Cecilia Miozzo from total SA11 rotavirus genomic RNA and subcloned by Iva Afrikaonova for eukariotic transient expression into pCDNA3 under the T_7 promoter, to generate pCDNA3-NSP2 [3].

Result (1)

In the past few years, the characterization of the rotavirus structural and non-structural proteins had a big improvement. In particular in our laboratory, it was extensively characterised the phosphorylation of NSP5 both *in vivo* and *in vitro*, as well as its interaction with another non-structural viral protein (NSP2) and the functional and biochemical consequences.

Viroplasms in rotavirus infected cells

We started to focus particular attention on the study of NSP5 phosphorylation, and its interaction with NSP2 based on the results of NSP5 co-immunoprecipitation with NSP2 from infected cells, and involvement of NSP2 in the hyperphosphorylation of NSP5 [3, 19]. Early electron microscopy studies demonstrated that both rotavirus non-structural proteins NSP5 and NSP2 localised in viroplasms of infected cells at the early stages of infection [148]. The significance of the presence of NSP5 and NSP2 in viroplasms is not known, although it has been hypothesised that these proteins are involved in RNA stabilisation and in the support of virus packaging and replication. The cross-linking of NSP5 with NSP2 and VP1 in viral infected cells described in our laboratory supports this view [3, 19].

We decided to investigate the distribution of NSP5 in infected cells. Figure 1 shows an immunostaining of rotavirus infected cells. NSP5 localisation in viroplasms was evidenced with a specific anti-NSP5 antibody and indirect immunoperoxidase reaction. Rotavirus viroplasms (arrows) appear as circular cytoplasmic structures with a strong NSP5 staining on the rim, suggesting a large accumulation of this protein on their surface.

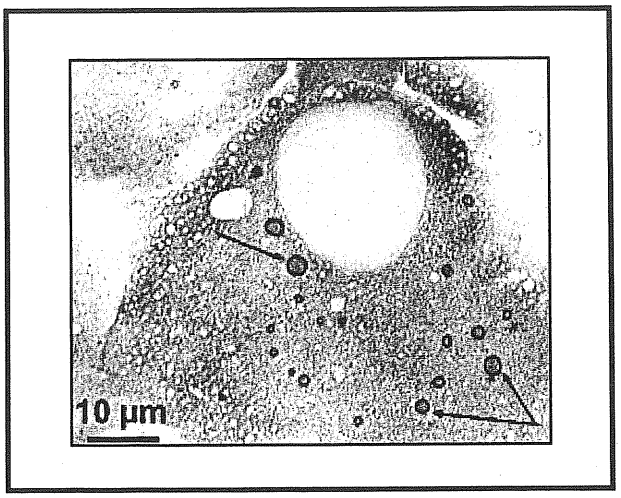

Figure 1: Immunostaining of rotavirus infected cell. Rotavirus viroplasms are immunostained with anti-NSP5 antibody (arrows).

To further investigate the structure and, eventually, the relative spatial ultrastructural localisation of NSP5 and NSP2 in viroplasms, we decided to perform electron microscopy (EM) experiments, in collaboration with Piero Giulanini (Univerity of Trieste). Figure 2 shows an electronic transmission of rotavirus infected cells. The result is an image where the different subcellular compartments can be seen highly contrasted. Rotavirus viroplasms appear as highly electrondense structures (vir) of a variable size from around 300 to 500 nm. Immature transiently enveloped (e) and mature non-enveloped (ne) virions in the lumen of the ER can be also clearly detected.

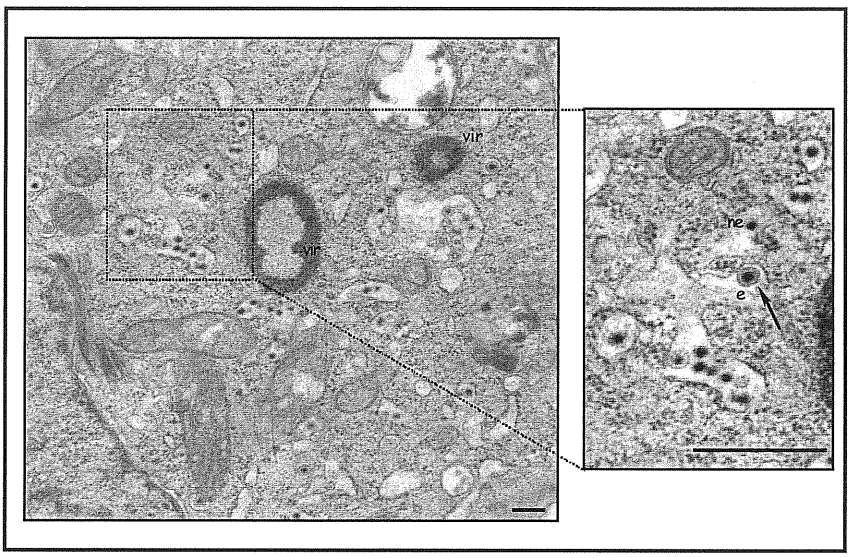

Figure 2: Transmission electron microscopy of a rotavirus infected cell. Viroplasms are highly electrondense structures (vir). Immature enveloped (e) and non enveloped (ne) virions are emerging from the ER. Scale bar, 300 nm.

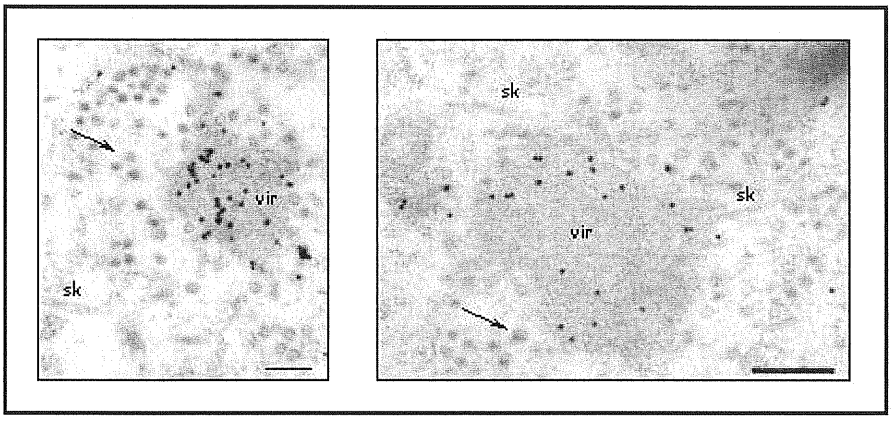

Figure 3: Immunogold NSP5 localisation. Electron anti-NSP5 immunolocalization of rotavirus infected cells. 1 nm-diameter large gold-conjugated secondary anti-mouse antibody revealed specific NSP5 protein accumulation in viroplasms (vir). Interestingly, no NSP5 diffuse background is seen. Interestingly, virions under maturation (arrows) do not show gold labelling. Long cytoskeleton elements could be seen (sk). Scale bar, 300 nm.

To identify the NSP5 localisation within rotavirus viroplasms, we performed immuno-electron microscopy experiments. Rotavirus infected cell monolayers were first reacted with a polyclonal mouse anti-NSP5 antibody and then embedded in the resin (pre-embedding technique). For the secondary immunoreaction, we chose 1 nm-diameter large gold-conjugated anti-mouse antibody, because they are clearly distinguishable from the less defined biological structures. As shown in Figure 3, anti-NSP5 gold immunolabelling identified specifically viroplasms (vir) and no unspecific reaction was found diffused in the cytoplasm or associated to immature viruses (arrows). Interestingly, fine cytoskeleton elements (sk) are also evident that seem to originate from viroplasms.

NSP5 and NSP2 can form "viroplasm-like structures"

Since NSP5 and NSP2 are found in virus infected cells in viroplasms [148], we decided to investigate their distribution in cells co-transfected with both genes, in the absence of any other rotavirus protein and rotavirus replication. Elsa Fabbretti started this work during her PhD project and during the last part I was involved, in particular for the characterisation of the phosphorylation of NSP5.

To achieve this aim, we used the T7 DNA polymerase recombinant vaccinia virus (strain vTF7.3) [60, 61] that represents an efficient cytoplasmatic expression system for T_7-dependent constructs. After vaccinia infection, MA104 cells were transfected with plasmids containing the complete ORF of NSP5 and NSP2 (pCDNA3-NSP5 and pCDNA3-NSP2). We assayed the expression of both expressed NSP5 and NSP2 proteins by immunofluorescence using confocal (laser scanning) light microscopy analysis. We used specific anti-NSP2 (mouse) and anti-NSP5 (guinea pig) antibodies, which were later visualised with green and red fluorescence respectively.

As shown in Figure 4, NSP5 and NSP2 independent expression resulted in homogeneous distribution in the cytoplasm of the transfected cells. However, when both proteins were co-expressed, organisation of discrete structures with regular spherical shape became evident. For their similarity to rotavirus viroplasms (Figure 4), we called them viroplasm-like structures (VLS) [57]. With this confocal analysis we demonstrated that NSP5 and NSP2 truly interact *in vivo* co-localising in VLS.

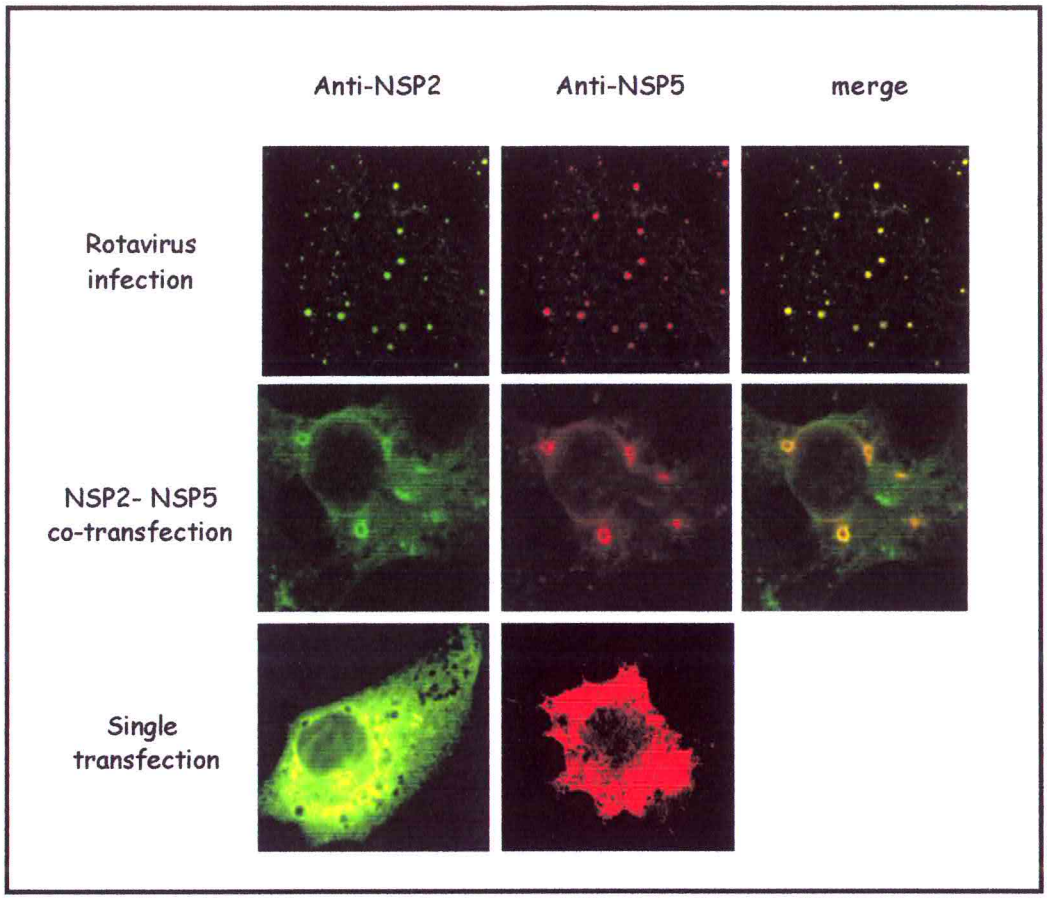

Figure 4: Double immunofluorescence of viroplasms and viroplasm-like structures (VLS). SA11 rotavirus infected cells and NSP5-NSP2 co-expressing cells were subjected to double immunofluorescence to detect VLS. FITC and RITC contemporaneous immunostaining permitted to visualise respectively NSP2 (green) and NSP5 (red) localisation. pCDNA3-NSP2 and pCDNA3-NSP5 single transfected cells showed homogeneous protein cytoplasmatic distribution. The rightmost panel shows the superimposition of the two independently acquired images [57].

VLS obtained by NSP5 and NSP2 co-expression are similar to rotavirus viroplasms, but a difference on protein "density" can be appreciated. While VLS appear as "empty" spheres, viroplasms are complex structures. The presence of the other viral proteins as well as the RNA in virus infected cells, could certainly account for the difference in morphology between viroplasms and VLS. However, this morphology in part could also depend on the conditions used for fixing the samples.

In addition, interesting information resulted from analysis of images obtained by serial confocal sections. Figure 5 represents four different longitudinal panels (collected in 0.5 μm steps) of the same NSP5-NSP2 co-transfected cell. The result highly suggested that VLS have a near spherical shape [57].

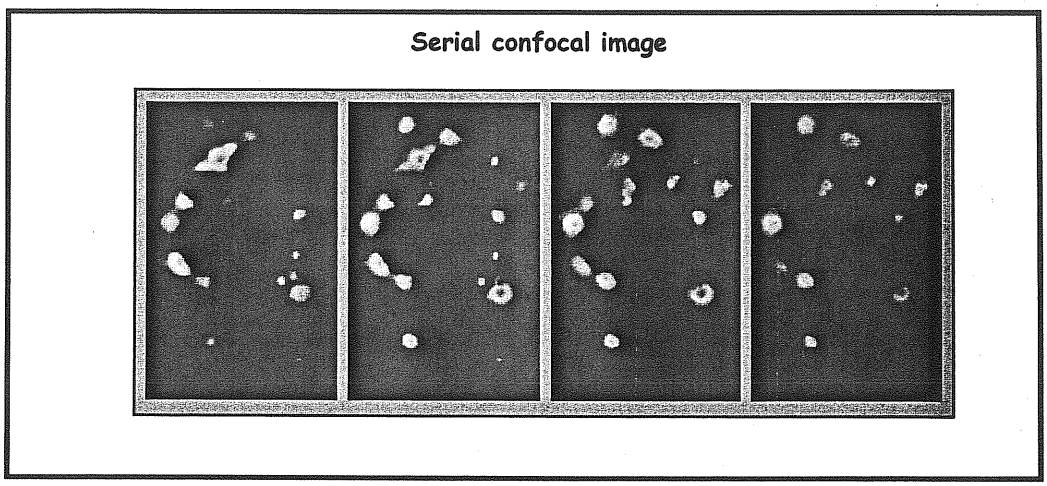

Figure 5: Serial laser confocal images of a NSP2 and NSP5 co-transfected cell. Cells were immunoreacted with anti-NSP5 antibody to detect VLS. Parallel confocal sections were collected in 0.5 mm steps [57].

In vivo phosphorylation state of NSP5 mutants

Since NSP5-NSP2 interaction was well characterised and NSP5 showed a strong phosphorylation, we characterised NSP5 in terms of hyperphosphorylation and we decided to construct a series of NSP5 deletion mutants. NSP5 does not share any homology with other known proteins, so we had no hypothesis on its tertiary structure. We decided to divide it arbitrarily in 4 regions and a short C-terminus sequence of 18 aa long ("tail"), which does not contain any serine or threonine. A schematic representation of wt NSP5 and all the N-, C- and internal deletion mutants obtained, is shown in Figure 6. In wt NSP5, the number of Serine and Threonine residues per domain is indicated, as well as the basic-acid-basic region (BAB), characterised by highly charged aminoacids and the interesting SDS repetitions (Figure 11, page 21). The mutants were named according to the specific regions deleted.

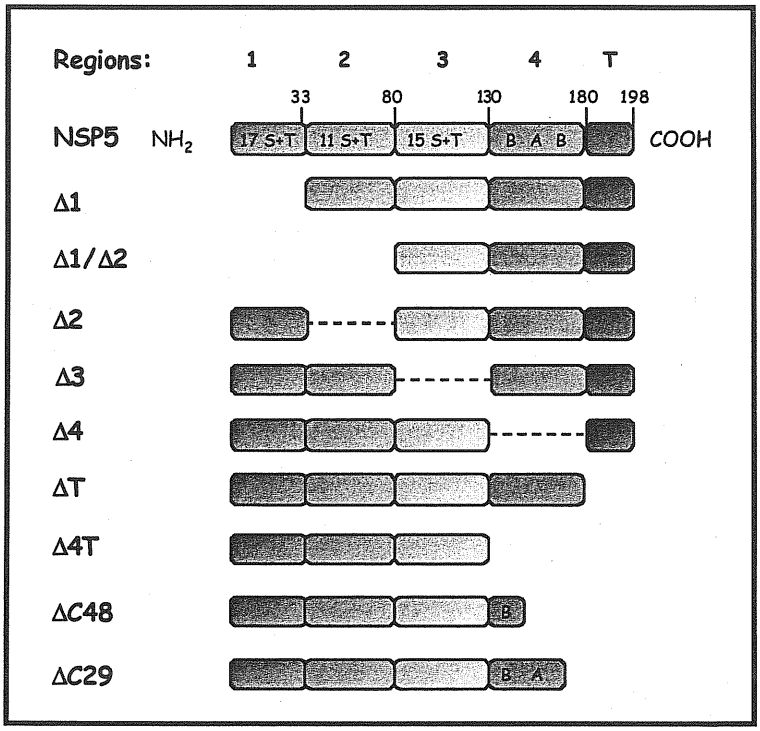

Figure 6: Schematic representation of NSP5 deletion mutants. In each region of wt NSP5 is indicated the relative Ser+Thr content. B-A-B indicates the 49 aa long highly charged (61% of charged residues) basic-acid-basic domain. The last 18 aa represent the "tail" (=T).

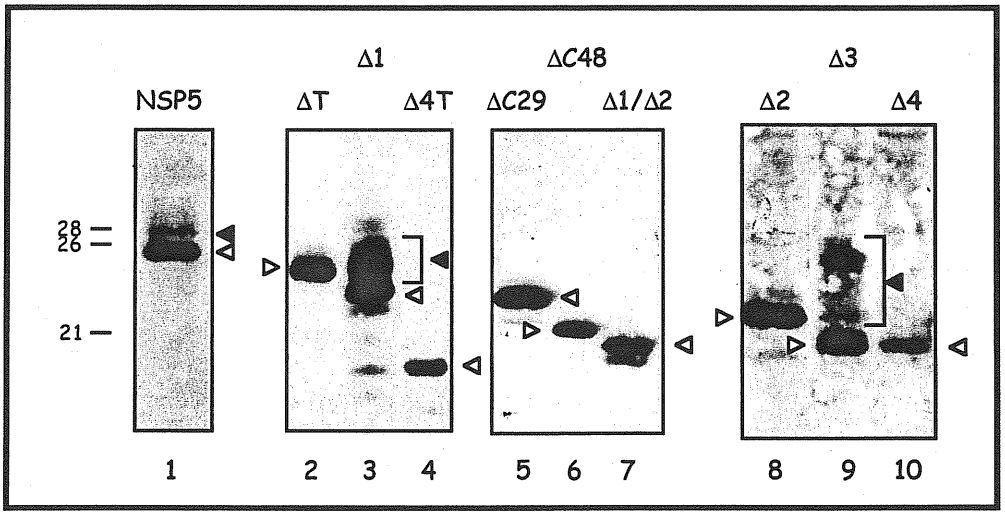

Figure 7: Anti-NSP5 Western immunoblotting of extracts of each independently transfected NSP5 deletion construct. Filled arrowheads indicate λ-Ppase sensitive hyperphosphorylated species with reduced gel mobility. Relative molecular masses in kDa are shown to the left [57].

All mutant constructs were transfected in MA104 cells to investigate their electrophoretic mobility and phosphorylation state in comparison to NSP5. Hyperphosphorylation of wt NSP5, Δ1 and Δ3 can be easily assessed because it largely affects their migration on SDS-PAGE and is λ-Ppase sensitive, even though, we know that NSP5 can also be phosphorylated without changes in mobility [4]. The Western

immunoblotting in Figure 7 shows that all the mutants are well expressed in MA104 cells, and some of them (Δ1 and Δ3) present a stronger shifted mobility than NSP5 wild type. All the species with reduced gel mobility are hyperphosphorylated forms as verified with treatment with λ-Ppase [3, 19]. The phosphorylation shift of NSP5 transiently transfected is quite reduced in comparison with the pattern obtained in rotavirus infected cells (data not shown). This could be due to the absence of the other viral proteins, as NSP2, which can responsible of the hyperphosphorylation of NSP5.

Moreover, all the other deletion mutants did not present any mobility shift as shown in Figure 7 (ΔT, Δ4T, Δ2, Δ4, ΔC29, ΔC48, ΔN80). Nevertheless, we analysed the phosphorylation state of all the NSP5 deletion mutants with transient transfection in MA104 cells and followed by ^{32}Pi *in vivo* labelling and immunoprecipitation (Figure 8). Figure 8 indicates that only Δ1 and Δ3 mutants show spontaneous hyperphosphorylation, detectable in Western immunoblotting (Figure 7, lanes 3 and 9) as well as in $^{32}P_i$ *in vivo* labelling (Figure 8, lanes 2 and 4).

In particular, Δ3 hyperphosphorylation produced an enormous mobility shift from around 21 kDa up to 29-30 kDa (Figure 7 lane 9, and Figure 8 lane 4). All the other N- and C-terminal deletion mutants (ΔT, Δ4T, ΔC29, ΔC48 and ΔN80) did not show any mobility change in SDS-PAGE (Figure 7 lanes 2, 4, 5, 6 and 7), even tough Δ1/Δ2, ΔT and ΔC29 can be labelled *in vivo* with $^{32}P_i$ (Figure 8 lanes 3, 6 and 7). Interestingly, the two internal deletion mutants, Δ2 and Δ4 were not phosphorylated (Figure 7, lanes 8 and 10; Figure 8, lanes 5 and 10). As expected, wt NSP5 phosphorylation was also observed (Figure 8, lane 1).

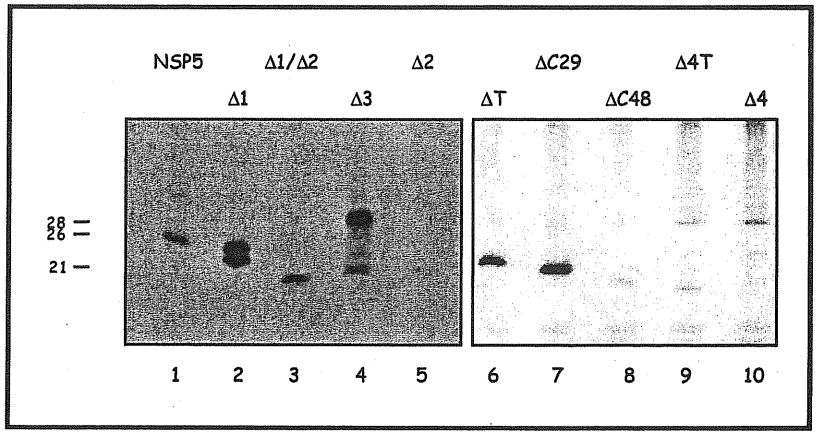

Figure 8: *In vivo* phosphorylation of NSP5 deletion mutants. Immunoprecipitations of cells transfected with the indicated NSP5 deletion mutant constructs and labeled *in vivo* with $^{32}P_i$. Relative molecular masses in kDa are shown to the left [133].

The hyperphosphorylation of the two internal deletion mutants suggests that in wt NSP5 there are structural inhibitory constrains (region 1 and 3) whose elimination allows some conformational modification to better expose the phosphorylation sites. The different NSP5 regions might interact in a such way to maintain a general inhibitory effect, that is removed by NSP2 interaction, as suggested by the enhanced phosphorylation of NSP5 after cross-linking and in co-transfected cells [3, 19]. Our hypothesis was that NSP2 may play a key role in the conformational change of NSP5 during virus infection.

NSP5 mutants and VLS formation

Since NSP5 phosphorylation and VLS formation are both related to the NSP5/NSP2 interaction, we decided to investigate the capacity of the different NSP5 mutants to form VLS *in vivo*. The different NSP5 mutants were thus co-expressed together with NSP2 and tested for their capacity to assemble VLS. Figure 9 shows a series of different anti-NSP5 immunofluorescence assays of cells transfected either with the single NSP5 deletion mutants (left) or co-transfected together with NSP2 (right). Mutants lacking either N-terminal (Δ1) (Figure 9) or C-terminal (ΔT, ΔC29, ΔC48, and Δ4T) portions were completely inactive in forming VLS [57] (data not shown).

Figure 9 presents Δ1 as an example of one of the NSP5 mutants unable to organise VLS. Cells transfected with Δ1 alone (a) or co-transfected together with NSP2 (b), showed the same diffuse localisation of Δ1 protein. Similar results were obtained with mutant ΔN80, ΔT, ΔC29, ΔC48 and Δ4T (not shown). Interestingly, the NSP5 internal deletion mutant, which lacks the third domain (Δ3), was the only one able to produce VLS when co-expressed with NSP2 (d), even though smaller than the ones obtained with wt NSP5. Two other internal deletion mutants, Δ2 and Δ4, lacking respectively the second and the fourth (B-A-B) region, were not sufficient to form VLS in presence of NSP2 (Figure 9f and not shown). Δ4, however, showed a non-homogeneous distribution with irregular spots and short spikes produced even in the absence of NSP2 (not shown). On the other hand, mutant Δ2, even though sensitive to the presence of NSP2, produced irregular structures rather than the spherical VLS (f). Taken together these data indicate that both N- and C-terminal region of NSP5 are required for VLS formation [57].

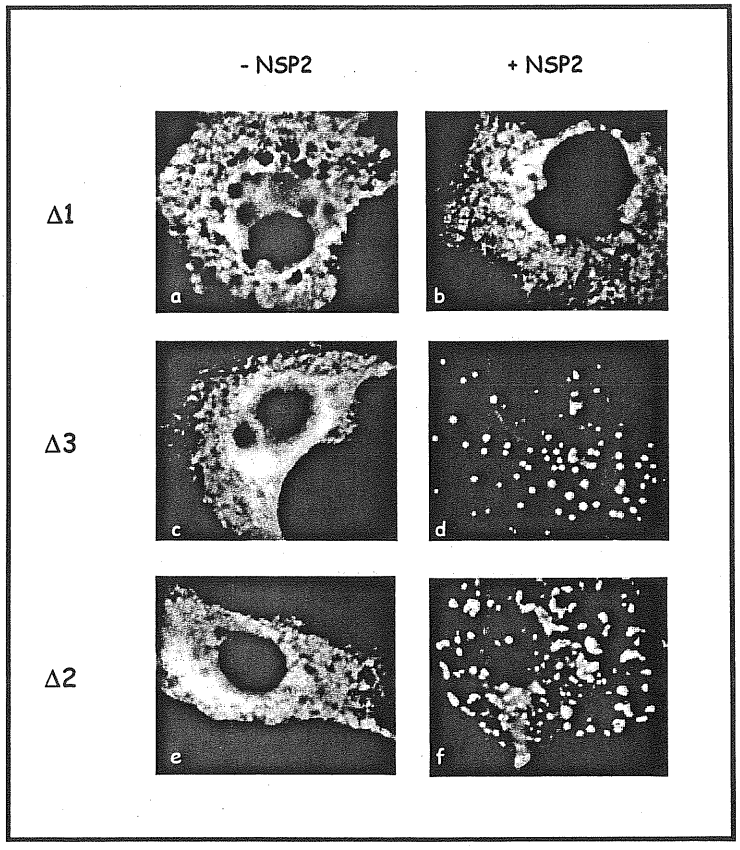

Figure 9: NSP5 mutants and VLS formation. Anti-NSP2 (right) and anti-NSP5 (left) immunofluorescence of cells expressing NSP5 deletion mutants either alone (a, c, e) or in presence of NSP2 (b, d, f). As example of VLS negative phenotype, Δ1 co-expression with NSP2 is shown (b). VLS were detected when Δ3 is co-expressed with NSP2 (d). Peculiar phenotype is observed with mutant Δ2 (f).

New NSP5 domain combination mutants and their characterisation

At this point it was clear that the division of NSP5 in different domains results in differently characteristic phenotypes. To better investigate the role of the NSP5 domains in the phosphorylation, we decided to construct two new mutants indicated in Figure 10. We named them: Δ1/Δ3, Δ1/ΔT, 4T.

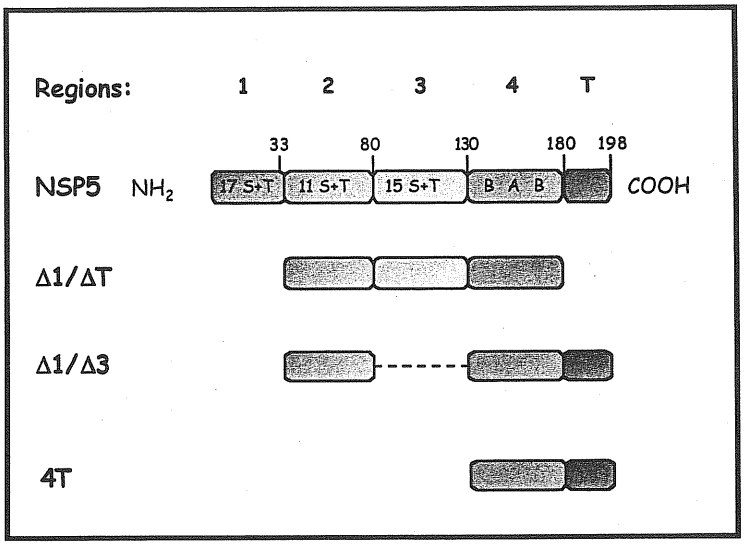

Figure 10: Schematic representation of Δ1/ΔT, Δ1/Δ3, 4T mutants.

A preliminary series of experiments was performed to characterise the new NSP5 deletion mutant Δ1/Δ3, which lacks the two regions identified as internal inhibitors. Interestingly, analysis of the *in vivo* expression of Δ1/Δ3 by Western immunoblotting (Figure 11A) and by *in vivo* ^{32}Pi-labelling (Figure 11B) showed typical pattern of hyperphosphorylation, as demonstrated by the sensitivity to λ-Ppase (Figure 11A). Mutants Δ1/ΔT and 4T did not show any hyperphosphorylation (data not shown).

These results indicated that Δ1/Δ3 is the minimal NSP5 deletion mutants able to maintain a hyperphosphorylated pattern similarly to NSP5, suggesting that the fourth region play a relevant role in the process leading to its own phosphorylation.

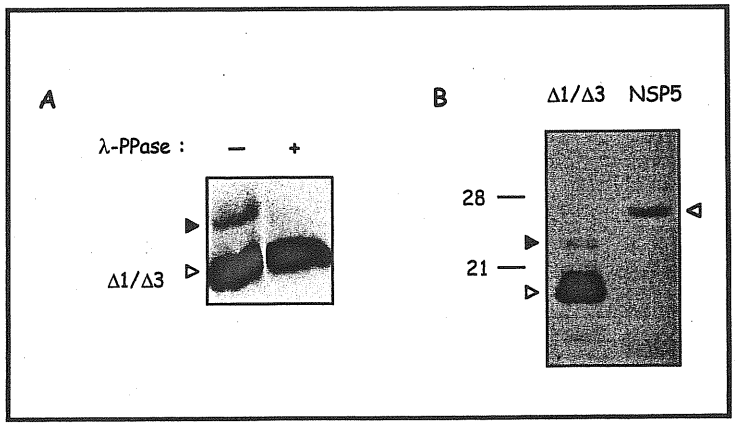

Figure 11: Characterisation of Δ1/Δ3 *in vivo*. **A)** Anti-NSP5 Western immunoblotting of Δ1/Δ3 transfected cells. **B)** *In vivo* ^{32}Pi-labeling of Δ1/Δ3 transfected cells; as control wt NSP5 protein was also ^{32}Pi-labeled. Filled arrowheads indicate λ-Ppase sensitive hyperphosphorylated species with reduced gel mobility [54].

NSP5 activates an NSP5-specific kinase(s)

It has been previously suggested by us and other authors [17, 176, 185] that NSP5 has an "autophosphorylation" activity. In order to study the putative NSP5 kinase activity, we developed an *in vitro* phosphorylation assay, which allowed us to obtain the characteristic PAGE mobility shift of hyperphosphorylated NSP5. This study of my PhD was a shared project with the PhD student Catherine Eichwald.

The *in vitro* hyper-phosphorylation assay consisted in the transfection of NSP5 deletion mutants in MA104 cells and tested their cellular extracts for eventual kinase activity *in vitro* on specific substrates, as the *in vitro* synthesised ^{35}S-Met-labelled NSP5 deletion mutants (TNT). The substrates were immunoprecipitated and electrophoresed on SDS-PAGE gel. The kinase activity of the tranfected cellular extracts were indicated on he autoradiography by mobility shifts of the substrates due to their phosphorylation.

We selected as a substrate in the assay the *in vitro* translated NSP5 mutant Δ1 (Figure 6) for the following reasons: i) it appears as a single not hyperphosphorylated band, of around 20 kDa in SDS-PAGE (Figure 12A, lane 1), ii) it becomes hyperphosphorylated when expressed in MA104 transfected cells (Figure 7 and 8) in similar way of wild type NSP5 in infected cells [3, 57] and iii) it is the most efficiently phosphorylated of all the mutants tested (see Table 1). In this assay the kinase activity of the cellular extracts transfected with NSP5 mutants is determined as the capability to instruct PAGE mobility shift of the [^{35}S] labelled Δ1 protein.

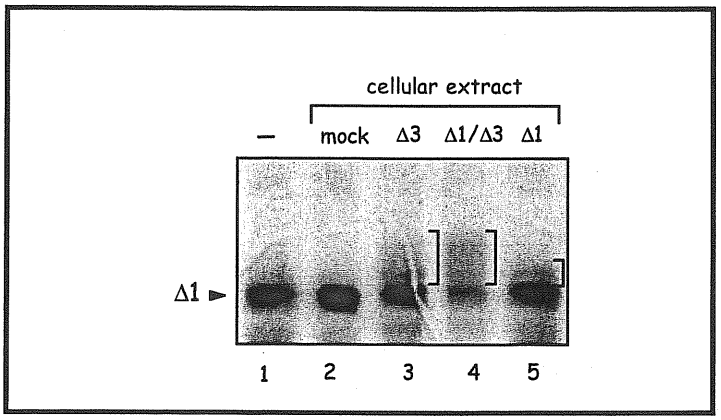

Figure 12: *In vitro* shift-phosphorylation assay. Analysis of immunoprecipitates of the *in vitro* translated, [^{35}S]-methionine labelled mutant Δ1, incubated with cellular extracts from cells transfected with the indicated mutants [54].

Table 1:

Protein	Activity of cellular extracts [a]	Activity as substrate [b]
NSP5	–	+/-
Δ1	+	+
Δ2	–	+
Δ3	+	+
Δ4	–	–
ΔT	–	–
Δ4T	n.d.	–
4T	–	–
Δ1/Δ3	+	–
Δ1/Δ3 (S→A)	+	–

a: using as substrate Δ1 mutant
b: Δ1/Δ3 cellular extract used as a source of cellular kinase(s)
+: present; -:absent; n.d.: no determined

We tested several cellular extracts derived from either untransfected cells or from cells transfected with NSP5 or NSP5 deletion mutants. Extracts containing mutant Δ1, Δ3 and Δ1/Δ3, but not extracts from mock-transfected cells had phosphorylation activity (Figure 12). Treatment with λ-Ppase confirmed that PAGE mobility changes corresponded to hyperphosphorylated forms of the substrate (data not shown). In agreement with this result, these three mutants are hyperphosphorylated *in vivo* in transfected cells (Figure 8 and 11). Conversely, extracts from cells transfected with the wild type NSP5 showed a marginal effect (Table I), consistent with its low phosphorylation in transfected cells, in the absence of viral replication [3, 57].

Interestingly, extracts transfected with the two mutants that lack region 3 (Δ3 and Δ1/Δ3), showed the highest phosphorylation activities. Extracts from cells transfected with other mutants, such as Δ2, Δ4 or ΔT did not show significant activity. Table I reports the activities of all mutants tested. In all cases, similar amounts of transfected proteins were used, as judged by Western blotting analysis. From these results it appears that domains 2, 4 and T are absolutely required for extracts' activities. Other mutants were also tested as substrates in this assay (Table 1).

The phosphorylated shifted forms of Δ1 were only achieved with extracts from cells transfected with NSP5 mutants that showed hyperphosphorylation *in vivo*. This result suggested that, either the activity resides in the transfected protein itself or, alternatively, the transfected protein induces or activates an otherwise inactive cellular kinase(s). To discriminate between these two hypotheses, a His_6 tagged version of Δ1/Δ3 protein was purified from transfected cellular extracts on a nickel column. The purified His_6–Δ1/Δ3 and all the different fractions were analysed by Western blotting (Figure 13).

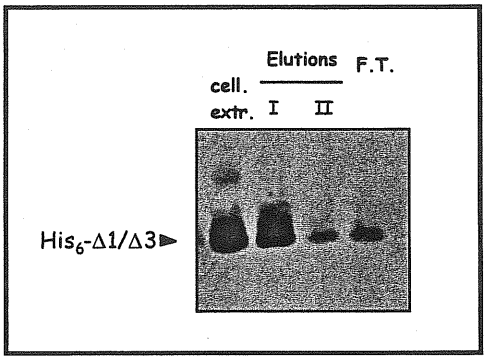

Figure 13: Western immunoblotting, using anti-NSP5 serum, of different fractions of the purification of His_6-Δ1/Δ3 from transfected cellular extracts. Cellular extract corresponds to the input, while flow trough (F.T.) is the fraction not retained to the nickel column.

Purified His_6–Δ1/Δ3 was used in the *in vitro* phosphorylation assay as well as the cellular extract containing His_6–Δ1/Δ3 and the results are shown in Figure 14. The His_6–Δ1/Δ3 transfected cellular extract had phosphorylation activity (lane 4), while the purified protein did not (lane 6).

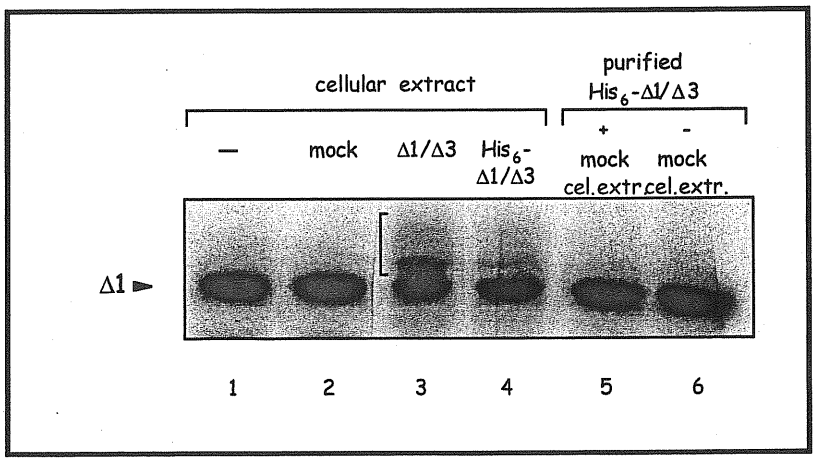

Figure 14: *In vitro* shift-phosphorylation assay. His_6-Δ1/Δ3 was purified with nickel column. Arrowheads indicate the unphosphorylated Δ1 substrate and vertical brackets the position of mobility shifted phosphorylated forms [54].

From these results we hypothesised the possibility that the transfected NSP5 mutant can form a complex with a cellular kinase, thus activating its own phosphorylation. However, this is unlikely since addition of purified His_6–Δ1/Δ3 to a mock cellular extract did not reconstitute the phosphorylation activity of the cellular extract on the substrate Δ1 (Figure 14, lane 5). This suggests that expression of the protein is necessary to promote activation of the cellular kinase(s). Nevertheless, hyperphosphorylation of NSP5 in virus-infected cells occurs also in the presence of Actinomycin D, an inhibitor of cellular transcription, as demonstrated by Catherine Eichwald. This indicates that transcriptions of new cellular genes are not required for the emergence of the kinase(s) activity (data not shown). In conclusion, phosphorylation and capacity to activate the cellular kinase(s) appear to be distinct characteristics of NSP5. Indeed, mutation of four serine residues within domain 4 [mutant Δ1/Δ3 (S→A)], that completely abolished phosphorylation of the protein expressed *in vivo* (see below), did not affect its ability to activate the cellular kinase(s) (Table 1 and see below).

Mapping phosphorylation sites of NSP5

Since Δ1/Δ3 continued to show the interesting pattern of phosphorylation characteristic of NSP5, we wanted to map the phosphorylation sites on the recombinant protein. We constructed a variety of NSP5 deletion mutants, as GST fusion proteins. None of these proteins produced in bacteria showed any phosphorylation activity (Figure 15), neither when they were incubated with purified His_6–Δ1/Δ3 from transfected cells (data not shown). These evidences strengthen the idea that NSP5 has not kinase activity. However, some of the mutants, as well as wild type NSP5, served as substrates when incubated *in vitro* with a cellular extract from Δ1/Δ3 transfected cells, as a source of enzyme. As shown in Figure 15 only mutants containing region 4 were phosphorylated indicating that most of the phosphorylation occurs within this domain, and suggesting that *in vivo* phosphorylation sites could reside in this region.

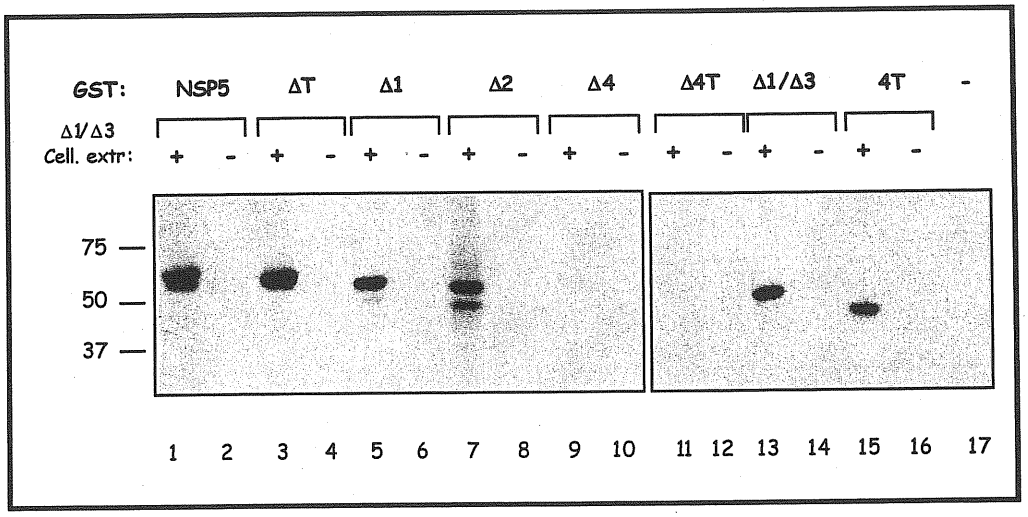

Figure 15: Mapping phosphorylation sites of NSP5. SDS-PAGE analysis of *in vitro* phosphorylated ([γ-^{32}P]ATP) GST-NSP5 mutant proteins by Δ1/Δ3 transfected cellular extract. Lane 5: GST negative control [54].

We previously reported that NSP5 phosphorylation takes place in Ser and Thr residues [4]. For a further characterisation of phosphorylation sites we mutated to alanine four serines (Ser^{153}, Ser^{155}, Ser^{163} and Ser^{165}) within region 4 in mutant Δ1/Δ3, present in a particular acidic amino acid context (ADSDSEDYVLDDSDSDDG) (Figure 16A). This new mutant was expressed as GST fusion protein [GST-Δ1/Δ3(S→A)] and tested for its ability to be phosphorylated *in vitro* by Δ1/Δ3 cellular extracts (Figure 16B). The point mutations on the 4 four serine reduced dramatically the phosphorylation signal of GST-Δ1/Δ3(S→A) in comparison of the wt GST–Δ1/Δ3 (Figure 16B).

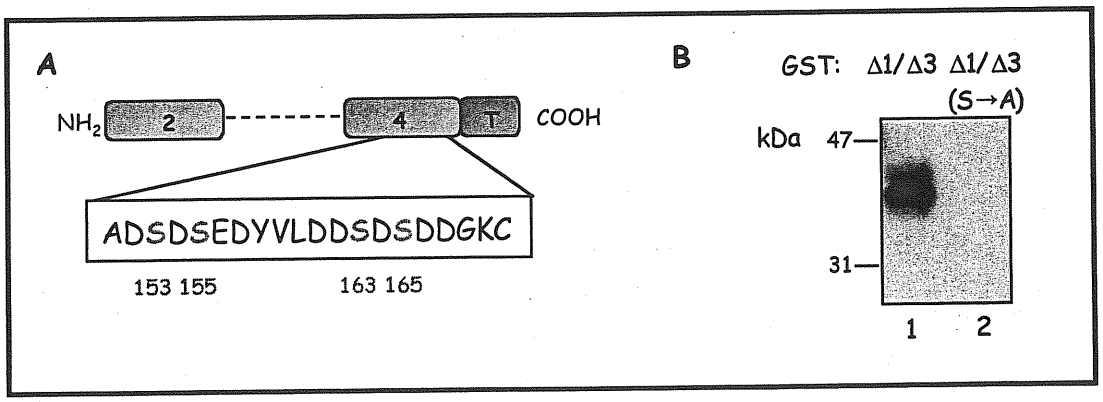

Figure 16: Characterisation of Ser→Ala mutants. **A)** Scheme of Δ1/Δ3(S→A) mutant. The position of four Ser mutated to Ala within region 4 are indicated. **B)** *in vitro* phosphorylation assay with [γ-^{32}P]ATP of substrates GST-Δ1/Δ3 and GST-Δ1/Δ3 (S→A) incubated wit the Δ1/Δ3 transfected cellular extract [54].

Further confirmation that the four serines are the main phosphorylation sites was obtained with phosphorylation *in vivo* using [^{32}Pi]. Figure 17 shows immunoprecipitates

of different transfected Δ1/Δ3 Ser→Ala mutants following labelling with [^{32}Pi]. The four serines appeared to be sites of phosphorylation, and the only mutant that showed no phosphorylation was the one with all four serines mutated (lane 9). All lanes in Figure 17 contained comparable amounts of transfected protein, determined by Western immunoblotting (data not shown). The double band corresponded to low mobility hyperphosphorylated forms as judged by λ–Ppase sensitivity (Figure 11A).

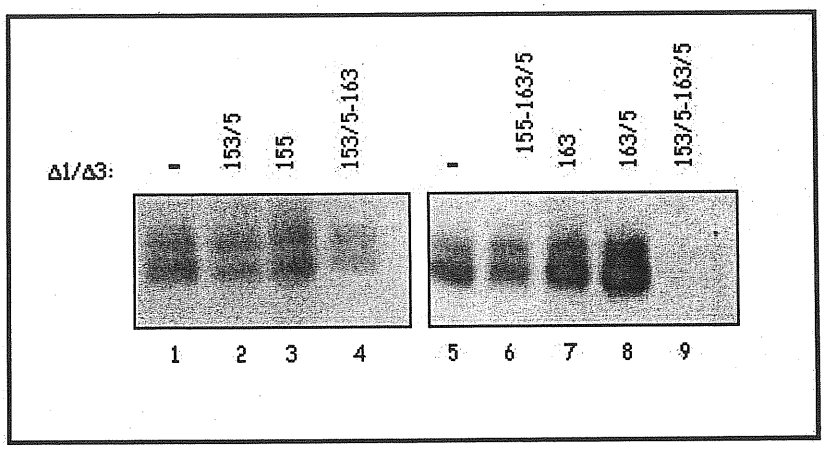

Figure 17: Characterisation of Ser→Ala mutants. Immunoprecipitates of [^{32}P$_i$] *in vivo* labelled MA104 cells transfected with the indicated mutant constructs. Numbers indicate the mutated Ser residues [54].

NSP5 is substrate of CK2 *in vitro*

From sequence analysis of NSP5 with Prosite-EMBL/http://www.ebi.ac.uk emerged that the four serines within the particular acidic amino acid sequence, SDSE and SDSD, are characteristic substrates for casein kinase II (CK2) (Figure 11, page 21 sites CK2 and PKC on NSP5) [197]. We therefore tested, whether recombinant CK2 was able to phosphorylate the different NSP5 mutants. We used the recombinant human CK2, as a GST fusion protein, active to phosphorylate the β-casein (Figure 18 lane 1). Figure 18 shows that GST-CK2α/β was able to phosphorylate NSP5 and all mutants containing region 4, namely Δ1/ΔT, Δ1/Δ3 and Δ2. This phosphorylation appeared to be restricted to serines 153, 155, 163 and 165, since mutant GST-Δ1/Δ3(S→A) was not phosphorylated by CK2 (lane 6). This result is in complete agreement with the lack of phosphorylation of this mutant *in vivo* (Figure 17) and *in vitro* (Figure 16).

Since CK2 is able to phosphorylate in vitro GST-NSP5, we wanted to understand if CK2 was able to induce the characteristic phosphorylation shift of NSP5. For this purpose, we used the recombinant GST-CK2α/β in the *in vitro* phosphorylation assay, which allows us to follow the phosphorylation shift of the NSP5. We used the *in vitro* translated His_6-Δ1 as substrate. The left panel of Figure 19 shows both, the [^{35}S] label of the *in vitro* translated substrate and the [^{32}P] label from [γ^{32}P]ATP. On the right panel only the [^{32}P] radioactivity was detected. In these conditions CK2 was able to convert, similarly to the transfected cellular extracts, part of the substrate into mobility shifted forms. These results suggested that CK2 or a CK2-like enzyme could be involved in NSP5 phosphorylation. In particular, it seems that the CK2-like enzyme is involved in the phosphorylation, which causes the shift of the substrate. In fact, the [^{35}S] label His_6-Δ1 substrate, indicated with a grey arrowhead in Figure 19 left panel (~26 kDa), is not labelled in the right panel. This result demonstrated that the incorporation of [γ^{32}P]ATP by a CK2-like enzyme occurs only for the shifting of the His_6-Δ1 substrate.

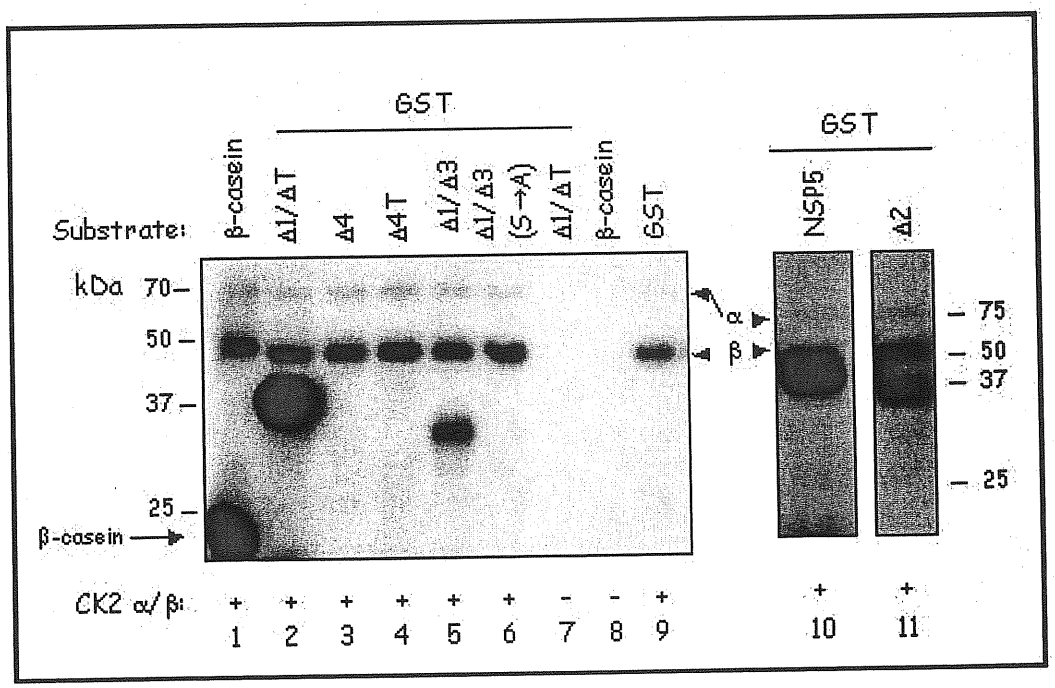

Figure 18: NSP5 is a substrate of casein kinase 2 (CK2). SDS-PAGE analysis of an *in vitro* CK2 phosphorylation assay with [γ^{32}P]ATP. Different GST-NSP5 mutants were used as substrates for GST-CK2α/β. Positive and negative controls of the kinase assays are indicated in lanes 1, 7, 8 and 9 [54].

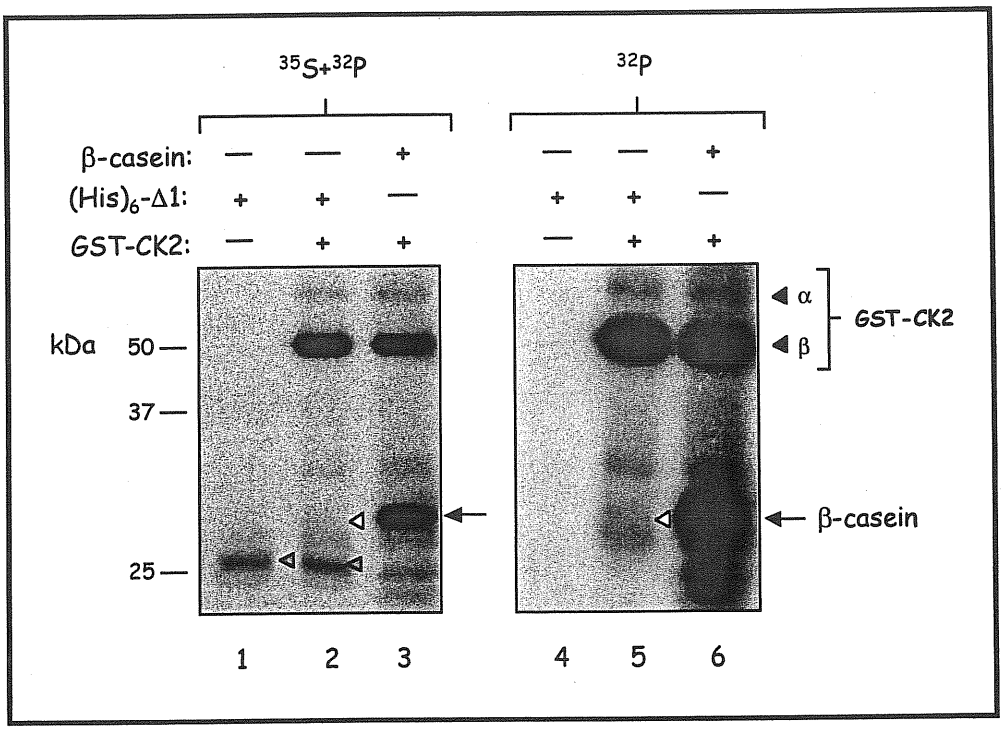

Figure 19: Purified *in vitro* translated [^{35}S]His$_6$-Δ1 was used as substrate in the presence (lanes 1 and 3) or absence (lanes 2 and 4) of GST-CK2α/β. The two panels show autoradiography of the same gel, detecting ^{35}S+^{32}P (left) and ^{32}P (right). Filled and open arrowheads indicate the His$_6$-Δ1 precursor and hyperphosphorylated forms, respectively. Autophosphorylated GST-α and GST-βCK2 subunits are indicated [54].

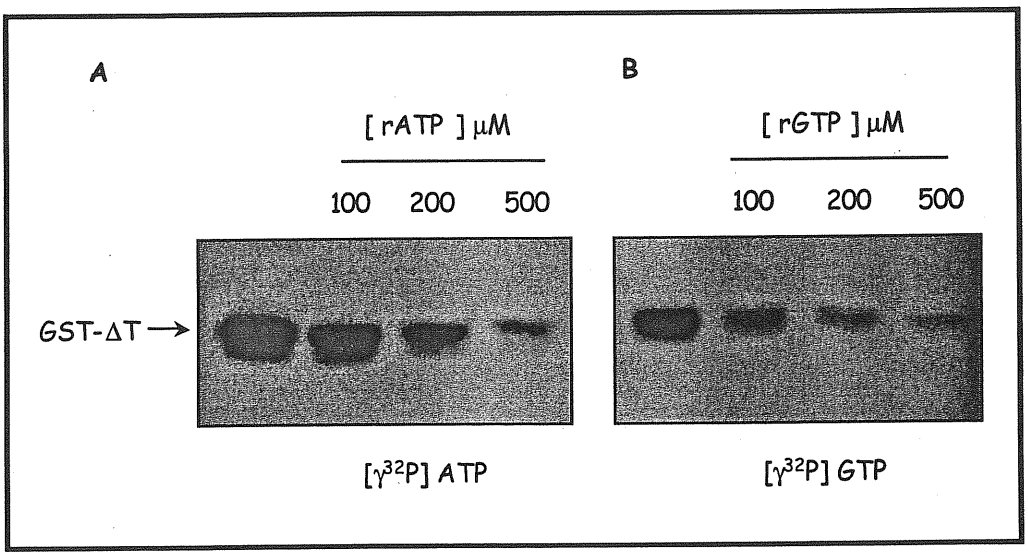

Figure 20: SDS-PAGE of immunoprecipitated *in vitro* phosphorylated ([γ^{32}P]ATP or [γ-^{32}P]GTP) GST-ΔT mutants. GST-ΔT was incubated with cellular extract form Δ1/Δ3 transfected cells and different concentration of unlabelled rATP (panel A) and rGTP (panel B).

Another indication, that NSP5 can be a substrate for CK2, comes from the evidence that CK2 is one of the few kinases capable of utilising GTP as a phosphor donor. Thus, the phosphorylation assay with [γ^{32}P]GTP was performed using transfected cellular extract as a source of enzyme for the phosphorylation of GST-NSP5. Figure 20 shows the *in vitro* phosphorylation using [γ-^{32}P]ATP or [γ-^{32}P]GTP as phosphor donor and GST-NSP5 mutant. To verify that NSP5 is not a substrate for other kinases, we tested some commercial protein-kinase available in our laboratory, as cdc2 and Erk2. We tested these two kinases on GST deletion mutant of NSP5 (Figure 21) and on specific substrates (data not shown). The phosphorylation assay demonstrated that GST-NSP5 deletion mutant is not substrate for cdc2 and Erk2.

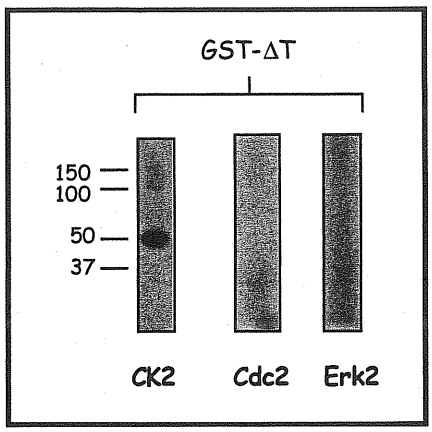

Figure 21: SDS-PAGE of immunoprecipitated GST-ΔT incubated *in vitro* with [γ^{32}P]ATP and 5 units of recombinant CK2, cdc2 and Erk2.

CK2 Inhibitors and phosphorylation assay

Since CK2 is able to phosphorylate NSP5 *in vitro*, we wanted to investigate the possible role of CK2 *in vivo* during viral infection. To obtain evidence of the involvement of CK2 in the phosphorylation of NSP5, we thought to use the well characterised CK2 inhibitors. Based on the present knowledge, CK2 inhibitors may fall in three categories (Figure 22):

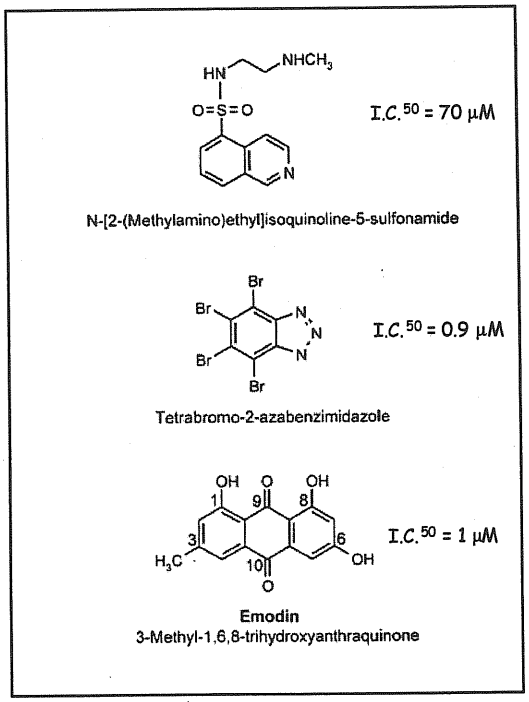

Figure 22: The three classes of CK2 inhibitors [14].

(i) Isoquinoline derivatives. The lowest Ki (Inhibition Constant) value, however, is about 70 μM, denoting a quite modest affinity, especially considering that another acidophilic protein kinase, CK1, is inhibited much more efficiently (Ki = 5 μM). (ii) Halogenated benzimidazole/benzotriazole derivatives, whose parent compound has to be considered 5,6-dichloro-1-(-D-furanosyl)-benzimidazole, commercially available as DRB and whose inhibitory potential correlates with the number and the size of halogen substituents. In particular, the tetrabromo derivative of azabenzimidazole (TBB) inhibits CK2 with a Ki value around 1 μM, whereas it is very poorly effective on several other protein kinases tested, and it inhibits CK1 much less potently (Ki = 39 μM). A drawback of tetrabromo-2-azabenzimidazole (TBB) is its very low solubility in water. (iii) The natural anthraquinone derivative emodin (Figure 22), extracted from the rhizomes of *Rheum palmatum*, a herbal medicine widely used in the Orient as anti-inflammatory and anti-cancer drug [14]. Emodin, in comparison with TBB is more water soluble and has been recently reported to inhibit CK2 with an IC^{50} value around 1μM, while being poorly effective on other Ser/Thr protein kinases [166]. In some way, this observation is surprising, because emodin was reported in the literature as a relatively specific inhibitor of tyrosine protein kinases , with special reference to the receptor kinase Her-2 neu. The latter property is believed to underlie its potential to counteract cell transformation. However, CK2 is definitely more sensitive than Her-2 neu to emodin inhibition, as judged from

their Ki values (1 versus 21 μM), raising the possibility that some of the effects of emodin are mediated by CK2 rather than protein-tyrosine kinase inhibition. Therefore, emodin represents a promising lead for developing more potent and selective inhibitors of CK2 [14].

TBB [13] and emodin [14] were crystallised with *Zea mays* CK2α, showing the way of interaction of these two compounds and the CK2 ATP-binding site. Specially, TBB appears to be mainly dictated by the reduced size of active site, which in most other protein kinases is too large for making stable interactions with this inhibitor [13].

These two ATP/GTP competitive inhibitors of protein kinase CK2, were also tested on several different kinases in *in vitro* phosphorylation assays, concluding that this two compounds are the most specific inhibitors of CK2 known to date [13]. Moreover, the glycosaminoglycan heparin and dichlororibofuranosyl-benzimidazole (DRB) are the first drugs used for inhibition of CK2 but they are relatively non-specific, the former being a polyanion that interacts with many enzymes on the basis of charge and the latter being a general inhibitor of transcription when used on intact cells. Then, DRB has been tested only on a small number of protein kinases and inhibits the other class of ubiquitous CKs (CK1) almost as efficiently as CK2 [122]. By contrast, TBB discriminates between CK2 and CK1, being much more effective with the former [166].

Thus, to obtain some indications about the role of CK2 and NSP5 phosphorylation, we tested the effect of TBB and emodin as CK2 inhibitors in *in vivo* and *in vitro* assays.

CK2 Inhibitors affect the phosphorylation state of NSP5

Three different experiments were performed to test the activity of the inhibitors on the phosphorylation of NSP5. We used the TBB and emodin as specific drugs for CK2, and staurosporine to check if other kinases were involved in this process of phosphorylation. Staurosporine is a compound of large spectrum, mainly used to inhibit CaM, myosin light chain kinase, PKC, PKA and PKG with $I.C._{50}$ from 0,7 to 20 nM.

In a first experiment we tested the phosphorylation activity of the Δ1/Δ3 cellular extract with [γ-^{32}P]ATP on a GST NSP5 deletion mutant (GST-ΔT). Figure 23 shows an autoradiography of an *in vitro* phosphorylation assay using TBB, emodin and staurosporine during the reaction. TBB and Emodin can inhibit the phosphorylation of GST-ΔT while staurosporine can not.

From sequence analysis of NSP5 with Prosite-EMBL/http://www.ebi.ac.uk emerged that NSP5 shows also some protein kinase C phosphorylation sites (Figure 11,

page 21). For this reason we wanted to test if PKC's inhibitors could have some effect on NSP5 phosphorylation. We chose GO6983 and Bisindolylmaleimide as specific protein-kinase C inhibitors, but none of them were able to inhibit the GST-NSP5 phosphorylation *in vitro* (data not shown).

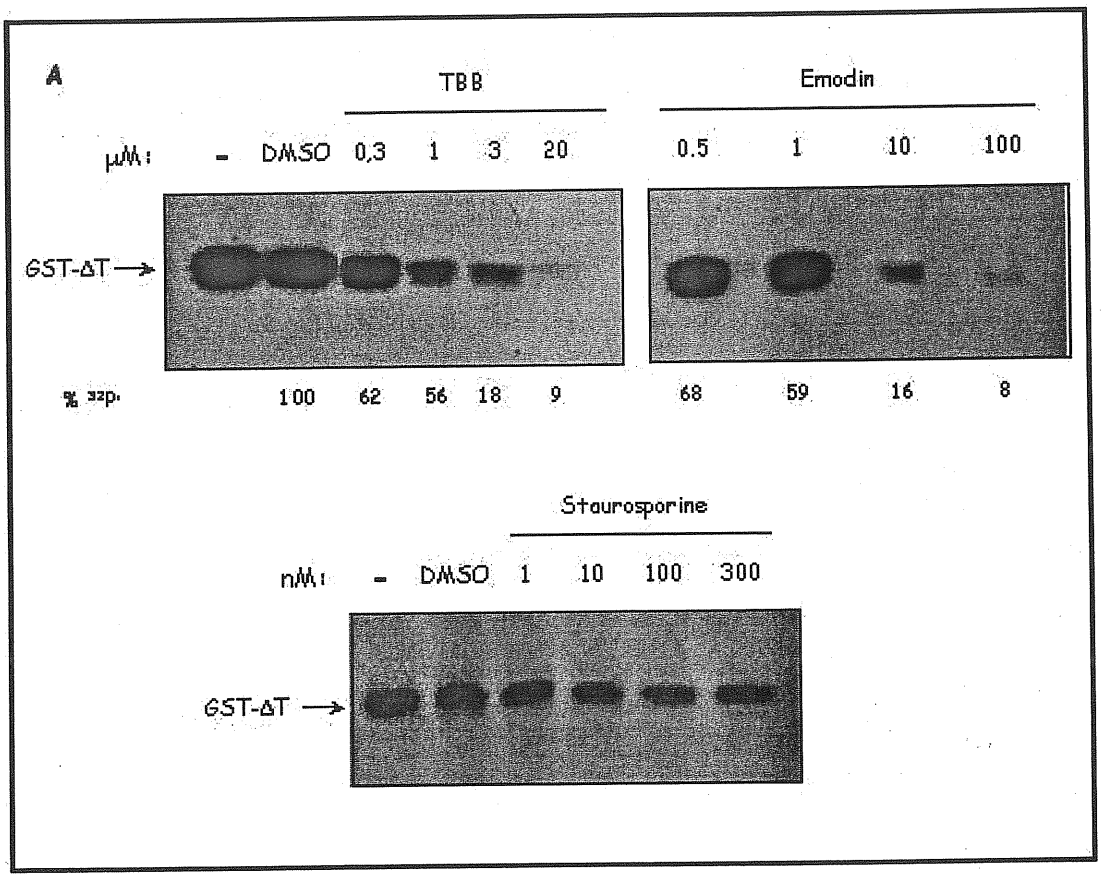

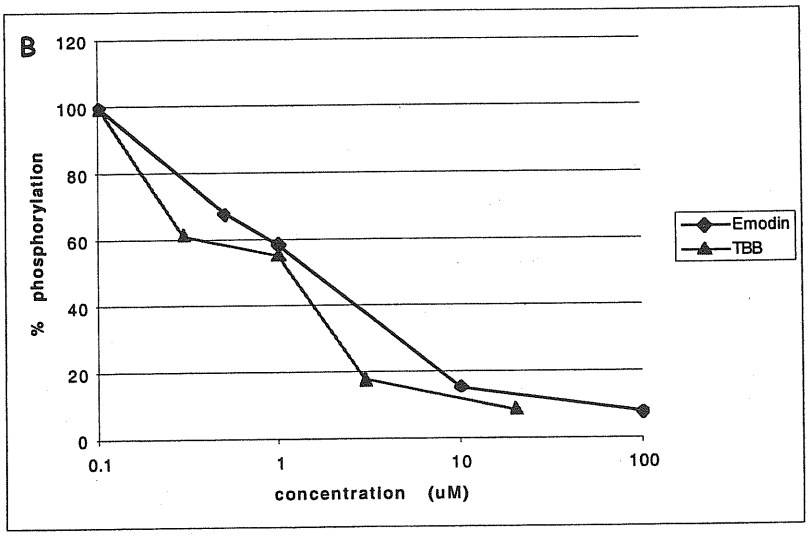

Figure 23: A) SDS-PAGE of immunoprecipitated, *in vitro* phosphorylated GST-ΔT mutant. GST-ΔT mutant was incubated with Δ1/Δ3 transfected cellular extract and [γ-^{32}P]ATP. TBB, Emodin or Staurosporine were added at the indicated concentrations **B)** inhibition plot.

In a second phosphorylation assay *in vitro* we incubated transfected Δ3 cellular extract with [γ-^{32}P]ATP , and TBB or Staurosporine at different concentration. Afterwards Δ3 was immunoprecipitated using anti-NSP5 serum. In Figure 24 we show that TBB inhibited the phosphorylation of Δ3 protein, while Staurosporine did not even at concentration 125 times higher of its I.C.^{50} (I.C.^{50}=2 nM).

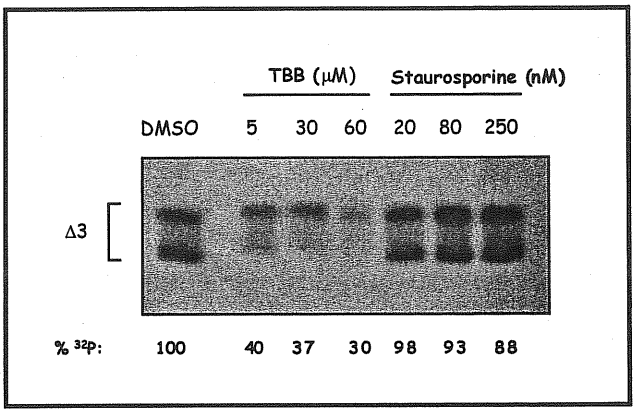

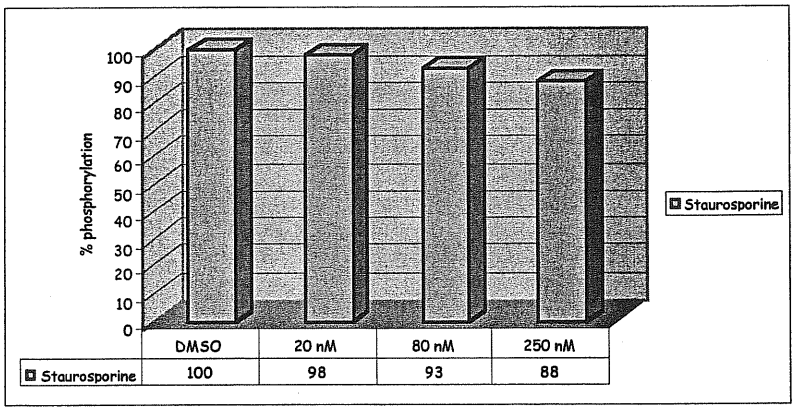

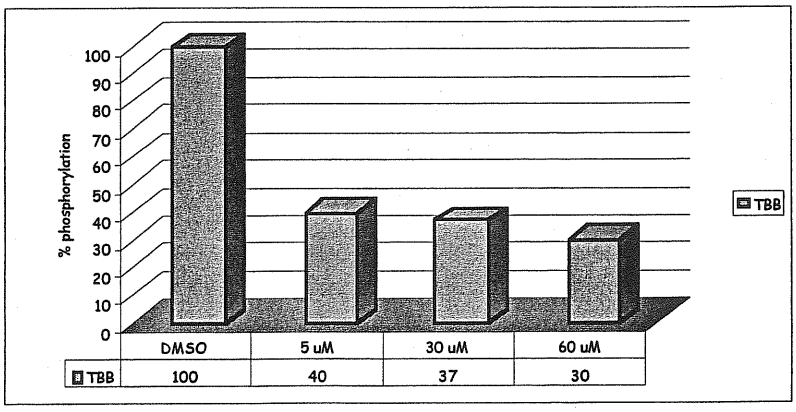

Figure 24: SDS-PAGE of immunoprecipitated *in vitro* phosphorylated Δ3 transfected cellular extract. Δ3 was incubated with [γ-^{32}P]ATP and TBB or Staurosporine as indicated.

In the third assay we tested the TBB *in vivo* on MA104 cells infected with SA11 rotavirus. We added to the medium of SA11 infected cells 70 μM TBB at different time post virus absorption or with DMSO for the control. The infected cells were lysed at the fifth hour post infection. The total cellular extracts were analysed by Western immmunoblotting with anti-NSP5 serum. Figure 25 shows that when the inhibitor is incubated immediately after the absorption of the virus and It was maintained in the medium for 4 hours, the viral NSP5 cannot be detected. When the TBB was added at the 4th hour post infection NSP5 started to be visible in Western immunoblotting.

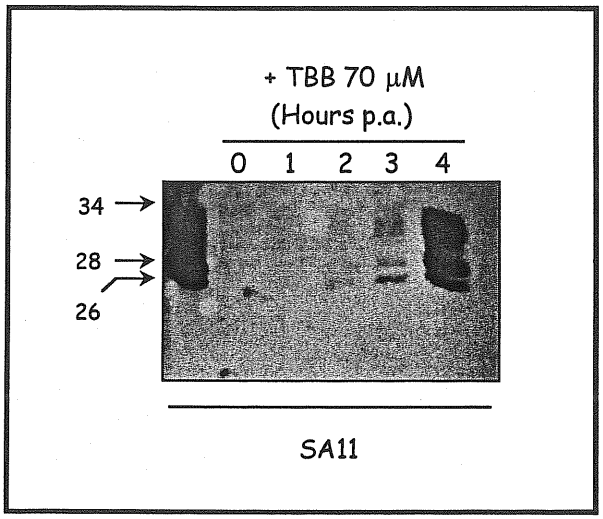

Figure 25: Westerm immunoblotting of total cellular extracts of MA104 cells infected with SA11. TBB was added in the medium at different times post infection (p.i.) of the virus.

From this experiment we understood that TBB seemed to have a strong effect on the production of the viral NSP5 and probably on the whole viral replicative cycle, because also NSP2 was affected in the same way (data not shown).

To figure out the effect of TBB specifically on the phosphorylation of NSP5 we performed an *in vivo* labelling with ^{32}Pi of infected cells with SA11 rotavirus to investigate directly the pattern of phosphorylation of NSP5. Initially, MA104 cells were infected with SA11. At 4th hour post infection cells were treated with cycloheximide (CHX) to inhibit protein synthesis, and incubated with the CK2 inhibitors (TBB and Emodin). After 10 min ^{32}Pi was added to the medium for 1 hour. Then, cells were lysed and NSP5 was immunoprecipitated with the specific serum. The Figure 26 shows the autoradiografy of the gel.

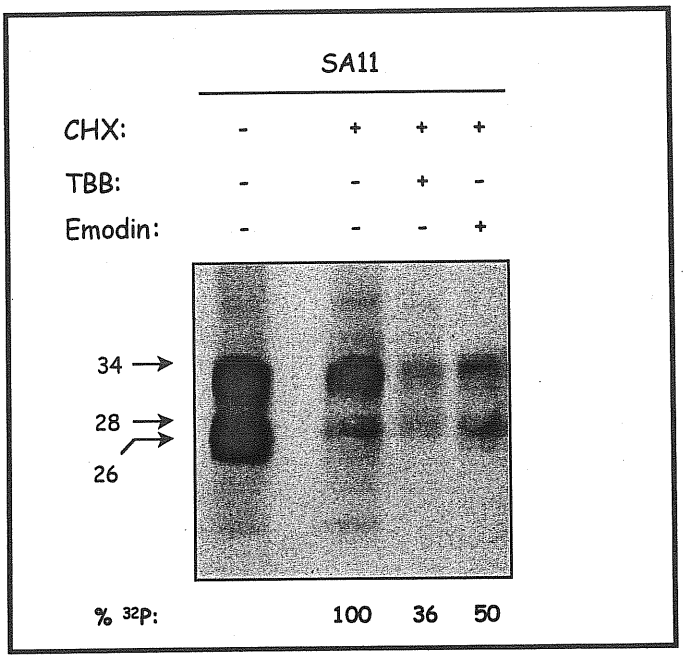

Figure 26: *In vivo* phosphorylation of NSP5 in rotavirus infected cells. Immunoprecipitations of infected cellular extracts treated with CHX and with CK2 inhibitors as indicated. The cells were labeled *in vivo* with $^{32}P_i$. Relative molecular masses in kDa are shown to the left

Since CHX decreased sensibly the quantity and the level of phosphorylation of NSP5, we used it as a reference control of phosphorylation. TBB and Emodin were both able to reduce the level of phosphorylation of NSP5 at 36% and 50%.

At the light of these experiments we demonstrated that CK2 inhibitors showed a very strong effect on the *in vitro* phosphorylation of the GST-Δ1, inhibiting the phosphorylation activity of the transfected cellular extracts. These results strongly suggested that CK2 could be the enzyme involved in the phosphorylation of NSP5. However, the *in vivo* experiments did not showed so dramatic effects of TBB and Emodin on the NSP5 phosphorylation during rotavirus infection. At the end we can propose that CK2 or a CK2-like enzyme are responsible for the phosphorylation of NSP5.

Introduction (2)

The determination of a gene function is one of the most important aspects of the functional genomics as a follow up of different genome projects, as well as in the biotechnology and pharmaceutical gene-discovery efforts. In general, the classical approach to solve the problem of identifying the function of the gene is to inactivate the gene itself and to study the resulting phenotype. In principle, the function of a gene can be inactivated at several levels using genotypic and phenotypic knock-out methods. These methods include:

- ✓ Gene knock-out by homologous recombination
- ✓ Dominant negative mutations
- ✓ RNA-based methods as antisense-RNA, ribozymes and RNA interference (RNAi)
- ✓ Protein knock-out system

Since the function of NSP5 is still unknown and it is not possible to perform reverse genetics with rotavirus, in our laboratory we chose the protein knock-out system through the use of intracellular antibodies (intrabody) as a possible strategy to understand the role of NSP5 during the viral cycle.

Intracellular antibodies (intrabodies)

The immunoglobulins (Ig) are the most popular class of proteins naturally designed as recognition molecules with high specificity and affinity properties. They provide virtually an unlimited repertoire of binding molecules with a wide range of applications, specially in biomedical science.

Naturally, antibodies work in extracellular compartments, since they are molecules secreted from activated B cells or anchored as receptors on their cellular membrane. Based on their characteristic expression, all antibodies pass through the endoplasmic reticulum (ER)

where specific chaperones assist their normal assembly and the oxidanting environment permits the formation of the disulfide bonds important for their folding (Figure 1).

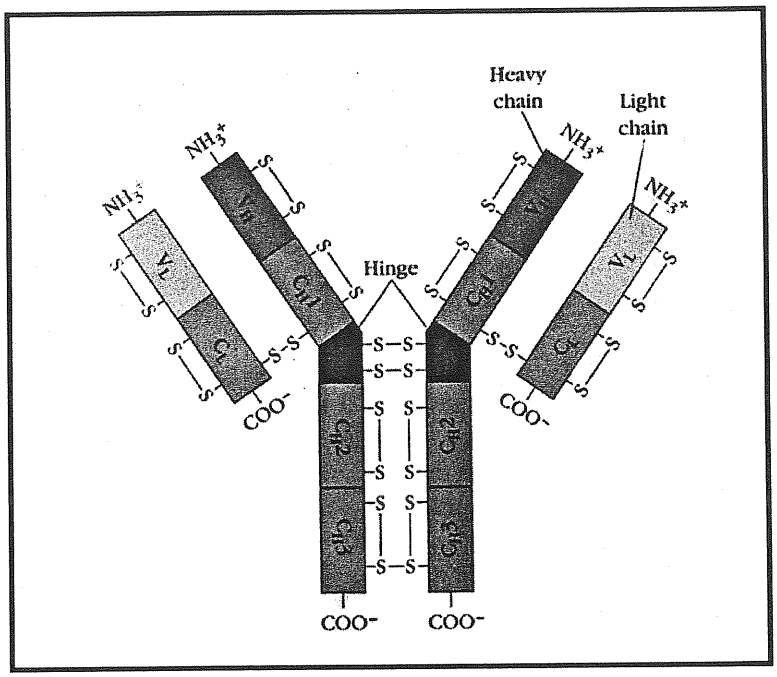

Figure 1: General structure of antibody. Two heavy and two light chains constitute the immunoglobulin molecule. Each chain contains a variable (V) and a constant (C) region composed. Two antigen-binding sites are made up of a heavy V region (V_H) and a light V region (V_L). The intra-chain and inter-chain disulphide bonds are indicated in the figure.

Since many proteins are expressed intracellularly, in different places of the cells, such as nucleus, cytoplasm or other specific cellular compartments (like ER, Golgi, peroxisomes etc.), the Igs can not be used directly *in vivo* to interact with them and eventually block their activities. However, numerous functional studies have illustrated that in some cases recombinant antibodies, in the scFv or Fab formats (Figure 2) expressed in the cytoplasm of a cell, are able to fold and assemble correctly maintaining their high affinity and selective-binding properties against their antigens [14, 57, 56]. All these results determined the growth of protein knock-out applications using intracellular antibodies (intrabodies or Ib) to modulate cellular physiology and metabolism by a wide variety of mechanisms, which has also been termed "intracellular immunisation" [33].

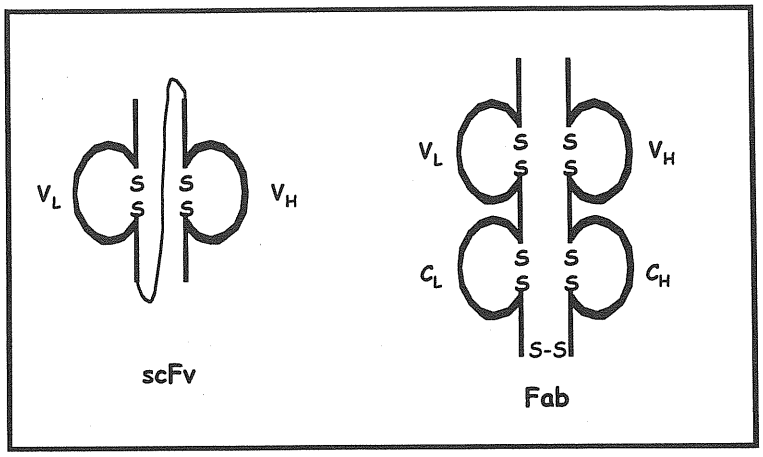

Figure 2: Structure of the antibody fragments. ScFv fragments are created expressing two variable regions (V_L an V_H) covalently joined by a polypeptide linker. Fab is a Ig fragment constitute by V_L-C_L linked to VH-C_H by an intrachain disulphide bond.

Assembly, folding and stability of intrabodies

One of the problems encountered during initial phase of the application of the intracellular antibodies was related to the shorter half-life of the antibody fragments (scFv and Fab) expressed in the cytoplasm of cells as compared to their secretory counterparts [11]. It was initially surmised that the expression of antibodies in the cytoplasm was made more difficult by the reducing environment, which would hinder the formation of intrachain disulfide bonds linking the two b-sheets of antibody domains [11, 47, 15]. Nevertheless the presence of the central disulfide bond is not essential for the β-barrel architecture, which makes up V fragments. Furthermore some natural antibodies lack a disulfide bond in the heavy chain variable domain [64] as a result of somatic mutation. These observations have inspired attempts to engineer antibodies that do not rely on the formation of the disulfide bond for proper folding in the cytoplasm.

Of particular interest has been the introduction of designed mutations that stabilise antibody fragments lacking the two cysteine residues involved in the disulfide bond formation. Moreover, it has been demonstrated that the intradomain disulfide bridge contributes about 4-5 kcal/mol to the stability of the antibody domains (Figure 3) [75, 53]. Therefore, antibody fragments expressed in the reducing environment are destabilised compared with the same molecules containing disulfides, although some of them are likely to fold to the correct native structure. This fact is believed to be responsible for the frequently

observed reduced function of cytoplasmically expressed antibody fragments [55], as well as for their high tendency to aggregate [10]. Nevertheless, a larger number of cytoplasmically expressed antibody fragments were reported to show specific biological effects and several solutions have been proposed, including engineering antibodies to obtain stable disulfide-free forms [57], or the use of a stable disulfide-free non-antibody scaffold [7] to increase stability for cytoplasmic expression of the antibody fragments [80].

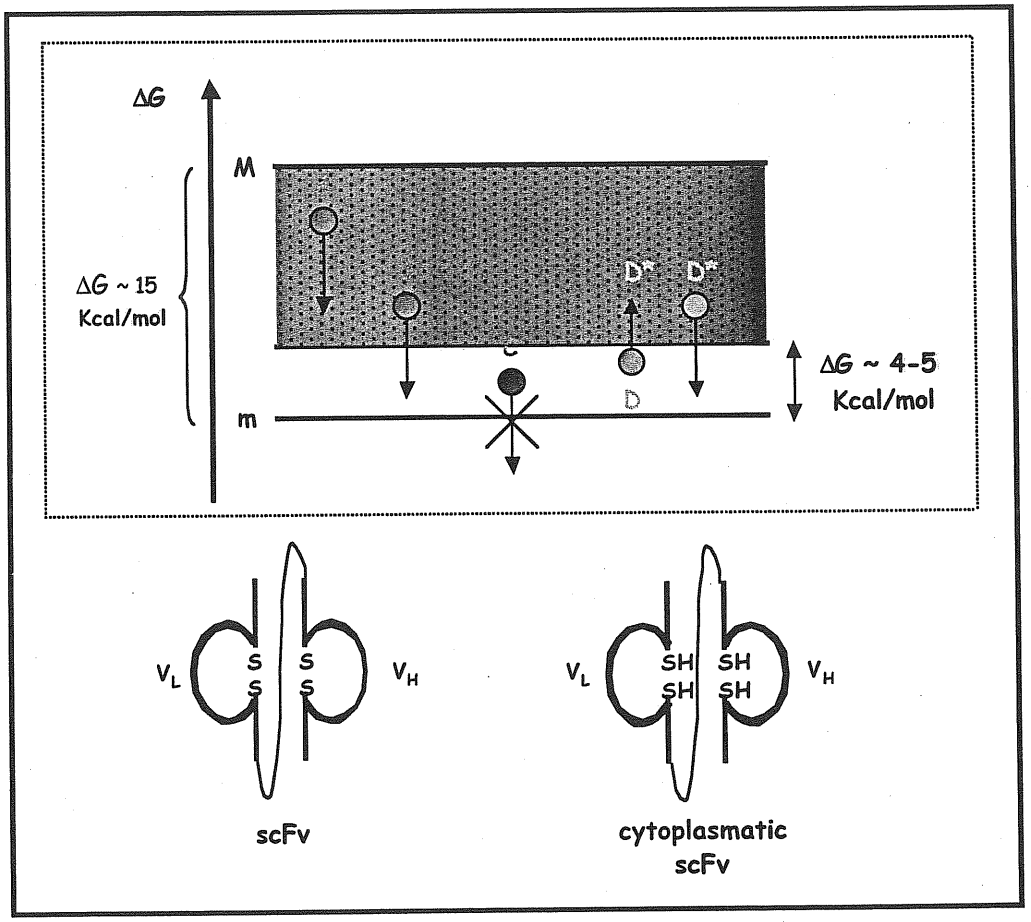

Figure 3: The folding of antibody domains is restricted to a range between a minimum (m) and maximum (M) value of DG (free energy) contributed by many residues in the frameworks [57]. Different scFv fragments have different overall stabilities. Some scFvs could tolerate the removal of intrachain disulphide bonds and remain folded because they are in the upper part of folding stability plot (A and B), while those that are in the lower part will not (C). Moreover, there are some mutations that could stabilise antibody fragments rendering them tolerant to the absence of the disulphide bonds (D*).

Application of intrabodies

Up to now, intracellular immunisation has been mainly applied with the aim to:

- block or interfere on protein-protein or protein-DNA interactions (PLCg1 [82]; Gcn4p [80]; p53 [19]; murine leukaemia virus RT [27]; Bcl-2 [51]; HIV-1 Vif [29])
- modulate enzyme function (e.g. a-1,3-galactosyltransferase [72], HIV-1 integrase [42]; HIV-1 Reverse Transcriptase [26, 28, 45]) by occluding active sites, sequestering substrates or fixing enzymes in an active (on) or inactive (off) conformation;
- block protein functions by diverting them from their usual cellular compartment, for example by:
  - ✓ sequestering protein in the cytoplasm (e.g. $p21^{ras}$, ATF-1, Tat, Rev, HIV integrase)
  - ✓ recruiting in the nucleus non-nuclear proteins (caspase3 [58], or
  - ✓ retention in the ER proteins that are normally destined to the cell surface or other compartments (e.g. IL-2Ra, Erb2 [34-30]; CCR5 receptor [68]; gp120 [17-3]; HCV core protein [32, 61].

Thus, the expression of a specific intrabody (Ib) can have a direct neutralisation effect on the antigen, or alternatively a successful strategy is to divert the antigen/antibody complex to a different intracellular compartment to inhibit the function of selected antigens [8, 14, 15].

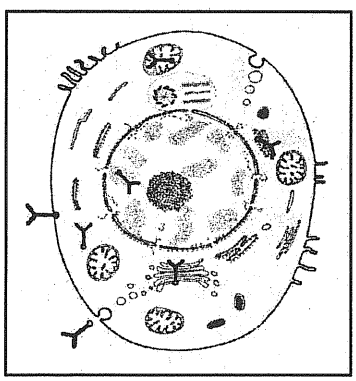

Figure 4: Targeting of intracellular antibodies. Illustration of how some of the known targeting signals can be exploited to lead the intracellular trafficking of the antibodies in eukariotic cells. For example, intrabodies can be directed to the nucleus, or the mithocondrion, the plasma membrane and the ER using specific targeting signals (see table 1).

Compartment	Signal
Secretory	**MGWSLILLFLVAVATGVHS** Wild type leader sequence at N-terminus [43]
Cytosol	**None** Leader-less [8, 9]
Nuclear	**DPKKKRKV**: nuclear localisation sequence of Large T-antigen of SV40 virus at N- or C- termini [37]
Mithocondrial	**MSVLTPLLLRGLTGSARRLPVPRAK** (N-teminal presequence of the mithocondrial enzyme cytochrome C oxidase)[11]
Endoplasmic Reticulum (ER)	Wild type leader sequence and **SEKDEL** (C-erminal tetrapeptide sequence sufficient to cause retention in the ER) sequence at C-terminal[11, 30, 36]
ER lumen membrane	Wild type leader sequence and m chain transmembrane domain at C-terminal: **NLWTTASTFIVLFLLSLFYTTVTLF** (in non B cells model) [79]
Plasma membrane	Wild type leader sequence and γIg G1 (**WTTITIFITLFLLSVCYSATVTFF**) or εIg and αIg [6] Wild type leader sequence m mutated chain transmembrane domain at C-terminal: **NLWVVAAVFIVLFLLSLFYSTTVTLFTMD** (in non B cells model) of T cell receptor, met receptor and PDGF receptor [79]

Table 1: Signals used for targeting antibody to different cell compartments.

Antigen diverting and inactivation activity

Several examples show the applications of intrabody (**Ib**) to block or alter the normal expression of the antigens often associated at tumoral phenotype.

IL-2Rα plays a key role in T cell-mediated immune responses, and is constitutively expressed in some T and B cells leukemias, most notably in T cell leukaemia (ATL), which is caused by HTLV-1. The intracellular stable expression of ER-tagged scFv (KDEL-tag-scFv) specific for the a subunit of the receptor for human interleukin 2 (IL-2Rα) in T-cells exhibited a complete loss of cell-surface IL-2Rα expression and was no longer responsive to IL-2, due to the retention of the Il-2Rα in the ER by the tagged scFv [62].

Another example of antigen/antibody retention in the ER has been applied for the Erb2 transmembrane protein. Erb2 is a receptor tyrosine kinase, member of the epidermal growth factor receptor (EGFR)-related family. Erb2 is overexpressed in a variety of human tumors, including breast and ovarian carcinoma, where it correlates with an unfavourable prognosis. The expression of two KDEL-tagged Ib showed to markedly decrease the expression on the cell-surface of erb2 in NIH3T3 fibroblasts transformed by activated ErbB-2 and more importantly to determine reversion to the non-transformed phenotype of the cells [5]. Moreover, the Erb2-dependent signal transductions were impaired [30].

Dysregulated cyclin E expression is found in a large number of breast cancers. Ectopic over expression of cyclin E results in accelerated G(1) progression, chromosome instability and a reduced requirement of growth factors. Nuclear–tagged antibody fragment anti cyclin E has been selected intracellularly and stably expressed in the breast cancer cell line SKBR3. This intrabody determined the inhibition of growth of this breast cancer cell line [69].

An effective approach for the therapy of chronic myelogenous leukaemia and other c-myb-dependent malignancies has been investigated by the ablation of the c-Myb function with an intracellular scFv expression. The nuclear-tagged form of the antibody fragment has been stably and tetracycline-inducible expressed in the leukaemia cell line K562 showing inhibition of the transactivation activity of c-Myb and cellular proliferation [38, 39].

An interesting effect of an intrabody has been described for a fatal neurodegenerative disorder. Huntington's disease (HD) is caused by (abnormal) overexpression of the protein hungtintin (htt) involved in an abnormal formation of insoluble aggregates in affected neurons, with a toxic function and inducing death in subpopulation of neurons. A scFv specific intrabody has been characterised to inhibit cell death induced by this pathological aggregation of htt. It seems that this particular scFv (MW7) may act, not by inhibiting the formation of aggregates but rather by imposing a conformational change to mutated htt, enhancing the turnover of the complex through proteosome-mediated degradation [40, 41].

A well studied example of protein inactivation by Ib is the case of $p21^{ras}$, a protein involved in cell growth and differentiation. Several works demonstrated applications of different tagged forms of Ib (scFv and Fab) to perturb the function of $p21^{ras}$. Different Ib were transfected in morphologically transformed cells with active *ras*, determining phenotypic reversion to a non-transformed morphology [13, 18, 9, 8].

Other reports showed the application of Ib to block the transcription factor ATF-1 in the cytoplasm interfering with its normal migration into the nucleus. The expression of ATF-1 and CREB is upregulated in metastatic melanoma cells and recently it has been described a significant reduction in CRE-dependent promoter activation in MeWo melanoma cells. In addition, the expression of anti ATF-1 scFv in melanoma cells suppressed their tumorigenicity and metastatic potential in nude mice. Moreover, this scFv rendered the melanoma cells susceptible to induced-apoptosis *in vitro* and caused massive apoptosis in

tumors transplanted subcutaneously into nude mice, confirming the potential usage of anti-ATF-1 scFv as an inhibitor of tumor growth and metastasis of solid tumor *in vivo* [35].

In conclusion the most important aspect of all these works is that intrabodies may have a prominent role in cancer gene therapy in the future.

Interference on the viral cycle

Baltimore et al. in 1988 [2] described for the first time the introduction of an antibody moiety into a cell that leads to resistance of the cell to productive infection by viral pathogen, a sort of "intracellular immunisation". After this works several viral models were investigated to determine an active intracellular immunisation of cells using the intrabodies as human gene therapy. HIV has been the most studied virus, but intracellular immunisation was also performed in other viral systems.

Intrabodies and HIV

Several intrabodies directed against structural, regulatory or enzymatic proteins of HIV-1 have been studied [63](Integrase RT). Encouraging results have been reported with antibodies direct against the envelope glycoprotein gp120. Interestingly, production of intrabodies as ER-tagged-scFv, or as secreted Fab, blocked incorporation of gp120 into virion particles and the syncytial formation [3, 46]. In addition, the secreted Fab specific for gp120 was transduced in human lymphocytes using adeno-associated virus vector (AAV) resulted in resistance to HIV-1 infection of several primary. Thus this approach may provide a therapeutic benefit for HIV-1-infected patients by reducing of virus infection and by inhibiting direct and indirect HIV cytopathic effects [17].

Other studies have reported targeting of the regulatory protein Rev. Cytoplasmic anti-Rev Ib were able to inhibit transport of Rev to the nucleus, thereby preventing viral mRNA processing and HIV-1 production and syncytial formation by the cell. Again human lymphocytes transduced with retroviral vectors expressing these Ib were resistant to HIV-1 infection [23, 22].

The cytoplasmic expression of anti-Tat scFv blocked Tat-mediated transactivation of HIV-1 LTR (using a CAT reporter gene) as well as the cytoplasm-nuclear transport of Tat in

mammalian cells, resulting in a strong resistance to HIV-1 infection in stably transfected lympocytes [49].

Another alternative strategy to block somehow HIV-1 infection was obtained by expression of an ER tagged form of a scFv specific for the CCR5 receptor. Polymorphism studies on CCR5 gene have shown that deletion of the functional receptor or reduced expression of the gene can have beneficial effect in preventing HIV-1 infection or delaying disease. So an ER-tagged scFv blocked surface expression of human and rhesus CCR5 receptor and preventing cellular interactions with CCR5-dependent HIV-1 and SIV [68], offering a new strategy for viral gene therapy. A similar work was presented also for the CXC-chemkine receptor 4 (CXCR4), which acts as a co-receptor for T cell of HIV-1 [12].

Intrabodies and other viruses

Tavlodoraky has performed the first strategy of plant immunoprotection against virus through Ib in 1993 [70]. A constitutive expressed cytoplasmic scFv raised against the coat protein of the artichoke mottle crinkle virus (AMCV) was able to specifically shield transgenic plants from viral attack, reducing the infection incidence and causing a delay in symptoms development upon challenge with abnormally high titer of viral inocula.

In other viral system, it has been expressed an intrabody (scFv) able to inhibited hepatitis B virus (HBV) DNA replication. HBV replication can only take place in the viral nucleocapside made of HBV core protein (HBc), where the bifunctional progenome RNAs serves as template for viral DNA synthesis conducted by HBV-P protein (viral DNA-dependent polymarese which works also as Reverse trascriptase and RNAse H).

The authors generated an anti-HBVc scFv and showed its marked effect on HBV DNA replication through inhibition of the reverse transcription process from HBV progenome RNA to ss-DNA in human hepatoblastoma-derived cell line that produce HBV [81].

In another example, it has been reported an efficient block of virus infection of canine parvovirus (CPV) by intracellular immunisation with an antibody fragment specific for the viral capsid protein. The successful strategy was first conducted by microinjecting the antibody and the also by transfecting the scFv fused to EGFP. In this case the mechanism of intracellular neutralisation is not known, but the antibodies would likely bind directly the incoming virus in the cytoplasm, interfering with capsid functions [74].

Finally, another example of phenotypic knock-out strategy is the application of the intracellular ER-tagged scFv to achieve a functional inhibition of the oncoprotein latent membrane protein 1 (LMP1) in Epstein Barr Virus (EBV)-transformed B lymphocytes. The LMP1 of EBV is a transmembrane protein that is essential for the transformation of B lymphocytes. LMP1-mediated-upregulation of Bcl-2 is thought to be an important element in the process of transformation. The neutralisation approach, based on the expression of ER-scFv, markedly reduced LMP1 protein level and Bcl-2 expression in EBV-transformed B lymphocytes [52].

Screening of intracellular antibodies

Hybridoma-cell lines represent an immediately available source of well characterised and affinity maturated antibodies that can readily be converted in the recombinant format as scFv or Fab. Recent advances in antibody engineering allow the *de novo* construction of antibody fragments libraries and the selection of desired specificity antibodies by a screening "*in vitro*" with phage display or "*in vivo*" with the two-hybrid system. The first technical approaches was the **phage display** [66] based on the expression of peptides on the surface of phage particles by cloning the gene encoding the antibody fragments into the phage genome, as a fusion with a coat protein. Later it has been set for the antibody fragments expression [48]. These resulting particles can be affinity-purified on immobilised antigen. After washing and elution steps, the selected phages are amplified by infection of *E.coli*. This cycle can be repeated several times (Figure 5).

This technique has been used to select antibodies from large repertoires. Two type of repertoires can be chosen. Immunised repertoires where the V genes used to assemble the antibody fragments are taken from mice immunised by antigen, and naïve repertoires where the V regions are taken from peripheral blood lymphocytes of non-immunised individuals (human, mice etc.). The main advantage of the first method is that antibodies selected from immunised repertoires are expected to have high affinities on the basis that immunisation could have induced a large bias toward B-cells specific for the immunogen and having undergone affinity maturation. Obviously the main drawback of such method is that an immunisation is required for each antigen. In this respect, naïve libraries are very convenient since once they are constructed they can be used almost indefinitely against a diverse panels

of antigens. Most importantly, these libraries can be built using human B-cells, thereby allowing the direct isolation of human antibodies. A major drawback of naïve repertoire is that they need to be very large to yield reasonable affinities. Typically a naïve library of 10^{10} clones is expected to yield affinities in the 10^{-8} M range [16, 65].

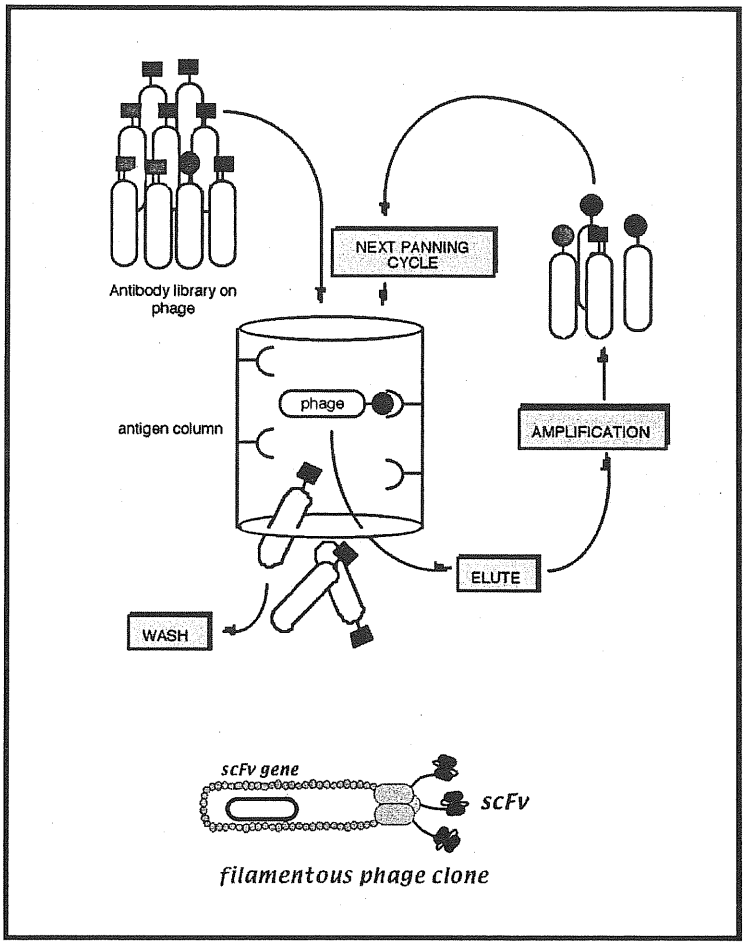

Figure 5: Phage antibody technology. Scheme showing one complete panning cycle.

The new and very promising application of recombinant antibodies with intracellular activity induced researchers to find new and more convenient methods for the selection of intrabodies able to maintain their specificity in a non-natural environment as the cellular cytoplasm. The **two-hybrid system**, originally developed in 1989 [25], is a good experimental system to monitor intracellular protein-protein interactions, based on the screening of a library (a large repertoire of proteins) for a specific protein of interest. An intrinsic characteristic of this *in vivo* screening is that the protein-protein interactions occur in the

intracellular reducing environment, namely cytoplasm and nucleus. For this reason, if a scFv fragments can be successfully expressed in a two-hybrid system, monitoring their interaction with a corresponding antigen, it should allow the isolation of those scFv fragments, which successfully bind to the antigen under intracellular conditions [15]. Such a system was firstly performed using a large number of known antigen/scFv interactions, giving good results [77 21]. So, this system validates the specificity of the interactions between antigens and scFvs. This new technology started to be used as an effective new strategy of scFv selection, named intracellular antibody capture technology (IACT) [76].

Since this technology has been recently developed, up to now all the application of intrabodies were derived from screening of libraries with phage display or from engineering classical monoclonal antibodies (from hybridomas) formatted as recombinant fragments. These selected scFvs have been adapted to intracellular expression in mammalian cells, but with unpredictable success.

Two-hybrid system and intrabodies

The main procedure of the new strategy of selection in yeast with the two-hybrid system based on *in vivo* interaction is outlined in Figure 6.

Up to now few works have described selection of scFv libraries with the two-hybrid system in yeast. In these works the interactions between selected Ib and antigen have been then verified *in vitro* with biochemical approaches (as ELISA or Western immunoblotting), and *in vivo* in mammalian cells with other approaches, as mammalian two-hybrid system, immunoprecipitation and co-localisation in immunofluorescence.

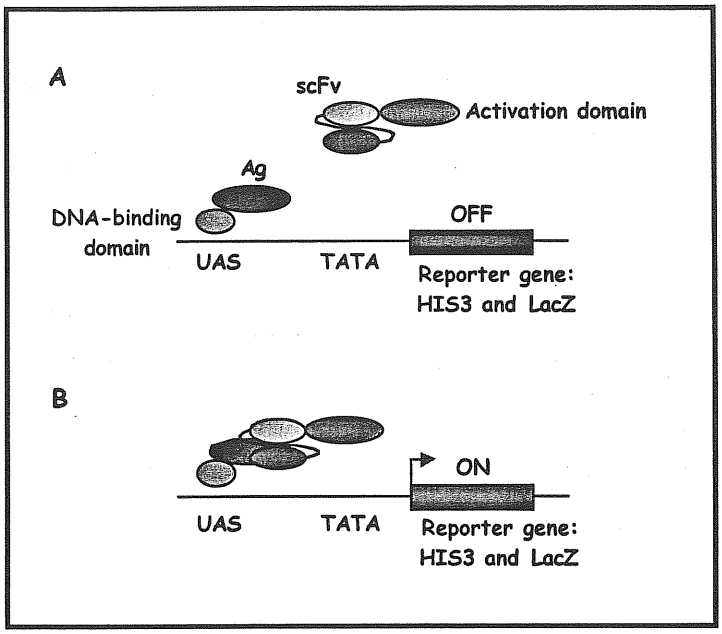

Figure 6: Schematic view of the *in vivo* selection with the use of the antigen-antibody two-hybrid system. **A)** The antigen (Ag) fused to the DNA-binding domain of *E.coli* repressor LexA is expressed in the yeast strain L40 carrying two reporter genes, lacZ and HIS3, under control of the LexA regulatory sequence. This hybrid protein (bait) can bind to its operator site (upstream activation sequence, UAS) but will not activate transcription. A second plasmid, which expresses the scFv fragments fused to the herpes simplex virus type 1 VP16 transcriptional activation domain, is introduced into the same strain; this hybrid protein (fish) does not bind to the UAS because it lacks the DNA-binding domain. **B)** The interaction between the two fusion proteins through the antigen and the scFv results in the formation of a transcription factor composed of a DNA-binding domain and an activation domain which can activate the expression of the reporter genes (HIS3 and LacZ).

In the first work of IACT has been screened a naïve human scFv library by two-hybrid system in yeast to isolate specific binders able to recognise the microtubule-associated protein **TAU**, found in neuofribillary lesion of Alzheimer's disease brains. In this work a fine analysis of the Ib *in vitro* has been conducted with different biochemical approaches, to validate, quantify and map the interactions among the scFvs and antigen TAU and its deletion mutants. In this work for the first time co-transfection in mammalian cells of the scFvs with nuclear localisation signals (NLS) and the cytoplasmic antigen TAU showed the re-localisation of the antigen TAU by the anti-TAU-scFv-NLS through their interaction *in vivo* [76] (FIG). Moreover, the expression in neuronal cell lines of one of the anti-TAU scFv was shown to inhibit the neurotrophin-mediated neurite outgrowth (Melchionna T. and Visintin M. personal communication).

At the same moment, several Ib recognising **BCR-ABL** protein were fished out from the same human scFv library. The recognition activities of these Ib for BCR-ABL protein were confirmed with the mammalian-two-hybrid system, where the specific binding was monitored through activation of a luciferase reporter gene in mammalian cells, and Western immunoblotting, as primary antibody to recognise the blotted antigen [71].

Another example is the screening of a human scFv library with two-hybrid system permitted to find scFvs direct against the transcriptional factor **ATF-2**. In this work the authors showed the ability of these scFvs to work in Western immunoblotting, and in mammalian-two-hybrid system [54].

Up to now only one work has been published describing a correlation of the expression of a two-hybrid system selected intrabodies and a specific phenotype in mammalian cells. This very interesting work reported the biological effects of the binding of intracellular scFv to Syk. They elucidate the functions of Syk, a protein tyrosin kinase involved a signal transduction pathway in most hemopoietic cell types, including B cells and mast cells, with the application of intrabodies. The cells stably expressing the scFv revealed an inhibition of the tyrosine phosphorylation and activation of Btk and PLC-γ2, while other partners involved in the same signalling pathway are not impaired. These intrabodies inhibit selectively the link between Syk and Btk and PLC-γ2 for their subsequent tyrosine phosphorylation [20].

The IACT is a powerful technique that allows the isolation of intrabodies able to fold in reducing environments, to be expressed in cytoplasm of mammalian cells. For this purpose a library of scFvs was created from immunised mice to select binders able to recognise rotavirus NSP5, and then to express them in the cytoplasm of mammalian cells.

This could allow us to understand the role of this non-structural protein during the viral cycle using this protein knock-out strategy.

Aims (2):

1. Construction of a scFv library from immunised mice with recombinant NSP5 protein.
2. Selection of the scFv library by two-hybrid system in yeast to "fish out" competent intracellular scFvs specific for NSP5.
3. Identification of the families of the variable regions of the specific anti-NSP5 scFvs.
4. Expression of the intrabodies in mammalian cells: localisation in the cytoplasm and in the nucleus of transfected MA104 cells.
5. Diversion of the localisation of the antigen (NSP5) in transfected cells through interaction with anti-NSP5 intrabodies.
6. Protein knock-out of rotavirus NSP5 in infected cells using intracellular antibodies (intrabodies) as a possible passive intracellular immunisation.
7. Purification of the anti-NSP5 scFvs form periplasm of *E.coli*: possible utilisation as a general tool in different laboratory techniques.

Materials and Methods (2)

Plasmids

There are several vectors for use with the two-hybrid system and in general they have a number of features in common. Not all the vectors in use can be utilized for this purpose, in particular the choice of terminal fusion for the scFv fragment can be crucial because of the steric hindrance of the molecule.

The two-hybrid vectors described here were plasmids that contain replicators and genetic markers that allow their selection and maintenance both in *S.cerevisiae* and in *E.coli*. The drug resistance markers and replicators that allowed selection and maintenance in *E.coli* were standard (*bla* and *ori* sequences respectively), whereas those that allowed use in yeast were more specialized.

pBTM116 (bait vector) [33] (Figure 2 page 99) 5-kb DNA-binding domain vector was used to generate fusions of the target antigen with the complete lexA coding sequence, with downstream polylinker for cloning genes of interest to generate in-frame protein fusions to LexA, expressed from the yeast ADH1 promoter. It contains TRP1 gene, a selectable marker for yeast and the yeast 2μ origin of replication. The plasmids contain ADH1 transcription terminators, downstream from the promoter and the cloning-fusion sites.

A PCR amplification was performed on pCDNA-NSP5 using 5'primer (5'-CCGGAATTCATGTCTCTCAGCATTG-3') and 3' primer (5'-GCGGGATCCTTACAAATCTTCGATC-3'), digested EcoRI and BamHI, inserted with the two primers, and cloned in bait vector EcoRI/BamHI obtaining pBMT116-NSP5.

The constructs were obtained with the same strategy but with the opportune couple of primers on the relative pCDNA construct: 5' primer (5'-CCGGAATTCATGTCTCTCAGCATTG-3') and 3' primer SP6 for pBMT116-ΔT, pBMT116-Δ4T, pBMT116-ΔC48, pBMT116-ΔC29, pBMT116-Δ4, pBMT116-Δ2. All the clones were sequenced to verify the sequence of the PCR products and to confirm the correct fusion at 5' with LexA.

pVP16/D (fish vector) (Figure 2 page 99) was a variant pf VP16* [33] 7.5-kb activation domain vector, was used to generate fusions of a scFv library with the VP16 activation domain, with upstream polylinker for cloning genes of interest to generate in-frame fusions to VP16, expressed from the yeast ADH1 promoter. It contains LEU2 gene, a nutritional marker that must be used in conjunction with special host strains, as L40, that carry the appropriate complementable mutations. It contains also two SV40 large antigen nuclear localization sequences (NLS) fused to the VP16 acidic activation domain and the yeast 2μ origin of replication. ATG indicates the initial of transcription of the polylinker of the activation domain VP16/D vector. The pVP16/D polylinker was engineered for suitable cloning from library, which has BssHII-NheI cloning sites for scFv fragments, e.g. from pDAN3 scFv libraries [65]. The plasmids contain ADH1 transcription terminators, downstream from the promoter and the cloning-fusion sites.

The first modification on VP16* were done on the polylinker, inserting a linker in the original sites SfI/XhoI (disrupting them) and inserting BssHII and NheI sites in frame with the 5' and 3' Nuclear Localization Signals (NLS) creating pVP16/B. The two

oligonulceotides (5'-CGCGCATACAGCTAGCGTT-3') and (5'-TCGAAACGCTAGCTGTATG-3') were annealed and inserted as linker.
The second modification were done reducing the length of the DNA coding for VP16 transactivation domain of Herpes simplex virus type I from 401 to 479 aa. In particular a PCR was conducted on pVP16/B, with a 5' primer (5'-CGCGCATACAGCTAGCGTT-3') and with 3' primer (5'-CGGGGATCCCTACCCACCGTACTCGTCAAT-3'). The amplification product were digested BssHII/BamHI and inserted in pVP16/B-BssHII/BamHI. In this way a stop codon was inserted after the 479 aa of VP16 protein, before the BamHI site, creating pVP16/C.
A human scFv fragments (BssHI-V_L-SalI-**linker218**-XhoI-V_H-NheI) was cloned in BssHI/NheI sites of pVP16/C, creating pVP16/D. This final vector contains the linker 218 [78] in frame with the V_L and V_H regions, with the 2 NLSs and VP16 (Figure 2 page 99).
pDAN3 vector (REF) was digested BssHI/NheI to insert the scFv (BssHII-NheI) from pVP16/D-scFv constructs, obtaining pDAN3-A19, -A22 and -D24.
pDAN3ATG vector was obtained from pDAN3 (gently provided by D. Sblattero and A. Bradbury) digested with HindIII/BssHII (eliminating the pelB sequence) and inserting a liker with an ATG start codon in frame with BssHII sites. The two oligonulceotides (5'-AGCTTGTCGACCATGGG-3') and (5'-CGCGCCCATGGTCGACA-3') were annealed and inserted in pDAN3-HindIII/BssHII. pVP16/D-A19, -A22, -D24, -14, -20, -SchCH$_2$ were digested BssHII/NheI to subcloned the fragments in pDAN3ATG, obtaining pDAN3ATG-A19, -A22, -D24, -14, -20, -SchCH$_2$. These are intermediate vectors for subcloning the scFv formats in eukariotic (pCDNA3 and pEGFP-N1).
The pDAN3ATG-A19, -A22, -D24, -14, -20, -SchCH$_2$ constructs were digested HindIII/NheI to subclone the scFv in pCDNA vector, obtaining pCDNA-A19, -A22, -D24, -14, -20, -SchCH$_2$.
The scFv in pCDNA vectors were tagged with two nuclear localization signals (NLS) form SV40 L-antigen.
The oligonucleotides containing two tandem repeated NLSs were annealed
(5'-CTAGT**GATCCAAAAAAGAAGAGAAAGGTA**GATCCAAAAAAGAAGAGAAAGGTAG-3') and (5'-CTAGCTACCTTTCTCTTCTTTTTTGGATCTACCTTTCTCTTCTTTTTTGGATCA-3') and inserted in the NheI site, disrupting the 5' NheI and maintaining the 3' NheI site obtaining pCDNA-A19(NLS), -A22(NLS), -D24(NLS), -14(NLS), -20(NLS), -SchCH$_2$(NLS).
pR4(NLS) was gently provided by M. Visintin.
The multicloning site pEGFP-N1 was modified to permit the subcloning of the scFv form pCDNA-scFvs. The pEGFP-N1 was digested NheI/ApaI, Two oligonucleotides (5'-CTAGT**AAGCTTCAAGGCTAGCCGGGCC**-3') and (5'-CGGCTAGCCTTGAAGCTTA-3'), carrying HindIII and NheI sites, were annealed and inserted in the pEGFP-N1-NheI/ApaI. The sticky ends of this linker disrupted the 5' NheI site and reformed the 3' ApaI site. pEGFP-A19, -A22, -D24, -SchCH$_2$ were obtained subcloning A19, -A22, -D24 and -SchCH$_2$ HindIII/NheI from pCDNA-scFvs constructs in the pEGFP-HN HindIII/NheI.

Yeast strain

The yeast strain L40 [33] contains lexA operator-responsive reporters chromosomally integrated; the genotype of L40 is: Mata *his*3Δ200 *trp*1-901 *leu*2-3, 112 *ade*2 LYS2::(lexAop)$_4$-HIS3 URA3::(lexAop)$_8$-*lac*Z GAL4.

Minimal HIS3 and GAL1 promoters fused to multimerized LexA binding sites drive the expression of the HIS3 and LacZ coding sequences, respectively. The expression of HIS3 permits the growth of the transformed yeast in selective medium while the expression of

LacZ, which encodes the enzyme β-galactosidase, can be monitored using a colorimetric assay based on the activity of β-galactosidase: the $lacZ^+$ yeasts form blue colonies in the presence of the chromogenic substrate 5-bromo-4-chloro-3-indolyl-βD galactoside (X-gal). This strain is deficient for TRP and LEU (auxotrophic phenotype) and cannot grow on minimal medium lacking those nutrients unless functional TRP1 and LEU2 genes are introduced. Moreover, this strain carries the ade2 mutation, which confers a red colour (due to a red pigment accumulation) on medium containing limiting amounts of adenine that turns darker as the colony age.

Preparation of media and reagents

Yeast strains, which employ auxotrophic mutations as markers, were grown on nutrient-rich media at 30°C to minimize selections for revertants. Strains to be preserved were grown to logarithmic phase on YPD plates in 3-4 days; the yeast was then scraped up with sterile inoculation loop and suspended in a 15-30% (v/v) glycerol-YPD medium; yeast were stored indefinitely at -70°C (the vials should be vortex briefly before freezing at -70°C to avoid cells settling to the bottom of the tube).

When needed, the yeast strain was revived by transferring a small portion of the frozen sample onto YPD plates (yeast L40 colonies should appear slightly pink onto YPD plates and grow to >2 mm in diameter); yeast was also stored at 4°C on YPD plates for up to 2 months.

YPD medium
10 g yeast extract (Difco # 0127-17)
20 g peptone (Difco # 0118-17)
20 g bacto-agar (Difco # 0140-01)
2% glucose
Added H_2O to 950 ml. Adjusted pH to 5.8 then adjust to 1 L. Autoclaved 121°C for 15 min.

YPA medium
10 g yeast extract
20 g peptone
20g bacto-agar
0.1g Adenine hemisulfate salt
Added H_2O to 950 ml. Adjusted pH to 5.8 then adjust to 1 L. Autoclaved 121°C for 15 min.

YC medium
1. YNB w/o aa & $(NH_4)_2SO_4$:
1.2 g yeast nitrogen base, w/o amino acids and ammonium sulfate (Difco # 0335-15-9)
20 g bacto-agar
Added H_2O to 800 ml. The solution were adjusted to pH 5.8 and autoclaved 121°C for 15 min.
2. Salts:
5.4g NaOH
10g succinic acid (Sigma # S-7501)
5g ammonium sulfate (Sigma # A-3920)
3. Glucose:
22g D-glucose
Dissolve in 16 ml H_2O
Add H_2O to 100 ml and dissolve all components one by one. Added glucose and H_2O to make a final volume of 150 ml.
4. amino acids MIX:
5.8 g NaOH
1 g Adenine hemisulfate salts
1 g L-Arginine HCl (Sigma # A-5131)
1 g L-Cysteine (Sigma # C-8277)
1 g L-Threonine (Sigma # T-8625)

0.5 g L-Aspartic acid (Sigma # A-4534)
0.5 g L-Isoleucine (Sigma # I-7383)
0.5 g L-Methionine (Sigma # M-9625)
0.5 g L-Phenylalanine (Sigma # P-5030)
0.5 g L-Proline (Sigma # P-4655)
0.5 g L-Serine (Sigma # S-5511)
Dissolve in 80 ml H_2O
5. L-Tyrosine (Y):
0.5 g L-Tyrosine (Sigma # T-3754)
0.2 g NaOH
Dissolvd in 10 ml by heating
6. Omitted aminoacid solutions:
L-Histidine (H) (Sigma # H-9511):
5 g/l H_2O
Uracil (U) (Sigma # U-0750) :
10 g/l H_2O (+2 pellets NaOH)
L-Leucine (L) (Sigma # L-1512):
10 g/l H_2O
L-Lysine HCl (K) (Sigma # L-1262):
10 g/l H_2O
L-Tryptophan (W) (Sigma # T-0254):
10g/lH_2O

Added to aminoacid MIX the L-Tyrosine solution and H_2O to make a final volume of 100 ml. Filter-sterilized, aliquoted and stored at -20°C for up to 1 year.
Filter-sterilize and aliquot individually omitted amino acids (aa) solutions (H, W, L, K, U) and stored at -20°C for up to 1 year.

All the components were mixed as suggested in Table 2:

	YNB w/o aa & $(NH_4)_2SO_4$	Salts	Aa MIX	W	H	U	L	K	H_2O
-W	800	150	10		10	10	10	10	
-L	800	150	10	10	10	10		10	
-WL	800	150	10		10	10		10	10
-UW	800	150	10		10		10	10	10
-WHUK	800	150	10				10		30
-WHULK	800	150	10						40

Table 2: All the indicated volumes are expressed in ml.

LiAc transformation (small-scale)

This protocol was made by Clontech laboratories. The expected transformation efficiency was 10^3-10^4 / µg plasmid DNA.

Materials

- 10X LiAc buffer: 1 M LiAc, pH 7.5 adjusted with diluted glacial acetic acid filter-sterilized (lithium acetate dehydrate – Sigma # L-6883)
- 50% (w/v) filter-sterilized PEG 4000: polyethylene glycol, avg. mol. wt.=3350-Sigma # P-3640. (Solution must be kept in a tightly sealed glass bottle to avoid evaporation)
- 10X TE buffer: 100 mM Tris, 10 mM EDTA pH7.5, filter-sterilized
- 100% DMSO: dimethyl sulfoxide
- 10 mg/ml denatured herring testes carrier DNA (Clontech # K1606)

Procedure

Day 1: Inoculate few colonies of L40 in 50 ml of YPD and incubated for 16-18 hr with shaking at 250 rpm at 30°C to place the culture at mid log phase the next day (OD_{600} > 1.5).
Note. Use only glass flasks carefully washed with ultra pure, pyrogen-free water and sterilized by autoclaving 15 min at 121°C.

Day 2:

1) Dilute the overnight culture to OD_{600} 0.2-0.3 in 300 ml of YPD prewarmed to 30°C. Grow at 30°C for 3 hours with shaking (230 rpm)

2) Pellet the cells by centrifugation (1000 X g for 5 min) at room temperature, discard the supernatant and resuspend the pellet in 50 ml of H_2O.

3) Centrifuge the cells again as in 2), decant the supernatant

4) Resuspend the pellet in 1.5 ml of freshly prepared 1X TE/LiAc (10mM TE, 0.1M LiAc)

5) Prepare in a tube a mixture of:

- ✓ 0.1 µg LexA-Ag vector construct
- ✓ 0.1 µg scFv-VP16 vector construct (if you need to test specific antigen-antibody partners)
- ✓ 0.1 mg herring testes carrier DNA
- Add 0.6 ml of a sterile PEG/LiAc (0.1 M LiAc, 10mM TE, PEG 4000 40%) to the tube and vortex to mix
- Incubate 30 minutes at 30°C with shaking (230 rpm)
- Add 70 µl of DMSO, mix gently by inversion and heat shock for 15 min in a 42°C water bath.
- Chill cells on ice
- Pellet cells by centrifugation (20 sec at maximum speed)
- Remove supernatant and resuspend cell in 0.5 ml of sterile 1X TE; spread 100 µl for single transformation or 250 µl for a co-transformation on each 100 mm plate.

LiAc transformation (maxi-scale) (protocol #1)

The following transformation protocol was made by Invitrogen laboratories. This protocol was applied for cDNA library transformation when a higher efficiency of transformation (≅10^6/µg DNA) was needed.

Materials

500 µg scFv/VP16/D DNA

150 ml YC-UW

- ✓ 2 l YPAD
- ✓ 1 l YPA
- ✓ 1.5 l YC-UWL + 10 YC-UWL plates (100mm)
- ✓ 1.5 l YC-WHULK + 100 YC-WHULK plates (100mm)
- ✓ 100 ml 10X TE
- ✓ 20 ml 10X LiAc
- ✓ 1 ml of 10 mg/ml denatured salmon sperm

150 ml 50% PEG 4000

20 ml DMSO

Procedure:

1. **Day1**: grow L40 yeast containing bait plasmid in YC-UW O/N
2. **Day2**: inoculate 100 ml of YC-WU with an aliquot of the overnight culture in order to find a dilution that places the 100 ml culture to logarithmic phase the next day
3. **Day3**: transfer enough overnight culture in 1 l of prewarmed to 30°C YPAD to produce an OD_{600} = 0.3
4. Grow at 30°C for 3 hours
5. Centrifuge the cells at 1500 X g for 5 min at room temperature
6. Wash pellet in 500 ml of 1X TE then centrifuge again the cells at 1500 X g for 5 min at room temperature

7. Resuspend pellet in 20 ml 1X LiAc, 0.5X TE and transfer to a new flask
8. Add 500 µg DNA library and 1 ml denatured salmon sperm
9. Add 140 ml of 1X LiAc, 40% PEG 3350, 1X TE; mix and incubate for 30 min at 30°C with gently shaking
10. Add 17.6 ml of DMSO; swirl to mix
11. Heat shock for 10 minutes at 42°C in a water bath swirl occasionally to mix
12. Rapidly cool at room temperature cells in a water bath diluting with 400 ml YPA
13. Pellet cells by centrifugation and wash with 500 ml YPA
14. After centrifugation resuspend pellet in 1 l of prewarmed YPAD
15. Incubate at for 1 hour at 30°C with gently shaking
16. Pellet cells from 1 ml: resuspend in 1 ml YC-UWL; spread 100 µl of a 1:1000, 1:100, 1: 10 dilutions for transformation efficiency controls
17. Pellet cells from the remaining culture
18. Wash pellet with 500 ml YC-UWL
19. Resuspend in 1l of prewarmed YC-UWL and incubate O/N at 30°C with gently shaking
20. **Day4:** pellet cells and wash twice with 500 ml of YC-WHULK
21. Resuspend final pellet in 10 ml of YC-WHULK
22. Spread dilutions of the total on YC-UWL plates to compare to the number of primary transformants
23. Spread the remaining transformation suspension on YC-WHULK plate

LiAc transformation (maxi-scale) (protocol#2)

The same protocol as above but at step 19, the pellet was resuspended in 10 ml. Spread dilutions of the total on YC-UWL plates to compare to the number of primary transformants. Spread the remaining transformation suspension on YC-WHULK plate.

β-galactosidase filter assay

Materials

Nitrocellulose filter circles (Millipore)
Buffer Z (60 mM Na_2HPO_4, 40 mM NaH_2PO_4, 10 mM KCl, 1mM $MgSO_4$, pH 7.0)
50 mg/ml 5-bromo-4-chloro-3-indoyl βD-galactoside
Whatman filter circles
Liquid nitrogen

Procedure

Patch yeast colonies to a nitrocellulose filter circle
Lift filter and place colony side up on a pre-cooled aluminium boat floating upon a sea of liquid nitrogen
After 20 seconds, immerse boat and filter for 5 seconds
Allow the filter to come to room temperature and place on top of Whatman filter circle incubated with 3 ml of Z buffer containing 30 µl of X-gal
Incubate the filter for up to 5 hours. Blue coloration is indicative of β-galactosidase activity.

Preparation of crude yeast lysate for SDS-PAGE analysis

To verify that the bait fusion protein is properly synthesized, an SDS-PAGE and immunoblot analysis on crude yeast lysate must be performed.

Material

master plate with bait-containing positive and control yeasts
antibody to LexA (Invitrogen) or monoclonal/polyclonal to fusion protein

Laemmli sample buffer 4x.

Procedure

Day 1: Incubate overnight at 30°C a 5-ml culture of the bait being tested and relative controls in the appropriate YC medium.

Day 2: From each overnight culture start a new 5-ml culture at OD_{600}= 0.15. Incubate at 30°C until the culture has reached OD_{600}= 0.5-0.7.

Remove 1.5 ml to a tube and centrifuge cells 3 min at maximum speed

Remove the supernatant and working rapidly resuspend in 50 µl of 4x Laemmli sample buffer.

Vortex and place immediately the tube on dry ice.

Boil 5 min and centrifuge 1 min at maximum speed the sample before loading it on SDS-PAGE.

Western immunoblot analysis

The general procedure was described in the previous section. In this case polyclonal antibodies anti-LexA (1:5000) (Invitrogene) and anti-VP16 (1:200) (Clontech) were used followed by anti-rabbi-HPR. While for scFv tagged with SV5, anti-SV5 monoclonal antibody [31] was used at 1:5000.

Constrution of the scFv library

RNA extraction from spleen:

The second step in a two-hybrid assay was the construction of the "fish". In our case, the fish was a scFv library single scFv fused in frame with VP16.

Material

glass homogeniser

choloroform RNAzol TM B kit

isopropanol

ethanol

Procedure

RNA was extracted (RNAzol B kit TEL-TEST, INC®) from the spleen of GST-NSP5 immunised mice. The immunisation protocol is describe at page 40.

1) homogenised spleen with RNAzol ™ B solution (2 ml per 100 mg tissue) with a few strokes in a glass homogenizer.
2) Add 1/10 of chloroform to the homogenate, and shack vigorously for 15 min and let it stay on ice for 5 min.
3) centrifuge the suspension at 12.000xg at 4°C for 15 min. After the centrifugation two phases are formed: the lower blue phenol chloroform phase and the colourless upper aqueous phase whereas the DNA and proteins are in the interphase and organic phase.
4) transfer the aqueous phase to a fresh tube and add an equal volume of isopropanol and store the sample for 15 min at 4°C.
5) centrifuge for 15 min at 4°C at 12.000xg. Precipitated RNA is as a white-yellow pellet at the bottom of the tube.
6) remove the supernatant and wash the pellet once with 75% ethanol by vortexing.
7) centrifuge 8 min at 4°C at 7.500 g.
8) dissolve the RNA pellet in 30 µl DEPC-(diethylpyrocarbonate) water.

cDNA preparation

In an eppendorf tube add the following in order:

- ✓ 1 µl random primers (50 pmol/µl)

- ✓ 3 µl of total RNA (1-5 µg)
- ✓ 8 µl dNTP mix (2.5 mM each dNTP)

1) Heat to 80°C for 3 min and let cool down to about 40° C, spin briefly and add:
   - ✓ 2 µl PCR buffer II (PerkinElmer)
   - ✓ 4 µl $MgCl_2$ 25 mM (PerkinElmer)
   - ✓ 1 µl Rnase inhibitor (20U/µl) (PerkinElmer)
   - ✓ 1 µl MuLV Reverse Trascriptase (PerkinElmer) and mix gently by pipetting up and down
2) Incubate 42°C for 60 min
3) Inactivate at 95°C for 5 min and place the tube on ice.

PCR amplification of V_L and V_H fragments

PCR was carried out using 1/4 of the obtained cDNA. The PCR reactions were performed as follows:

- ✓ 1 µl VKmixFOR (50 pmol/µl)
- ✓ 1 µl VHmixBACK (50 pmol/µl)
- ✓ 10 µl PCR buffer II (PerkinElmer)
- ✓ 4 µl $MgCl_2$ 25 mM (PerkinElmer)
- ✓ 1 µl Taq polymerase Gold 5U/µl (PerkinElmer)
- ✓ sterile distilled water up to 100 µl and mix gently by pipetting up and down

95°C	1 min	30 cycles
60°C	1 min	
72°C	1min 30 sec	
72°C	10 min	
4°C	24h	

A mixture of degenerated primers was used for the PCR of the cDNA. The sequences were reported on Orlandi et al. [50].

Aliquots of PCR reactions were checked on 1.5% agarose gel. PCR products were gel-purified using the electroelution procedure.

Purified V_L PCR products were digested with BssHII and SalI, while V_H PCR products were digested with XhoI and NheI and inserted into pVP16/D in two different steps (Figure 7 page 104).

The ligations mix were electroporated into electrocompetent DH5αF' (Gibco BRL, Rockville, MD) [*F'/endA1 hsdR17(r_K-mK+) supE44 thi-1 recA1 gyrA (Nal^r) relA1 Δ(lacZYA-argF)U169 deoR (ϕ80dlacΔ(lacZ)M15*] and plated on LB 100µg/ml ampicillin plates to obtain the V_L-V_H scFv library. An aliquote of bacteria was used to inoculate a o/n bacterial culture to recover the scFv library DNA (Jetstar®).

The library DNA was transformed into L40 yeast strain expressing the antigen (bait) (Ag-L40) using large-scale lithium acetate transformation. Positive clones were selected using auxotrophic markers for both plasmids and for uracil, lysine and histidine prototrophy [33]. Histidine-positive colonies and controls were lysed in liquid nitrogen and assayed for β-galactosidase activity on filters as described before. All positive clones were grown in selective medium to isolate the plasmid of the scFv (fish) and re-transformed in Ag-L40 yeast for the secondary screening. Moreover, all the positive scFv were sequenced.

Plasmid isolation from yeast

The rapid procedure for the isolation of plasmid DNA from 4 ml of liquid colture of yeast is based on the method from QIAprep Spin Miniprep Kit. Plasmid DNA isolated from yeast is contaminated by yeast genomic DNA: the procedure described below has been successfully used for transformation of *E.coli,* for restriction analysis, PCR screening and sequencing.

Finger printing analysis

Each individual V region of scFv gives an own "fingerprint". Fingerprinting carried out on V genes will give a number of discrete bands. They can be carried out on V regions amplified from cDNA from individual clones: a good library contains different fingerprinting each clone.

Pick one clone with a toothpick and dissolve it in 50 µl ddH_2O. Use 2 µl in PCR reaction mix:

2 µl colony in water
2 µl PCR buffer with 25mM $MgCl_2$ 10X (PerkinElmer)
1.6 µl dNTPs 2.5 mM each dNTP
0.1 µl Taq polymerase Gold 5U/µl (PerkinElmer)
1 µl VP16seq/VP16HSV 10 pmol/µl
1 µl linker for/back10 pmol/µl
ddH_2O up to 20 µl

94°C –1 min	30 cycles
55°C –1 min	
72°C –1 min 30 sec	

72°C-10 min
4°C-24h

Check PCR amplifications on a 1.5% agarose gel, using 3 ml each PCR reaction mix. After verification, use the other 17 µl of reaction mix for digestion:

17 µl DNAmix
0.5 µl BstNI (20U/µl)
3 µl NEB buffer 2 (10X)
0.3 µl BSA (10mg/ml)
9.2 µl ddH_2O

Put to incubate at 60°C for 2 hours. Add 5 µl 6X gel loading buffer to each tube and load on 2% agarose gel. Run 60V-120 min.

Secondary screening of positive Ag-scFv two-hybrid interactions

The final validation for positive and specific interactions was assessed testing Ag and scFvs for His and lacZ gene activation in co-transformed in L40 yeast strain. The specificity of interaction was tested using an irrelevant antigen, as lamin.

Transformation controls for a well-behaved "fish"

When the positive clones are definitively isolated, a test of a well-behaved "fish" was performed as shown in Table 3:

Table 3:

"bait"	"fish"	YC selective medium	HIS3 phenotype	lacZ phenotype
Lamin/BTM116		-WUK		white
Lamin/BTM116		-WUKH	/	
	scFv/VP16	-UKL		white
	scFv/VP16	-UKH	/	
Lamin/BTM116	scFv/VP16	-WUKL		white
Lamin/BTM116	scFv/VP16	-WULKH	/	
Ag/BTM116	scFv/VP16	-WULKH	+	blue

Antibodies Cross-linking to Protein-A Sepharose beads

1 ml of Protein-A Sepharose beads (Pharmacia) was washed twice with 3 volumes of iced PBS by centrifugation at 10.000xg for 30 sec and equilibrated with 3 volumes with incubation buffer (0.2 M $Na_2B_4O_7$ pH 9). 500 μl of binding solution were added to the beads with 20 μl of anti-SV5 monoclonal antibody. After a rocking incubation of 1.5 h at RT, the beads were washed three times with 2 volumes of incubation buffer to eliminate the excess of immunoglobulins. The covalent cross-linking between IgG and protein A was performed treated the beads with 20 mM di-methylpimelidate (DMP Pierce) in incubation buffer for 45 min a RT on a rocker. The reaction was stopped by washing the beads 3 times with stopping solution (0.2 M ethanolamine pH 8) and with a rocking incubation for 2 h at RT with gentle rocking. The beads were washed three times with 2 volumes of PBS and twice with TNN, prepared for the immunoprecipitation of cellular extracts.

Expression of soluble antibody fragments

The scFvs were expressed from the plasmid pDAN3 in HB2151 non suppressor strain [*K12, ara Δ(lac-pro), thi/F' proA+B+, lacI^{q}ZΔ*M15]

Day1:

Inoculate clones directly from the plate in 10 ml 2YT, 100 μg/ml ampicillin, 2% glucose. Incubate in a 30°C shaker overnight at 250 rpm.

Day2:

Inject 5 ml of the overnight stock to 500 ml 2YT, 100 μg/ml ampicillin, 0.1% glucose
Incubate in a 37°C shaker at 250 rpm until bacteria reach O.D.$_{600}$ of 0.6
Induce with 0.5 mM IPTG
Incubate in a 30°C shaker for 4 hours
Collect cells by centrifuging in 500 ml plastic bottles at 6000 rpm for 10 min
Resuspend pellet in 12.5 ml PPB buffer (200 mg/ml Sucrose, 1mM EDTA, 30 mM Tris-HCl pH 8, and one tablet Complete, EDTA-free protease Inhibitor Cocktail Tablets, Boehringer Mannheim). Keep on ice for 20 min
Spin down cells in centrifuge at 5000 rpm for 15 min at 4°C
Collect supernatant
Resuspend pellet in 12.5 ml of 5 mM $MgSO_4$ buffer. Incubate on ice for 20 min
Spin down cells in centrifuge at 5000 rpm for 15 min at 4°C
Collect the supernatant
Load supernatants into dialysis tubing and dialyze overnight in 5L PBS buffer. Change buffer more than once if possible

Day3:

Collect the dialyzed soluble samples and store on ice until Ni-NTA agarose resin column purification, as described above.

Result (2)

The replication cycle of rotavirus occurs totally in the cytoplasm of mammalian cells. Its non-structural proteins function as part of the replication complex, as chaperones to transport RNAs or proteins to the sites of RNA replication, assembly and packaging. Properties of most non-structural proteins are only beginning to be understood. Reverse genetic for rotavirus has not yet been described and it would dramatically enhance the ability of investigation in finding out the role of each viral protein in effecting specific cellular responses. Nevertheless, up to now temperature sensitive mutants and genome reassortment studying are the only described approaches to study the function of the rotavirus proteins. Even though, the function of NSP5 during viral replication and packaging is still unknown. Based on the strong limitation of the lack of reverse genetics, we decided to apply the Intracellular Antibody Capture Technology as a protein knock-out system of rotavirus NSP5 in collaboration with M. Visintin and A. Cattaneo (International School for Advanced Studies in Trieste) for the application of. This strategy uses the two-hybrid system to isolate intracellular competent antibody V regions (in scFv format) able to recognise the non-structural protein NSP5 in the cytoplasm of infected cells. This new strategy could permit to figure out the role of NSP5 and it could allow us its application as "intracellular immunisation" for Rotavirus infection.

The two-hybrid system for antibody-antigen interactions

The classical two-hybrid system in yeast [25] was adapted to monitor the interaction of scFv fragments with their corresponding antigens, under condition of intracellular expression. The procedure is outline in Figure 1 and described in Material and Methods (2).

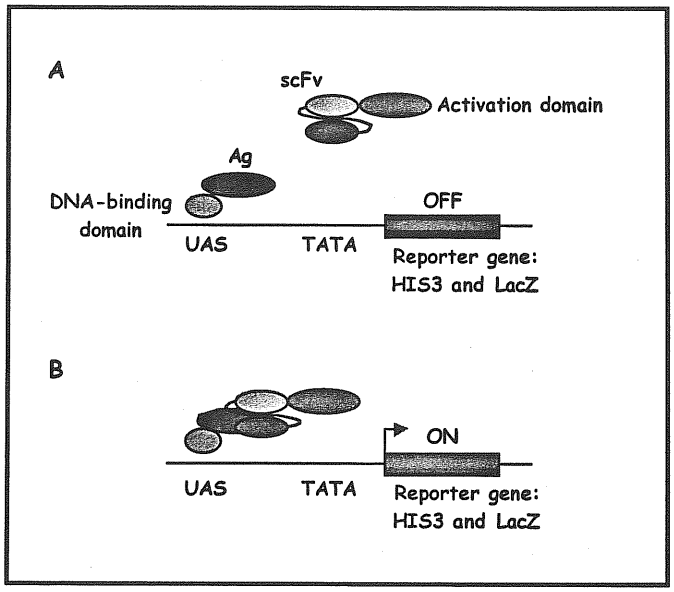

Figure 1: Dual selection/screen using the two-hybrid system. **A)** The antigen (Ag) fused to the DNA-binding domain of *E.coli* repressor LexA is expressed in the yeast strain L40 carrying two reporter genes, lacZ and HIS3, under control of the LexA regulatory sequence. This hybrid protein (bait) can bind to its operator site (upstream activation sequence, UAS) but will not activate transcription. A second plasmid, which expresses the scFv fragments fused to the herpes simplex virus type 1 VP16 transcriptional activation domain, is introduced into the same strain; this hybrid protein (fish) does not bind to the UAS because it lacks the DNA-binding domain. **B)** The interaction between the two fusion proteins through the antigen and the scFv results in the formation of a classical transcription factor composed of a DNA-binding domain and an activation domain which can activate the expression of the reporter genes (HIS3 and LacZ).

In our system, the bait vector is the pBMT116 plasmid [33]. This vector contains a target antigen fused at the C-terminus of DNA-binding domain of the *E.coli* repressor LexA [4] for the expression the bait fusion protein. It contains the TRP1 marker gene for the growth selection in yeast (Figure 2A).

The fish vector (pVP16/D) expresses a library of scFv fragments (V_L-V_H) in frame with two nuclear localisation signals (NLS) located at the N- and C- termini of the scFv followed by the activation domain of the herpes simplex virus type 1 VP16 transcription factor [33]. In this case the vector expresses the LEU2 gene for nutritional selection in yeast (Figure 2B). The pVP16/D was obtained in our laboratory modifying pVP16* [33], by inserting a particular multicloning sites (MCS), which would permit a simpler cloning of scFv fragments from libraries available for phage display technology. In addition, the VP16 transactivation factor sequence of Herpers Simplex Virus type 1 (HSV-1) [33] was reduced at the minimal sequence of the transactivation domain of VP16 protein from 401-479 aa. This protein motif was fused to the C-terminus of V_H (Figure 8).

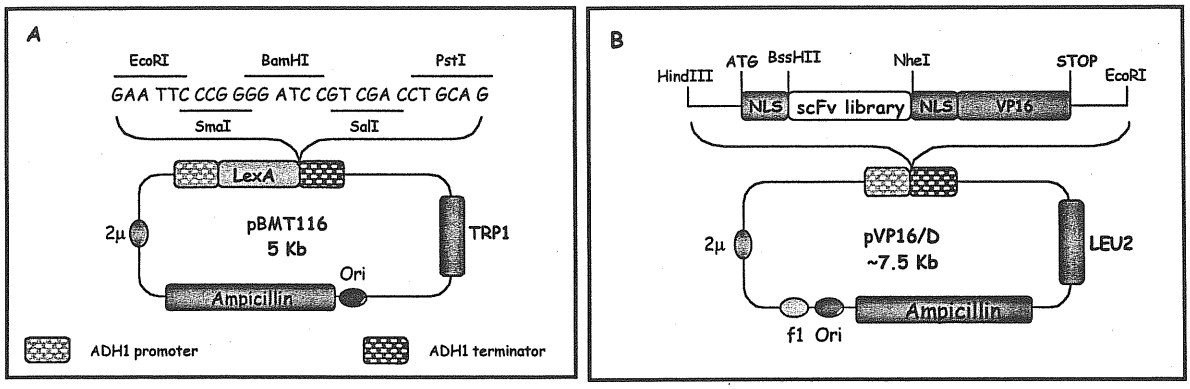

Figure 2: Schemes of the vectors used in the two-hybrid system. **A)** The pBMT116 vector. **B)** The pVP16/D vector.

The L40 strain (Mata *his*3D200 *trp*1-901 *leu*2-3,112 *ade*2 LYS2::(lexAop)$_4$-HIS3 URA3::(lexAop)$_8$-*lac*Z GAL4) is deficient for Trp (W) and Leu (L) (auxotrophic phenotype) and it carries in its genome the yeast biosynthetic HIS3 gene and the bacterial LacZ gene under control of the minimal promoter containing the LexA binding site [33]. Moreover, L40 strain is LYS2+ and URA3+, able to growth in absence of Lys (K) and Uracil (U), because it was originated by insertion of these two genes in a precursor strain, deficient in the synthesis of them [33].

The selection of the library was performed transfecting sequentially the bait and fish vectors in the L40 yeast strain. When the antigen and the scFv fragment are co-expressed in the cytoplasm of yeast and they interact with each other, the complex, driven by the NLS, migrates into the nucleus and binds the UAS *via* LexA (bait). In this way the complex activates the transcription *via* VP16 restoring histidine independent growth of the yeast colonies (Figure 1). The screening for interacting clones is carried out by nutritional selections as histidine (H) and for triptophan (W) and leucin (L), because they are the selection marker genes present in bait and fish vector respectively (Figure2). The selective medium also lacks Ura and Lys, because they are expressed by the L40 strain, thus maintaining it under selection (Figure 1). Moreover, the interaction is confirmed with the β-galactosidase activity assay,

Preparation of the NSP5 bait-antigen

To perform the two-hybrid system in yeast it is essential to test the bait, in this case the antigen NSP5, to rule out any unspecific trans-activation activity on the two reporter genes. Full length NSP5 was first cloned in the pBMT116 vector, and transformed in the L40 yeast strain. Growth of colonies on medium lacking Histidine, followed by β-galactosidase assay, revealed that LexA-NSP5 was able to activate the two reporter genes, thus making this bait not adequate for the scFv library selection (Figure 3, panel a). We then decided to test the activity of some NSP5 deletion mutants already available in our laboratory. Figure 4 indicates a scheme of all the NSP5 deletion mutants used in this test. Their coding regions were amplified by PCR and cloned in the pBMT116 vector in fusion with LexA. Figure 3 shows the β-galactosidase assay of all tested NSP5 deletion mutants. LexA-Δ2, -Δ4 and -ΔC48 appear to perform well as bait, because these three deletion mutants don't show activation of the two reporter genes (Figure 3 panels b, d and f).

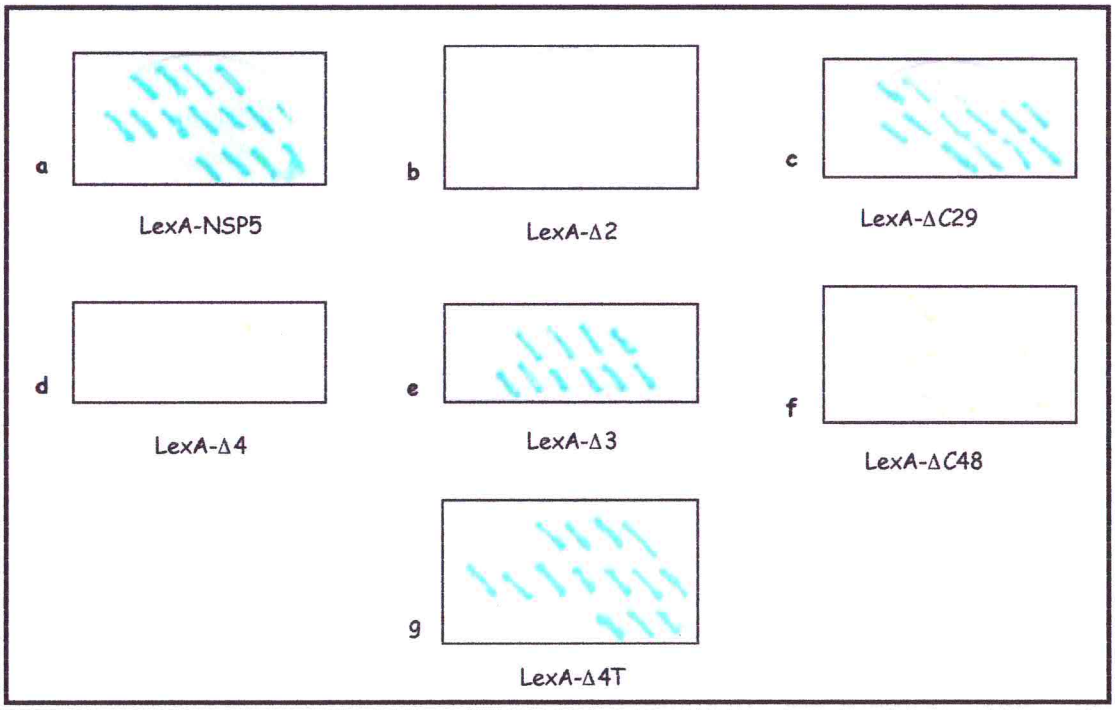

Figure 3: β-galactosidase assay performed on colonies grown on –WUK plates to test different baits. a, NSP5 full length; b-g, different NSP5 deletion mutants.

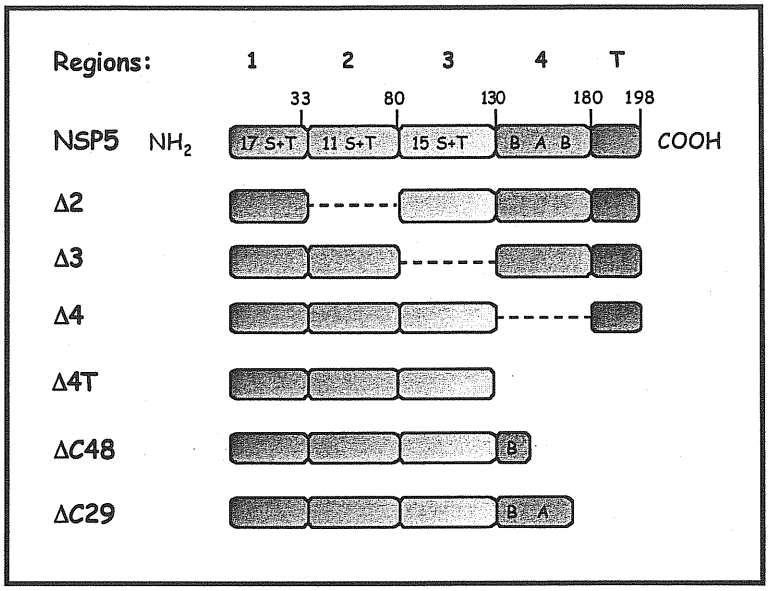

Figure 4: Schematic representation of NSP5 deletion mutants. In each region of wt NSP5 is indicated the relative Ser+Thr content. B-A-B indicates the 49 aa long highly charged (61% of charged residues) basic-acid-basic domain. The last 18 aa represent the "tail" (=T).

All three good baits were well expressed in yeast as shown in the Western immuoblotting of total yeast extracts (Figure 5).

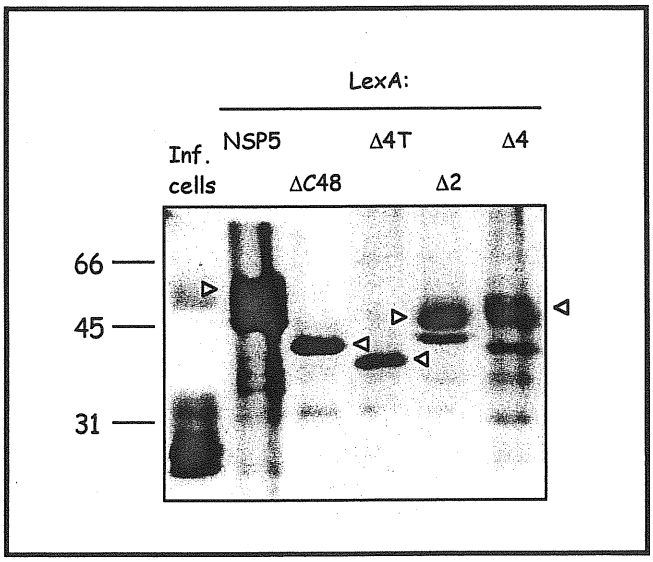

Figure 5: Western immunoblotting using anti-NSP5 sera of total yeast extracts electrophored on SDS-PAGE gel. The yeast was transformed with the indicated baits (LexA fusion proteins). SA11 infected cellular extract is the positive control (lane 1). The open arrowheads indicate the correct position of the fusion proteins.

Among these constructs we chose LexA-Δ2 to screen the scFv library, because it is the mutant with a deletion of only region 2, while the region 4 is maintained. As shown in the Result (1) (Figure 15) region 4 appeared to be essential for NSP5 phosphorylation. We chose this mutant because NSP5 presents a particular pattern of phosphorylation [1], involving exactly the region 4. For this reason, we decided maintain this region in the bait in order to have the possibility to fish out scFvs able to recognise this portion of the protein.

Preparation of the scFv library from immunised mice

Up to now the scFv libraries available for the two-hybrid system have been produced as human naïve library cloned in pVP16* vector from V_H-V_L phage-display libraries [67, 73]. We decide to prepare a new V_L-V_H library from immunised mice, because this could enhance the probability to find V_L-V_H combinations from mature and high affinity immunoglobulins (Ig) against the antigen, and also because mice are responsive animal for the immunisation with a rotavirus protein NSP5.

The first step consisted in immunisation of mice with recombinant NSP5 fused to GST. Immunesera were tested in Western blotting on NSP5 cellular extracts of MA104 cells infected with SA11 and uninfected cells, as negative control (Figure 6).

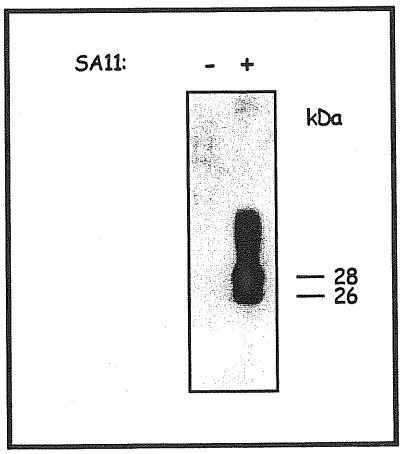

Figure 6: Western immunoblotting of total cellular extracts of uninfected and SA11-infected MA104 cells using a serum of immunised mouse.

In the second step we extracted RNA from splenocytes of three positive animals and a mixture of all three RNA preparations was used as template in RT-PCR to amplify the

fragments of both V_L and V_H repertoires. We used a set of degenerate primers homologous to frameworks 1 and 4 of the different V_L and V_H families [50]. In Material and Method (2) section the strategy is described more precisely. The V_L and V_H fragments were sequentially cloned in the pVP16/D vector to generate the library of scFvs (pVP16/D V_LV_H) for the two-hybrid system selection (Figure 7). The C-terminus of the V_L fragment is joined to the N-terminus of V_H fragment by a flexible linker of 18 aminoacidic residues GSTSGSGKPGSGEGSSGT derived from the "218 linker" [78] (Figure 8).

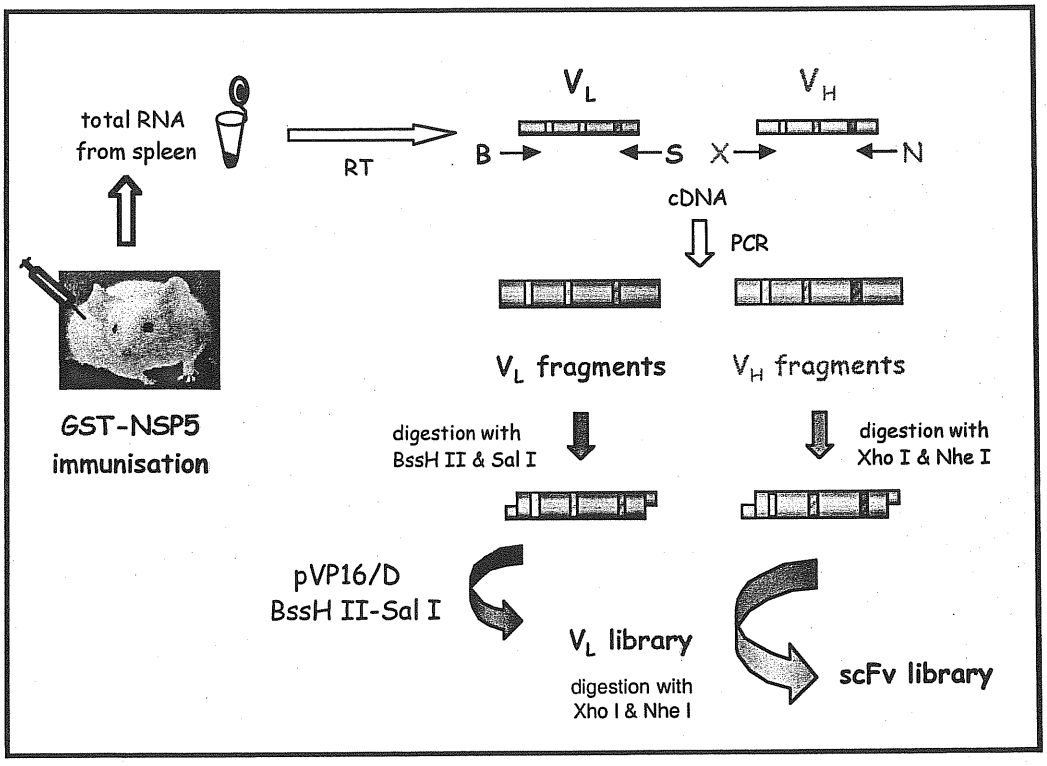

Figure 7: Scheme of the strategy for the preparation of scFv library. The blue bars indicate the V_H repertoires while the yellow the V_L. The colourful rectangles in the V fragments represent the CDRs surrounded by the frameworks.

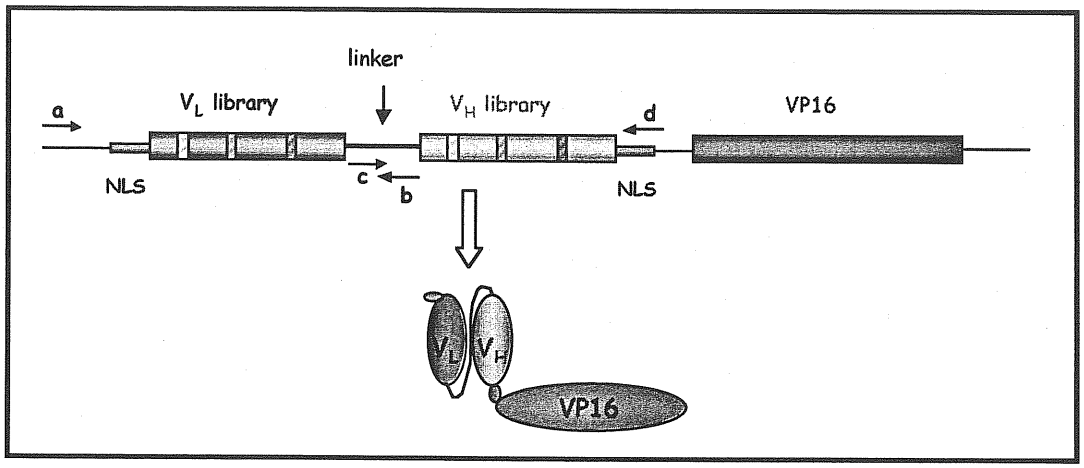

Figure 8: Scheme of the pVP16/D V_LV_H construct and the expressed fusion protein in yeast. NLS are the nuclear localisation signals. The primers for the PCR used in the screening of the library's diversity are indicated as a-b and c-d.

The partial library pVP16/DV_L was tested for the diversity by finger printing analysis of several different colonies out of $1x10^5$ totally obtained. This was done performing PCRs directly on different bacterial colonies, using primers (a and b) specific for the vector pVP16/D to amplify the V_L cloned regions (Figure 8). The PCR products were digested with BstNI, an enzyme with a short sequence recognition (4bp), which cuts frequently in coding regions. The patterns obtained for each colony were different and Figure 9A shows an example of 10 reactions.

The partial V_L library was then used to clone the amplified V_H fragments. We obtain $4x10^4$ clones and also in this case a number of randomly picked colonies were analysed for the V_H diversity. Figure 9B shows the patterns of different colonies analysed by fingerprinting using primers c and d (Figure 8).

The results indicated that the mouse scFv library in the pVP16/D vector (pVP16/D V_LVH) contained a total of $\underline{4x10^4}$ clones with diversity larger than 90% as detected from our analysis.

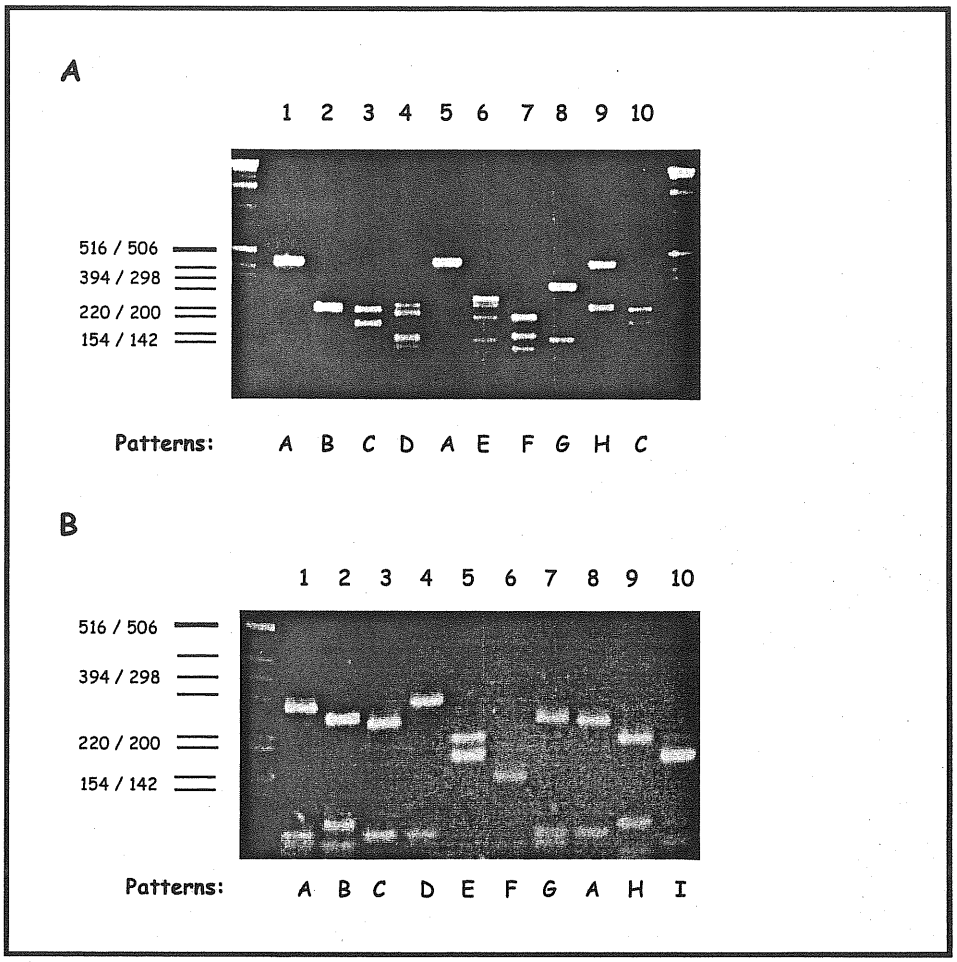

Figure 9: Finger print analysis of 10 different bacterial colonies. Each PCR product was digested with BstNI and electrophoresed on 2% agarose gel. The upper panel **(A)** shows the finger printing of ten different V_L fragments from colonies containing pVP16/D V_L constructs (half-library), while the lower panel **(B)** shows the pattern of ten different V_H fragments from colonies containing pVP16/D V_L V_H (scFv library).

Screening of the scFv library

First selection

In the first selection, we transformed L40-Δ2 (using protocol #1) with 100 µg of pVP16/D V_LV_H, obtaining an efficiency of $2x10^6$ colonies/µg of DNA. We plated 1/1000 of the total yeast culture on selective medium (-WULKH) and we obtained 2000 colonies. This selective medium does not contain all the aminoacids responsible for the selection of all the elements of the two-hybrid system. (W: bait vector, L: library vector, H: interaction of the bait and fish, U and K to avoid any genetic reversion of the L40 strain). 100 clones were

randomly picked on selective plates and replated on the two selective plates (-WULKH), to perform the β-galactosidase assay and to characterise the DNA by finger printing. All the 100 colonies were positive in the β-galactosidase assay (data not shown).

PCR analysis was then performed directly on 100 yeast colonies using primers (a and d, Figure 8) specific for the vector pVP16/D to amplify the whole (V_L and V_H) cloned scFv. 73 reactions gave a PCR product (data not shown). We performed the finger print analysis and found out 11 different patterns each one differently represented (Figure 10).

Finger printing patterns	Number of colonies
A3	32
A19	2
A17	1
A22	8
B5	11
B6	8
B11	2
C14	1
D3	4
D14	1
D24	4

The pVP16/D plasmids were isolated from the 11 representative yeast clones and used to transform bacteria to recover a quantity of plasmid DNA sufficient to perform the second screening. The 11 constructs (pVP16/D scFv) were retransformed in L40 yeast expressing the antigen Δ2 (L40-Δ2) to eliminate possible false positive clones. In addition, they were also transformed into L40 strain expressing an irrelevant bait (LexA-lamin) in order to verify their specificity for the antigen. Also this second screening was performed with nutritional selection for histidine followed by the β-galactosidase activity assay.

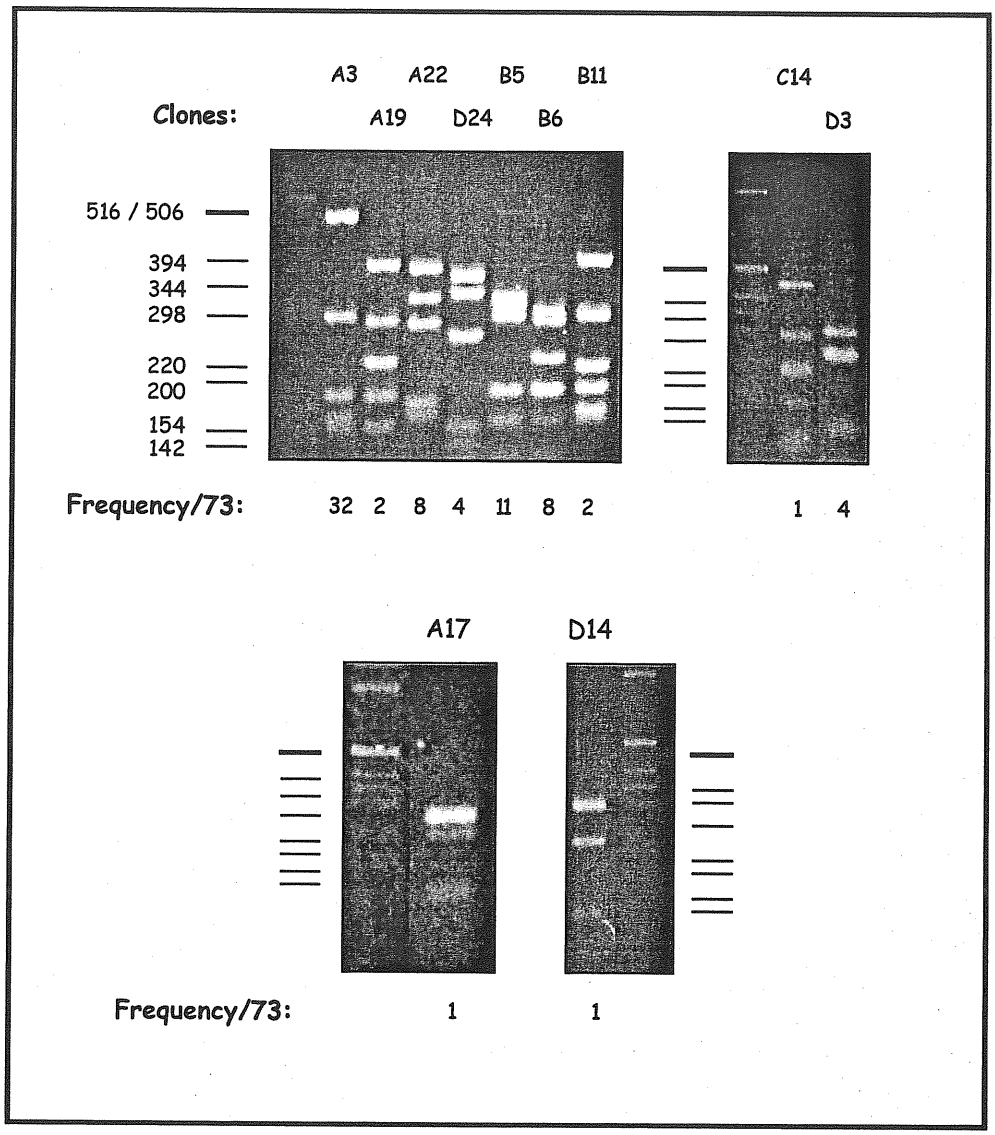

Figure 10: Finger print analysis of the 73 PCR products obtained from positive blue colonies.

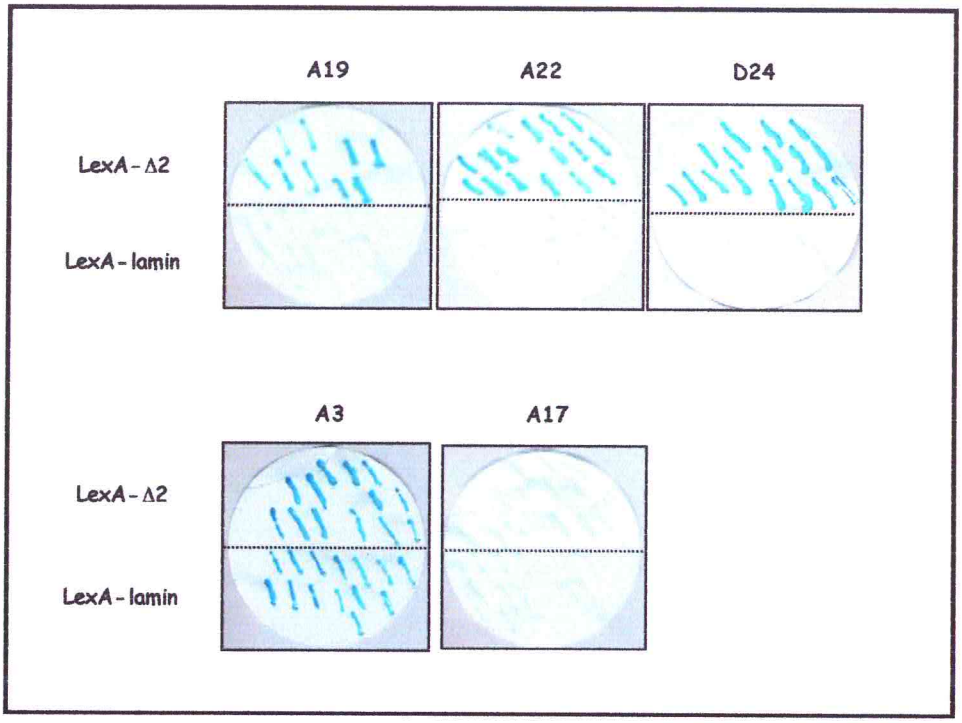

Figure 11: β-galactosidase assay performed on colonies grown on-WULK plates. The assay shows three specific scFvs are A19, A22 and D24, the false positive A17 and the unspecific A3

From this screening three clones (A19, A22, D24) showed specificity for LexA-Δ2, five recognised lamin (A3, B5, B6, B11, D3), and three were false positive because didn't recognise again LexA-Δ2 (A17, D14, C14) (Figure 11). With this screening protocol we fish out 3 scFvs specific for Δ2 out of 11 different scFvs. Nevertheless, a quite high number of unspecific scFvs and false positives were isolated. Eliminating the number of false positive scFvs (3), which are normally frequent during two-hybrid system selection, ~40% (3 out 8) were in the end specific. Analysing the protocols used for the transformation of the library, we decided to perform some modifications on protocol 1 to reduce the selection of redundant clones, since some of them like the non-specific A3, B5 and B6 or specific as A22 were highly repeated.

ScFvs expression in yeast

The A19, A22 and D24 yeast colonies, carrying LexA-Δ2 and each scFv, were grown on selective medium (-WULKH) to verify in Western immunoblotting the expression of the two partners: the Δ2 bait and the scFvs (Figure 12). Either the bait (Δ2) or the scFvs are well expressed in yeast.

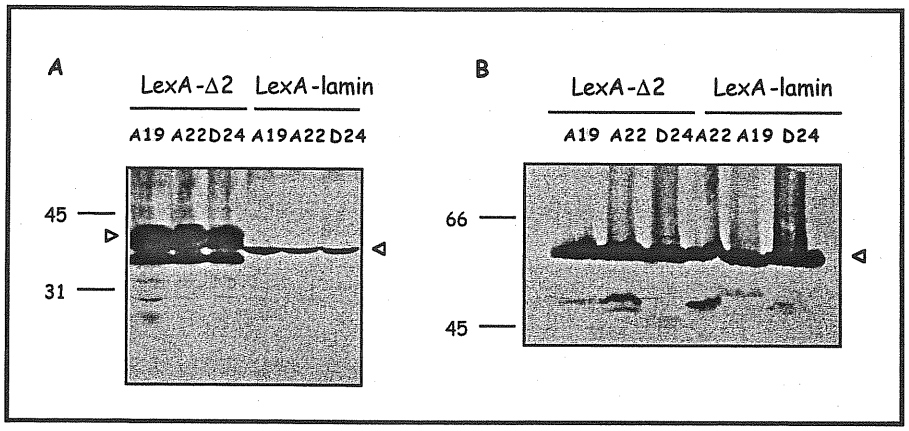

Figure 12: Western immunblotting of total extracts of yeast cotransformed with LexA-Δ2 or LexA-lamin and the scFvs (A19, A22, and D24). The total yeast extracts containing the bait and the scFv were loaded on two separate SDS-PAGE gels. Panel **A** shows the presence of the bait, using anti-LexA antibody and panel **B** shows the scFvs using anti-VP16 antibody.

Second selection

From the first selection we found ~60% (5 out 8) of non-specific scFvs. We thought that this high drawback was due to a positive selection of the most "stable" scFvs during the growth on last step of the library transformation. To avoid this disadvantage, we modified the protocol#1 for the library selection in protocol#2 (page 92). Essentially, we decided to eliminate the step of growth in liquid medium after transformation, proceeding directly to the plating on the selective plates (-WULKH).

We therefore performed a second selection of the same library (pVP16/D V_LV_H) on the LexA-Δ2 bait, obtaining an efficiency of transformation of $4x10^5$ /μg DNA. We plated 1/100 of the total yeast culture on selective medium (-WULKH) and obtaining 200 colonies. All of them were picked and replated on the two selective plates (-WULKH), to perform the β-galactosidase assay and to characterise the DNA by finger printing. Only 4 colonies out 200 were negative in the β-galactosidase assay (data not shown).

The pVP16/D scFv plasmids were extracted from 20 blue yeast colonies, growth in liquid selective medium (-WULKH), and used to transform bacteria. PCR was performed on bacteria colonies, followed by the finger printing analysis. We found 6 different patterns each one differently represented (Figure 13).

Finger printing patterns	Number of colonies
A3	13
A22	3
7	1
11	1
14	1
20	1

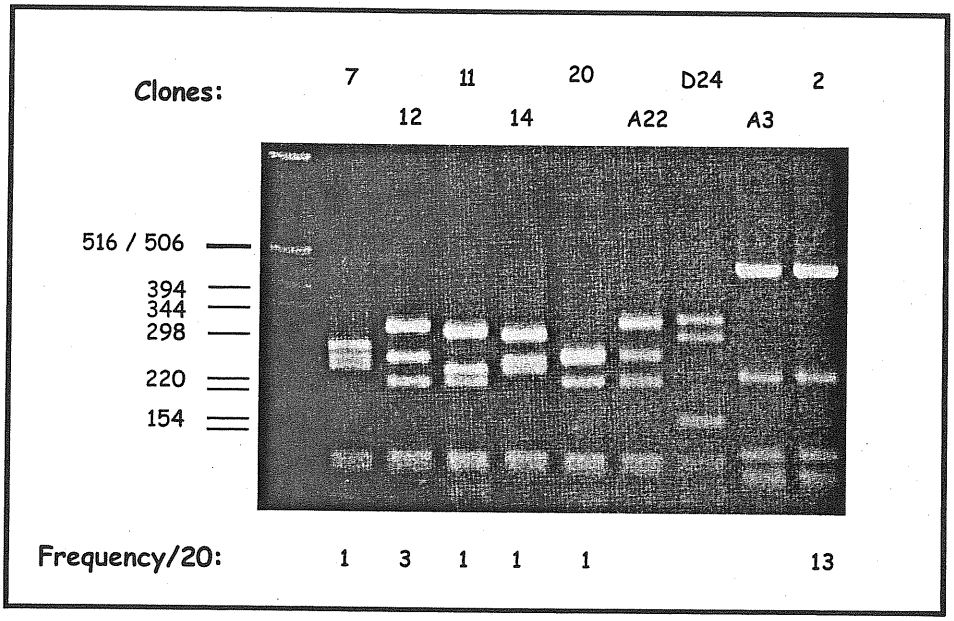

Figure 13: Comparison of selected finger printing patterns from 20 PCR products from positive blue clones. A22, D24 and A3 were used as reference finger printing patterns.

Four patterns (7, 11, 14 and 20) were different from the previously selected ones, while 2 corresponded to the pattern of the clone A3 (Δ2 non specific) and A22 (Δ2 specific). The 4 new scFv plasmids were used to perform a second screening in L40-Δ2 and in L40-lamin yeast strain. None of them recognised lamin, and two were strongly positive for LexA-Δ2 (14 and 20) (Figure 14), while clone 7 and 11 were only weakly positive (data not shown).

In this screening the total number of unspecific clones is still quite high, 65% (13 out 20) in comparison with the first screening 44% (32 out 73), while if we consider the efficiency to fish out good clones appears to be higher. In fact, from only 20 colonies analysed we fished out 5 good scFvs (7, 11, 14, 20 and A22). This is a higher number than the positive clones (3) found during the first selection based on 73 PCRs. In conclusion, the efficiency to find specific scFv was ~ 80% in the second screening using the second protocol (5 out 6) with respect to 40% (3 out 8) using the first protocol.

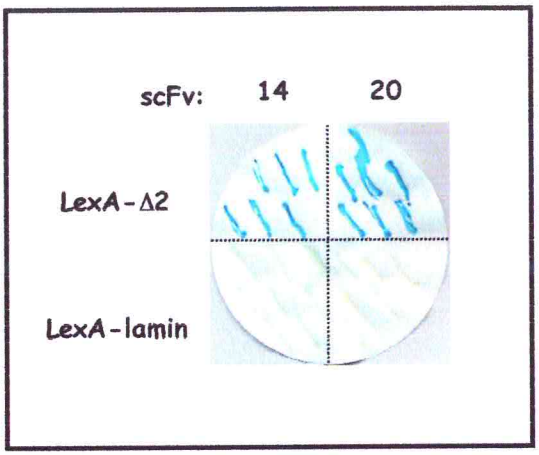

Figure 14: β-galactosidase assay performed on colonies grown on -WULK plates. The scFvs 14 and 20 interact specifically with the bait LexA-Δ2, while not with the irrelevant bait LexA-lamin.

Is this library selectable for other antigens?

To find out if the pVP16/D V_L-V_H library could be a source of scFvs specific for other different antigens, inspite of the fact that it was derived from immunised animals, we decide to perform a screening against another protein: ShcA.

The Shc family of adapter proteins are involved in signalling events that lead to mitogenesis as differentiation in several receptor systems [44]. ShcA is widely expressed, but has been not revealed in haematopoietic cells. ShcA shows three isoformes, 46, 52 and 66kDa, which are splicing variants of a single gene. ShcA contains N-terminal phosphotyrosine-binding (PTB) domain, central proline-rich (CH_1) domain and C-terminal Src-homology (SH_2) domain [44]. The p66 ShcA isoform encodes an additional NH_2-terminal CH_2 domain, which is unique within the ShcA family (Figure 15).

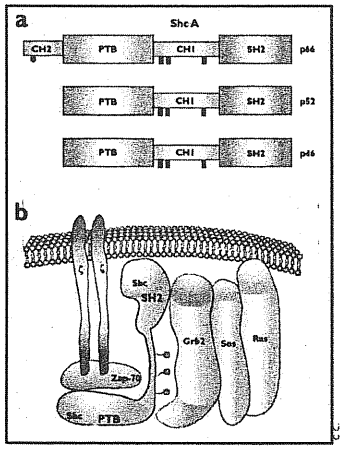

Figure 15: Scheme of protein ShcA family [59]. p66 isoform shows a unique domain called CH_2.

Michela Visintin (ISAS, Trieste) screened the mouse pVP16/D V_L-V_H library against the N-terminal CH_2 domain of the p66 isoform of ShcA ($ShcCH_2$). Protocol 2 was used obtaining an efficiency of transformation of $5x10^5/\mu g$ DNA. PCR and finger printing analysis were performed using 20 yeast colonies grown on -WULKH plates. One clone showed a shorter PCR product (13b, data not shown) and it was excluded. Figure 16 shows 8 different patterns observed out of 20 electrophoresed on agarose gel, each one differently represented.

Finger printing patterns	Number of colonies
1b	1
2b	1
3b	6
4b	6
8b	1
10b	2
16b	1
20b	1

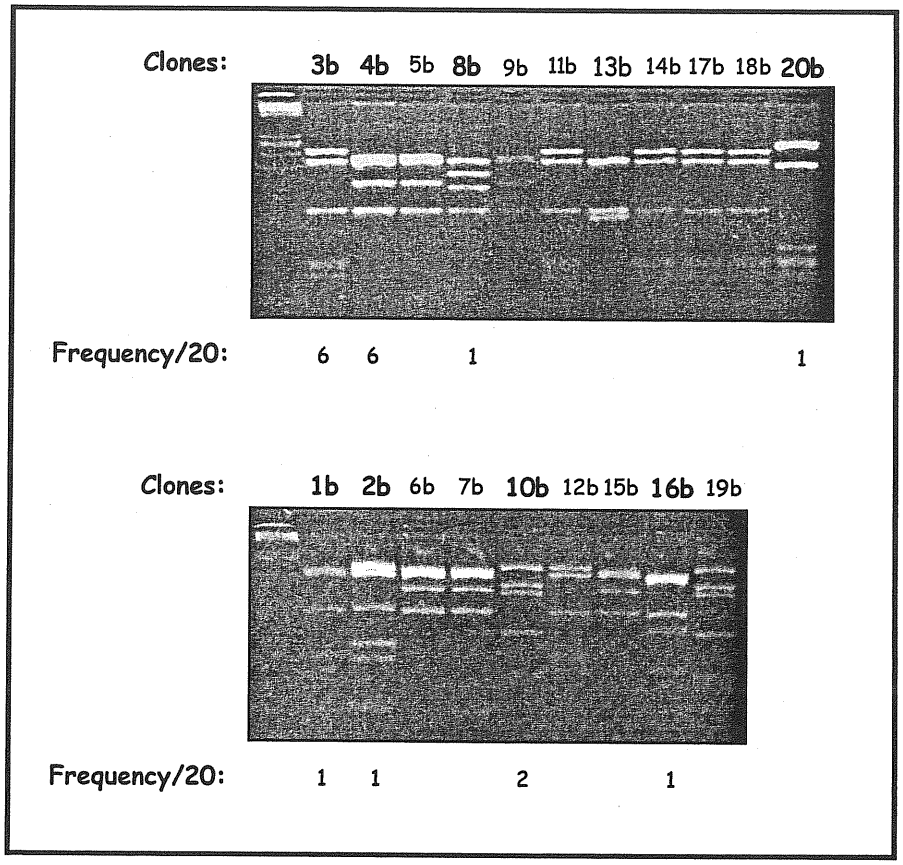

Figure 16: Finger printing of 20 positive clones selected against LexA-ShcCH$_2$. In bold are marked the finger printing patterns of the representative clones.

All 20 scFvs were tested in the second screening in L40 expressing ShcCH$_2$ or the irrelevant bait LexA-lamin. Figure 17 shows the β-galactosidase assay of –WULK plates with L40 yeast expressing bait and fish as indicated. 16 scFvs were found specifically positive against LexA-ShcCH$_2$ yeast. Two clones (10b and 19b) were strongly positive against the lamin (irrelevant bait) and 2 weakly (9b, and 6b) (Figure 17).

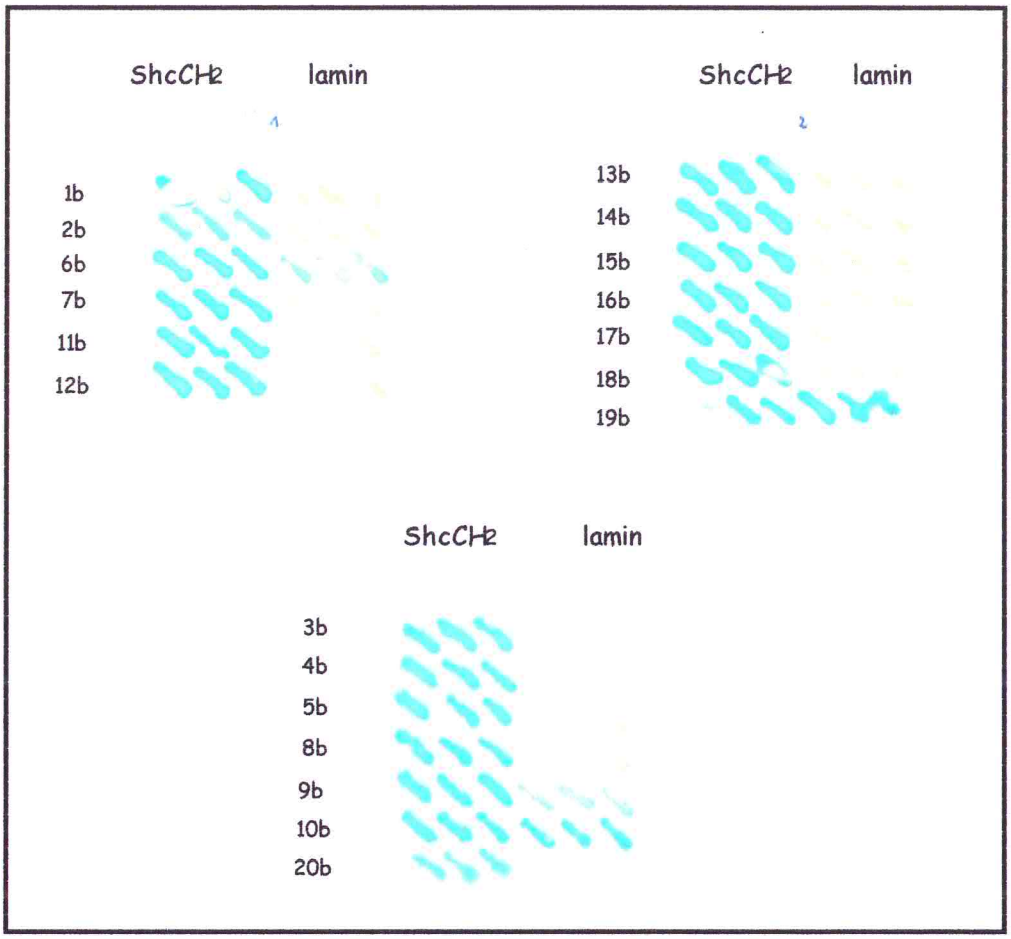

Figure 17: β-galactosidase assay of 20 scFvs performed on colonies grown on -WULK plates. The scFvs were tested with the bait LexA–$ShcCH_2$, and the irrelevant LexA-lamin.

With this screening we can conclude an important feature of this pVP16/D V_L-V_H library, hat it could be a source of scFvs able to recognise different antigens in the two-hybrid-system, eventhough it was derived from an immunised repertoire of immunoglobulins.

Analysis of the sequences of the intrabodies

The five sequenced intrabodies (A19, A22, D24, 14 and 20) were analysed and aligned using http://www.ebi.ac.uk/clustalw/. Figure 18 indicates the V_L and V_H alignment and the positions of the CDR1, 2 and 3 are indicated in violet.

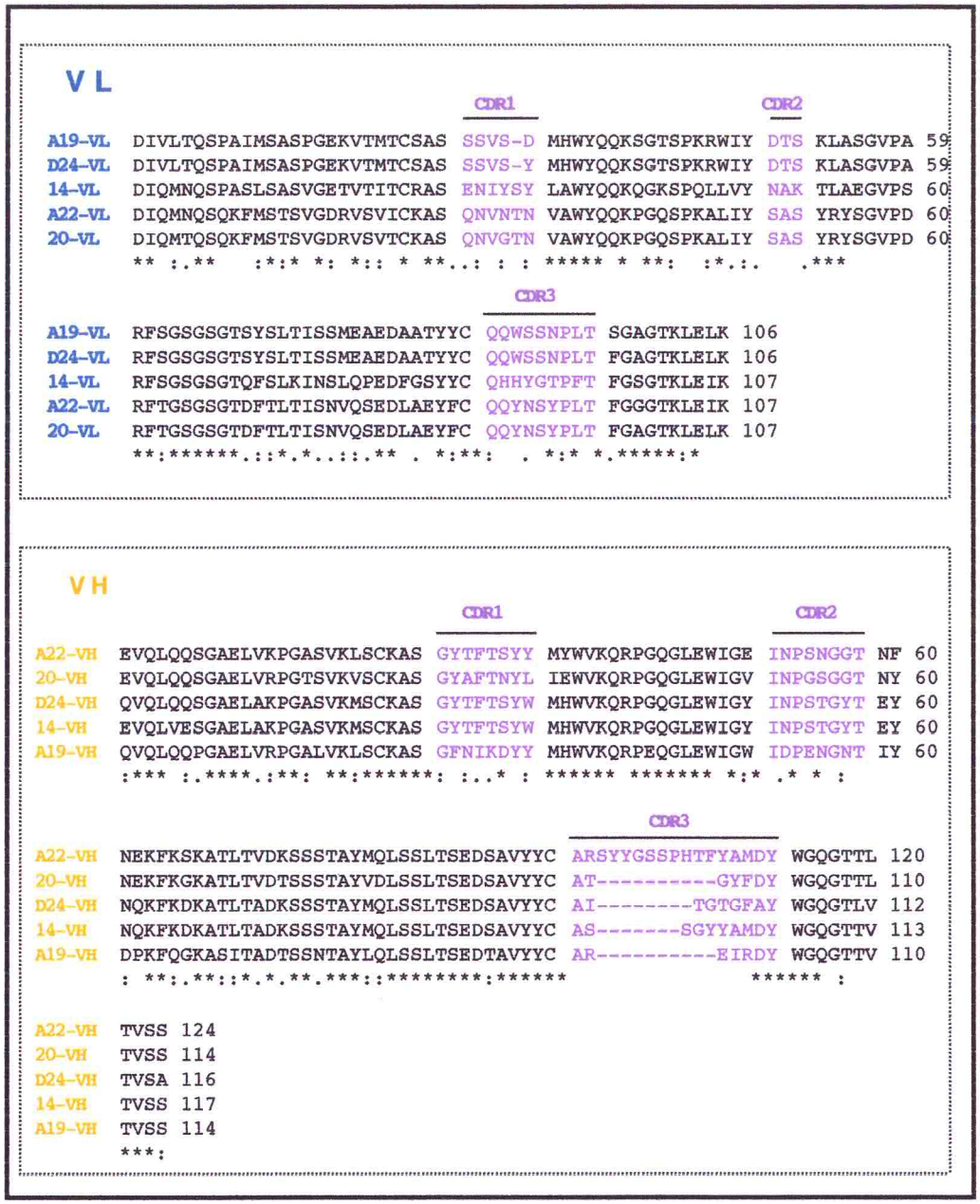

Figure 18: Alignment of V_L and V_H of the anti-Δ2 scFvs with http://www.ebi.ac.uk/clustalw/. In violet are indicated the CDR 1,2 and 3 while in black the 4 frameworks
"*"the residues are identical in all sequences in the alignment.
":"conserved substitutions.
"."semi-conserved substitutions.

We performed also an analysis of all the V_L and V_H regions of the five scFvs using the better database available for the mouse immunoglobulins: http://imgt.cines.fr. The database performed automatically the DNA alignments of the V_H and V_L sequences with germline sequences of mouse immunoglobulins indicating the J genes for both variable regions and D genes for V_H regions (Table 1).

Variable regions	Ig germline genes	aa difference	Ig J genes	IgHD genes	
A19 V_H	HV14S2		HJ4	n.d	GL
A19 V_L	KV4-59	CDR1 (Y→D)	KJ5		SM
A22 V_H	HV1S120		HJ4	FL16.1 (♦)	GL
A22 V_L	KV6-15	FR1 (T→I) CDR1 (G→N)	KJ2		SM
D24 V_H	HV1S27	FR1 (A→G, R→K) CDR1 (T→W) CDR2 (S→T) FR3 (T→A)	JH3	Q52 (♦)	SM
D24 V_L	KV4-59		KJ5		GL
14 V_H	HV1S27	FR1(A→G, R→K) CDR1 (T→W) CDR2 (S→T) FR3 (T→A)	HJ4	ST4	SM
14 V_L	KV12-44		KJ4		GL
20 V_H	HV1S23 H1S130	Shuffling* FR3 (P →L)	HJ2	Q52	GL
20 V_L	KV6-15		KJ5		GL

Table 1: The table reports the germline genes for each variable region of the 5 selected scFvs, the position of eventual different aa, the J genes for V_L and V_H and D genes for the V_H regions. GL indicates germline variable regions, SM indicates somatic mutated variable regions. * 20 V_H represents a particular case of shuffling of 2 different variable heavy regions during PCR reaction. In this case the VH regions is a hybrid fragment from two different germline genes: FR1 to CDR2 from IGHV1S23 gene and the FR3 from IGH1S130 gene. We considered it a germline gene. (♦) represents N nucleotides added during V-D-J recombination at 5' and 3' of the D gene.

This analysis suggested that during our *in vivo* selection of intrabodies by two-hybrid system, we obtained variable regions from germline genes (A19 V_H, A22 V_H, D24 V_L,14 V_L 20 V_H and 20 V_L) as well as from somatic mutated ones (A19 V_L, A22 V_L, D24 V_H,14 V_H.

The scFv 20 contained both variable fragments, which we considered derived from a germline genes. In particular, the V_H region was found as hybrid of two germline genes probably fused during the PCR reaction. A particular situation emerged from two scFvs D24 and 14, which presented the same variable heavy region V_H (HV1S27 germline gene) carrying the same point mutations (five), in the CDR1 and CDR2. Since the same somatic mutations formed through two indipendent events (two different lymphocytes) is a impossible process, we thought that most probably the variable region (from FR1 to FR3) was joined with two different CDR3 during the PCR amplification, creating hybrid molecules. In the Discussion (2) we described more in detailed other possible explanations. Other variable regions (A19 V_L, A22V_L, 20 V_H) presented mutations only in FR1 and/or CDR1. The main result from this computational analysis showed that we can not draw important conclusions regarding the advantage of using a scFv library from immunised mice, because the relative small number of clones identified (five) and the fact that we found a low number of somatic mutations.

Expression of the intrabodies in mammalian cells

An important step for the application of the intrabodies *in vivo* is to test whether they can be expressed in the cytoplasm of mammalian cells or targeted in some intracellular compartment to divert the Ag in order to subtract it from its usual environment.

In our case we chose to express the intrabodies as cytoplasmic and nuclear tagged proteins in order to divert NSP5 into the nucleus (Figure 19).

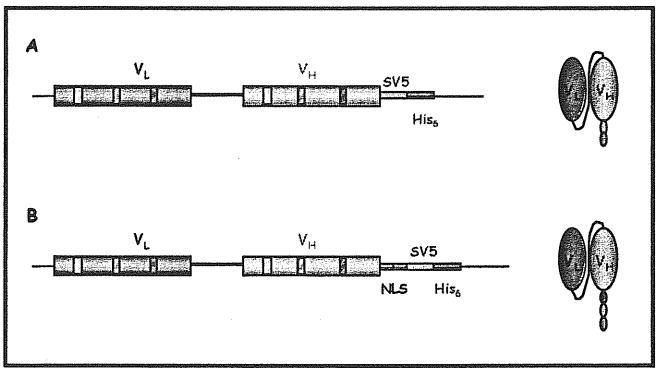

Figure 19: Scheme of the scFv formats for cytoplasmic and nuclear localisation. The scFvs carry an SV5 tag and a His_6 tag at its C-terminus. Panel **A** shows the cytoplasmic format, while thepnel **B** the nuclear format. NLS indicates the nuclear localisation signal responsible of diverting the scFvs into the nucleus of mammalian cells.

For this purpose, 5 specific intrabodies for NSP5 (A19, A22, D24, 14 and 20) and the irrelevant $ShcCH_2$ (clone $ShcCH_2$ 3b) specific for ShcA were cloned in the pcDNA3 vector in order to express them intracellularly in mammalian MA104 cells. We chose this cell line because it is the usual host for rotavirus replication, so we could investigate the effect of these specific scFvs during the viral cycle.

We tested the expression of the intrabodies in mammalian cells by Western blotting using monoclonal antibody against the SV5 tag [31] (Figure 20). A time course of transient transfection was performed for only two scFvs (A19, D24) and we monitored the expression level of the protein at 28 up to 36 hour post-transfection (p.t.) (Figure 20). Moreover, the scFvs were expressed also as nuclear diverted protein through a tandem repetition at its C-terminus of two nuclear localisation signals (NLS) from SV40 (Figure 19). The scFvs (cytoplasmic localisation) and scFvs(NLS) were expressed in MA104 cells previously infected with T_7 DNA polymerase recombinant vaccinia virus (strain vTF7.3). After 16 hours we performed the cellular lyses and the cellular exctrats were loaded on SDS-PAE gel. Figure 20 shows the total cellular extracts tested in Western immuoblotting using the anti-SV5 monoclonal antibody.

All the scFvs were well expressed in MA104 cells in transient transfection either between 28-36 hours p.t. or with T_7-vaccinia virus system after 16 hours as cytoplasmic and nuclear tagged proteins.

In a second step we tested the interaction of the scFvs and the antigen by co-transfection of the scFvs with Δ2 protein, the NSP5 deletion mutant used for the selection of the library in yeast. In particular, the nuclear tagged scFvs were co-transfected with Δ2 in MA104 cells and their interaction was analysed by immunofluorescence and immunoprecipitation assays.

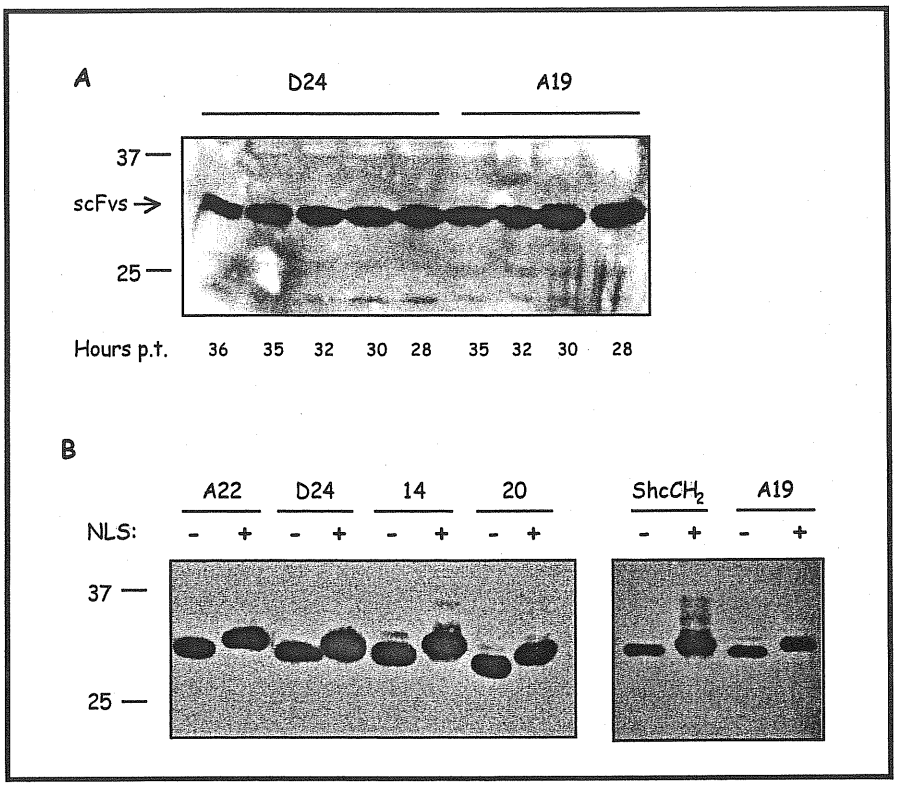

Figure 20: Western immunoblotting of total cellular extracts of MA104 transfected with scFvs using anti-SV5 monoclonal antibody.
Panel A shows the total cellular extracts of transfected MA104 with two scFvs (A19 and D24) harvested at different times. Panel B shows all the scFvs expressed with the T_7-vaccinia virus system. The scFv(NLS) and scFv are indicated as nuclear tagged and cytoplasmic expressed protein.

Immunofluorescence analysis: Δ2 and the intrabodies

The interaction between scFvs and the Δ2 antigen in mammalian cells was investigated with immunofluorescence assays. The antigen Δ2 (like full length NSP5 and its mutants) is known to be a cytoplasmic protein [1] (Figure 21, panel f). The scFv was visualised using a monoclonal antibody specific for the SV5 tag located downstream of the NLS (Figure 19), followed by an anti-mouse RITC conjugated antibody. The antigen Δ2, fused with EGFP at its N-terminal, was detected directly as green fluorescence.

Figure 21 shows an immunofluorescence analysis performed at 30 hours p.t. of MA104 cells transfected either with scFvs(NLS) or Δ2-EGFP. The scFv(NLS) migrates into the nucleus of the transfected cells, while the antigen Δ2-EGFP is diffused in the cytoplasm. In both cases the distribution of the proteins is clearly homogeneous.

When the two constructs expressing Δ2-EGFP and scFv(NLS) were co-transfected, the distribution of both partners changed dramatically. Figure 22 shows the scFvs with the Δ2-EGFP forming characteristic aggresomes in the cytoplasm of the cells with a perfect co-localisation of the two partners (antigen and intrabody). The scFvs were not able to migrate into the nucleus any longer, while the antigen (Δ2-EGFP) is no longer homogenously distributed in the cytoplasm.

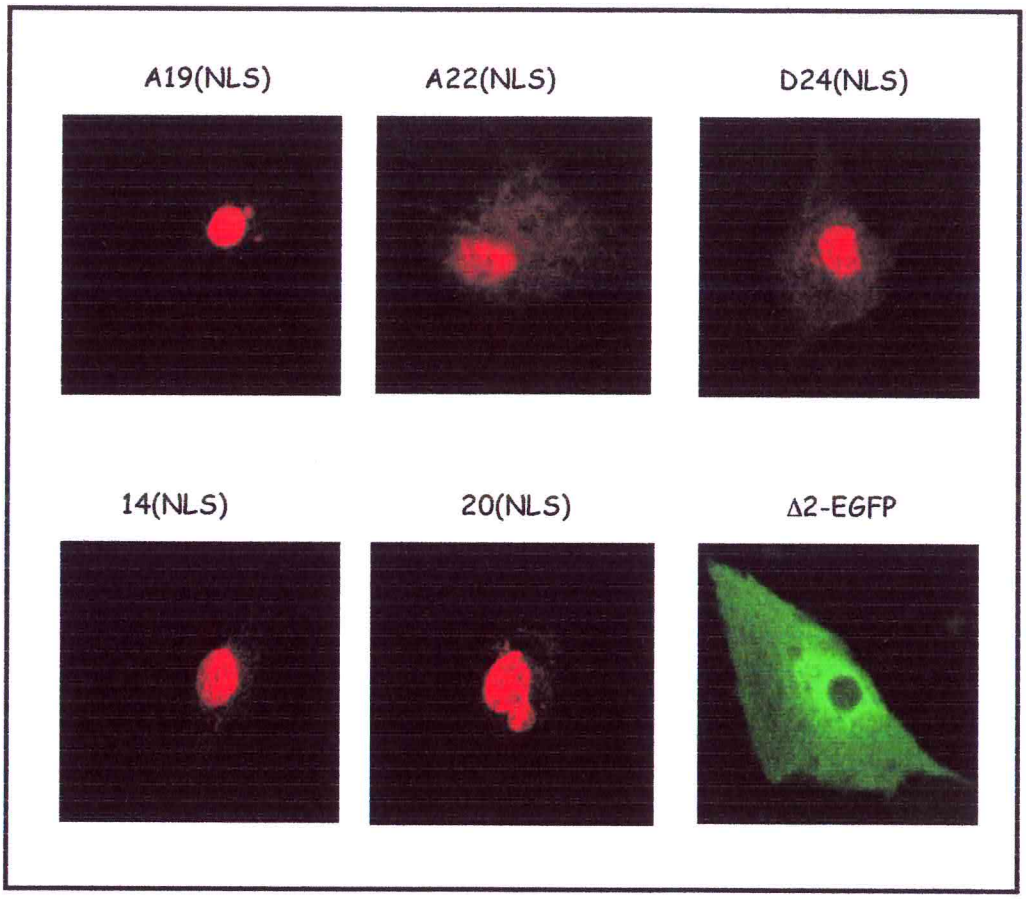

Figure 21: Immunofluorescence of a single transfection of scFvNLS and Δ2-EGFP in MA104 cells. Different intrabodies are tagged into the nucleus (red), while the antigen Δ2-EGFP is in the cytoplasm of the cell (green).

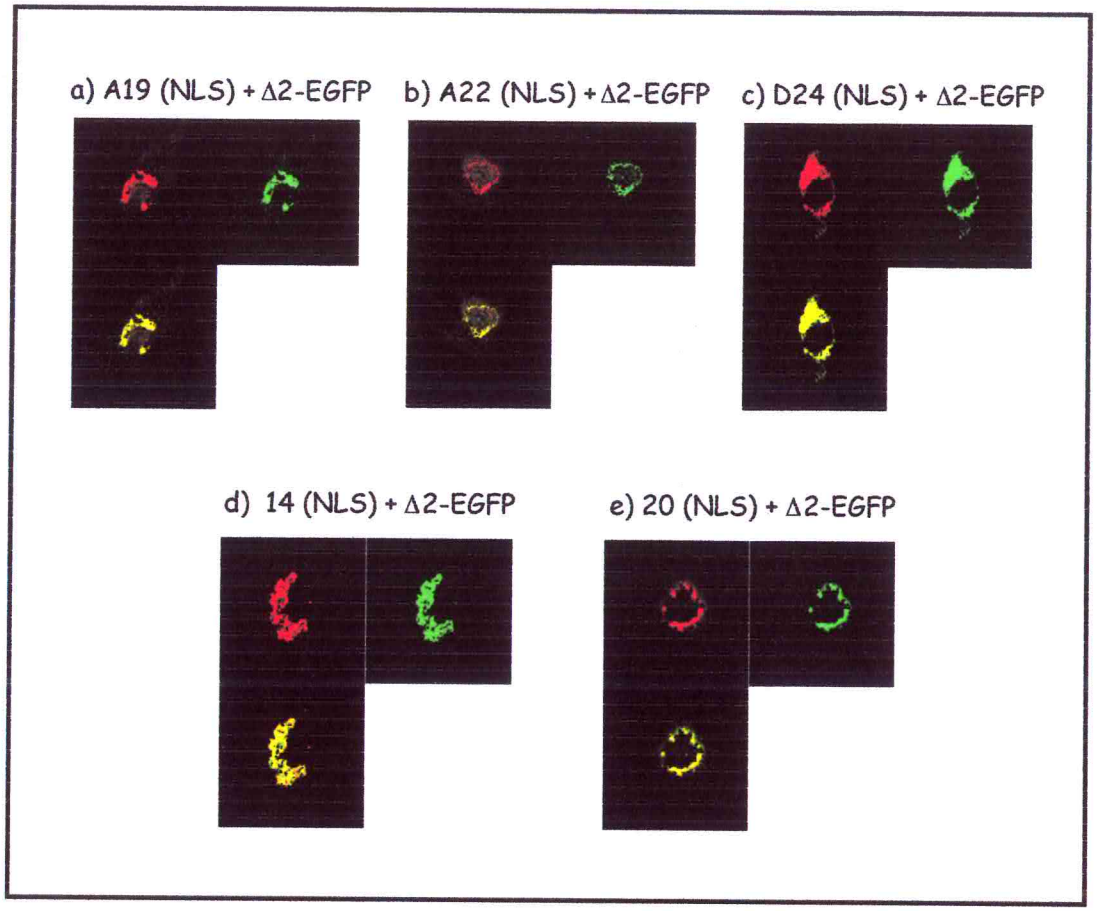

Figure 22: Confocal immunofluorescence of MA104 cells co-transfected with scFvs(NLS) and Δ2-EGFP. The scFvs were visualised with anti-SV5 antibody (red) and Δ2-EGFP antigen (green).

To confirm that only a specific interaction between antigen and intrabody determines the formation of these cytoplasmic aggregates, we used an irrelevant intrabody, specific for β–galactosidase (R4NLS). When Δ2-EGFP and R4-NLS are co-expressed in MA104 cells, R4NLS migrates into the nucleus, while the antigen distribution is not impaired (Figure 23 panel a). This was also the case for another intrabody, anti-ShcCH$_2$ (ShcCH$_2$) which also localised into the nucleus while the antigen remained in the cytoplasm, demonstrating no interaction between the two co-transfected partners (Figure 23 panel b).

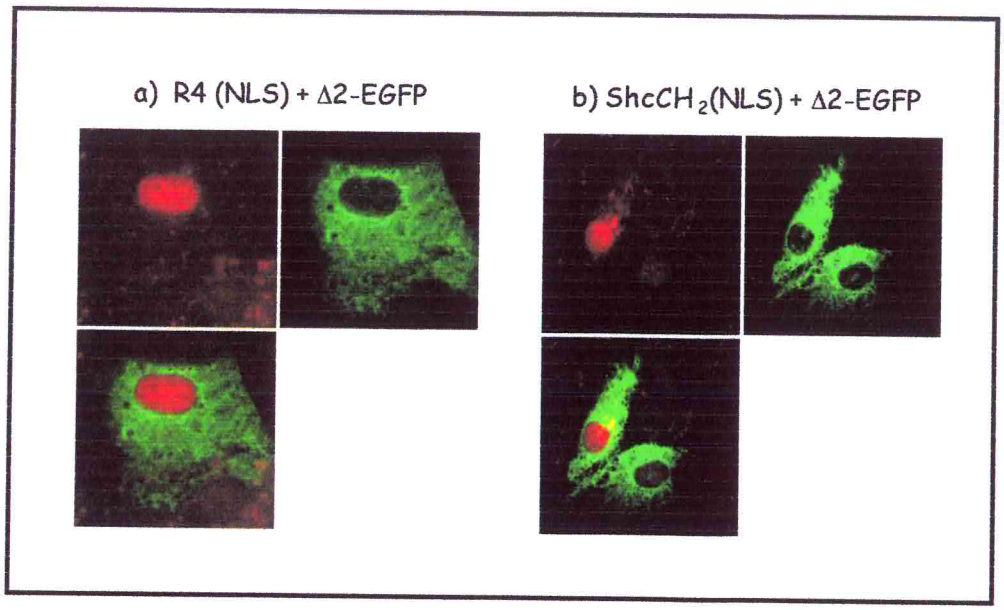

Figure 23: Confocal immunofluorescence of MA104 cells co-transfected with Δ2-EGFP (green) and $ShcCH_2$(NLS) or R4(NLS) (red).

As a second negative control we used an irrelevant cytoplasmic antigen, NSP2-EGFP. Also NSP2-EGFP shows a homogeneous distribution in the cytoplasm (Figure 24 panel a), which is maintained when co-transfected with scFv A19(NLS) (Figure 24 panel b). Figure 24 panel b clearly shows the migration of the A19(NLS) into the nucleus of the MA104 co-transfected cells.

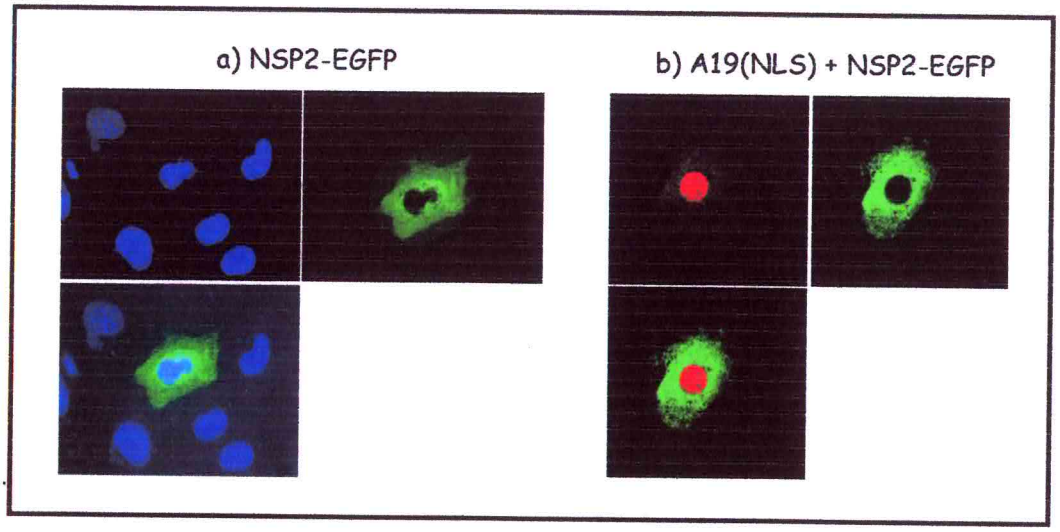

Figure 24: Confocal immunofluorescence of MA104 cells transfected with NSP2-EGFP (**a**) (green) and with NSP2-EGFP and A19(NLS) (red) (**b**). In the single transfection (**a**) the nucleus is indicated in blue.

The other anti-Δ2 intrabodies [A22(NLS), D24(NLS), 14(NLS) and 20(NLS)] were also co-transfected with NSP2-EGFP. As shown in Figure 25, all of them have the same general behaviour of intrabodies not interacting with an unspecific antigen (NSP2).

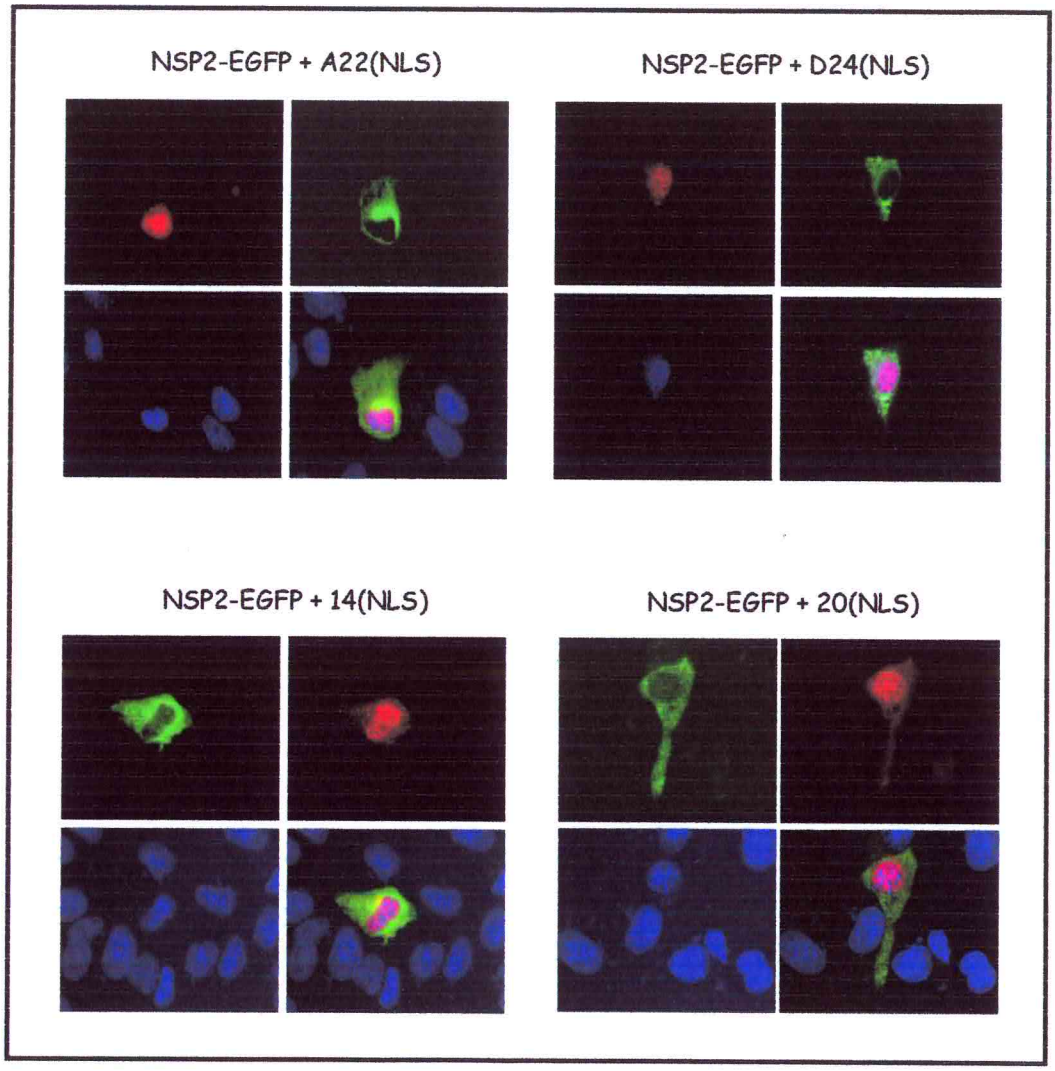

Figure 25: Immunofluorescence of MA104 cells co-transfected with EGFP-NSP2 (green) and with different scFvs(NLS) (red) as indicated

The immunofluorescence assay was also performed with all the scFvs without NLS, and therefore expressed in the cytoplasm of MA104 cells. All of them showed homogeneous distribution in the cytoplasm, although partial migration into the nucleus was observed, probably due to internal nuclear-like localisation signals (data not shown).

However, aggresomes appeared in the cytoplasm of cells co-transfected with Δ2-EGFP and the svFvs (without NLS), with co-localisation of the two components similarly to what we previously observed. On the other hand, the negative control $ShcCH_2$, which forms aggregates in the cytoplasm *per se*, does not co-localise with Δ2-EGFP antigen (Figure 26).

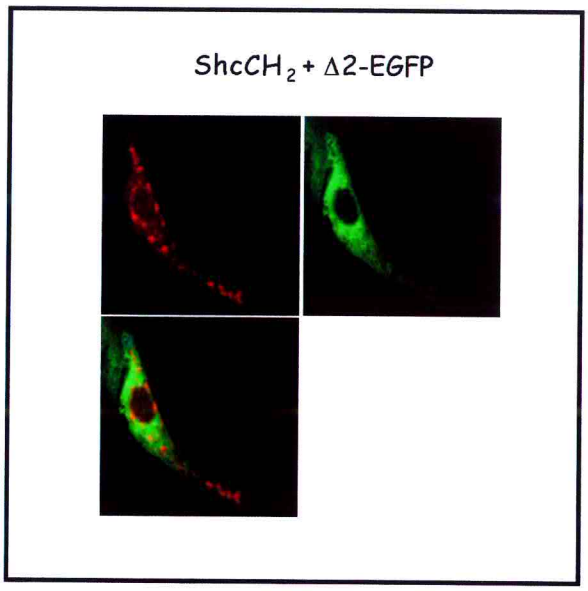

Figure 26: Confocal immunofluorescence of MA104 cells co-transfected with $ShcCH_2$ (red) and Δ2-EGFP (green).

All the results demonstrated that the specific interaction between the scFv(NLS) co-transfected with the antigen (Δ2-EGFP) were able to form the aggresomes. In this way the specific interaction dramatically perturbed the distribution of the two partners, scFvs(NLS) did not migrate into the nucleus any longer, while the antigen (Δ2-EGFP) was not homogenously distributed in the cytoplasm of the transfected cells. The characteristic aggresomes in the cytoplasm of co-transfected cells showed a perfect co-localisation of the two partners (antigen and intrabodies), confirming the interaction between the two molecules. The control experiments demonstrated no aggresomes formation and no antigen-divertion with the irrelevant scFvs [R4(NLS) and Shc(NLS)] co-transfected with Δ2-EGFP.

A similar result was obtained with an irrelevant antigen (NSP2-EGFP) and the 5 scFs(NLS) specific for NSP5. In these control experiments the scFvs(NLS) were able to migrate into the nucleus, while the antigens (Δ2-EGFP or NSP2-EGFP) are homogenously distributed in the cytoplasm.

Immunoprecipitation: Δ2 and the intrabodies

In a second experimental approach to study the intrabody-antigen interaction, we checked if the intrabodies were able to immunoprecipitate the antigen when co-transfected in MA104 cells (Figure 27). We co-expressed the two partners [Δ2 and scFvs(NLS)] in MA104 cells previously infected with T7 DNA polymerase recombinant vaccinia virus. After 16 hours we performed the cellular lysis and immunoprecipitation of the intrabodies using the anti-SV5 monoclonal antibody.

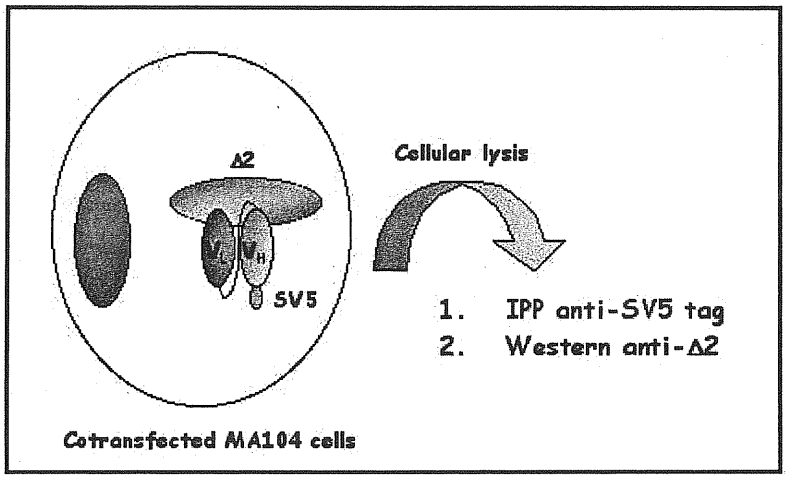

Figure 27: Scheme of the *in vivo* interactions between Δ2 and the scFvs detected by immunoprecipitation followed by Western blotting.

The cellular lysis and all the steps during the immunoprecipitation were done constantly in the presence of 5 mM dithiothreitol (DTT) or 20 mM N-ethylenmaleimide (NEM), an alkylating agent which reacts with the free SH groups, preventing formation of disulphide bonds. Panel A of Figure 28 shows that A19(NLS) was able to immunoprecipitate the co-transfected Δ2 antigen, but not an irrelevant antigen as NSP2, confirming its specificity for Δ2. Moreover, $ShcCH_2$(NLS) used also as a negative control, was not able to immunprecipitate the antigen Δ2 (Figure 28). The other intrabodies were also tested in the

same assay. Panel B shows that D24(NLS) and 20(NLS) can recognise the antigen Δ2 under the same conditions , while A22(NLS) and 14(NLS) can not.

With these experiments we could observe a stable interaction of the A19, A22 and D24 *in vivo*, which can be maintained *in vitro* quite easily, while for the two other scFvs (A22 and 14) the interaction seems very weak. In fact the washing steps during the immunoprecipitation are sufficient to disrupt the interactions between the partners.

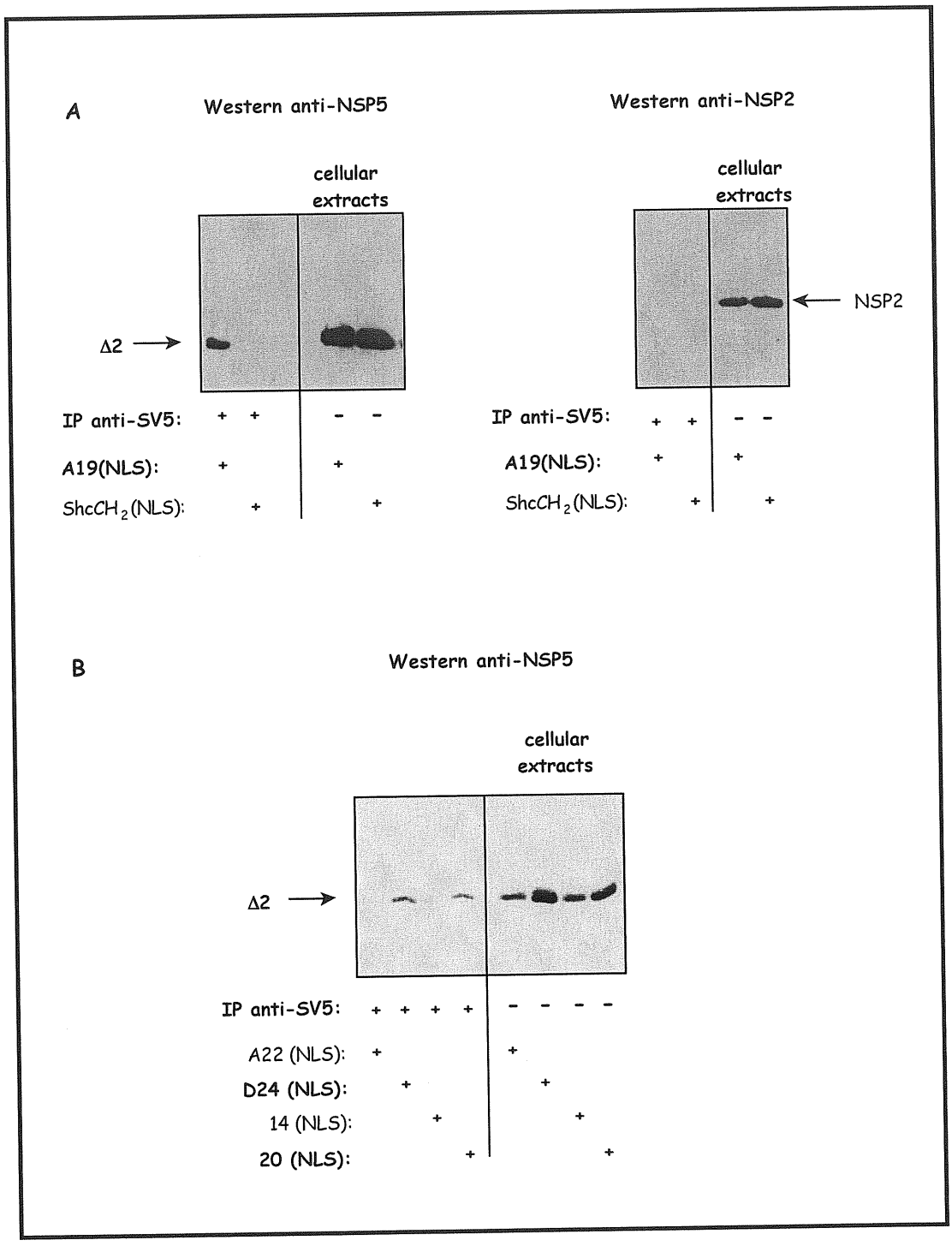

Figure 28: Western immunoblotting of immuoprecipitated (using anti-SV5) cellular extracts transfected with Δ2 or NSP2 (irrelevant antigen) using anti-NSP5 or anti-NSP2 sera as indicated. The scFvs are fused to the SV5 tag.

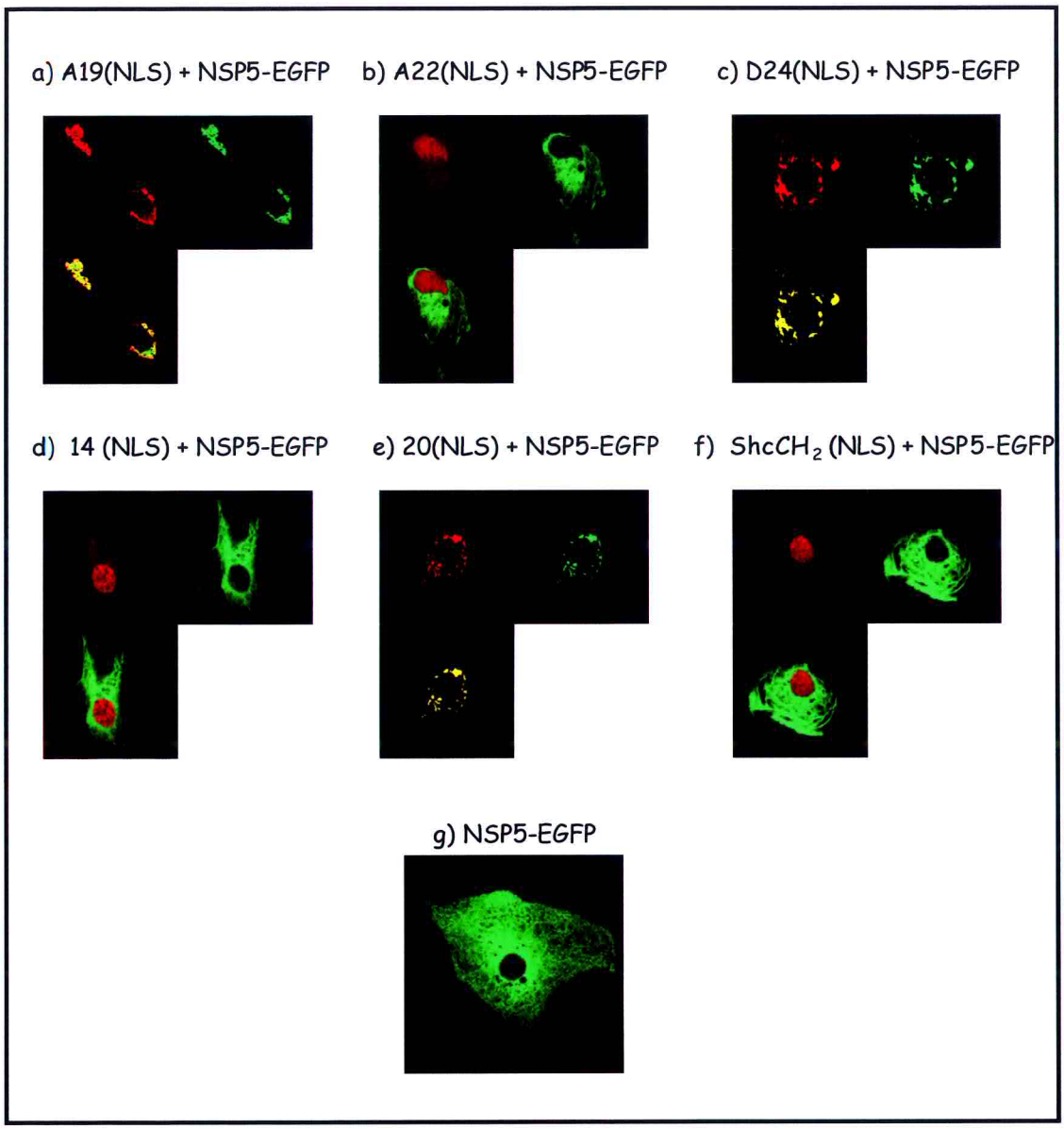

Figure 29: Immunofluorescence of scFvs(NLS) (red) and EGFP-NSP5 (green) cotransfected in MA104 cells. Panel g shows a single transfection of the antigen EGFP-NSP5 (green).

Immunofluorescence analysis: NSP5 wild type and the intrabodies

The same strategies used to test the interaction between Δ2 and the intrabodies, were also applied for the NSP5 protein, to verify whether the scFv were able to recognise the wild type protein. This was a very important step to determine which intracellular antibody could be expressed in mammalian cells for the "*in vivo* intracellular immunisation" against rotavirus infection. Figure 29 shows the results of the confocal microscopy of scFv(NLS) and NSP5-EGFP co-transfected MA104 cells. The A19(NLS), D24(NLS) and 20(NLS), have the same behaviour observed before with Δ2-EGFP (Figure 25) while A22(NLS) (b) and 14(NLS) (d) appear not to interact with wild type NSP5 showing a similar distribution of the negative control $ShcCH_2$(NLS) (f).

From these results we can conclude that three scFvs [A19(NLS), D24(NLS) and 20(NLS)] are able to perturb the distribution of the wild type protein in transfected cells, rendering these molecules valuable tools to study a possible interference with the role of NSP5 during the viral replicative cycle of Rotavirus.

Rotavirus infection of cells expressing intrabodies

The previous experiment suggested us to utilise some scFvs (in particular A19, D24 and 20) for cellular immunisation against rotavirus infection because able to recognise the wild type NSP5 protein in co-transfected MA104 cells. For this purpose we subcloned the scFv of A19, D24 and $ShcCH_2$ (as control in the pEGFP-N1 vector. The scFv proteins were fused to the N-terminus EGFP. The pscFvs-EGFP constructs were transfected in MA104 cells, which were then infected with Rotavirus (strain OSU) at 30 hours post-transfection. Immunofluorescence experiments were performed using anti-NSP5 or anti-NSP2, separately to detect viroplasms in the cytoplasm of infected cells. The state of rotavirus infectivity was analysed in cells in relation to the effect of "intracellular immunisation" expressing the green scFv fusion proteins. We found that cells expressing A19-EGFP and D24-EGFP showed a remarkable difference in the number of viroplasms in comparison to the controls ($ShcCH_2$-EGFP and EGFP alone).

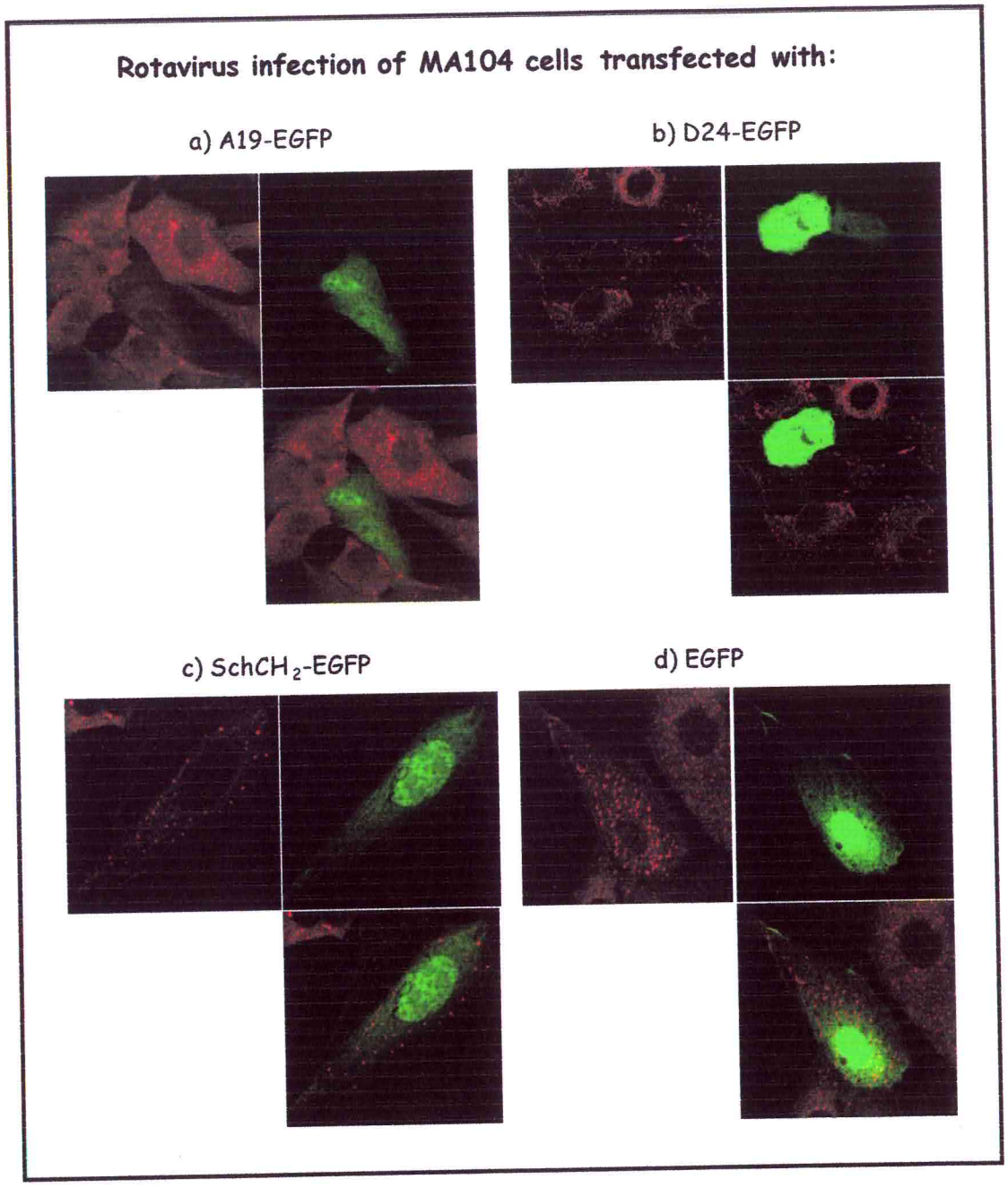

Figure 30: Immunofluorescence of rotavirus (strain OSU) infected MA104 cells previously transfected with EGFP-A19, -D24 and $-ShcCH_2$ or EGFP alone (green). The NSP5 protein of rotavirus is detected in red. Similar results were obtained in the immunofluorescence experiments using anti-NSP2 serum (data not shown).

The results presented in Figure 30 are preliminary data obtained from two different transfection experiments and with two anti-NSP5 intrabodies (A19-EGFP and D24-). Experiments with 20-EGFP are in preparation. The scFvs-EGFP (A19, D24 and $ShcCH_2$), shown in Figure 30, had a homogenous cytoplasmic distribution in absence of virus, although few cells showed aggregation of the green proteins in the cytoplasm (data not shown).

The important aspect of these experiments was indicated by the absence or a very low number of viroplasms (less then 5) in cells transfected with A19-EGFP and D24- (Figure 30, panel a and b), while $ShcCH_2$-EGFP and EGFP alone did not compromis the formation of viroplasms. In fact in these transfected cells, used as control, the number of viroplasms per cells were normal (up to 50) (Figure 30, panel c and d).

The number of viroplasm positive cells was counted in cells expressing each scFv-EGFP (approximately 150). The percentage of viroplasm positive cells was plotted as shown in Figure 31. The plot shows the relative percentage of viroplasm positive cells in relation to the control EGFP detectable by anti-NSP5 or anti-NSP2 sera. The percentage of viroplasms positive cells expressing EGFP alone was considered as reference value of 100%. $ShcCH_2$-EGFP is an alternative control of the effect of an irrelevant scFvs on the viral infection.

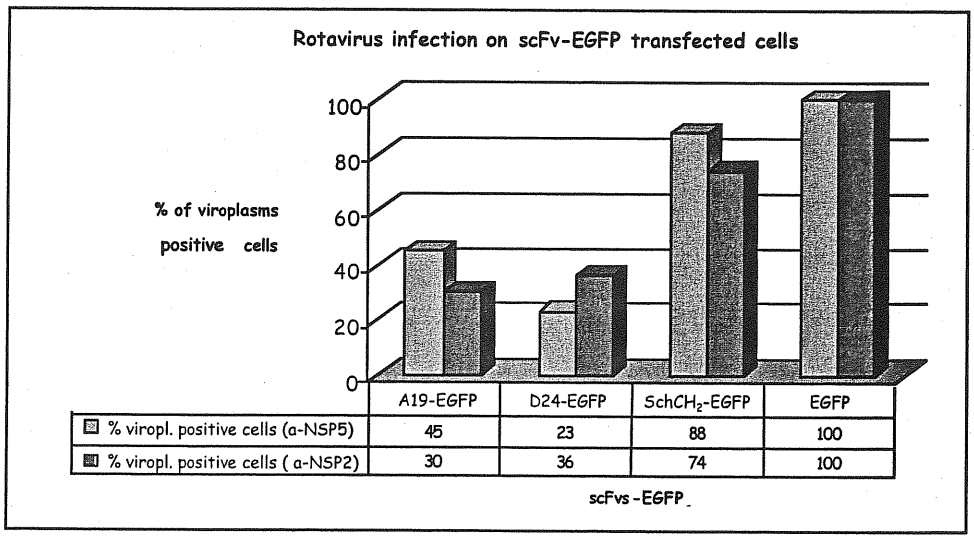

Figure 31: The plot indicates the relative percentages of viroplasms positive cells transfected with the three scFvs-EGFP (A19-EGFP, D24- and $ShcCH_2$-) in relation of the percentage obtained from the positive control of transfected cells with EGFP alone. The number of viroplasms positive cells expressing EGFP alone was considered the reference value of 100%. $ShcCH_2$-EGFP is an alternative control of the effects of a scFv on the viral infection.

The percentage of cells transfected with A19-EGFP and D24- intrabodies and with cytoplasm viroplasms (more than 5 viroplasms per cell) was from 23% to 46% (Figure 31). These preliminary data shows a quite strong inhibitory role of these two specific anti-NSP5 scFvs (A19 and D24) on viroplasm formation in the cytoplasm of infected cells. In fact 60%-70% of cells expressing the EGFP-intrabodies were viroplasm negative cells. Moreover, the irrelevant intrabody (ShcCH$_2$-EGFP), used as a control, did not show strong effect on the viroplasms formation during the infection, because around 80% of the cells contained a large number of viroplasms (Figure 31). It is important to mention that in cells, in which viroplasms formation was inhibited by the intrabodies, there was no background of SP5 (or NSP2) distributed in the cytoplasm.

Expression of the scFvs in bacteria

Up to now scFv molecules has been largely used in laboratory research as common tool, in Western immunoblotting, ELISA, immunoprecipitation and immunofluorescence as well as antibodies. For this reason, the anti-NSP5 intrabodies (A19, A22, D24) were subcloned in pDAN3, an expression vector for prokaryotic cells (Figure 32) to have the have an alternative antibodies fragment to the polyclonal sera obtained from guinea pigs and mice vaccinated with NSP5 recombinant protein. The scFv are fused with a leader peptide (pelB) at the N-terminus to promote the expression of the protein in the periplasm of the bacteria. In this way scFvs can form the disulfide bonds among cysteins, due to the presence of the oxidising environment in this compartment.

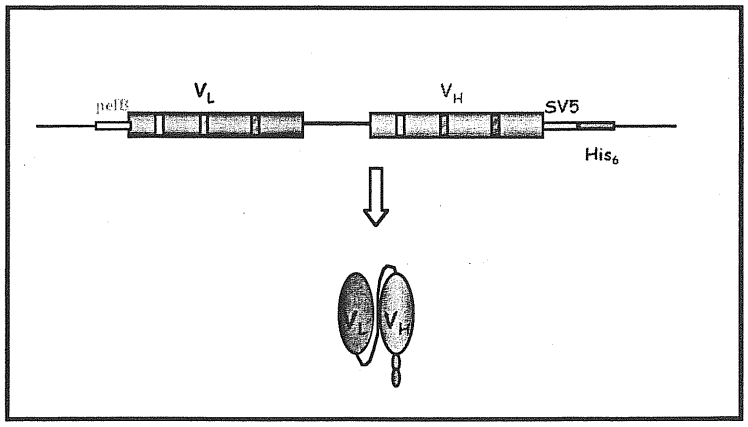

Figure 32: Scheme of the prokariotic expression vector pDAN3 and the protein expressed in *E.coli.*

The three scFv were expressed in HB2151 *E.coli* bacteria strain. HB2151 is a non-suppresser strain for the amber stop codon. The expression of scFv was induced by IPTG and the protein was extracted from the bacterial periplasmic fraction, where intra-chain disulfide bonds are formed and purified from the extract by nickel column (Figure 33).

The three scFv were used in ELISA assay and Western immunoblotting to recognise the antigen, but none of them gave a positive result. We thought three possible conclusions:

a) Δ2 in Western blotting is denaturated suggesting that the intrabodies are conformational antibody fragments.

b) the coated antigen (GST-NSP5) in the ELISA was purified from GST columns in denaturing conditions.

c) the conformation state of the intrabodies, produced in the oxidising environment of the periplasmic bacteria, could be perturbed by the formation of the disulfide bonds, modifying the recognition specificities.

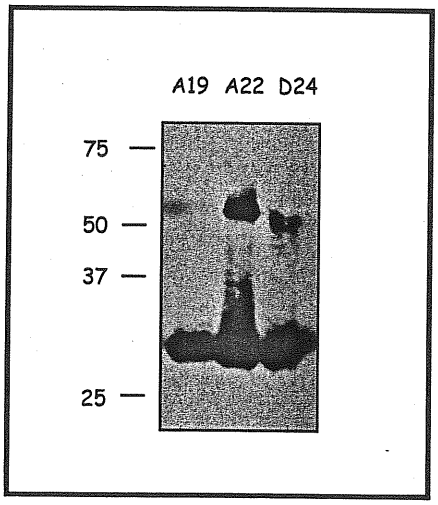

Figure 33: Western immunoblotting of the nickel column purified scFv from periplasmic extract of *E.coli*, using anti-SV5.

These results suggest that selection of *in vivo* competent antibodies by the two hybrid-system favours the selection of the conformational intrabodies as opposed to scFv recognising linear epitopes. Moreover, it appears that the expression of intracellular antibodies in oxidising environment, like the periplasmic bacterial compartment, can affect their conformational state and activity, similarly to what occurs when scFvs selected *in vitro* are tested in the cytoplasm of mammalian cells, where the reducing environment abolishes

the formation of intra-chain disulphide bonds. However, in some case it has been shown that scFv selected as intrabodies were able to function also as secreted molecules [76] [71].

In our case the selected intrabodies are not functional when expressed in bacteria even though the intracellular activity was the most important aspect for our research. In fact our aim of the application of intracellular antibody capture technology was intracellular immunisation against rotavirus infection.

Discussion (1)

A characteristic feature of rotavirus infected cells is the formation of large accumulations of viral proteins and viral RNA in precise sites of the cytoplasm, called viroplasms. From previous study, NSP2 and NSP5 were shown to localise in viroplasms from the early stages of infection [148]. The study of the phenotype of different rotavirus ts-mutant viruses, has suggested that rotavirus viroplasms are the elective subcellular place of replication and packaging of newly made virus particles. At the non-permissive temperature, cells infected with tsE-mutants (a replication defective temperature-sensitive mutant, mapping in gene encoding NSP2), are defective in the formation of viroplasms [68], and produce large number of empty particles, indicating that NSP2 is involved in the correct organisation and formation of viroplasms which in turn play an essential role in genome packaging and replication. The function of NSP5 in viroplasms is still not known, since nor ts-mutants NSP5 were ever found neither any other NSP5 negative mutant, strongly suggesting NSP5 importance in the replicative virus cycle.

Our laboratory has been involved for many years in the study of the non-structural protein NSP5. In particularly we focus our attention to the study of its particular phosphorylation state, and the characterisation of its interaction with NSP2 in the context of viroplasms formation. In this thesis we pointed out particular attention to the phosphorylation of NSP5 to characterise its putative "autokinase" activity, largely described also by other researchers and its phosphorylation state in the context of the viral replicative cycle and NSP2 interaction.

The phosphorylation of NSP5 appears as a complex process, which generates different phosphorylated isoforms with an apparent MW ranging from 26 to 32-34 kDa. This event, conveniently called hyperphosphorylation, takes place in the context of rotavirus replication while in cells transfected with only NSP5 is much less evident. In this latter case NSP5 appears as a main band of 26 kDa and a minor band of 298 kDa, with almost absence of the hyperphosphorylated forms (higher than 28 kDa) [4, 16, 156].

O-glycosylation also modifies NSP5 post-translationally [74] mainly involving isoforms of 26 and 28 kDa [4].

In our laboratory was previously demonstrated the interaction of NSP5 with other two viral proteins, the viral RNA-polymerase VP1 and the non-structural protein NSP2

with chemical cross-linking (DSP) experiments. Moreover, an important consequence of NSP2-NSP5 interaction was highlighted with co-transfection experiments where the *in vivo* phosphorylation of NSP5 strongly changed, producing a pattern that resembles the one obtained in virus infected cells [4].

The presence of NSP2 and NSP5 in viroplasms and the NSP5 biochemical modifications following interaction with NSP2 (hyperphosphorylation), prompted us to investigate the cytoplasmic distribution of the two proteins in transfected cells. We showed that co-expressing NSP5 and NSP2 in mammalian cells in the absence of any other viral protein and rotavirus replication, originate structures significantly similar to those found in infected cells, that we have called viroplasm-like structures (VLS). Confocal microscopy has demonstrated the precise spatial co-localisation of the two proteins in viroplasms as well as on the rim of VLS, strongly confirming their interaction. All the replication machinery composed of the structural proteins (VP1, VP2, VP3 and VP6) and the RNA are present in viroplasm of infected cells, reflecting a more complex structure than VLS. However, VLS are formed in the absence of replication [57]. These data permit to link NSP5 protein to the complex context of rotavirus morphogenesis. Replication components are not yet fully characterised, but the purification of an active replicase complex with anti-NSP2 antibody [8], has permitted to hypothesize that NSP2 may have a fundamental role in rotavirus replication. In particular NSP2 has higher affinity for ss- rather than for ds-RNA [175], suggesting that it may stabilise ssRNA template to present it to the polymerase VP1 for replication. Even for NSP5 it was recently showed a nonspecific ss-dsRNA and DNA interaction proposing a possible role in the cooperation with NSP2 in the destabilization of RNA secondary structures and packaging and/or prevention of the interferon-induced dsRNA-dependent activation of the protein kinase PKR [189]. However, this possibility was accurately investigated in our laboratory, and no indications of RNA binding activity of NSP5 was ever found.

Recently, the crystal structure NSP2 has been very well characterised especially for its interaction with RNA and for its NTPase activity. However, in this work nothing was mentioned about the interaction with NSP5 and their biological function *in vivo* and in viroplasm formation. For this purpose Catherine Eichwald in our laboratory is conducting a study of the NSP5 regions involved in interaction with NSP2 *in vitro* and *in vivo*. Regions 1 and the tail (last C-terminus 18 aa) appear to be responsible for the binding with NSP2.

The ability of NSP5 and NSP2 in forming VLS suggests the possibility that viroplasms could be structurally organized by a primary protein-protein (NSP5-NSP2) interaction that does not require other components. This interaction could have an early structural function in the virus replicative cycle as an organizer for replicative functional viroplasms. In order to map the NSP5 regions relevant for VLS formation and to verify the importance of NSP5 hyperphosphorylation in this process, several NSP5 deletion mutants were analysed. With the co-transfection of NSP2 and the different NSP5 mutants, we concluded that the N- and C-terminal regions (region 1 and 4T) of NSP5 are required for formation of discrete cytoplasmic structures (VLS), even if the mutant Δ2 (lacking region 2) did not form the spherical VLS when co-expressed with NSP2, but rather irregular structures.

Moreover, the *in vivo* phosphorylation assay showed that mutants, lacking regions 1 and/or 3 (Δ3, Δ1 and Δ1/Δ3), undergo spontaneous hyperphosphorylation generating species of decreased gel mobility [57], without any further dependence from NSP2 [3]. The results obtained with Δ1 or Δ3 suggest a constantly "open" state of the molecule in terms of favoring phosphorylation. The elimination of the first or the third region appears to result in a structural change of the protein that abolishes the intrinsic inhibitory control of the NSP5 hyperphosphorylation, thus mimicking NSP2-dependent hyperphosphorylation of wt NSP5. We hypothesize that the N-terminal portion of NSP5 (region 1) plays an inhibitory role on NSP5 hyperphosphorylation, probably through interactions that may involve the region between aminoacids 81 and 130 (region 3). An interesting possibility is that Δ1 and Δ3 hyperphosphorylations are due to changes in the structural molecular constraints present in the wt that during infection are modulated by interaction with NSP2. In this view, a complex NSP5 tertiary structure may control also the hyperphosphorylation on specific serine/threonine sites, which may be structurally accessible only after interaction with NSP2.

Conformational changes can result from the interaction of NSP5 with itself or with NSP2. NSP5-NSP2 interaction was also confirmed using the yeast two-hybrid system [156] (Catherine Eichwal's results). It was also reported that the last C-terminal 10 residues of NSP5 are involved in the formation of NSP5-NSP5 oligomers or of heterocomplexes between NSP5 and NSP6, a polypeptide encoded by the alternative ORF of gene segment 11 [72, 185]. However, NSP6 is poorly studied, and NSP6 is not equally expressed in all rotavirus strains. All the N- and C-terminal mutants (Δ1/Δ2, ΔT, ΔC29,

ΔC48 and Δ4T) did not show a change in mobility in *in vivo* ^{32}P labeling, even though Δ1/Δ2, ΔT and ΔC29 become phosphorylated [57], and without sensitivity to the presence of NSP2 [3]. From this study of NSP5 mutants phosphorylation, we found that the deletion of the last C-terminal highly conserved regions (region 4 and T) completely silences protein phosphorylation, and in particular the last C-terminal 18 residues (tail) ΔT) are sufficient to abolishes NSP5 hyperphosphorylation. Other groups also confirmed these data [185].

The VLS formation experiments allowed us to conclude that the phosphorylation state of NSP5 is not sufficient to organize discrete cytoplasmic structures (VLS), based on the results that some mutants with a strong hyperphosphorylation were not able to form the VLS, while the interaction with NSP2 appears to be an essential event [57]. However, the exact timing and course of events that leads to VLS formation is not yet completely clear.

Another important aspect from the *in vivo* phosphorylation assay was the relation between the presence of regions 2, 4 or T (tail) in the transfected NSP5 mutants and their phosphorylation patterns. All mutants containing these three regions show a strong mobility shift due to phosphorylation, because of λ-Ppase sensitivity. In other words, NSP5 deletion mutants lacking region 1, 3 or both (Δ1, Δ3 and Δ1/Δ3) efficiently instruct PAGE mobility shift. We then decided to investigate the problem of the "autophosphorylation" of NSP5 that appear to be due to kinase activity of NSP5 itself.

This study was done in closed collaboration with Catherine Eichwald who performed the *in vitro* shift-phosphorylation assay, which allowed us to obtain *in vitro* the characteristic PAGE mobility shift of hyperphosphorylated NSP5. Cellular extracts transfected with NSP5 or its deletion mutants were used as source of enzyme on a NSP5 mutant, which worked as substrate. In this way we demonstrated that the NSP5 phosphorylation is an intermolecular reaction (in *trans*), and that cellular extracts containing NSP5 deletion mutants lacking either domain 1, 3 or both (Δ1, Δ3 or Δ1/Δ3, respectively) efficiently instruct PAGE mobility shift to an *in vitro* translated NSP5-derived substrate. Consistent with these results, these same mutants were previously described to undergo mobility shift phosphorylation *in vivo* [57]. The cellular extracts transfected with mutants lacking regions 2, 4 or T or not transfected (mock) are not able to hyperphosphorylate the substrate. Besides, we saw a marginal phosphorylation activity of extracts containing wild type NSP5. This is not surprising since, when expressed alone, NSP5 is very little phosphorylated producing mainly 26 kDa protein while, upon

co-expression with NSP2 it becomes hyperphosphorylated [3, 57]. Regions 1 and 3 appear again to play an inhibitory role (region 3 being stronger than region 1) in the capacity of their corresponding cellular extracts to work as kinase(s), as revealed by the strong activity of mutants Δ1, Δ3 and Δ1/Δ3.

Since mutant Δ1/Δ3 and the histidine-tagged version (His_6-Δ1/Δ3) was the shortest deletion mutant able to maintain the hyperphosphorylation activity *in vivo* and *in vitro*, we tested the purified protein as a putative kinase. The *in vitro* phosphorylation assay was negative using either the purified His_6-Δ1/Δ3 or in combination with a mock cellular extract to test for a possible complementation between cellular kinase(s) and the purified His_6-Δ1/Δ3.

Taken together these results indicate that NSP5 is not itself a kinase, but rather it activates a cellular kinase(s) for its own phosphorylation, otherwise inactive in the untransfected cellular extracts. Noteworthy, phosphorylation appeared not to be required for kinase activation, since mutant Δ1/Δ3 (Ser→Ala), which lacks four serines in region 4 and did not show phosphorylation was still able to induce the cellular kinase(s). However, the presence of the regions 2, 4 and T seemed essential for the activation of the cellular kinase(s).

At this point we mapped the phosphorylation sites on NSP5 using GST fusion proteins of NSP5 and its deletion mutants, which were used as substrates in a second *in vitro* phosphorylation assay. Interestingly, all GST fusion proteins were unable to show autophosphorylation, further indicating the lack of kinase activity of NSP5. Instead, transfected cellular extracts were used as a source of enzyme. All the tested mutants lacking region 4 were not phosphorylated by Δ1/Δ3 cellular extract. In particular four serines within region 4 were mapped as main phosphorylation sites of NSP5.

In the previous *in vitro*-shift phosphorylation assay the substrates showed a clear mobility shift when phosphorylated, in this second assay the GST fusion protein substrates do not show mobility shift. The type of substrate could explain the reason of this difference. In the first assay, we used *in vitro* translated proteins, produced in rabbit reticulocytes lyses (TNT) while in the second case the proteins were produced in bacteria and fused with Glutathione S-Transferase (GST~29 kDa) with higher total molecular weight which could impair a mobility shift on the PAGE. Alternatively, the fact that these proteins were produced in bacteria did not exclude the possibility that unspecific phosphorylation took place affecting the PAGE mobility pattern.

Analysis of the sequence of NSP5 with the http://www.ebi.ac.uk [Prosite-EMBL] showed within region 4 two motifs SDSE and SDSD, mapped to serines 153, 155, 163 and 165, located in an acidic region with homology to CK2 phosphorylation sites [112]. In fact, we showed that recombinant CK2 was able to phosphorylate GST-NSP5 *in vitro* precisely in those positions. The contribution of the recombinant CK2 is very important in conferring the mobility shift of the substrate Δ1 in the *in vitro* shift-phosphorylation assay.

Moreover, an important additional strong indication of the involvement of a CK2 in the phosphorylation of NSP5 derived from the *in vitro* phosphorylation performed with [γ-^{32}P]GTP instead of [γ-^{32}P]ATP based on the fact that CK2 is one of the few kinases capable of utilizing GTP as a phosphor donor. However, this does not demonstrate that CK2 is the kinase responsible for NSP5 phosphorylation *in vivo* or that other kinases may not be involved. However, these results suggested that the cellular kinase(s) activated by NSP5 is a CK2-like enzyme. The CK2 inhibitors Emodin and TBB were tested *in vitro* and *in vivo* to check the possible effect of these compounds on the NSP5 phosphorylation. The effects of TBB and Emodin on NSP5 phosphorylation *in vitro* were very impressive, while the use of them *in vivo* during rotavirus infection were not so strong, but effective (reduction of 65% and 50% of the phosphorylation). Moreover, we showed that treatment of cells with TBB at early time of infection affected the expression of NSP5 protein (as NSP2) as detected in cellular extracts by Western blotting (Figure 26). An interesting suggestion emerged from a research, presented in Introduction (1) (page 37), in which CK2 inhibitors showed an inhibitory effect on the viral transcription of HIV1-1 [45]. They suggested that CK2 activity could be functionally linked, either directly or indirectly, to a viral or a cellular component(s) critical for HIV-1 transcription. The conclusion of the authors could suggest a possible role of TBB by some indirect (or direct) effects on rotaviral transcription through inhibition of the activity of CK2.

Since NSP5 contains some phosphoacceptor sites also for protein kinase C (PKC), located in regions 1, 2 and 4 we also tested GO6983 and Bisindolylmaleimide, specific inhibitors for PKC and Staurosporine, a large spectrum compound mainly used to inhibit CaM kinase, myosin light chain kinase, PKC, PKA and PKG. All of them were not able to affect the phosphorylation of NSP5 both *in vitro* and *in vivo*. At the light of these

experiments the putative PKC sites on NSP5 did not seem involved in the phosphorylation of NSP5 by protein kinase C.

Up to now CK2 has been described to phosphorylate several viral proteins of both DNA and RNA viruses [53 79, 94, 95, 116, 127, 129] with the exception of viruses of the *Reoviridae* family. Here we reported the involvement of CK2 or a CK2-like enzyme responsible for the phosphorylation of NSP5 providing strong evidence against the putative "autokinase" activity. However, the function of NSP5 in the cycle of Rotavirus remains unknown. Since also the functional significance of NSP5 phosphorylation is not known, it is possible to speculate that phosphorylation and interaction with cellular kinase(s) may be important events in viral replication to regulate the viral life cycle. An essential role of NSP5 in the viral cycle is suggested also by the lack of temperature-sensitive mutants for NSP5, up to now never isolated.

All these results highly support the idea that NSP5 hyperphosphorylation is finely regulated at different steps and suggest that initial activation of NSP5-dependent cellular kinase(s) allows the further hyperphosphorylation of NSP5.

With the results obtained with the *in vivo* ^{32}P labeling and *in vitro* shift-phosphorylation assay we hypothesized a model to describe the hyperphosphorylation of NSP5. As said before during a first step NSP5 is responsible for the induction of a cellular kinase, and in the second it is involved for its own phosphorylation by this activated kinase. In this model NSP5 works as kinase activator, and then as substrate. In the *in vivo* ^{32}P labeling assay we can not separate these two events, and in this way the phosphorylation step is totally dependent on the first one. For example Δ2 could not active the cellular kinase, resulting negative in this assay, even tough in the *in vitro* shift-phosphorylation assay it was a substrate. However, with the *in vitro* shift-phosphorylation assay we separated the two functions of NSP5 analysing one or the other using different combinations of substrates and sources of enzyme. Only from this second experiment we can conclude that regions 2, 4 and T are important for the activation of the cellular kinase and probably involved in the interaction with CK2 or CK2-like enzyme. In the other hand, the regions 4 and T could be essential for the hyperphosphorylation shifting. However, the phosphorylation of NSP5 seemed to be a more complex process, because some mutants can be phosphorylated *in vivo* but did not show any mobility shift in PAGE (^{32}P in vivo labeling). Moreover, this kind of phosphorylation was not appreciated in the *in vitro* shift-phosphorylation assay, because the substrates were already radiolabeled

(^{35}S-methionine). For this mutants (ΔT, ΔC29, Δ1Δ2) the process oh phosphorylation could be different involving another cellular kinase, which can not confer mobility shift to the proteins.

Many questions concerning the importance of the phosphorylation process of NSP5 await the development of a reverse genetic system or alternative strategies. Even though the biological function of NSP5 remains to be elucidated, the data presented in this thesis delineate meaningful aspects of NSP5 phosphorylation.

Scheme of the results:

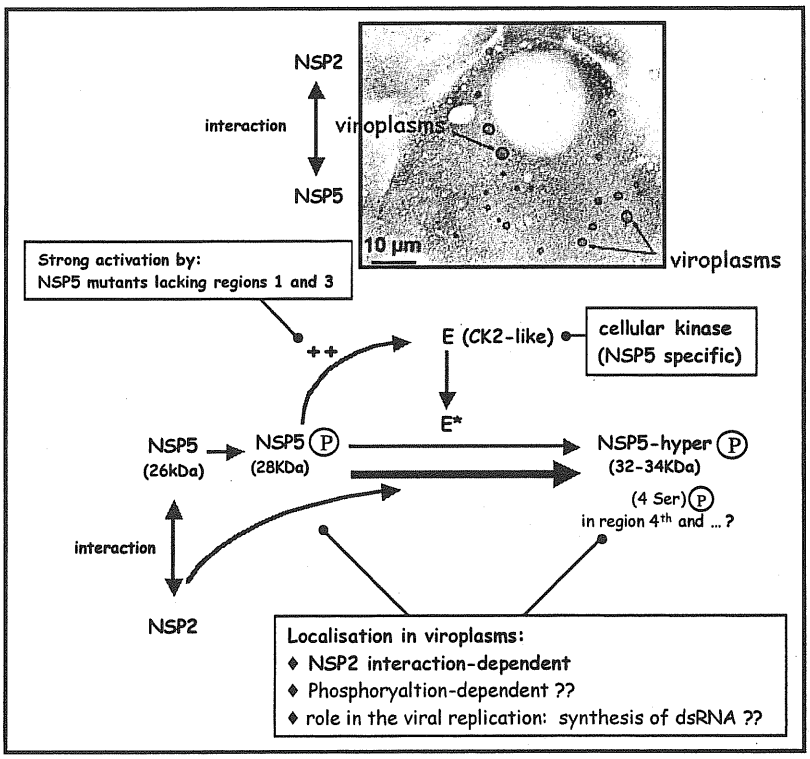

Discussion (2)

The determination of the functions of proteins is one of the most intriguing aspects of functional genomic, in several biological sectors and biotechnological pharmaceutical projects. Among different genotypic and protein knock-out systems we chose the intracellular antibody capture technology (IACT) as a new method for the isolation of intracellular antibodies (intrabodies) able to fold in cellular cytoplasm (reducing environment) recognising intracellular antigens *in vivo*. Since this technology has been recently developed, up to now all the application of intrabodies were derived from screening of libraries with phage display or from engineering classical monoclonal antibodies (hybridomas) formatted as recombinant fragments. These selected scFvs have been adapted to intracellular expression in mammalian and plant cells, but with unpredictable and low success. However, increasing number of reports in the literature describe the effects of intrabodies selected *in vivo* by the two-hybrid system for "intracellular immunisation", in the case of viral proteins or pathogenic molecules, and as for "immunomodulation" [24] interfering with cellular metabolism.

In this thesis it is presented the application of IACT technology in rotavirus research as a protein knock-out strategy to allow us to understand the role of the non-structural protein NSP5 during the viral cycle, since its function is not fully understood and up to now no reverse genetic approach is possible. Part of the work was conducted in collaboration with M. Visintin and A. Cattaneo (ISAS, Trieste Italy), who provided us the techniques.

The IACT technology [76] is based on the selection of intracellular antibodies in scFv format using the two-hybrid system. We used the rotavirus non-structural protein 5 (NSP5) as bait, while the library consisted of a mouse repertoire of antibody V region fragments obtained from mice immunised with the same protein.

First, NSP5 was tested as bait for the two-hybrid system, and it showed a very strong transactivation activity when transformed alone in L40 yeast. This activity could be explained first by the presence of a nuclear localisation signal (KRLKK) found recently in

LexA [60] and secondly by the potential transactivation activity of the acidic region at the C-terminus of NSP5 (Basic-Acid-Basic) (Figure 12), common in the eukariotic transactivation factors for the interaction with the RNA-polymerase complex. On the light of these results, we first tested different C-terminus deletion mutants and other available in our laboratory as possible alternative baits in the two-hybrid system. Δ2, Δ4 and ΔC48 showed a good behaviour, while ΔT (deletion of only 18 aa of the C-terminus), and ΔC29 showed transactivation activity. Also mutant ΔC68 showed a very strong activity even though it lacks the whole regions 4 and the T.

Among the three good baits we chose Δ2 mutant for the screening of the scFv library, because it maintain the region 4, which is mainly involved in the particular pattern of phosphorylation of NSP5. With this particular deletion mutant we maintained the possibility to fish out scFvs able to recognise this portion of the protein.

We modified the original VP16* plasmid [33] introducing a new multicloning site in pVP16/D for the possibility to exchange the scFvs cassette from this two-hybrid system vectors with the phage display vector used in our laboratory (pDAN3 V_H-V_L) using the same restriction enzymes. This change rendered the cloning of the scFvs very simple for their expressions as Histidine tagged proteins in bacteria and as fusion protein on the phage surface. In addition, the VP16 transactivation factor sequence of Herpers Simplex Virus type 1 (HSV-1) was reduced to the minimal sequence able to work as transactivation domain, which consists in the last 78 aa of the whole VP16 protein. In this way we eliminated an irrelevant sequence (~ 150 aa) located at the C-terminal of the 78 aa with unknown function. In this format the pVP16/D vector was tested and it presented a very good activity.

The pVP16/D V_L-V_H library was screened in yeast L40 strain, using two-hybrid system against LexA-Δ2 bait. From two different protocols of selections we obtained a total of 5 scFvs strongly specific for NSP5 (A19, A22, D24, 14 and 20).

We used two different protocols of selection. The first permitted to obtain three clones (A19, A22, D24) specific for LexA-Δ2 out of 11 different scFvs, screening 73 colonies. Of the remaining 8 scFvs five were "polyreactive", because able to recognise an irrelevant bait (LexA-lamin) and three were false positive. An important apect, which

convinced us to change protocol, was the high number of repeated clones. Analysing the protocol #1 of transformation we decided to modify it in order to reduce this number. We thought that this drawback was probably due to the overnight incubation of the transformed yeast in liquid medium before plating on selective medium. Thus, we developed protocol #2 in which the yeast was directly plated immediately after transformation of the library. We thus obtained 3 different positive clones ot of 20 analysed, while with protocol #1 we obtained 3 out of 73. In addition, with this new protocol we reduced the non-specific scFvs from 5 to 1, even tough its frequency was still high. The reason of the presence of such high background is unknown.

An interesting aspect comes from the fact that even though the mouse scFv library was generated from splenocytes of immunised mice, the immunisation procedure with NSP5 protein didn't compromise the quality and variability of the library. In fact the screening for ShcA antigen of the same library permitted to find several specific intrabodies for this protein. This result points out the fact that this library could be useful for other different antigens as a source of intracellular scFvs.

From this selection we had the opportunity to use one ($ShcCH_2$3b) of the first intrabodies specific for $ShcCH_2$ derived from a mouse library as a negative control for the next experiments in mammalian cells.

Computational analysis (http://www.ncbi.nlm.nih.gov/igblast/ and http://imgt.cines.fr) was performed on the nucleotide sequences of the variable region of the 5 selected anti-NSP5 scFvs to understand the role of the immunisation of mice and the intrabodies, derived directly from germline genes or carrying somatic mutations during affinity maturation events. This result showed that with the *in vivo* selection by two-hybrid system we selected different specific intrabodies, containing at least one somatic mutated variable region. Moreover, the scFv 20 contained a variable fragment V_H which we considered derived from a germline gene. In particular, this region was found as hybrid of two germline genes probably fused during the PCR reaction. A particular situation emerged from two scFvs D24 and 14, which presented the same variable heavy region V_H (HV1S27 germline gene) carrying the same point mutations (five), in the CDR1 and CDR2. Since the

same somatic mutations formed through two indipendent events (two different lymphocytes) is a impossible process, we could explain this event in different way: i) these mutations could represent a polymorfism of the germline genes; ii) the database used could lack of some sequences; iii) the most probably explanation could be that the same part of the variable region (from FR1 to FR3) was joined with two different CDR3 during the PCR amplification, creating hybrid molecules.

From our results we can not draw any conclusion regarding the advantage of using a scFv library from immunised mice, because the relative small number of clones identified (five) and the fact that we found a relative important and low number of somatic mutations.

The main aim of our study was to express the selected anti-NSP5 scFvs in mammalian cells as a tool for "intracellular immunisation". The 5 anti-Δ2 intrabodies were tested in MA104 cells by transfection assays. All of them showed a very good expression in MA104 cells both with the classical transient transfection and with the T_7-vaccinia virus system. The scFvs were efficiently produced in the cytoplasm and in the nucleus as tagged proteins. In the immunofluorescence assays on co-transfected cells the intrabodies [A19(NLS), A22(NLS), D24(NLS), 14(NLS) and 20 (NLS)] efficiently interacted with the antigen Δ2-EGFP in a specific manner creating the characteristic structures called aggresomes [13]. The distribution of an irrelevant scFv [Shc(NLS)] or an irrelevant antigen (NSP2-EGFP) in co-transfected cells where never perturbed demonstrating that the formation of aggresomes were due to the specific Ag-intrabody interactions.

We tested the scFvs also in immunoprecipitation assays, adding 5mM DTT or 20 mM N-etylmaleimide to maintain the redox of the cytoplsmic environment during the experiments, limiting any possible biophysical change that can compromise their interaction. Only two scFv [A22(NLS) and 14(NLS)] were unable to maintain binding activity for the rotavirus antigen, while the other three [A19(NLS), D24(NLS) and 20 (NLS)] bound the Ag Δ2 during the *in vitro* immunoprecipitation. These results suggested that probably a weak interaction occurred between the antigen and the A22 and 14 intrabodies, making them unstable during the washing steps, while a stronger interaction happened for the three other scFvs, thus suggesting higher affinities.

The 5 scFvs specific for the Δ2 mutant were also tested in immunofluorescence assay with the full length NSP5 (NSP5-EGFP). Three scFvs A19(NLS), D24(NLS) and 20 (NLS) showed a behaviour totally similar to the Δ2-EGFP.

Two intrabodies (A22 and 14) did not change the NSP5 cytoplasmic distribution when cotransfected with NSP5 and they did not work in the immunoprecipitation. It is therefore possible that both of them have a weak interaction with NSP5 or alternatively, that they are directed against a structure of the mutant absent in the wild type NSP5 protein. The result of this assay was very important to choose those anti-NSP5 intrabodies for intracellular inmmunisation against rotavirus infection.

Preliminary experiments suggested very interesting results of the two anti-NSP5 intrabodies A19 and D24, which prevented viroplasm formation in infected cells. We performed transfections with these two scFv fused with EGFP in MA104 cells followed by rotavirus infection. Only the cells transfected with the two specific anti-NSP5 intrabodies showed a significantly reduction in the number of viroplasms positive cells. In fact only 23% to 46% of the cells showed a normal number of viroplasms in the cytoplasm of infected cells. At the same time the specificity of this "intracellular immunisation" was confirmed using an irrelevant intrabody as $ShcCH_2$-EGFP and EGFP protein alone demonstrating no reduction in the viroplasm formation in these transfected cells.

Confirmation of these results would indicted NSP5 as essential protein for virus replication, probably because it is required for a correct architecture of the viroplasms as a true viroplasms factory.

An interesting characteristic emerged from these experiment, because it was not observed background of NSP2 and/or NSP5 distributed in cytoplasm of "immunised cells". This characteristic suggests that:

a) half-lives of NSP5 and NSP2 could be affected by the absence of viroplasms, since in infected cells practically all NSP5 proteins (and NSP2) were only found in viroplasms.
b) most of the proteins detected in infected cells come from mRNAs produced in the viroplasms. Therefore, the absence of viroplasms could impair the general level of the protein production as NSP5 and NSP2 themselves.

More experiments are in progress to investigate the effects of the intrabodies on the replicative cycle of rotavirus. Since the constitutive stable expression of scFvs in mammalian cells showed quite strong toxicity (data not shown), we produced an MA104 cell line expressing cytoplasmically anti-NSP5 intrabody (A19) induceble by pronasterone (an insect hormone). With this new system we hope to be able to see the "intracellular immunisation" effects for example on virus production, dsRNA synthesis since all the cells will express the scFvs.

From our experiments in bacteria appeared that the expression of intracellular antibodies in oxidising environment, like the periplasmic bacterial compartment, can affect their conformational state and activity, similarly to what occurs when scFvs selected *in vitro* are tested in the cytoplasm of mammalian cells, where the reducing environment abolishes the formation of intra-chain disulphide bonds. We were unfortunate that these scFvs can not be used as monoclonal antibody specific for NSP5 in the common laboratory techniques like Western immunoblotting and immumofluorescence. However, the intracellular activity was the most important aspect for our research. In fact our aims for the application of intracellular antibody capture technology were i) to find out the role of NSP5 in the context of viroplsm formation and viral replication ii) to achieve a methods for "intracellular immunisation" against rotavirus infection.

Conclusions (1):

1. *In vivo* interaction of NSP5 and NSP2 determine the formation of viroplasm-like structures (VLS) in cotransfected MA104 in the absence of other viral proteins.
2. The *in vivo* phosphorylation assay demonstrated that NSP5 deletion mutants lacking region 1 and/or 3 undergo spontaneous hyperphosphorylation in the absence of other viral proteins.
3. Regions 2, 4 and T (tail) are important for NSP5 mobility shift induced by phosphorylation.
4. The phosphorylation state of NSP5 does not seem necessary to organize the VLS, instead the interaction with NSP2 plays an essential role.
5. Purified histidine-tagged NSP5 from transfected cells did not show kinase activity.
6. NSP5 is not a kinase *per se*, rather an activator of cellular kinase(s) for its own phosphorylation.
7. NSP5 regions 2, 4 and T (tail) are important to activate a cellular kinase(s) for its own phosphorylation.
8. Four serines (153, 155, 163, 165) within region 4 are the main phosphorylation sites of NSP5.
9. Recombinant casein kinase II (CK2) is able to phosphorylate NSP5 exactly on the four serines in region 4.
10. The cellular kinase(s) activated by NSP5 use GTP and ATP as phosphate donor, strongly suggesting a possible role of a CK2-like enzyme
11. Emodin and TBB (tetrabromo-2-azabenzimidazole), specific casein kinase 2 inhibitors, dramatically reduced the NSP5 phopshorylation in *in vitro* assays
12. The CK2-inhibitors were effective also *in vivo* to inhibit the NSP5 phosphorylation but in lesser extent, suggesting a possible role of other cellular kinase(s)

Conclusions (2):

1. scFv library were constructed from immunised mice with the recombinant NSP5 protein by selection with two-hybrid system in yeast.
2. Five scFvs (A19, A22 D24, 14 and 20) were selected against a deletion mutant of NSP5 (Δ2).
3. The scFv library can be used as a repertoire of competent intracellular scFvs against antigens different than the one used for immunisation.
4. The five scFv can interact specifically with Δ2 in cotransfected cells, altering the normal localisation of the viral antigen.
5. Three scFvs (A19, D24 and 20) immunoprecipitate the cotransfected antigen (Δ2) from cellular extract.
6. Three scFvs (A19, D24 and 20) are able to interact specifically with the wild type NSP5 in cotransfected cells but not to immunoprecipitate it from cellular extract.
7. Intrabodies (A19 and D24) transiently transfected in mammalian cells are able to reduce the viroplasm formation in rotavirus-infected cells.

References (1):

1. Acs, G. et al. Mechanism of reovirus double-stranded ribonucleic acid synthesis in vivo and in vitro. *J Virol* **8**, 684-9. (1971).
2. Affranchino, J. L. & Gonzalez, S. A. Deletion mapping of functional domains in the rotavirus capsid protein VP6. *J Gen Virol* **78**, 1949-55. (1997).
3. Afrikanova, I., Fabbretti, E., Miozzo, M. C. & Burrone, O. R. Rotavirus NSP5 phosphorylation is up-regulated by interaction with NSP2. *J Gen Virol* **79**, 2679-86. (1998).
4. Afrikanova, I., Miozzo, M. C., Giambiagi, S. & Burrone, O. Phosphorylation generates different forms of rotavirus NSP5. *J Gen Virol* **77**, 2059-65. (1996).
5. Allende, J. E. & Allende, C. C. Protein kinases. 4. Protein kinase CK2: an enzyme with multiple substrates and a puzzling regulation. *Faseb J* **9**, 313-23. (1995).
6. Altenburg, B. C., Graham, D. Y. & Estes, M. K. Ultrastructural study of rotavirus replication in cultured cells. *J Gen Virol* **46**, 75-85. (1980).
7. Aponte, C., Mattion, N. M., Estes, M. K., Charpilienne, A. & Cohen, J. Expression of two bovine rotavirus non-structural proteins (NSP2, NSP3) in the baculovirus system and production of monoclonal antibodies directed against the expressed proteins. *Arch Virol* **133**, 85-95 (1993).
8. Aponte, C., Poncet, D. & Cohen, J. Recovery and characterization of a replicase complex in rotavirus- infected cells by using a monoclonal antibody against NSP2. *J Virol* **70**, 985-91. (1996).
9. Arias, C. F., Romero, P., Alvarez, V. & Lopez, S. Trypsin activation pathway of rotavirus infectivity. *J Virol* **70**, 5832-9. (1996).
10. Au, K. S., Chan, W. K., Burns, J. W. & Estes, M. K. Receptor activity of rotavirus nonstructural glycoprotein NS28. *J Virol* **63**, 4553-62. (1989).
11. Au, K. S., Mattion, N. M. & Estes, M. K. A subviral particle binding domain on the rotavirus nonstructural glycoprotein NS28. *Virology* **194**, 665-73. (1993).
12. Ball, J. M., Tian, P., Zeng, C. Q., Morris, A. P. & Estes, M. K. Age-dependent diarrhea induced by a rotaviral nonstructural glycoprotein. *Science* **272**, 101-4. (1996).
13. Battistutta, R., De Moliner, E., Sarno, S., Zanotti, G. & Pinna, L. A. Structural features underlying selective inhibition of protein kinase CK2 by ATP site-directed tetrabromo-2-benzotriazole. *Protein Sci* **10**, 2200-6 (2001).
14. Battistutta, R. et al. The replacement of ATP by the competitive inhibitor emodin induces conformational modifications in the catalytic site of protein kinase CK2. *J Biol Chem* **275**, 29618-22 (2000).
15. Bican, P., Cohen, J., Charpilienne, A. & Scherrer, R. Purification and characterization of bovine rotavirus cores. *J Virol* **43**, 1113-7. (1982).
16. Blackhall, J., Fuentes, A., Hansen, K. & Magnusson, G. Serine protein kinase activity associated with rotavirus phosphoprotein NSP5. *J Virol* **71**, 138-44. (1997).
17. Blackhall, J., Munoz, M., Fuentes, A. & Magnusson, G. Analysis of rotavirus nonstructural protein NSP5 phosphorylation. *J Virol* **72**, 6398-405. (1998).
18. Bowman, G. D. et al. Crystal structure of the oligomerization domain of NSP4 from rotavirus reveals a core metal-binding site. *J Mol Biol* **304**, 861-71. (2000).

19. Boyle, J. F. & Holmes, K. V. RNA-binding proteins of bovine rotavirus. *J Virol* **58**, 561-8. (1986).
20. Browne, E. P., Bellamy, A. R. & Taylor, J. A. Membrane-destabilizing activity of rotavirus NSP4 is mediated by a membrane-proximal amphipathic domain. *J Gen Virol* **81**, 1955-9. (2000).
21. Brunet, J. P. et al. Rotavirus infection induces cytoskeleton disorganization in human intestinal epithelial cells: implication of an increase in intracellular calcium concentration. *J Virol* **74**, 10801-6. (2000).
22. Bryant, H. E. et al. Interaction between herpes simplex virus type 1 IE63 protein and cellular protein p32. *J Virol* **74**, 11322-8. (2000).
23. Butera, S. T. et al. Compounds that target novel cellular components involved in HIV-1 transcription. *Mol Med* **1**, 758-67. (1995).
24. Casola, A. et al. Interleukin-8 gene regulation in intestinal epithelial cells infected with rotavirus: role of viral-induced IkappaB kinase activation. *Virology* **298**, 8-19. (2002).
25. Chaibi, C., Cotte-Lafitte, J., Servin, A. L., Quero, A. M. & Geniteau-Legendre, M. in *The world of microbes* (ed. IUMS) 463 (Paris, 2002).
26. Chan, W. K., Au, K. S. & Estes, M. K. Topography of the simian rotavirus nonstructural glycoprotein (NS28) in the endoplasmic reticulum membrane. *Virology* **164**, 435-42. (1988).
27. Chan, W. K., Penaranda, M. E., Crawford, S. E. & Estes, M. K. Two glycoproteins are produced from the rotavirus neutralization gene. *Virology* **151**, 243-52. (1986).
28. Charpilienne, A., Lepault, J., Rey, F. & Cohen, J. Identification of rotavirus VP6 residues located at the interface with VP2 that are essential for capsid assembly and transcriptase activity. *J Virol* **76**, 7822-31. (2002).
29. Chasey, D. & Lucas, M. Detection of rotavirus in experimentally infected piglets. *Res Vet Sci* **22**, 124-5. (1977).
30. Chen, D., Gombold, J. L. & Ramig, R. F. Intracellular RNA synthesis directed by temperature-sensitive mutants of simian rotavirus SA11. *Virology* **178**, 143-51. (1990).
31. Chen, D., Luongo, C. L., Nibert, M. L. & Patton, J. T. Rotavirus open cores catalyze 5'-capping and methylation of exogenous RNA: evidence that VP3 is a methyltransferase. *Virology* **265**, 120-30. (1999).
32. Chen, D. & Patton, J. T. De novo synthesis of minus strand RNA by the rotavirus RNA polymerase in a cell-free system involves a novel mechanism of initiation. *Rna* **6**, 1455-67. (2000).
33. Chen, D. Y. & Ramig, R. F. Determinants of rotavirus stability and density during CsCl purification. *Virology* **186**, 228-37. (1992).
34. Chizhikov, V. & Patton, J. T. A four-nucleotide translation enhancer in the 3'-terminal consensus sequence of the nonpolyadenylated mRNAs of rotavirus. *Rna* **6**, 814-25. (2000).
35. Chnaiderman, J., Diaz, J., Magnusson, G., Liprandi, F. & Spencer, E. Characterization of a rotavirus rearranged gene 11 by gene reassortment. *Arch Virol* **143**, 1711-22 (1998).
36. Ciarlet, M. & Estes, M. K. Interactions between rotavirus and gastrointestinal cells. *Curr Opin Microbiol* **4**, 435-41. (2001).
37. Clark, S. M., Roth, J. R., Clark, M. L., Barnett, B. B. & Spendlove, R. S. Trypsin enhancement of rotavirus infectivity: mechanism of enhancement. *J Virol* **39**, 816-22. (1981).

38. Cohen, J. Ribonucleic acid polymerase activity associated with purified calf rotavirus. *J Gen Virol* **36**, 395-402. (1977).
39. Conner, M. et al. in *The world of microbes* (ed. IUMS) 179 (Paris, 2002).
40. Connolly, J. L. et al. Reovirus-induced apoptosis requires activation of transcription factor NF-kappaB. *J Virol* **74**, 2981-9. (2000).
41. Coulson, B. S., Londrigan, S. L. & Lee, D. J. Rotavirus contains integrin ligand sequences and a disintegrin-like domain that are implicated in virus entry into cells. *Proc Natl Acad Sci U S A* **94**, 5389-94. (1997).
42. Crawford, S. E. et al. Characterization of virus-like particles produced by the expression of rotavirus capsid proteins in insect cells. *J Virol* **68**, 5945-22. (1994).
43. Crawford, S. E. et al. Trypsin cleavage stabilizes the rotavirus VP4 spike. *J Virol* **75**, 6052-61. (2001).
44. Critchfield, J. W., Butera, S. T. & Folks, T. M. Inhibition of HIV activation in latently infected cells by flavonoid compounds. *AIDS Res Hum Retroviruses* **12**, 39-46. (1996).
45. Critchfield, J. W., Coligan, J. E., Folks, T. M. & Butera, S. T. Casein kinase II is a selective target of HIV-1 transcriptional inhibitors. *Proc Natl Acad Sci U S A* **94**, 6110-5. (1997).
46. Cuadras, M. A., Feigelstock, D. A., An, S. & Greenberg, H. B. Gene expression pattern in Caco-2 cells following rotavirus infection. *J Virol* **76**, 4467-82. (2002).
47. Das, T. et al. Role of cellular casein kinase II in the function of the phosphoprotein (P) subunit of RNA polymerase of vesicular stomatitis virus. *J Biol Chem* **270**, 24100-7. (1995).
48. Das, T., Schuster, A., Schneider-Schaulies, S. & Banerjee, A. K. Involvement of cellular casein kinase II in the phosphorylation of measles virus P protein: identification of phosphorylation sites. *Virology* **211**, 218-26. (1995).
49. Denisova, E. et al. Rotavirus capsid protein VP5* permeabilizes membranes. *J Virol* **73**, 3147-53. (1999).
50. Deo, R. C., Groft, C. M., Rajashankar, K. R. & Burley, S. K. Recognition of the rotavirus mRNA 3' consensus by an asymmetric NSP3 homodimer. *Cell* **108**, 71-81. (2002).
51. Dormitzer, P. R., Sun, Z. Y., Wagner, G. & Harrison, S. C. The rhesus rotavirus VP4 sialic acid binding domain has a galectin fold with a novel carbohydrate binding site. *Embo J* **21**, 885-97. (2002).
52. Dowling, W., Denisova, E., LaMonica, R. & Mackow, E. R. Selective membrane permeabilization by the rotavirus VP5* protein is abrogated by mutations in an internal hydrophobic domain. *J Virol* **74**, 6368-76. (2000).
53. Dupuy, L. C., Dobson, S., Bitko, V. & Barik, S. Casein kinase 2-mediated phosphorylation of respiratory syncytial virus phosphoprotein P is essential for the transcription elongation activity of the viral polymerase; phosphorylation by casein kinase 1 occurs mainly at Ser(215) and is without effect. *J Virol* **73**, 8384-92 (1999).
54. Eichwald, C., Vascotto, F., Fabbretti, E. & Burrone, O. R. Rotavirus NSP5: Mapping Phosphorylation Sites and Kinase Activation and Viroplasm Localization Domains. *J Virol* **76**, 3461-70. (2002).
55. Estes, M. K. in *Virology* (eds. Kniper, D. M. & Howley, P. M.) 1747 (Lippincott Williamns & Wilkins, Philadelphia, 2001).
56. Estes, M. K. & Morris, A. P. A viral enterotoxin. A new mechanism of virus-induced pathogenesis. *Adv Exp Med Biol* **473**, 73-82 (1999).

57. Fabbretti, E., Afrikanova, I., Vascotto, F. & Burrone, O. R. Two non-structural rotavirus proteins, NSP2 and NSP5, form viroplasm- like structures in vivo. *J Gen Virol* **80**, 333-9. (1999).
58. Feng, N. et al. Inhibition of rotavirus replication by a non-neutralizing, rotavirus VP6-specific IgA mAb. *J Clin Invest* **109**, 1203-13. (2002).
59. Fuentes-Panana, E. M., Lopez, S., Gorziglia, M. & Arias, C. F. Mapping the hemagglutination domain of rotaviruses. *J Virol* **69**, 2629-32. (1995).
60. Fuerst, T. R., Earl, P. L. & Moss, B. Use of a hybrid vaccinia virus-T7 RNA polymerase system for expression of target genes. *Mol Cell Biol* **7**, 2538-44 (1987).
61. Fuerst, T. R., Niles, E. G., Studier, F. W. & Moss, B. Eukaryotic transient-expression system based on recombinant vaccinia virus that synthesizes bacteriophage T7 RNA polymerase. *Proc Natl Acad Sci U S A* **83**, 8122-6 (1986).
62. Fukuhara, N., Yoshie, O., Kitaoka, S. & Konno, T. Role of VP3 in human rotavirus internalization after target cell attachment via VP7. *J Virol* **62**, 2209-18. (1988).
63. Gault, E. et al. A human rotavirus with rearranged genes 7 and 11 encodes a modified NSP3 protein and suggests an additional mechanism for gene rearrangement. *J Virol* **75**, 7305-14. (2001).
64. Giambiagi, S., Gonzalez Rodriguez, I., Gomez, J. & Burrone, O. A rearranged genomic segment 11 is common to different human rotaviruses. *Arch Virol* **136**, 415-21 (1994).
65. Gilbert, J. M. & Greenberg, H. B. Cleavage of rhesus rotavirus VP4 after arginine 247 is essential for rotavirus-like particle-induced fusion from without. *J Virol* **72**, 5323-7. (1998).
66. Ginn, D. I., Ward, R. L., Hamparian, V. V. & Hughes, J. H. Inhibition of rotavirus in vitro transcription by optimal concentrations of monoclonal antibodies specific for rotavirus VP6. *J Gen Virol* **73**, 3017-22. (1992).
67. Glass, R. I., Bresee, J. S., Parashar, U., Miller, M. & Gentsch, J. R. Rotavirus vaccines at the threshold. *Nat Med* **3**, 1324-5. (1997).
68. Gombold, J. L., Estes, M. K. & Ramig, R. F. Assignment of simian rotavirus SA11 temperature-sensitive mutant groups B and E to genome segments. *Virology* **143**, 309-20. (1985).
69. Gombold, J. L. & Ramig, R. F. Analysis of reassortment of genome segments in mice mixedly infected with rotaviruses SA11 and RRV. *J Virol* **57**, 110-6. (1986).
70. Gombold, J. L. & Ramig, R. F. Assignment of simian rotavirus SA11 temperature-sensitive mutant groups A, C, F, and G to genome segments. *Virology* **161**, 463-73. (1987).
71. Gonzalez, R. A., Espinosa, R., Romero, P., Lopez, S. & Arias, C. F. Relative localization of viroplasmic and endoplasmic reticulum-resident rotavirus proteins in infected cells. *Arch Virol* **145**, 1963-73 (2000).
72. Gonzalez, R. A., Torres-Vega, M. A., Lopez, S. & Arias, C. F. In vivo interactions among rotavirus nonstructural proteins. *Arch Virol* **143**, 981-96 (1998).
73. Gonzalez, S. A. & Burrone, O. R. Porcine OSU rotavirus segment II sequence shows common features with the viral gene of human origin. *Nucleic Acids Res* **17**, 6402. (1989).
74. Gonzalez, S. A. & Burrone, O. R. Rotavirus NS26 is modified by addition of single O-linked residues of N- acetylglucosamine. *Virology* **182**, 8-16. (1991).

75. Gonzalez, S. A., Mattion, N. M., Bellinzoni, R. & Burrone, O. R. Structure of rearranged genome segment 11 in two different rotavirus strains generated by a similar mechanism. *J Gen Virol* **70**, 1329-36. (1989).
76. Groft, C. M. & Burley, S. K. Recognition of eIF4G by rotavirus NSP3 reveals a basis for mRNA circularization. *Mol Cell* **9**, 1273-83. (2002).
77. Guerrero, C. A. et al. Integrin alpha(v)beta(3) mediates rotavirus cell entry. *Proc Natl Acad Sci U S A* **97**, 14644-9. (2000).
78. Halaihel, N. et al. Direct inhibitory effect of rotavirus NSP4(114-135) peptide on the Na(+)-D-glucose symporter of rabbit intestinal brush border membrane. *J Virol* **74**, 9464-70. (2000).
79. Haneda, E., Furuya, T., Asai, S., Morikawa, Y. & Ohtsuki, K. Biochemical characterization of casein kinase II as a protein kinase responsible for stimulation of HIV-1 protease in vitro. *Biochem Biophys Res Commun* **275**, 434-9. (2000).
80. Harada, S. et al. Casein kinase II (CK-II)-mediated stimulation of HIV-1 reverse transcriptase activity and characterization of selective inhibitors in vitro. *Biol Pharm Bull* **22**, 1122-6. (1999).
81. Helmberger-Jones, M. & Patton, J. T. Characterization of subviral particles in cells infected with simian rotavirus SA11. *Virology* **155**, 655-65. (1986).
82. Hewish, M. J., Takada, Y. & Coulson, B. S. Integrins alpha2beta1 and alpha4beta1 can mediate SA11 rotavirus attachment and entry into cells. *J Virol* **74**, 228-36. (2000).
83. Horie, Y. et al. Diarrhea induction by rotavirus NSP4 in the homologous mouse model system. *Virology* **262**, 398-407. (1999).
84. Hua, J., Chen, X. & Patton, J. T. Deletion mapping of the rotavirus metalloprotein NS53 (NSP1): the conserved cysteine-rich region is essential for virus-specific RNA binding. *J Virol* **68**, 3990-4000. (1994).
85. Hua, J., Mansell, E. A. & Patton, J. T. Comparative analysis of the rotavirus NS53 gene: conservation of basic and cysteine-rich regions in the protein and possible stem-loop structures in the RNA. *Virology* **196**, 372-8. (1993).
86. Hua, J. & Patton, J. T. The carboxyl-half of the rotavirus nonstructural protein NS53 (NSP1) is not required for virus replication. *Virology* **198**, 567-76. (1994).
87. Ijaz, M. K. et al. Inhibition of rotavirus infection in vitro and in vivo by a synthetic peptide from VP4. *Vaccine* **16**, 916-20. (1998).
88. Ivanov, K. I., Puustinen, P., Merits, A., Saarma, M. & Makinen, K. Phosphorylation down-regulates the RNA binding function of the coat protein of potato virus A. *J Biol Chem* **276**, 13530-40. (2001).
89. Jayaram, H., Taraporewala, Z., Patton, J. T. & Prasad, B. V. Rotavirus protein involved in genome replication and packaging exhibits a HIT-like fold. *Nature* **417**, 311-5. (2002).
90. Jourdan, N. et al. Rotavirus is released from the apical surface of cultured human intestinal cells through nonconventional vesicular transport that bypasses the Golgi apparatus. *J Virol* **71**, 8268-78. (1997).
91. Kabcenell, A. K. & Atkinson, P. H. Processing of the rough endoplasmic reticulum membrane glycoproteins of rotavirus SA11. *J Cell Biol* **101**, 1270-80. (1985).
92. Kattoura, M. D., Chen, X. & Patton, J. T. The rotavirus RNA-binding protein NS35 (NSP2) forms 10S multimers and interacts with the viral RNA polymerase. *Virology* **202**, 803-13. (1994).

93. Kattoura, M. D., Clapp, L. L. & Patton, J. T. The rotavirus nonstructural protein, NS35, possesses RNA-binding activity in vitro and in vivo. *Virology* **191**, 698-708. (1992).
94. Kim, J., Lee, D. & Choe, J. Hepatitis C virus NS5A protein is phosphorylated by casein kinase II. *Biochem Biophys Res Commun* **257**, 777-81. (1999).
95. Kohl, A., di Bartolo, V. & Bouloy, M. The Rift Valley fever virus nonstructural protein NSs is phosphorylated at serine residues located in casein kinase II consensus motifs in the carboxy-terminus. *Virology* **263**, 517-25. (1999).
96. Kojima, K., Taniguchi, K., Urasawa, T. & Urasawa, S. Sequence analysis of normal and rearranged NSP5 genes from human rotavirus strains isolated in nature: implications for the occurrence of the rearrangement at the step of plus strand synthesis. *Virology* **224**, 446-52. (1996).
97. Kordasti, S., Sjovall, H., Lundgren, O. & Svensson, L. in *The world of microbes* (ed. IUMS) 180 (Paris, 2002).
98. LaMonica, R. et al. VP4 differentially regulates TRAF2 signaling, disengaging JNK activation while directing NF-kappa B to effect rotavirus-specific cellular responses. *J Biol Chem* **276**, 19889-96. (2001).
99. Lawton, J. A., Estes, M. K. & Prasad, B. V. Three-dimensional visualization of mRNA release from actively transcribing rotavirus particles. *Nat Struct Biol* **4**, 118-21. (1997).
100. Lawton, J. A., Estes, M. K. & Prasad, B. V. Comparative structural analysis of transcriptionally competent and incompetent rotavirus-antibody complexes. *Proc Natl Acad Sci U S A* **96**, 5428-33. (1999).
101. Liu, M., Mattion, N. M. & Estes, M. K. Rotavirus VP3 expressed in insect cells possesses guanylyltransferase activity. *Virology* **188**, 77-84. (1992).
102. Londrigan, S. L. et al. Growth of rotaviruses in continuous human and monkey cell lines that vary in their expression of integrins. *J Gen Virol* **81**, 2203-13. (2000).
103. Lopez, S. & Arias, C. F. Protein NS26 is highly conserved among porcine rotavirus strains. *Nucleic Acids Res* **21**, 1042. (1993).
104. Lu, B., Ma, C. H., Brazas, R. & Jin, H. The major phosphorylation sites of the respiratory syncytial virus phosphoprotein are dispensable for virus replication in vitro. *J Virol* **76**, 10776-84. (2002).
105. Ludert, J. E. et al. Genetic mapping indicates that VP4 is the rotavirus cell attachment protein in vitro and in vivo. *J Virol* **70**, 487-93. (1996).
106. Ludert, J. E., Krishnaney, A. A., Burns, J. W., Vo, P. T. & Greenberg, H. B. Cleavage of rotavirus VP4 in vivo. *J Gen Virol* **77**, 391-5. (1996).
107. Ludert, J. E. et al. Identification of mutations in the rotavirus protein VP4 that alter sialic-acid-dependent infection. *J Gen Virol* **79**, 725-9. (1998).
108. Ludert, J. E., Michelangeli, F., Gil, F., Liprandi, F. & Esparza, J. Penetration and uncoating of rotaviruses in cultured cells. *Intervirology* **27**, 95-101 (1987).
109. Lundgren, O. et al. Role of the enteric nervous system in the fluid and electrolyte secretion of rotavirus diarrhea. *Science* **287**, 491-5. (2000).
110. Maass, D. R. & Atkinson, P. H. Rotavirus proteins VP7, NS28, and VP4 form oligomeric structures. *J Virol* **64**, 2632-41. (1990).
111. Mansell, E. A., Ramig, R. F. & Patton, J. T. Temperature-sensitive lesions in the capsid proteins of the rotavirus mutants tsF and tsG that affect virion assembly. *Virology* **204**, 69-81. (1994).

112. Marin, O. et al. Tyrosine versus serine/threonine phosphorylation by protein kinase casein kinase-2. A study with peptide substrates derived from immunophilin Fpr3. *J Biol Chem* **274**, 29260-5. (1999).
113. Martin, S. et al. in *The world of microbes* (ed. IUMS) 472 (Paris, 2002).
114. Mason, B. B., Graham, D. Y. & Estes, M. K. In vitro transcription and translation of simian rotavirus SA11 gene products. *J Virol* **33**, 1111-21 (1980).
115. Mathieu, M. et al. Atomic structure of the major capsid protein of rotavirus: implications for the architecture of the virion. *Embo J* **20**, 1485-97. (2001).
116. Matsushita, Y. et al. In vitro phosphorylation of the movement protein of tomato mosaic tobamovirus by a cellular kinase. *J Gen Virol* **81**, 2095-102. (2000).
117. Mattion, N. et al. Rearrangement of genomic segment 11 in two swine rotavirus strains. *J Gen Virol* **69**, 695-8. (1988).
118. Mattion, N. M. et al. Genome rearrangements in porcine rotaviruses: biochemical and biological comparisons between a supershort strain and its standard counterpart. *J Gen Virol* **71**, 355-62. (1990).
119. Mattion NM, M. D., Both GW, Estes MK. Expression of rotavirus proteins encoded by alternative open reading frames of genome segment 11. *Virology* **181**, 295-304 (1991).
120. McCrae, M. A. & McCorquodale, J. G. Molecular biology of rotaviruses. V. Terminal structure of viral RNA species. *Virology* **126**, 204-12. (1983).
121. McIntyre, M. et al. Biophysical characterization of rotavirus particles containing rearranged genomes. *J Gen Virol* **68**, 2961-6. (1987).
122. Meggio, F., Shugar, D. & Pinna, L. A. Ribofuranosyl-benzimidazole derivatives as inhibitors of casein kinase-2 and casein kinase-1. *Eur J Biochem* **187**, 89-94 (1990).
123. Mendez, E., Lopez, S., Cuadras, M. A., Romero, P. & Arias, C. F. Entry of rotaviruses is a multistep process. *Virology* **263**, 450-9. (1999).
124. Michel, Y. M., Poncet, D., Piron, M., Kean, K. M. & Borman, A. M. Cap-Poly(A) synergy in mammalian cell-free extracts. Investigation of the requirements for poly(A)-mediated stimulation of translation initiation. *J Biol Chem* **275**, 32268-76. (2000).
125. Mirazimi, A., Nilsson, M. & Svensson, L. The molecular chaperone calnexin interacts with the NSP4 enterotoxin of rotavirus in vivo and in vitro. *J Virol* **72**, 8705-9. (1998).
126. Mirazimi, A. & Svensson, L. ATP is required for correct folding and disulfide bond formation of rotavirus VP7. *J Virol* **74**, 8048-52. (2000).
127. Miriagou, V., Stevanato, L., Manservigi, R. & Mavromara, P. The C-terminal cytoplasmic tail of herpes simplex virus type 1 gE protein is phosphorylated in vivo and in vitro by cellular enzymes in the absence of other viral proteins. *J Gen Virol* **81**, 1027-31. (2000).
128. Mohan, K. V., Som, I. & Atreya, C. D. Identification of a type 1 peroxisomal targeting signal in a viral protein and demonstration of its targeting to the organelle. *J Virol* **76**, 2543-7. (2002).
129. Morrison, E. E., Wang, Y. F. & Meredith, D. M. Phosphorylation of structural components promotes dissociation of the herpes simplex virus type 1 tegument. *J Virol* **72**, 7108-14. (1998).
130. Musalem, C. & Espejo, R. T. Release of progeny virus from cells infected with simian rotavirus SA11. *J Gen Virol* **66**, 2715-24. (1985).

131. Nejmeddine, M. et al. Rotavirus spike protein VP4 is present at the plasma membrane and is associated with microtubules in infected cells. *J Virol* **74**, 3313-20. (2000).
132. O'Brien, J. A., Taylor, J. A. & Bellamy, A. R. Probing the structure of rotavirus NSP4: a short sequence at the extreme C terminus mediates binding to the inner capsid particle. *J Virol* **74**, 5388-94. (2000).
133. Okada, J., Kobayashi, N., Taniguchi, K. & Shiomi, H. Functional analysis of the heterologous NSP1 genes in the genetic background of simian rotavirus SA11. *Arch Virol* **144**, 1439-49 (1999).
134. Padilla-Noriega, L., Paniagua, O. & Guzman-Leon, S. Rotavirus protein NSP3 shuts off host cell protein synthesis. *Virology* **298**, 1-7. (2002).
135. Parashar, U. D., Bresee, J. S., R., G. J. & Glass, R. I. (http://www.cdc.gov/ncidod/eid/vol4no4/parashar.htm, 1998).
136. Park, K. J., Choi, S. H., Lee, S. Y., Hwang, S. B. & Lai, M. M. Nonstructural 5A protein of hepatitis C virus modulates tumor necrosis factor alpha-stimulated nuclear factor kappa B activation. *J Biol Chem* **277**, 13122-8. (2002).
137. Patton, J. T. Synthesis of simian rotavirus SA11 double-stranded RNA in a cell-free system. *Virus Res* **6**, 217-33. (1986).
138. Patton, J. T. & Chen, D. RNA-binding and capping activities of proteins in rotavirus open cores. *J Virol* **73**, 1382-91. (1999).
139. Patton, J. T. & Gallegos, C. O. Structure and protein composition of the rotavirus replicase particle. *Virology* **166**, 358-65. (1988).
140. Patton, J. T. & Gallegos, C. O. Rotavirus RNA replication: single-stranded RNA extends from the replicase particle. *J Gen Virol* **71**, 1087-94. (1990).
141. Patton, J. T., Hua, J. & Mansell, E. A. Location of intrachain disulfide bonds in the VP5* and VP8* trypsin cleavage fragments of the rhesus rotavirus spike protein VP4. *J Virol* **67**, 4848-55. (1993).
142. Patton, J. T., Jones, M. T., Kalbach, A. N., He, Y. W. & Xiaobo, J. Rotavirus RNA polymerase requires the core shell protein to synthesize the double-stranded RNA genome. *J Virol* **71**, 9618-26. (1997).
143. Patton, J. T., Salter-Cid, L., Kalbach, A., Mansell, E. A. & Kattoura, M. Nucleotide and amino acid sequence analysis of the rotavirus nonstructural RNA-binding protein NS35. *Virology* **192**, 438-46. (1993).
144. Patton, J. T. & Spencer, E. Genome replication and packaging of segmented double-stranded RNA viruses. *Virology* **277**, 217-25. (2000).
145. Patton, J. T. & Stacy-Phipps, S. Electrophoretic separation of the plus and minus strands of rotavirus SA11 double-stranded RNAs. *J Virol Methods* **13**, 185-90. (1986).
146. Patton, J. T., Wentz, M., Xiaobo, J. & Ramig, R. F. cis-Acting signals that promote genome replication in rotavirus mRNA. *J Virol* **70**, 3961-71. (1996).
147. Petrie, B. L., Estes, M. K. & Graham, D. Y. Effects of tunicamycin on rotavirus morphogenesis and infectivity. *J Virol* **46**, 270-4. (1983).
148. Petrie, B. L., Greenberg, H. B., Graham, D. Y. & Estes, M. K. Ultrastructural localization of rotavirus antigens using colloidal gold. *Virus Res* **1**, 133-52 (1984).
149. Pinna, L. A. Casein kinase 2: an 'eminence grise' in cellular regulation? *Biochim Biophys Acta* **1054**, 267-84. (1990).
150. Piron, M., Delaunay, T., Grosclaude, J. & Poncet, D. Identification of the RNA-binding, dimerization, and eIF4GI-binding domains of rotavirus nonstructural protein NSP3. *J Virol* **73**, 5411-21. (1999).

151. Piron, M., Vende, P., Cohen, J. & Poncet, D. Rotavirus RNA-binding protein NSP3 interacts with eIF4GI and evicts the poly(A) binding protein from eIF4F. *Embo J* **17**, 5811-21. (1998).
152. Pizarro, J. L., Sandino, A. M., Pizarro, J. M., Fernandez, J. & Spencer, E. Characterization of rotavirus guanylyltransferase activity associated with polypeptide VP3. *J Gen Virol* **72**, 325-32. (1991).
153. Poncet, D., Aponte, C. & Cohen, J. Rotavirus protein NSP3 (NS34) is bound to the 3' end consensus sequence of viral mRNAs in infected cells. *J Virol* **67**, 3159-65. (1993).
154. Poncet, D., Aponte, C. & Cohen, J. Structure and function of rotavirus nonstructural protein NSP3. *Arch Virol Suppl* **12**, 29-35 (1996).
155. Poncet, D., Laurent, S. & Cohen, J. Four nucleotides are the minimal requirement for RNA recognition by rotavirus non-structural protein NSP3. *Embo J* **13**, 4165-73. (1994).
156. Poncet, D., Lindenbaum, P., L'Haridon, R. & Cohen, J. In vivo and in vitro phosphorylation of rotavirus NSP5 correlates with its localization in viroplasms. *J Virol* **71**, 34-41. (1997).
157. Prasad, B. V., Burns, J. W., Marietta, E., Estes, M. K. & Chiu, W. Localization of VP4 neutralization sites in rotavirus by three- dimensional cryo-electron microscopy. *Nature* **343**, 476-9. (1990).
158. Prasad, B. V. & K., E. M. in *Structural biology of viruses* (ed. Chiu, B., Grecea) 239 (Oxford University Press, New York, Oxford, 1997).
159. Prasad, B. V. et al. Visualization of ordered genomic RNA and localization of transcriptional complexes in rotavirus. *Nature* **382**, 471-3. (1996).
160. Prasad, B. V., Wang, G. J., Clerx, J. P. & Chiu, W. Three-dimensional structure of rotavirus. *J Mol Biol* **199**, 269-75. (1988).
161. Raha, T. et al. N-terminal region of P protein of Chandipura virus is responsible for phosphorylation-mediated homodimerization. *Protein Eng* **13**, 437-44. (2000).
162. Rey, O. et al. The E7 oncoprotein of human papillomavirus type 16 interacts with F- actin in vitro and in vivo. *Virology* **268**, 372-81. (2000).
163. Rollo, E. E. et al. The epithelial cell response to rotavirus infection. *J Immunol* **163**, 4442-52. (1999).
164. Ruiz, M. C., Cohen, J. & Michelangeli, F. Role of Ca2+in the replication and pathogenesis of rotavirus and other viral infections. *Cell Calcium* **28**, 137-49. (2000).
165. Sapin, C. et al. Rafts promote assembly and atypical targeting of a nonenveloped virus, rotavirus, in Caco-2 cells. *J Virol* **76**, 4591-602. (2002).
166. Sarno, S. et al. Selectivity of 4,5,6,7-tetrabromobenzotriazole, an ATP site-directed inhibitor of protein kinase CK2 ('casein kinase-2'). *FEBS Lett* **496**, 44-8 (2001).
167. Schubert, U. et al. Human-immunodeficiency-virus-type-1-encoded Vpu protein is phosphorylated by casein kinase II. *Eur J Biochem* **204**, 875-83. (1992).
168. Schuck, P., Taraporewala, Z., McPhie, P. & Patton, J. T. Rotavirus nonstructural protein NSP2 self-assembles into octamers that undergo ligand-induced conformational changes. *J Biol Chem* **276**, 9679-87. (2001).
169. Shaw, A. L. et al. Three-dimensional visualization of the rotavirus hemagglutinin structure. *Cell* **74**, 693-701. (1993).
170. Shaw, R. D., Hempson, S. J. & Mackow, E. R. Rotavirus diarrhea is caused by nonreplicating viral particles. *J Virol* **69**, 5946-50. (1995).

171. Sheth, R. et al. Rotavirus stimulates IL-8 secretion from cultured epithelial cells. *Virology* **221**, 251-9. (1996).
172. Stirzaker, S. C., Whitfeld, P. L., Christie, D. L., Bellamy, A. R. & Both, G. W. Processing of rotavirus glycoprotein VP7: implications for the retention of the protein in the endoplasmic reticulum. *J Cell Biol* **105**, 2897-903. (1987).
173. Suzuki, H., Konno, T. & Numazaki, Y. Electron microscopic evidence for budding process-independent assembly of double-shelled rotavirus particles during passage through endoplasmic reticulum membranes. *J Gen Virol* **74**, 2015-8. (1993).
174. Taniguchi, K., Kojima, K. & Urasawa, S. Nondefective rotavirus mutants with an NSP1 gene which has a deletion of 500 nucleotides, including a cysteine-rich zinc finger motif- encoding region (nucleotides 156 to 248), or which has a nonsense codon at nucleotides 153-155. *J Virol* **70**, 4125-30. (1996).
175. Taraporewala, Z., Chen, D. & Patton, J. T. Multimers formed by the rotavirus nonstructural protein NSP2 bind to RNA and have nucleoside triphosphatase activity. *J Virol* **73**, 9934-43. (1999).
176. Taraporewala, Z. F. & Patton, J. T. Identification and characterization of the helix-destabilizing activity of rotavirus nonstructural protein NSP2. *J Virol* **75**, 4519-27. (2001).
177. Taraporewala, Z. F., Schuck, P., Ramig, R. F., Silvestri, L. & Patton, J. T. Analysis of a temperature-sensitive mutant rotavirus indicates that NSP2 octamers are the functional form of the protein. *J Virol* **76**, 7082-93. (2002).
178. Taylor, J. A., O'Brien, J. A., Lord, V. J., Meyer, J. C. & Bellamy, A. R. The RER-localized rotavirus intracellular receptor: a truncated purified soluble form is multivalent and binds virus particles. *Virology* **194**, 807-14. (1993).
179. Taylor, J. A., O'Brien, J. A. & Yeager, M. The cytoplasmic tail of NSP4, the endoplasmic reticulum-localized non- structural glycoprotein of rotavirus, contains distinct virus binding and coiled coil domains. *Embo J* **15**, 4469-76. (1996).
180. Thomas, K. W. et al. Respiratory syncytial virus inhibits apoptosis and induces NF-kappa B activity through a phosphatidylinositol 3-kinase-dependent pathway. *J Biol Chem* **277**, 492-501. (2002).
181. Tian, P., Ball, J. M., Zeng, C. Q. & Estes, M. K. The rotavirus nonstructural glycoprotein NSP4 possesses membrane destabilization activity. *J Virol* **70**, 6973-81. (1996).
182. Tian, P. et al. The rotavirus nonstructural glycoprotein NSP4 mobilizes Ca2+ from the endoplasmic reticulum. *J Virol* **69**, 5763-72. (1995).
183. Tian, P. et al. The nonstructural glycoprotein of rotavirus affects intracellular calcium levels. *J Virol* **68**, 251-7. (1994).
184. Timar Peregrin, A., Ahlman, H., Jodal, M. & Lundgren, O. Effects of calcium channel blockade on intestinal fluid secretion: sites of action. *Acta Physiol Scand* **160**, 379-86. (1997).
185. Torres-Vega, M. A. et al. The C-terminal domain of rotavirus NSP5 is essential for its multimerization, hyperphosphorylation and interaction with NSP6. *J Gen Virol* **81**, 821-30. (2000).
186. Valenzuela, S. et al. Photoaffinity labeling of rotavirus VP1 with 8-azido-ATP: identification of the viral RNA polymerase. *J Virol* **65**, 3964-7. (1991).
187. Varani, G. & Allain, F. H. How a rotavirus hijacks the human protein synthesis machinery. *Nat Struct Biol* **9**, 158-60. (2002).

188. Vende, P., Piron, M., Castagne, N. & Poncet, D. Efficient translation of rotavirus mRNA requires simultaneous interaction of NSP3 with the eukaryotic translation initiation factor eIF4G and the mRNA 3' end. *J Virol* **74**, 7064-71. (2000).
189. Vende, P., Taraporewala, Z. F. & Patton, J. T. RNA-binding activity of the rotavirus phosphoprotein NSP5 includes affinity for double-stranded RNA. *J Virol* **76**, 5291-9. (2002).
190. Weclewicz, K., Kristensson, K. & Svensson, L. Rotavirus causes selective vimentin reorganization in monkey kidney CV- 1 cells. *J Gen Virol* **75**, 3267-71. (1994).
191. Wells, S. E., Hillner, P. E., Vale, R. D. & Sachs, A. B. Circularization of mRNA by eukaryotic translation initiation factors. *Mol Cell* **2**, 135-40. (1998).
192. Wentz, M. J., Patton, J. T. & Ramig, R. F. The 3'-terminal consensus sequence of rotavirus mRNA is the minimal promoter of negative-strand RNA synthesis. *J Virol* **70**, 7833-41. (1996).
193. Wentz, M. J., Zeng, C. Q., Patton, J. T., Estes, M. K. & Ramig, R. F. Identification of the minimal replicase and the minimal promoter of (-)- strand synthesis, functional in rotavirus RNA replication in vitro. *Arch Virol Suppl* **12**, 59-67 (1996).
194. Whitfeld, P. L., Tyndall, C., Stirzaker, S. C., Bellamy, A. R. & Both, G. W. Location of sequences within rotavirus SA11 glycoprotein VP7 which direct it to the endoplasmic reticulum. *Mol Cell Biol* **7**, 2491-7. (1987).
195. Wickelgren, I. How rotavirus causes diarrhea. *Science* **287**, 409, 411. (2000).
196. Xu, A., Bellamy, A. R. & Taylor, J. A. BiP (GRP78) and endoplasmin (GRP94) are induced following rotavirus infection and bind transiently to an endoplasmic reticulum-localized virion component. *J Virol* **72**, 9865-72. (1998).
197. Yeager, M., Berriman, J. A., Baker, T. S. & Bellamy, A. R. Three-dimensional structure of the rotavirus haemagglutinin VP4 by cryo- electron microscopy and difference map analysis. *Embo J* **13**, 1011-8. (1994).
198. Yeager, M., Dryden, K. A., Olson, N. H., Greenberg, H. B. & Baker, T. S. Three-dimensional structure of rhesus rotavirus by cryoelectron microscopy and image reconstruction. *J Cell Biol* **110**, 2133-44. (1990).
199. Zandomeni, R., Zandomeni, M. C., Shugar, D. & Weinmann, R. Casein kinase type II is involved in the inhibition by 5,6-dichloro-1- beta-D-ribofuranosylbenzimidazole of specific RNA polymerase II transcription. *J Biol Chem* **261**, 3414-9. (1986).
200. Zeng, C. Q., Wentz, M. J., Cohen, J., Estes, M. K. & Ramig, R. F. Characterization and replicase activity of double-layered and single- layered rotavirus-like particles expressed from baculovirus recombinants. *J Virol* **70**, 2736-42. (1996).
201. Zhang, M., Zeng, C. Q., Morris, A. P. & Estes, M. K. A functional NSP4 enterotoxin peptide secreted from rotavirus-infected cells. *J Virol* **74**, 11663-70. (2000).

References (2):

1. Afrikanova, I., Miozzo, M. C., Giambiagi, S. & Burrone, O. Phosphorylation generates different forms of rotavirus NSP5. *J Gen Virol* **77 (Pt 9)**, 2059-65 (1996).
2. Baltimore, D. Gene therapy. Intracellular immunization. *Nature* **335**, 395-6. (1988).
3. Barbas, C. F., 3rd et al. Recombinant human Fab fragments neutralize human type 1 immunodeficiency virus in vitro. *Proc Natl Acad Sci U S A* **89**, 9339-43 (1992).
4. Bartel, P., Chien, C. T., Sternglanz, R. & Fields, S. in *Biotechniques* 920-4 (1993).
5. Beerli, R. R., Wels, W. & Hynes, N. E. Intracellular expression of single chain antibodies reverts ErbB-2 transformation. *J Biol Chem* **269**, 23931-6. (1994).
6. Bestagno, M. et al. Membrane immunoglobulins are stabilized by interchain disulfide bonds occurring within the extracellular membrane-proximal domain. *Biochemistry* **40**, 10686-92. (2001).
7. Beste, G., Schmidt, F. S., Stibora, T. & Skerra, A. Small antibody-like proteins with prescribed ligand specificities derived from the lipocalin fold. *Proc Natl Acad Sci U S A* **96**, 1898-903. (1999).
8. Biocca, S., Neuberger, M. S. & Cattaneo, A. Expression and targeting of intracellular antibodies in mammalian cells. *Embo J* **9**, 101-8 (1990).
9. Biocca, S., Pierandrei-Amaldi, P., Campioni, N. & Cattaneo, A. Intracellular immunization with cytosolic recombinant antibodies. *Biotechnology (N Y)* **12**, 396-9 (1994).
10. Biocca, S., Pierandrei-Amaldi, P. & Cattaneo, A. Intracellular expression of anti-p21ras single chain Fv fragments inhibits meiotic maturation of xenopus oocytes. *Biochem Biophys Res Commun* **197**, 422-7 (1993).
11. Biocca, S., Ruberti, F., Tafani, M., Pierandrei-Amaldi, P. & Cattaneo, A. Redox state of single chain Fv fragments targeted to the endoplasmic reticulum, cytosol and mitochondria. *Biotechnology (N Y)* **13**, 1110-5 (1995).
12. BouHamdan, M. et al. Inhibition of HIV-1 infection by down-regulation of the CXCR4 co- receptor using an intracellular single chain variable fragment against CXCR4. *Gene Ther* **8**, 408-18. (2001).
13. Cardinale, A., Filesi, I. & Biocca, S. Aggresome formation by anti-Ras intracellular scFv fragments. The fate of the antigen-antibody complex. *Eur J Biochem* **268**, 268-77. (2001).
14. Cattaneo, A. & Biocca, S. *Intracellular Antibodies: Development and Applications* (ed. Biocca, A. C. a. S.) (Springer-Verlag, New York, 1997).
15. Cattaneo, A. & Biocca, S. The selection of intracellular antibodies. *Trends in Biotechnology* **17**, 115-121 (1999).
16. Chames, P. & Baty, D. Antibody engineering and its applications in tumor targeting and intracellular immunization. *FEMS Microbiol Lett* **189**, 1-8. (2000).
17. Chen, J. D., Yang, Q., Yang, A. G., Marasco, W. A. & Chen, S. Y. Intra- and extracellular immunization against HIV-1 infection with lymphocytes transduced with an AAV vector expressing a human anti-gp120 antibody. *Hum Gene Ther* **7**, 1515-25. (1996).

18. Cochet, O. et al. Intracellular expression of an antibody fragment-neutralizing p21 ras promotes tumor regression. *Cancer Res* **58**, 1170-6. (1998).
19. Cohen, P. A., Mani, J. C. & Lane, D. P. Characterization of a new intrabody directed against the N-terminal region of human p53. *Oncogene* **17**, 2445-56. (1998).
20. Dauvillier, S. et al. Intracellular Single-Chain Variable Fragments Directed to the Src Homology 2 Domains of Syk Partially Inhibit FcepsilonRI Signaling in the RBL-2H3 Cell Line. *J Immunol* **169**, 2274-2283. (2002).
21. De Jaeger, G., Fiers, E., Eeckhout, D. & Depicker, A. Analysis of the interaction between single-chain variable fragments and their antigen in a reducing intracellular environment using the two- hybrid system. *FEBS Lett* **467**, 316-20. (2000).
22. Duan, L., Bagasra, O., Laughlin, M. A., Oakes, J. W. & Pomerantz, R. J. Potent inhibition of human immunodeficiency virus type 1 replication by an intracellular anti-Rev single-chain antibody. *Proc Natl Acad Sci U S A* **91**, 5075-9. (1994).
23. Duan, L., Zhu, M., Bagasra, O. & Pomerantz, R. J. Intracellular immunization against HIV-1 infection of human T lymphocytes: utility of anti-rev single-chain variable fragments. *Hum Gene Ther* **6**, 1561-73. (1995).
24. Eeckhout, D. et al. Isolation and characterization of recombinant antibody fragments against CDC2a from Arabidopsis thaliana. *Eur J Biochem* **267**, 6775-83 (2000).
25. Fields, S. & Song, O. A novel genetic system to detect protein-protein interactions. *Nature* **340**, 245-6 (1989).
26. Gargano, N., Biocca, S., Bradbury, A. & Cattaneo, A. Human recombinant antibody fragments neutralizing human immunodeficiency virus type 1 reverse transcriptase provide an experimental basis for the structural classification of the DNA polymerase family. *J Virol* **70**, 7706-12 (1996).
27. Gargano, N. & Cattaneo, A. Inhibition of murine leukaemia virus retrotranscription by the intracellular expression of a phage-derived anti-reverse transcriptase antibody fragment. *J Gen Virol* **78**, 2591-9. (1997).
28. Gargano, N. & Cattaneo, A. Rescue of a neutralizing anti-viral antibody fragment from an intracellular polyclonal repertoire expressed in mammalian cells. *FEBS Lett* **414**, 537-40 (1997).
29. Goncalves, J. et al. Functional neutralization of HIV-1 Vif protein by intracellular immunization inhibits reverse transcription and viral replication. *J Biol Chem* **277**, 32036-45. (2002).
30. Graus-Porta, D., Beerli, R. R. & Hynes, N. E. Single-chain antibody-mediated intracellular retention of ErbB-2 impairs Neu differentiation factor and epidermal growth factor signaling. *Mol Cell Biol* **15**, 1182-91. (1995).
31. Hanke, T., Szawlowski, P. & Randall, R. E. Construction of solid matrix-antibody-antigen complexes containing simian immunodeficiency virus p27 using tag-specific monoclonal antibody and tag-linked antigen. *J Gen Virol* **73 (Pt 3)**, 653-60 (1992).
32. Heintges, T., zu Putlitz, J. & Wands, J. R. Characterization and binding of intracellular antibody fragments to the hepatitis C virus core protein. *Biochem Biophys Res Commun* **263**, 410-8. (1999).
33. Hollenberg, S. M., Sternglanz, R., Cheng, P. F. & Weintraub, H. Identification of a new family of tissue -specific basic helix-loop-helix proteins with a two-hybrid system. *Molecular and Cellular Biology* **15**, 3813-3822 (1995).

34. Jannot, C. B., Beerli, R. R., Mason, S., Gullick, W. J. & Hynes, N. E. Intracellular expression of a single-chain antibody directed to the EGFR leads to growth inhibition of tumor cells. *Oncogene* **13**, 275-82. (1996).
35. Jean, D. et al. Inhibition of tumor growth and metastasis of human melanoma by intracellular anti-ATF-1 single chain Fv fragment. *Oncogene* **19**, 2721-30. (2000).
36. Jost, C. R. et al. Mammalian expression and secretion of functional single-chain Fv molecules. *J Biol Chem* **269**, 26267-73. (1994).
37. Kalderon, D., Richardson, W. D., Markham, A. F. & Smith, A. E. Sequence requirements for nuclear location of simian virus 40 large-T antigen. *Nature* **311**, 33-8. (1984).
38. Kasono, K. et al. Tetracycline-induced expression of an anti-c-Myb single-chain antibody and its inhibitory effect on proliferation of the human leukemia cell line K562. *Cancer Gene Ther* **7**, 151-9. (2000).
39. Kasono, K. et al. Functional knock-out of c-myb by an intracellular anti-c-Myb single- chain antibody. *Biochem Biophys Res Commun* **251**, 124-30. (1998).
40. Khoshnan, A., Ko, J. & Patterson, P. H. Effects of intracellular expression of anti-huntingtin antibodies of various specificities on mutant huntingtin aggregation and toxicity. *Proc Natl Acad Sci U S A* **99**, 1002-7. (2002).
41. Lecerf, J. M. et al. Human single-chain Fv intrabodies counteract in situ huntingtin aggregation in cellular models of Huntington's disease. *Proc Natl Acad Sci U S A* **98**, 4764-9. (2001).
42. Levy-Mintz, P. et al. Intracellular expression of single-chain variable fragments to inhibit early stages of the viral life cycle by targeting human immunodeficiency virus type 1 integrase. *J Virol* **70**, 8821-32. (1996).
43. Li, E. et al. Mammalian cell expression of dimeric small immune proteins (SIP). *Protein Eng* **10**, 731-6. (1997).
44. Luzi, L., Confalonieri, S., Di Fiore, P. P. & Pelicci, P. G. Evolution of Shc functions from nematode to human. *Curr Opin Genet Dev* **10**, 668-74 (2000).
45. Maciejewski, J. et al. Intracellular expression of antibody fragments directed against HIV reverse transcriptase prevents HIV infection in vitro. *Nat Med* **1**, 667-73 (1995).
46. Marasco, W. A., Haseltine, W. A. & Chen, S. Y. Design, intracellular expression, and activity of a human anti-human immunodeficiency virus type 1 gp120 single-chain antibody. *Proc Natl Acad Sci U S A* **90**, 7889-93. (1993).
47. Martineau, P., Jones, P. & G., W. Expression of an antibody fragment at high levels in the bacterial cytoplasm. *J Mol Biol* **280**, 117-127 (1998).
48. McCafferty, J., Griffiths, A. D., Winter, G. & Chiswell, D. J. Phage antibodies: filamentous phage displaying antibody variable domains. *Nature* **348**, 552-4. (1990).
49. Mhashilkar, A. M. et al. Inhibition of HIV-1 Tat-mediated LTR transactivation and HIV-1 infection by anti-Tat single chain intrabodies. *Embo J* **14**, 1542-51. (1995).
50. Orlandi, R., Gussow, D. H., Jones, P. T. & Winter, G. Cloning immunoglobulin variable domains for expression by the polymerase chain reaction. *Proc Natl Acad Sci U S A* **86**, 3833-7 (1989).
51. Piche, A. et al. Modulation of Bcl-2 protein levels by an intracellular anti-Bcl-2 single-chain antibody increases drug-induced cytotoxicity in the breast cancer cell line MCF-7. *Cancer Res* **58**, 2134-40. (1998).

52. Piche, A., Kasono, K., Johanning, F., Curiel, T. J. & Curiel, D. T. Phenotypic knock-out of the latent membrane protein 1 of Epstein-Barr virus by an intracellular single-chain antibody. *Gene Ther* **5**, 1171-9. (1998).
53. Pluckthun, A., Schaffitzel, C., Hanes, J. & Jermutus, L. In vitro selection and evolution of proteins. *Adv Protein Chem* **55**, 367-403. (2000).
54. Portner-Taliana, A. et al. In vivo selection of single-chain antibodies using a yeast two-hybrid system. *J Immunol Methods* **238**, 161-72. (2000).
55. Proba, K., Ge, L. & Pluckthun, A. Functional antibody single-chain fragments from the cytoplasm of Escherichia coli: influence of thioredoxin reductase (TrxB). *Gene* **159**, 203-7. (1995).
56. Proba, K., Honegger, A. & Pluckthun, A. A natural antibody missing a cysteine in VH: consequences for thermodynamic stability and folding. *J Mol Biol* **265**, 161-72 (1997).
57. Proba, K., Worn, A., Honegger, A. & Pluckthun, A. Antibody scFv fragments without disulfide bonds made by molecular evolution. *J Mol Biol* **275**, 245-53 (1998).
58. Rajpal, A. & Turi, T. G. Intracellular stability of anti-caspase-3 intrabodies determines efficacy in re-targeting the antigen. *J Biol Chem* **25**, 25 (2001).
59. Ravichandran, K. S. Signaling via Shc family adapter proteins. *Oncogene* **20**, 6322-30 (2001).
60. Rhee, Y., Gurel, F., Gafni, Y., Dingwall, C. & Citovsky, V. A genetic system for detection of protein nuclear import and export. *Nat Biotechnol* **18**, 433-7. (2000).
61. Richardson, J. H. & Marasco, W. A. Intracellular antibodies: development and therapeutic potential. *Trends Biotechnol* **13**, 306-10. (1995).
62. Richardson, J. H., Sodroski, J. G., Waldmann, T. A. & Marasco, W. A. Phenotypic knockout of the high-affinity human interleukin 2 receptor by intracellular single-chain antibodies against the alpha subunit of the receptor. *Proc Natl Acad Sci U S A* **92**, 3137-41. (1995).
63. Rondon, I. J. & Marasco, W. A. Intracellular antibodies (intrabodies) for gene therapy of infectious diseases. *Annu Rev Microbiol* **51**, 257-83. (1997).
64. Rudikoff, S. & Pumphrey, J. G. Functional antibody lacking a variable-region disulfide bridge. *Proc Natl Acad Sci U S A* **83**, 7875-8. (1986).
65. Sblattero, D. & Bradbury, A. Exploiting recombination in single bacteria to make large phage antibody libraries. *Nat Biotechnol* **18**, 75-80 (2000).
66. Scott, J. K. & Smith, G. P. Searching for peptide ligands with an epitope library. *Science* **249**, 386-90. (1990).
67. Sheets, M. D. et al. Efficient construction of a large nonimmune phage antibody library: the production of high-affinity human single-chain antibodies to protein antigens [published erratum appears in Proc Natl Acad Sci U S A 1999 Jan 19;96(2):795]. *Proc Natl Acad Sci U S A* **95**, 6157-62 (1998).
68. Steinberger, P., Andris-Widhopf, J., Buhler, B., Torbett, B. E. & Barbas, C. F., 3rd. Functional deletion of the CCR5 receptor by intracellular immunization produces cells that are refractory to CCR5-dependent HIV-1 infection and cell fusion. *Proc Natl Acad Sci U S A* **97**, 805-10. (2000).
69. Strube, R. W. & Chen, S. Y. Characterization of anti-cyclin E single-chain Fv antibodies and intrabodies in breast cancer cells: enhanced intracellular stability of novel sFv-F(c) intrabodies. *J Immunol Methods* **263**, 149-67. (2002).

70. Tavladoraki, P. et al. Transgenic plants expressing a functional single-chain Fv antibody are specifically protected from virus attack. *Nature* **366**, 469-472 (1993).
71. Tse, E. et al. Intracellular antibody capture technology: application to selection of intracellular antibodies recognising the BCR-ABL oncogenic protein. *J Mol Biol* **317**, 85-94. (2002).
72. Vanhove, B., Charreau, B., Cassard, A., Pourcel, C. & Soulillou, J. P. Intracellular expression in pig cells of anti- alpha1,3galactosyltransferase single-chain FV antibodies reduces Gal alpha1,3Gal expression and inhibits cytotoxicity mediated by anti-Gal xenoantibodies. *Transplantation* **66**, 1477-85. (1998).
73. Vaughan, T. J. et al. Human antibodies with sub-nanomolar affinities isolated from a large non-immunized phage display library. *Nat Biotechnol* **14**, 309-14. (1996).
74. Vihinen-Ranta, M., Yuan, W. & Parrish, C. R. Cytoplasmic trafficking of the canine parvovirus capsid and its role in infection and nuclear transport. *J Virol* **74**, 4853-9. (2000).
75. Visintin, M. & Cattaneo, A. *Selecting intracellular antibodies using the two-hybrid system* (ed. Dubel, R. K. S.) (Heidelberg, 2001).
76. Visintin, M. et al. The intracellular antibody capture technology (IACT): towards a consensus sequence for intracellular antibodies. *J Mol Biol* **317**, 73-83. (2002).
77. Visintin, M., Tse, E., Axelson, H., Rabbitts, T. H. & Cattaneo, A. in *Proc Natl Acad Sci U S A* 11723-8 (1999).
78. Whitlow, M. et al. An improved linker for single-chain Fv with reduced aggregation and enhanced proteolytic stability. *Protein Eng* **6**, 989-95. (1993).
79. Williams, G. T., Venkitaraman, A. R., Gilmore, D. J. & Neuberger, M. S. The sequence of the mu transmembrane segment determines the tissue specificity of the transport of immunoglobulin M to the cell surface. *J Exp Med* **171**, 947-52. (1990).
80. Worn, A. et al. Correlation between in vitro stability and in vivo performance of anti-GCN4 intrabodies as cytoplasmic inhibitors. *J Biol Chem* **275**, 2795-803. (2000).
81. Yamamoto, M. et al. Intracellular single-chain antibody against hepatitis B virus core protein inhibits the replication of hepatitis B virus in cultured cells. *Hepatology* **30**, 300-7. (1999).
82. Yi, K. S. et al. Inhibition of the EGF-induced activation of phospholipase C-gamma1 by a single chain antibody fragment. *Oncogene* **20**, 7954-64. (2001).